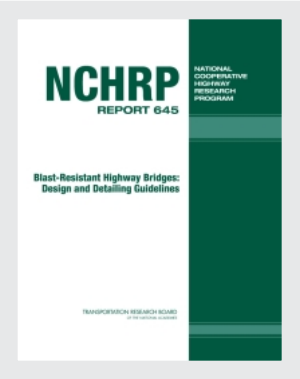

Blast-Resistant Highway Bridges: Design and Detailing Guidelines

DETAILS

0 pages | | PAPERBACK
ISBN 978-0-309-42995-5 | DOI 10.17226/22971

AUTHORS

NATIONAL COOPERATIVE HIGHWAY RESEARCH PROGRAM

NCHRP REPORT 645

Blast-Resistant Highway Bridges: Design and Detailing Guidelines

Eric B. Williamson
Oguzhan Bayrak
G. Daniel Williams
Carrie E. Davis
University of Texas at Austin
Austin, TX

Kirk A. Marchand
Aldo E. McKay
Protection Engineering Consultants
Dripping Springs, TX

John Kulicki
Wagdy Wassef
Modjeski and Masters, Inc.
Mechanicsburg, PA

Subject Areas
Bridges, Other Structures, and Hydraulics and Hydrology • Security

Research sponsored by the American Association of State Highway and Transportation Officials
in cooperation with the Federal Highway Administration

TRANSPORTATION RESEARCH BOARD

WASHINGTON, D.C.
2010
www.TRB.org

NATIONAL COOPERATIVE HIGHWAY RESEARCH PROGRAM

Systematic, well-designed research provides the most effective approach to the solution of many problems facing highway administrators and engineers. Often, highway problems are of local interest and can best be studied by highway departments individually or in cooperation with their state universities and others. However, the accelerating growth of highway transportation develops increasingly complex problems of wide interest to highway authorities. These problems are best studied through a coordinated program of cooperative research.

In recognition of these needs, the highway administrators of the American Association of State Highway and Transportation Officials initiated in 1962 an objective national highway research program employing modern scientific techniques. This program is supported on a continuing basis by funds from participating member states of the Association and it receives the full cooperation and support of the Federal Highway Administration, United States Department of Transportation.

The Transportation Research Board of the National Academies was requested by the Association to administer the research program because of the Board's recognized objectivity and understanding of modern research practices. The Board is uniquely suited for this purpose as it maintains an extensive committee structure from which authorities on any highway transportation subject may be drawn; it possesses avenues of communications and cooperation with federal, state and local governmental agencies, universities, and industry; its relationship to the National Research Council is an insurance of objectivity; it maintains a full-time research correlation staff of specialists in highway transportation matters to bring the findings of research directly to those who are in a position to use them.

The program is developed on the basis of research needs identified by chief administrators of the highway and transportation departments and by committees of AASHTO. Each year, specific areas of research needs to be included in the program are proposed to the National Research Council and the Board by the American Association of State Highway and Transportation Officials. Research projects to fulfill these needs are defined by the Board, and qualified research agencies are selected from those that have submitted proposals. Administration and surveillance of research contracts are the responsibilities of the National Research Council and the Transportation Research Board.

The needs for highway research are many, and the National Cooperative Highway Research Program can make significant contributions to the solution of highway transportation problems of mutual concern to many responsible groups. The program, however, is intended to complement rather than to substitute for or duplicate other highway research programs.

NCHRP REPORT 645

Project 12-72
ISSN 0077-5614
ISBN 978-0-309-11819-4
Library of Congress Control Number 2009944223

COPYRIGHT INFORMATION

NOTICE

The project that is the subject of this report was a part of the National Cooperative Highway Research Program conducted by the Transportation Research Board with the approval of the Governing Board of the National Research Council. Such approval reflects the Governing Board's judgment that the program concerned is of national importance and appropriate with respect to both the purposes and resources of the National Research Council.

The members of the technical committee selected to monitor this project and to review this report were chosen for recognized scholarly competence and with due consideration for the balance of disciplines appropriate to the project. The opinions and conclusions expressed or implied are those of the research agency that performed the research, and, while they have been accepted as appropriate by the technical committee, they are not necessarily those of the Transportation Research Board, the National Research Council, the American Association of State Highway and Transportation Officials, or the Federal Highway Administration, U.S. Department of Transportation.

Each report is reviewed and accepted for publication by the technical committee according to procedures established and monitored by the Transportation Research Board Executive Committee and the Governing Board of the National Research Council.

The Transportation Research Board of the National Academies, the National Research Council, the Federal Highway Administration, the American Association of State Highway and Transportation Officials, and the individual states participating in the National Cooperative Highway Research Program do not endorse products or manufacturers. Trade or manufacturers' names appear herein solely because they are considered essential to the object of this report.

Published reports of the

NATIONAL COOPERATIVE HIGHWAY RESEARCH PROGRAM

are available from:

Transportation Research Board
Business Office
500 Fifth Street, NW
Washington, DC 20001

and can be ordered through the Internet at:

http://www.national-academies.org/trb/bookstore

Printed in the United States of America

THE NATIONAL ACADEMIES

Advisers to the Nation on Science, Engineering, and Medicine

The **National Academy of Sciences** is a private, nonprofit, self-perpetuating society of distinguished scholars engaged in scientific and engineering research, dedicated to the furtherance of science and technology and to their use for the general welfare. On the authority of the charter granted to it by the Congress in 1863, the Academy has a mandate that requires it to advise the federal government on scientific and technical matters. Dr. Ralph J. Cicerone is president of the National Academy of Sciences.

The **National Academy of Engineering** was established in 1964, under the charter of the National Academy of Sciences, as a parallel organization of outstanding engineers. It is autonomous in its administration and in the selection of its members, sharing with the National Academy of Sciences the responsibility for advising the federal government. The National Academy of Engineering also sponsors engineering programs aimed at meeting national needs, encourages education and research, and recognizes the superior achievements of engineers. Dr. Charles M. Vest is president of the National Academy of Engineering.

The **Institute of Medicine** was established in 1970 by the National Academy of Sciences to secure the services of eminent members of appropriate professions in the examination of policy matters pertaining to the health of the public. The Institute acts under the responsibility given to the National Academy of Sciences by its congressional charter to be an adviser to the federal government and, on its own initiative, to identify issues of medical care, research, and education. Dr. Harvey V. Fineberg is president of the Institute of Medicine.

The **National Research Council** was organized by the National Academy of Sciences in 1916 to associate the broad community of science and technology with the Academy's purposes of furthering knowledge and advising the federal government. Functioning in accordance with general policies determined by the Academy, the Council has become the principal operating agency of both the National Academy of Sciences and the National Academy of Engineering in providing services to the government, the public, and the scientific and engineering communities. The Council is administered jointly by both the Academies and the Institute of Medicine. Dr. Ralph J. Cicerone and Dr. Charles M. Vest are chair and vice chair, respectively, of the National Research Council.

The **Transportation Research Board** is one of six major divisions of the National Research Council. The mission of the Transportation Research Board is to provide leadership in transportation innovation and progress through research and information exchange, conducted within a setting that is objective, interdisciplinary, and multimodal. The Board's varied activities annually engage about 7,000 engineers, scientists, and other transportation researchers and practitioners from the public and private sectors and academia, all of whom contribute their expertise in the public interest. The program is supported by state transportation departments, federal agencies including the component administrations of the U.S. Department of Transportation, and other organizations and individuals interested in the development of transportation. **www.TRB.org**

www.national-academies.org

CRP STAFF FOR NCHRP REPORT 645

Christopher W. Jenks, *Director, Cooperative Research Programs*
Crawford F. Jencks, *Deputy Director, Cooperative Research Programs*
David B. Beal, *Senior Program Officer, Retired*
Waseem Dekelbab, *Senior Program Officer*
Eileen P. Delaney, *Director of Publications*
Doug English, *Editor*

NCHRP PROJECT 12-72 PANEL
Field of Design—Area of Bridges

George A. Christian, *New York State DOT, Albany, NY* (Chair)
John A. Bryson, *Parsons Brinckerhoff Quade & Douglas, Inc., New York, NY*
Shyam Gupta, *Columbia, MO*
Sophia Hassiotis, *Stevens Institute of Technology, Hoboken, NJ*
Jugesh Kapur, *Washington State DOT, Olympia, WA*
Richard D. Land, *California DOT, Sacramento, CA*
Thomas Rummel, *Texas DOT, Austin, TX*
Jonathan C. Van Hook, *Florida DOT, Tallahassee, FL*
David G. Winget, *U.S. Army*
Theodore P. Zoli, III, *HNTB Corporation, New York, NY*
Sheila Rimal Duwadi, *FHWA Liaison*
Stephen F. Maher, *TRB Liaison*

AUTHOR ACKNOWLEDGMENTS

The research reported herein was performed for NCHRP Project 12-72 under the supervision of Dr. Eric B. Williamson, Associate Professor of Civil Engineering at the University of Texas at Austin (UT), who served as the project Principal Investigator.

Dr. Oguzhan Bayrak, Associate Professor of Civil Engineering at UT, Kirk A. Marchand, Managing Principal of Protection Engineering Consultants (PEC), Dripping Springs, Texas, and Dr. John Kulicki, President/CEO and Chief Engineer of Modjeski and Masters, Inc. (M&M), Mechanicsburg, Pennsylvania, served as co-Principal Investigators. Other researchers included G. Daniel Williams, Graduate Research Assistant and Ph.D. Candidate at UT, and Carrie E. Davis, Graduate Research Assistant and M.S. Candidate at UT.

Additional contributors included Aldo E. McKay, Project Engineer with PEC, James C. Ray, Research Engineer at the U.S. Army Corps of Engineers, Vicksburg, Mississippi, and Wagdy G. Wassef, Senior Associate at M&M.

FOREWORD

By Waseem Dekelbab
Staff Officer
Transportation Research Board

This report presents code-ready language containing general design guidance and a simplified design procedure for blast-resistant reinforced concrete bridge columns. It provides the results of experimental blast tests and analytical research on reinforced concrete bridge columns intended to investigate the effectiveness of a variety of different design techniques. The material in this report will be of immediate interest to bridge designers.

There is a need to protect the nation's bridges from intentional or accidental explosions. The impacts of these loads on buildings and military structures have been studied for many years, but design for resistance to explosive effects is a new area for bridge engineers. Much research and development has been done on the effectiveness of seismic strengthening details for buildings and bridges, and it has been suggested that these or similar bridge details, used in new construction or as a retrofit, may serve also to resist explosions and provide a predictable level of protection. There is a need to meld knowledge of seismic and extreme-event design for new and existing structures with the equally well-known field of blast-resistant design and the relatively new field of highway bridge blast-resistant design.

Under NCHRP Project 12-72, the research team was selected to develop design and detailing guidelines for improving the structural performance and resistance to explosive effects for new and existing bridges.

This research was performed under NCHRP Project 12-72 by the University of Texas at Austin with the assistance of Protection Engineering Consultants and Modjeski and Masters, Inc. The report fully documents the research leading to the developed design and detailing guidelines for blast-resistant reinforced concrete bridge columns.

CONTENTS

1 Summary

4 **Chapter 1** Introduction
4 1.1 Overview
5 1.2 Background and History
7 1.3 Research Approach

8 **Chapter 2** Research Background
8 2.1 Overview
8 2.2 Literature Review
8 2.2.1 Blast Loads and Shock Phenomena
13 2.2.2 Structural Response to Blast Loads
13 2.2.3 Dynamic Material Strength and Strain-Rate Effects
15 2.2.4 Application of Seismic Design to Blast-Loaded Bridges
18 2.2.5 Design Issues
24 2.3 Research Needs
24 2.3.1 Research Needs and Focus of Current Study
25 2.3.2 Blast-Resistant Design: Buildings versus Bridges
26 2.3.3 Current and Past Research on Highway Bridges
28 2.3.4 Summary
28 2.4 Focus of Current Work

30 **Chapter 3** Experimental Program
30 3.1 Overview
30 3.2 Phase I Load Characterization Study
30 3.2.1 Experimental Setup
31 3.2.2 Data Acquisition and Instrumentation Plan
31 3.3 Phase II Response Test
33 3.3.1 Background on Parameters Selected for Testing
37 3.3.2 Column Design
41 3.3.3 Reaction Structure Design
41 3.3.4 Data Acquisition and Instrumentation Plan
43 3.3.5 Column Construction
43 3.3.6 Small Standoff Test Setup
44 3.3.7 Spall/Breach Test Setup
45 3.4 Summary

46 **Chapter 4** Analytical Research Program
46 4.1 Overview
46 4.2 Current State-of-Practice: SDOF
49 4.3 Simplified Modeling and Software
49 4.3.1 Load Prediction Techniques
50 4.3.2 Response Prediction
55 4.3.3 Advanced Modeling Methods and Software

60 **Chapter 5** Observations and Research Findings
60 5.1 Overview
60 5.1.1 Phase I Tests
65 5.1.2 Phase II Tests
83 5.2 Observations from Analytical Programs
83 5.2.1 Strain Data
83 5.2.2 Actual Boundary Conditions
85 5.2.3 Actual Load Distribution
87 5.3 Summary
88 **Chapter 6** Design and Detailing Guidelines
88 6.1 Overview
88 6.2 Risk Assessment Guidelines for Bridges
89 6.3 Blast-Load Guidelines
90 6.4 Design and Detailing Guidelines for Columns
91 6.4.1 Design Category A
92 6.4.2 Design Category B
92 6.4.3 Design Category C
97 6.5 Analysis Guidelines for Columns
99 6.6 Summary
100 **Chapter 7** Analysis Guidelines
100 7.1 Overview
100 7.2 Simplified Analyses Guidelines
102 7.3 Airblast Modeling Using Computation Fluid Dynamics
105 7.4 Concrete Modeling
106 7.5 Coupled Analyses
107 7.6 Summary
108 **Chapter 8** Design Examples
108 8.1 Overview
108 8.2 Design Examples
109 8.2.1 Design Example 1
115 8.2.2 Design Example 2
123 8.2.3 Design Example 3
129 8.2.4 Design Example 4
133 8.3 Summary
134 **Chapter 9** Summary, Conclusions, and Recommendations
134 9.1 Summary of Research Program
135 9.2 Conclusions and Recommendations
135 9.2.1 Summary of Small Standoff Blast Tests
135 9.2.2 Summary of Local Damage Tests
135 9.2.3 Summary of Design Guidelines
136 9.3 Recommendations for Future Work
138 References
141 List of Variables

SUMMARY

Blast-Resistant Highway Bridges: Design and Detailing Guidelines

The possibility of terrorism against our nation's bridges is an ever-increasing threat in today's society. Data collected by the Mineta Transportation Institute indicate that at least 53 terrorist attacks worldwide specifically targeted bridges between 1980 and 2006, and 60% of those attacks were bombings. Moreover, accidental collapses of bridges in the U.S. and terrorist attacks against bridges in Iraq illustrate the large economic and socio-economic consequences of catastrophic bridge failures. To help ensure the safety of bridges in the U.S. and protect the nation's infrastructure, there is a need for design and detailing guidelines for blast-resistant highway bridges. To address this need, the National Cooperative Highway Research Program (NCHRP) funded NCHRP Project 12-72 to investigate highway bridges subjected to explosive loads.

Because bridge columns are integral to nearly all bridges regardless of the superstructure type, and because the loss of a key column could compromise the integrity of most bridges, the research team elected to focus its effort on reinforced concrete columns. The main goals of the research were to:

- Investigate the response of concrete bridge columns subjected to blast loads,
- Develop blast-resistant design and detailing guidelines for highway bridge columns, and
- Develop analytical models of blast-load distribution and the resulting column response that are validated by experimental data.

The research program consisted of two different phases of experimental testing, complemented by computational and analytical modeling. Phase I of the experimental test program included small-scale blast tests on square and round non-responding columns. These tests were conducted by the Engineering Research and Development Center of the U.S. Army Corps of Engineers at their test site in Vicksburg, Mississippi, and they were designed to determine how shock waves interact with slender structural members so that variations in pressures and impulses with both time and position along the height of a column could be studied. Phase II of the experimental testing program included close-in blast tests on half-scale reinforced concrete columns. These tests were conducted at a remote test site with help from Protection Engineering Consultants (PEC) and the Southwest Research Institute (SwRI). The test matrix included ten half-scale columns with three designs: a base design that represented a national survey of current bridge column specifications, a seismic design that reflected the current seismic detailing practices, and a blast design that consisted of a very dense mesh of transverse reinforcement. Along with these three designs, the five main parameters that were varied during the Phase II tests were scaled standoff, column geometry, amount of transverse reinforcement, type of transverse reinforcement, and splice location. The ten columns were tested with charges placed at small standoffs, and these tests were designed to observe the failure mode (i.e., shear or flexure) for the different column designs.

Each of the columns tested during the Phase II experimental program contained six strain gauges, and the strain data gathered during the tests were used to verify boundary conditions and blast-load distribution for each small standoff test. Three of the ten columns tested during the small standoff tests experienced significant shear deformation at the base, and the other seven columns displayed a combination of shear and flexural cracking. Six of the columns were re-tested using close-in or contact charges, and the objective of these local damage tests was to observe spall and breach patterns of blast-loaded concrete columns. Two of the six columns tested during the local damage tests experienced significant breach, and the other columns experienced spalling of concrete from their side and back faces. Computational and analytical research extended the knowledge gained from the experimental tests. This work included the use of simplified methods for predicting loads and response as well as detailed, nonlinear finite element analyses. The simplified models used widely available analysis procedures, including empirical models for predicting blast loads and single-degree-of-freedom models for computing response.

The experimental and analytical data gathered during this research program provided a basis for developing detailing guidelines and a general design procedure for blast-resistant bridge columns. These guidelines consist of three design categories, each of which contains increasingly demanding design requirements that specify greater amounts of transverse reinforcement as the design threat increases. Design Category A is the least restrictive of the three, requiring no special consideration for design threats associated with blast loads. Design Category B requires seismic detailing with the exceptions that larger than currently specified embedment lengths on the hooks of transverse reinforcement be used and plastic hinge detailing be used over the entire column height to account for uncertainties associated with the location of potential threat scenarios. Design Category C is for cases involving the most severe threats. Columns in this category must have a transverse reinforcement ratio that is 50% greater than that required for current seismic detailing and even larger embedment lengths on the hooks of transverse reinforcement than those used for Design Category B. Design Category C also requires a designer to conduct a single-degree-of-freedom dynamic response analysis to ensure that the ductility ratio and support rotation are less than recommended limits.

Test results indicate that measures other than structural hardening should be taken to help mitigate design threats with very small scaled standoffs corresponding to contact (and near-contact) charges because local damage failures such as breaching will begin to control response for these cases. All of the columns tested during the small standoff tests in this research fell into Design Category C, and the results of those tests, along with analytical work, provided the basis by which the limits used to define each of the design categories were established.

The following general guidelines are recommended for increasing the blast resistance of reinforced concrete bridge columns:

- Column performance improves significantly as standoff increases, and one of the best methods to reduce risk to a bridge is to increase the standoff. As such, the design categories allow a designer to capitalize on the fact that increasing standoff through the use of bollards, security fences, or vehicle barriers is a safe, efficient, and cost-effective alternative to increasing the design category and detailing requirements.
- Experimental and analytical data show that circular columns experience less net load than square columns subjected to the same charge weight and standoff distance. Therefore, bridge columns should employ circular cross sections whenever possible to reduce the applied net load of any threat. It should be noted, however, that square columns can be made blast resistant to an acceptable level with proper detailing and sizing.
- The cross-section size of a reinforced concrete column plays an important role on column performance, as this parameter controls the onset of breaching failure. As such,

increasing cross-section size will generally improve column resistance to blast loads, and a minimum column diameter of 30 in. is recommended for columns subjected to close-in blasts.

- Continuous spiral reinforcement provides better confinement and produces better overall behavior than discrete hoops for small standoffs and close-in threats and is preferable at all times. If design or construction constraints prevent the use of spiral reinforcement, columns should use hoops with an embedment length larger than that typically used for standard (i.e., gravity-controlled) and seismic designs.
- Increasing the transverse reinforcement ratio improves column response to blast loads. Experimental observations show that the blast designs, which employed very dense meshes of transverse reinforcement, performed better than the seismic designs, which in turn performed better than the gravity-load-controlled designs. Accordingly, the minimum amount of transverse reinforcement for a Category C column is now specified to be 50% greater than that which is currently specified for seismic designs, and this transverse reinforcement should extend over the entire height of the column to resist various potential threat scenarios.
- If possible, splicing of longitudinal reinforcement should be avoided, and removing splices from regions where charges may come into contact with a column can help minimize localized blast damage.

Finally, bridge engineers should remember that, while these design and detailing guidelines will increase the blast resistance of a bridge column, it is not possible to design a column to resist all possible threats. Bridge owners should conduct a thorough risk analysis to determine the most probable threats and have their bridges designed accordingly. A certain level of risk must be accepted for the extreme threat scenarios considered as part of this research. Failure should be expected if a sufficiently large quantity of explosive is placed close enough to any bridge column, regardless of the design and detailing.

CHAPTER 1

Introduction

1.1 Overview

The events of September 11, 2001, dramatically illustrated the catastrophic damage that terrorists can inflict on our civil structures. The attacks against the World Trade Center and Pentagon, unfortunately, were not isolated incidences of terrorist actions taken against U.S. assets. Over the last several decades there have been an increasing number of terrorist attacks that have led to tremendous losses. As a result of these events, the engineering community has become more aware of the need to design structures that can better withstand the effects of bomb blasts. For example, lessons learned from the Oklahoma City bombing in 1995 and the embassy attacks in Tanzania and Nairobi in 1998 have begun to shape current design guidelines for the prevention of progressive collapse.

In the area of transportation security, approximately 60% of terrorist attacks against highway infrastructure have consisted primarily of explosive attacks (Jenkins and Gerston, 2001), which highlights the need for blast-resistant structures. Although the chances of terrorist attacks directed against a bridge are typically assumed to be very small, the economic and socio-economic consequences can be extremely high. The majority of the current state of knowledge for the design of structures subjected to blast loads is based on and directed toward the performance of military structures and civilian buildings. There has been very little notable research on the blast-resistant design of highway bridges. Thus, to implement the design of bridges for security, experimental and analytical research are needed to evaluate the effectiveness of current blast-resistant design guidelines for buildings applied to bridges or to develop new design and detailing guidelines.

Since September 11th, several major efforts focused specifically on transportation security have been initiated. Nationally, several high-level groups have been assembled to develop recommendations and formulate both short- and long-term strategies for dealing with terrorist threats to bridges and other transportation assets. Among these efforts, the Blue Ribbon Panel on Bridge and Tunnel Security, organized through a joint effort of the FHWA and AASHTO, has been among the most significant. Following the efforts of the Blue Ribbon Panel, leading researchers at the FHWA developed both near-term and long-range research priorities to address important issues in the area of transportation security. A summary of the recommendations that have come from these and other groups can be found in the literature review presented in Chapter 2 of this report.

One of the first research projects initiated on bridge security following the attacks on September 11th was directed by the Texas Department of Transportation, along with funding from seven state DOTs and the FHWA. The focus of the research was on the development of mitigation strategies to improve the performance of a variety of different bridge types to potential terrorist courses of action. This study investigated cost-effective, unobtrusive design and retrofit options for a variety of bridge components and bridge structural systems based on parametric studies carried out using simplified analytical models (Winget et al., 2004). More recently, through other pooled-funded projects, the Army Corps of Engineers has looked at the performance of steel suspension bridge towers subjected to very severe close-in blasts, and they have also worked on a similar project for concrete towers for suspension and cable-stay bridges. Other research has focused on common bridge components, such as the multi-hazard pier study conducted by researchers at SUNY Buffalo (Fujikura et al., 2008), as well as the tests on prestressed girders coordinated by the Corps of Engineers (Transportation Pooled Fund Program, 2008). While these recent projects have provided tremendous insight into the performance of bridges subjected to explosions, this field is still quite new. Hence there is much that still needs to be learned regarding the design of bridges for security. An in-depth presentation on the current state of practice and relevant research on this topic can be found in Chapter 2 of this report.

1.2 Background and History

In order to develop an appreciation of the extent to which terrorists have targeted U.S. assets, it is helpful to review some previous incidents. The events highlighted below are not intended to be an exhaustive list, but they do illustrate the need for enhanced security.

On February 26, 1993, a bomb was detonated in the parking garage of one of the World Trade Center towers. As a result of this attack, 6 people were killed and 1,042 were injured. Damage was observed over seven floors, and property damage was over one-half billion dollars. According to the ASCE accident investigation (Wikipedia, 2008), the compartmentalized layout of the building structure was credited with minimizing the propagation of damage and preventing progressive collapse.

Two years after the bombing of the World Trade Center, on April 19, 1995, the Alfred P. Murrah building in Oklahoma City was attacked. The death toll from this event was much larger than that from the 1993 event. As a result of a large truck bomb, 169 people were killed, over 500 were injured, and damages exceeded $100 million. From an engineering perspective, there was great concern over the structural configuration of the Murrah building. This nine-story structure incorporated a transfer girder at the third floor that allowed the column spacing from the floors above to be doubled from 20 feet to 40 feet on the bottom three stories. Because the bomb blast likely caused the failure of three of the columns that supported the transfer girder, the high loads from the floors above could not be redistributed to the remaining columns. As a result, the Murrah building failed due to progressive collapse. Because of this event, research into progressive collapse has once again become a great concern to the structural engineering community, and engineering guidelines to resist progressive collapse have been developed by the Department of Defense (2005) and the General Services Administration (2003).

These events that took place on U.S. soil are very familiar to much of the population, yet several other events in recent years have shown that U.S. assets all over the world are susceptible to terrorist attacks. Though it is not necessary to describe all of these events in great detail, it is helpful to discuss the incidents that have implications related to structural engineering. One such event includes the bombing of the Khobar Towers in Saudi Arabia on June 25, 1996. This facility was used to house U.S. and allied forces. There were 19 fatalities and approximately 500 U.S. personnel wounded in the attack. Other events that raised awareness of the need to protect against terrorist activities took place on August 7, 1998. On this date, two U.S. embassy buildings were bombed in Africa. As a result of these attacks, 11 Americans were killed and over 30 were injured. The response of the two embassy buildings differed greatly. The embassy building in Tanzania fared quite well, and damage was limited. The Nairobi embassy building, however, suffered severe damage and underwent a partial collapse in a similar progressive fashion as the Murrah building.

Transportation targets have not been exempt from these types of attacks. In a 1997 report, Brian Jenkins describes over 550 terrorist attacks worldwide against transportation targets between 1975 and 1997. He states:

> We have seen an increase in attacks on public transportation as terrorism has increased over the past quarter century and more recently as terrorists have demonstrated greater willingness to kill indiscriminately. The Irish Republican Army's long-running terrorist campaign in the United Kingdom has included numerous attacks on rail lines, trains, subways, and stations. Palestinian terrorists have carried out numerous attacks on Israeli buses and bus stations. Algerian extremists directed their 1995 terrorist campaign in France against the subway and rail system. The first large-scale terrorist use of chemical weapons was carried out in Tokyo's subways, an ideal environment for chemical attack. Islamic extremists in New York planned to attack the city's bridges and tunnels in 1993 and its subways in 1997. (Jenkins, 1997)

Recent events around the world support Jenkins' position. On March 11, 2004, ten bombs exploded on four trains in three stations during the busy morning rush hour in Madrid, Spain. The bombings killed 191 people and injured hundreds of others. Results of the investigation following the attacks led to the arrest of several militants believed to be affiliated with al-Qaeda. More recently, public transportation in London became the target of terrorist attacks. On July 7, 2005, terrorists carried out a coordinated series of suicide bombings during the morning rush hour. In total, four different bombs exploded on three subway trains and one commuter bus, resulting in 52 deaths and approximately 700 people injured. These bombings were the largest and deadliest attacks on the transportation infrastructure ever to occur in London. Just two weeks later, on July 21, 2005, four attempted bomb attacks again disrupted London's transportation network. This time, however, authorities were able to prevent the attacks from taking place, and all main bombing suspects were arrested within a week of the incident.

In the aftermath of the events following September 11th, the potential threat against highway bridges became more pronounced to federal and state officials. While federal agencies such as FEMA and the Center for Defense Information had warned about highway structures being potential targets of terrorist acts, few state agencies had the resources or the expertise to implement any safety measures. Officials in California learned first-hand that the threat of terrorist action can lead to major disruptions in the transportation network. On

November 1, 2001, Governor Gray Davis held a press conference to announce that California had received intelligence that several of the state's bridges were threatened to be destroyed between November 2 and November 7. In response, security around the threatened bridges was substantially increased by assigning National Guard troops to protect the bridges. While the threats against these bridges were later determined to be non-credible, the disruption to traffic and the expense involved in providing security personnel to protect the bridges was significant.

In June 2003, a man in Ohio suspected of being a member of al-Qaeda was arrested for investigating the use of specialized equipment to sever the cables of one of the bridges in New York. The person arrested (Mohammed Rauf) was a truck driver who admitted he was an al-Qaeda agent who met with Osama bin Laden and high-ranking al-Qaeda leaders at an al-Qaeda terrorist training camp in Afghanistan. Rauf was later convicted of plotting to sabotage the bridge and launch a terrorist attack against the nation's capital, including derailing trains.

During our current conflict with Iraq, a self-proclaimed "anti-American" group threatened to carry out terrorist attacks against diplomatic compounds, airlines, and public transportation systems in eight U.S. allied countries (Fox News, 2004). Furthermore, insurgents in Iraq have routinely targeted bridges, and several significant collapses have occurred (which are detailed in Chapter 2 of this report). Thus, despite the heightened public awareness of potential terrorist acts, and despite the fact that more stringent security measures are in place now than before September 11th, terrorists appear to be as motivated as ever to attack U.S. targets. In fact, even after September 11th, terrorist attacks against American interests as a percentage of the total terrorist attacks worldwide have steadily increased. This conclusion is also supported by data discussed in the AASHTO/FHWA Blue Ribbon Panel Report (Blue Ribbon Panel on Bridge and Tunnel Security, 2003) in which data from the FBI show that terrorism against U.S. assets has been steadily increasing.

These events help illustrate that there is a growing need for engineers to be able to design structures to help minimize the consequences of a terrorist attack. Despite this awareness, the engineering profession does not currently have any consistent guidelines to help limit the effects of an attack. In the October 12, 1998, edition of *Engineering News Record,* Gene Corley, one of the principal investigators of the Oklahoma City bombing, commented that "while the military and federal government have developed methods to improve the blast resistance of their own buildings, they have not transferred these methods to civilian engineers." In fact, even today, more than 13 years after the bombing of the Murrah building, such guidelines are not readily available to the structural engineering community. In the November 7, 2001, issue of *Engineering News Record,* 90% of an estimated 3,000 architects that were involved in a web-based seminar on security issues "expressed frustration at the lack of risk assessment guidelines available to them for advising their clients." In response to these needs, at least for transportation assets, several organizations have begun to develop tools that engineers and planners can use to carry out vulnerability and threat assessments. For example, Science Applications International Corporation's (SAIC) 2002 publication, *A Guide to Highway Vulnerability Assessment for Critical Asset Identification and Protection,* was prepared for the AASHTO Security Task Force and provides a risk assessment procedure that is tailored specifically to the transportation infrastructure. Several other publications have appeared in the research literature offering procedures for carrying out risk assessments of transportation infrastructure, and Chapter 2 of this report includes a review of the relevant studies.

Although improvements have been made in recent years, there is still a great need for the available information on terrorist preparedness to be made accessible to structural engineers. In particular, because bridge engineers have not typically needed to consider structural integrity in response to a terrorist attack, current design guidelines do not consider the issue of bridge security. As a result, there is a need to compile available research literature and provide this information to transportation officials and highway bridge engineers. In fact, in response to the terrorist attacks on September 11th, AASHTO assembled a task force to consider transportation security, and now a subcommittee is focused entirely on this issue. Other professional organizations such as the Transportation Research Board (TRB) and the American Society of Civil Engineers (ASCE) have also established national committees to address the topic of transportation security. The primary charge of the AASHTO task force is to "establish guidance and share practices that help state DOTs prepare vulnerability assessments of their highway infrastructure assets, develop deterrence/surveillance/protection plans, develop emergency response plans and capabilities for handling traffic for major incidents on and off the transportation system, and assess and respond to military mobilization needs in each state."

In response to the September 11th tragedy and the subsequent events that suggested the vulnerability of our transportation infrastructure, research efforts have been initiated to address a large number of pressing needs. Due to the openness and ease of access to transportation assets, the transportation community faces a challenge much greater than that of individual building owners. Current priorities include port security, inspection of hazardous cargo, tunnel security, and bridge security. It is this last topic that is of relevance to the current report and the focus of this document.

1.3 Research Approach

The information included in this report summarizes the work completed for the National Cooperative Highway Research Program's (NCHRP) Project 12-72. The primary objective of this research was to develop design guidance for improving the structural performance and resistance to explosive effects for bridges. In order to meet this objective, it was essential to compile information on the response of structures subjected to blast loads. Limited information specifically focused on bridges was available in the open literature during the time that this research was conducted, but information on the behavior of blast-loaded building components was found to be useful in understanding the response of bridges subjected to blast loads. In addition, a thorough assessment of design principles and available technologies that are useful in protecting bridges from other extreme loading conditions such as earthquakes and vehicle crashes was made to determine their potential for application in improving bridge response to blast effects. This information has been compiled in the background and literature review appearing in Chapter 2 of this report.

Because of the great variety of bridges in the national inventory, it was necessary to develop a research program that addressed high priority needs in the design of bridges to resist explosions. While there are many types of bridges and structural systems in use, it was important to focus the research on areas that would yield critical information of national importance. In the second half of Chapter 2, the focus of the research project is explained, and details of the experimental and analytical testing programs are given in Chapters 3 and 4, respectively.

In Chapter 5, research findings are presented. This chapter provides information on the results of a two-phase experimental testing program and the corresponding analytical research program. Using the results of the experimental and analytical research, blast-resistant design guidelines are given in Chapter 6. The information is assembled using the AASHTO Load and Resistance Factor Design (LRFD) format so that the procedures can be presented in a format that is familiar to bridge engineers. Following these design guidelines, Chapter 7 includes recommendations for analyzing bridges subjected to blast loads. In this chapter, both simplified and detailed modeling approaches are covered.

To illustrate the application of the proposed analysis and design guidelines, detailed examples are provided in Chapter 8. In Chapter 9, the main findings are summarized, and recommendations for future research are given.

CHAPTER 2

Research Background

2.1 Overview

The purpose of conducting the research described in this report is to increase the security of the U.S. transportation infrastructure by providing the maximum possible contribution to the design and analysis of blast-resistant bridges given the available resources. Although the issues associated with various threats and the blast-resistant design of different bridge components will require many years of study, this work makes an important first step in the security of highway bridges by focusing on the areas of greatest need. The final work plan carefully considers information found in the literature, extensive past experience with blast testing and explosive effects on structures, and practical considerations concerning the importance of certain design issues and individual bridge components. This chapter describes the state of knowledge prior to the start of the current work and outlines the basis for the selected research plan.

2.2 Literature Review

While the field of blast-resistant bridges is relatively new, information regarding the design of blast-resistant buildings does exist in the literature, and a few recent and current studies do focus on bridges subjected to blast loads. Because sound research typically advances the state of knowledge by building on the foundation of the past, the literature review conducted for this project provides comprehensive coverage of basic blast-resistant design principles found in the literature and recent research related to both blast-resistant buildings and bridges, including an overview of seismic design and detailing provisions as they may apply to blast-loaded bridges. The review includes information regarding the analysis, design, and retrofit of structures to resist blast loads, along with information on the topics of bridge security, risk management, and vulnerability assessment. This chapter provides a brief summary of the most relevant information on a variety of topics relative to such a threat. As with any structural design, proper determination of the load and the resulting response is essential. To that end, the following section focuses primarily on airblast phenomenology and blast-wave propagation as they interact with structures, followed by current blast-resistant design guidelines and practices. Emphasis is given to reinforced concrete structures to be consistent with the focus of the test program.

2.2.1 Blast Loads and Shock Phenomena

Three principal effects of an explosion are important for structural design: the total impulse, the peak pressure, and fragments (velocity, distribution, and mass). While the first two aspects of blast loading can usually be computed if the explosive type, explosive weight, explosive shape, and standoff distance are known, the load imparted to a structure by fragments is often difficult to quantify because fragments are typically irregular in nature (Conrath et al., 1999). For terrorist threat scenarios involving vehicle-delivered bombs, however, fragment loads are negligible for structural design, though they still pose a human injury risk, because typical casings for terrorist weapons (i.e., car or truck parts, sheet metal, and plastic) are not massive (especially relative to cased military weapons) (Conrath et al., 1999). Because the focus of this research is on protecting bridge components subjected to blast effects associated with terrorist events, this review focuses primarily on airblast loading from uncased charges with no fragments.

The detonation of a high explosive is a high-rate chemical reaction producing a localized sudden release of energy that dissipates violently through a shock wave, which is a region of highly compressed air that radiates spherically away from an explosive source. This region of compressed air creates an overpressure and a dynamic pressure as it passes by a given point in space. Idealized curves for overpressure and dynamic pressure are shown in Figure 1. The overpressure is the pressure resulting from the explosion in excess of the ambient pressure, and

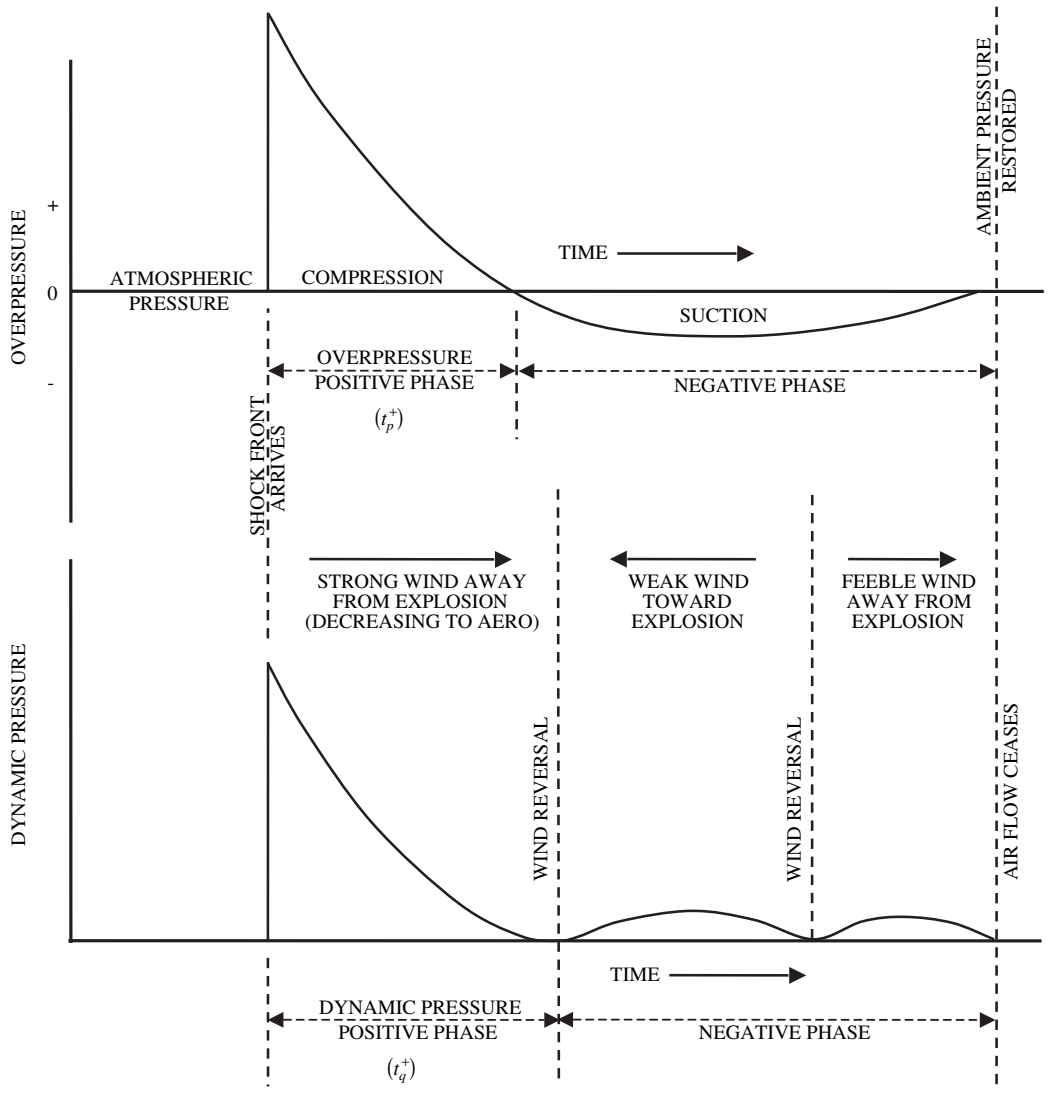

Figure 1. Overpressure and dynamic pressure variation with time (Glasstone and Dolan, 1997).

the dynamic pressure is the pressure of the resulting air flow. At the arrival of the shock front, the overpressure rises nearly instantaneously to its peak before decreasing to zero, at which time a small negative overpressure (i.e., suction) occurs. The dynamic pressure increases nearly instantaneously with the arrival of the shock front and consists of a strong wind away from the explosion, then a weak wind toward the explosion, and then a very weak or feeble wind away from the explosion. Unlike the overpressure, which is a measure of air pressure relative to the atmospheric pressure, the dynamic pressure always remains positive. There are two reasons for this phenomenon. The first is that the dynamic pressure is determined using the square of the wind velocity, making it positive regardless of the direction of the wind. The second is that the dynamic pressure is a measure of kinetic energy (i.e., "energy of motion"), which is a pressure without reference to another pressure.

The *incident wave* is the term used to describe the shock wave that radiates spherically from an explosion. This incident wave will reflect off any surface in its path, and the term *reflected wave* is used to describe the wave that reflects off a surface. The reflected wave travels at a higher velocity than the incident wave because it travels through air that has already been heated and compressed. As a result, waves reflecting off rigid surfaces (e.g., the ground) can potentially catch up to and merge with the incident wave to create a single wave front called a Mach front (Figure 2). At any point prior to the joining of the incident and reflected waves, two independent pressure peaks will occur, each of which is smaller than that of the single Mach front pressure amplitude. The point at which the incident and reflected waves merge is known as the triple point. An example of the two independent pressure peaks prior to the formation of the Mach front is shown in Figure 3. Figure 3a shows a

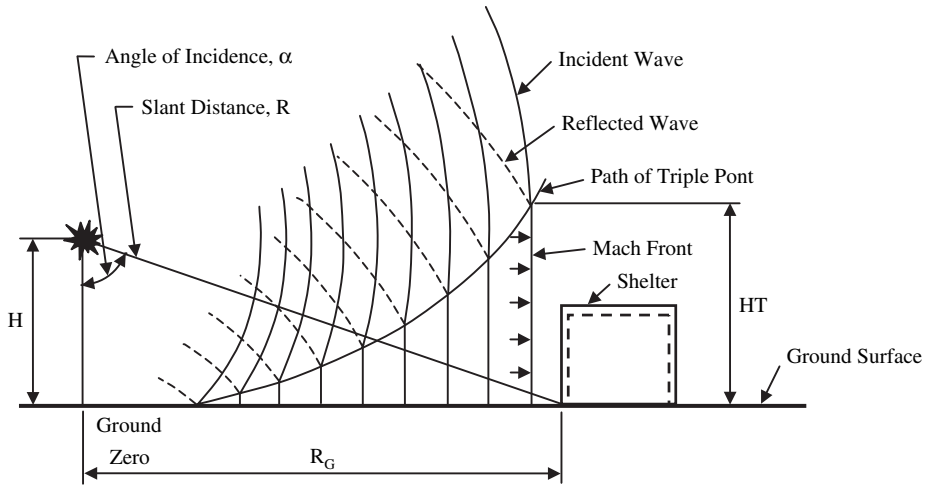

Figure 2. Unconfined air burst showing formation of Mach front (Department of the Army, 1990).

pressure–time history of a shock wave after the reflected wave and incident wave merge, forming a single incident wave, and Figure 3b shows a pressure–time history before the two waves merge, in which the separate incident and reflected waves are visible. The degree to which a wave reflects depends on the terrain over which the blast wave travels. Hilly land masses can increase blast effects in some areas but decrease them in others.

All pressure–time histories, except those very close to the detonation, have the same general assumed form shown in Figure 4, while the exact values that define the curve vary depending on the size of the explosive charge and the location of interest. For example, the peak pressure, P_{so}, decreases significantly with standoff distance, while the positive phase duration, t_o, increases with standoff. By definition, the impulse is equal to the area under the pressure–time history curve.

Different charge weights and standoff distances scale to create similar shock waves. "Self-similar blast waves are produced at identical scaled distances when two explosive charges of the same explosive material with similar geometry but of different weights are detonated in the same atmosphere" (Conrath et al., 1999). Scaling equations relate the parameters needed to define the curve in Figure 4, and the most common scaling relationship is the Hopkinson-Cranz or "Cube-Root" scaling law (Conrath et al., 1999), which is shown in Equation 1.

$$Z = \frac{R}{W_{TNT}^{1/3}} \tag{1}$$

where:

Z = scaled standoff (ft/lb$^{1/3}$)
R = standoff, distance between center of blast source and target (ft)
W_{TNT} = charge weight of explosive (lb equivalent TNT)

The charge weight, W_{TNT}, is in terms of a TNT-equivalent charge weight. TNT equivalencies relate the energy output

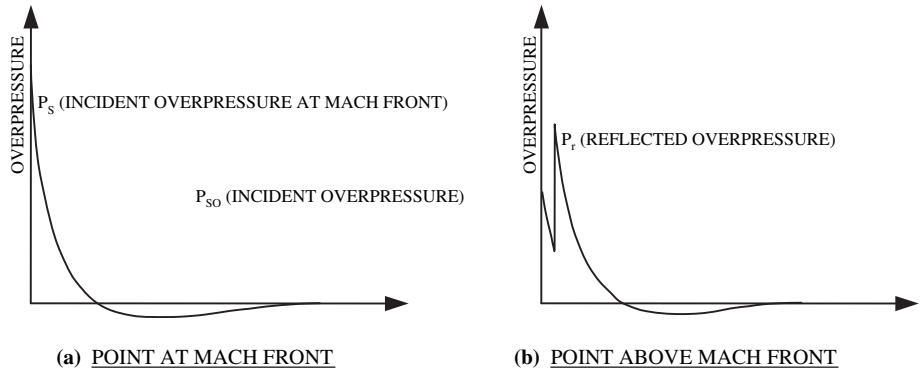

Figure 3. Two graphs showing difference in overpressure before and after formation of Mach front (Department of the Army, 1990).

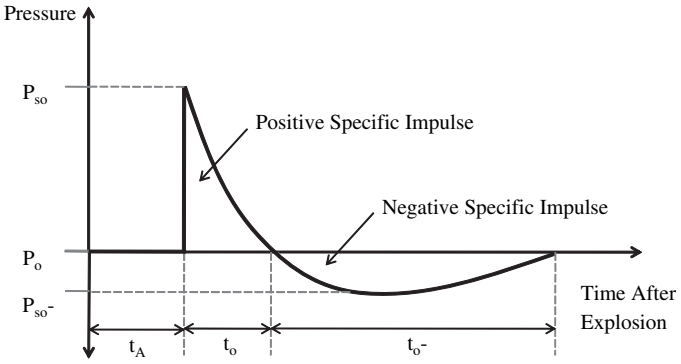

Figure 4. Idealized pressure–time curve for free-air explosion (Department of the Army, 1990).

of common explosives to that of TNT. In reality, a high explosive's TNT equivalency varies as a function of standoff, explosive geometry, target orientation, and atmospheric conditions. For the purposes of design, however, a given explosive's TNT equivalency is treated as a constant, which is the standard to which much of the available data have been reported. The Hopkinson-Cranz scaling law presented above has been verified experimentally using TNT equivalencies for scaled distances greater than 0.4 ft/lb$^{1/3}$ and may not be valid below this value.

The Hopkinson-Cranz scaling law enables the prediction of blast-load parameters for full-scale explosions using data from smaller-scale tests, and an engineer can create an idealized pressure–time curve for a free-air explosion, shown in Figure 4, with the TNT equivalent charge weight and standoff distance. A hemispherical burst on a perfect reflecting surface will double the effective charge weight, while a reflection factor of 1.8 is more realistic when significant ground cratering is present (Conrath et al., 1999). Commonly used "standard" airblast curves, often referred to as "spaghetti charts," exist to predict the parameters required to define an idealized blast wave; Figure 5 shows one of these charts. A vast collection of empirical data and theoretical predictions provides the basis for these charts, and curves exist for both hemispherical and spherical "free-field" bursts.

The transmission of a shock front through a fluid (i.e., air) is a nonlinear process, and the interaction of a blast wave with a structure is a complex problem leading to significantly magnified pressures and impulses. Figure 6 illustrates a blast wave reflecting off a structure. The magnification of the reflected pressure and impulse will vary depending on the magnitude of the peak incident overpressure and the orientation and location of the structure relative to the explosion source. Military design manuals (Department of the Army, 1986; Department of the Army, 1990) contain empirically derived

Notes:

P_{so}	=	Peak positive incident pressure (psi)
P_r	=	Peak positive normal reflected pressure (psi)
$i_s/W^{1/3}$	=	Scaled unit positive incident impulse (psi-ms/lb$^{1/3}$)
$i_r/W^{1/3}$	=	Scaled unit positive normal reflected impulse (psi-ms/lb$^{1/3}$)
$t_A/W^{1/3}$	=	Scaled time of arrival of blast wave (ms/lb$^{1/3}$)
$t_o/W^{1/3}$	=	Scaled positive duration of positive phase (ms/lb$^{1/3}$)
U	=	Shock front velocity (ft/ms)
W	=	Charge weight
$L_w/w^{1/3}$	=	Scaled wavelength of positive phase (ft/lb$^{1/3}$)

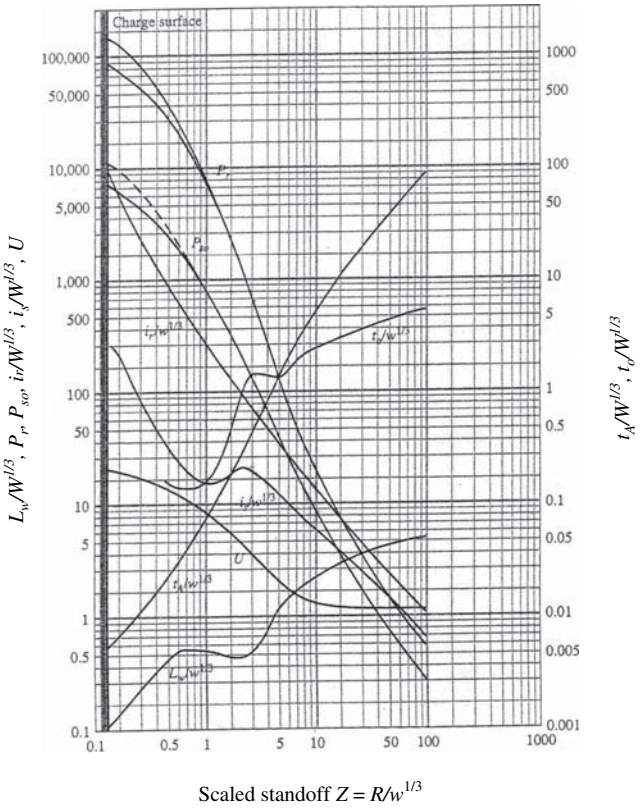

Figure 5. Positive phase airblast parameters for hemispherical surface TNT detonation at sea level (Department of the Army, 1990).

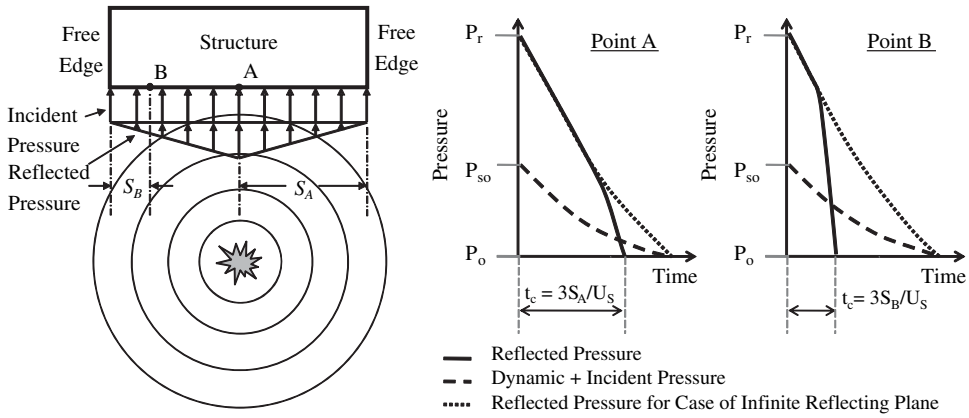

Figure 6. Blast wave reflecting off structure (U.S. Army Engineer Research and Development Center, 2003).

curves that provide the magnified values of the reflected pressure and reflected impulse as functions of the peak incident overpressure, the angle of incidence (i.e., the angle between a shock wave's direction of travel and a structure's surface normal vector), and charge weight.

Clearing effects on the front surface of a structure decrease the reflected pressure near free edges. When clearing occurs, the reflected pressure seeks relief toward the lower pressure regions at the free edges, forming a rarefaction (or relief) wave that propagates from the low-pressure region at the free edges to the high-pressure region at the middle of the surface. Therefore, the pressure differential between the free edge and front face causes the pressure at point B in Figure 6 to dissipate faster than at point A. According to TM 5-855-1 (Department of the Army, 1986), the clearing time at a given point on a reflective surface is the time required for the reflected pressure to dissipate from that point, and that time is given by Equation 2 (which is also known as the three-transits-to-edge-rule).

$$t_c = \frac{3S_x}{U_s} \tag{2}$$

where:

t_c = clearing time(s)
S_x = distance from nearest free edge to point of interest (ft)
U_s = shock front velocity (ft/s)

The type of blast load a structure must resist depends on the design threat and the type of structure. When a charge is detonated extremely close to a structure, it imposes a highly impulsive, high-intensity pressure load in a localized region of the structure. When a charge is detonated farther away, it produces a lower-intensity, longer-duration uniform pressure distribution over the entire structure. As the standoff increases, the pressure distribution over the surface becomes more uniform (Department of the Army, 1990). Because the shape and intensity of the loading can vary depending on the charge weight and standoff distance, three blast-loading categories exist: contact, close-in, and plane-wave. Figure 7 illustrates these categories (Department of the Army, 1990). A contact blast load consists of a high-intensity, non-uniform load where breaching is a typical response. Breach is defined as the complete loss of concrete through the depth of a cross-section. A close-in blast load is the result of a spherical shock wave striking a structure to produce a non-uniform load and

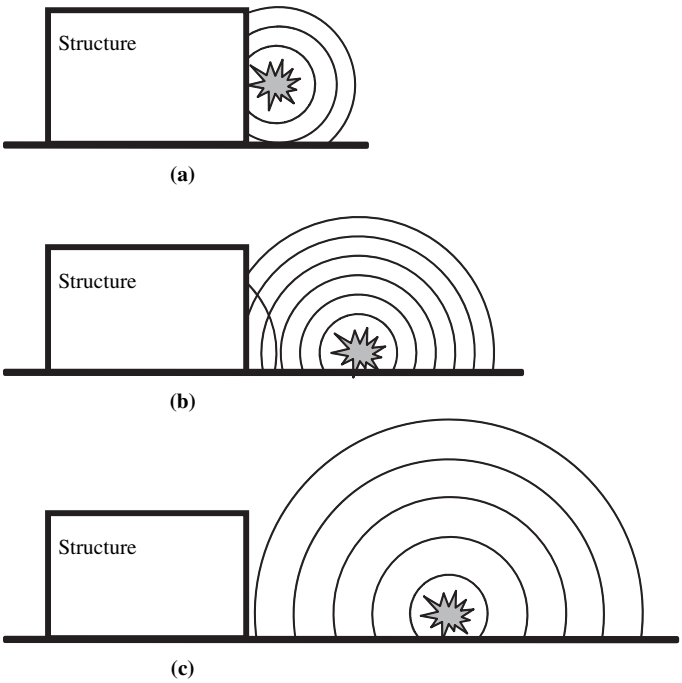

Figure 7. Blast-loading categories: a) contact, b) close-in, c) plane-wave (Departments of the Army, Air Force, and Navy and the Defense Special Weapons Agency, 2002).

an impulse-dominated response. A plane-wave blast load is a far-field explosion that produces essentially planar waves and a uniform load on each surface when it reaches a structure.

Additional load categories include unconfined free air burst (no immediate wave amplification), unconfined air burst (amplification from ground reflections), unconfined surface burst (amplification from ground reflections), confined fully vented explosion (one or more surfaces open to atmosphere), partially confined explosion (limited openings), and fully confined explosions. Most bridge loads will be either an unconfined air burst, unconfined surface burst, or a confined fully vented explosion (e.g., under the deck between girders).

2.2.2 Structural Response to Blast Loads

While the response of bridges to terrorist explosive threats is a relatively new topic for the structural engineering community, several observations from past incidents involving the performance of buildings during terrorist attacks and the response of bridges to cased military weapons can be made regarding the general expected response of blast-loaded bridges. Explosions located beneath a bridge deck will cause large uplift forces, and pressure buildup between girders and near the abutments can greatly amplify the applied load, as shown in Figure 8. Detonations directly between girders or at the abutments can generate extremely severe loads on the girders and deck, and underwater explosions can result in large water plumes that cause damage to structural components of bridges crossing waterways.

When designing for any explosion beneath the deck, it is best to sacrifice the deck and focus on saving the girders and columns. Longer girders typically are more resilient than shorter girders because of their greater mass, strength, and flexibility. Two cost-effective ways to strengthen bridges for blast loads are to provide continuous reinforcement in the tops of concrete girders for uplift resistance and to provide stiffeners for steel girders to prevent local buckling. In addition, using hinge restrainers or extended column seats can possibly prevent girders from falling off of the piers in the event of large deformations resulting from blast loads.

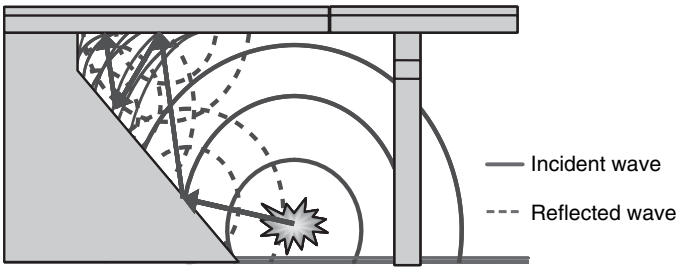

Figure 8. Blast-wave propagation during below-deck explosion (Winget et al., 2005).

Columns that are rigidly connected to the superstructure can experience tensile forces due to the uplift of girders during below-deck explosions. During above-deck explosions, columns can experience increased axial loads due to blast forces in addition to gravity loads. Although recent attacks in Iraq may suggest otherwise (ABC News, 2007), prior observations from military operations indicate that most substructures are generally large enough to withstand anticipated above-deck explosions (Winget, 2003).

Columns will experience significant shear forces from close-in charges for below-deck scenarios, and proper design requires enough transverse reinforcement to prevent shear failure and force a flexural failure. "When an explosion occurs below the deck of a bridge, bents and piers will be subjected to large lateral forces, possibly resulting in large deformations, shear, or flexural failures. Additionally, concrete cratering and spalling from the blast-wave impact may lead to significant losses of concrete, especially if the standoff distance is small" (Winget et al., 2004). Columns should be designed for lateral blast loads and resulting deflections in addition to the axial loads present due to gravity. Most bridge columns have much greater axial capacity than axial demand, however, and they experience service axial loads that are below their balance point. Therefore, ignoring the axial load is usually a conservative assumption for typical bridge columns subjected to lateral blast loads because the inclusion of axial loads will typically increase both shear and flexural resistance and improve performance. An exception to this guideline would be for cases in which the axial load is in excess of the balance point load and/or P-Δ (i.e., second-order) effects are significant, as they can be in tall, slender columns.

Very close-in or contact blasts create high-intensity blast pressures that often cause breaching (i.e., section loss) of a column, spalling of concrete cover from high-intensity blast pressures, back-face scabbing of concrete cover due to large deflections, and post-failure fragments. While blasts directly aimed at bridge structural members may be the first choice for a terrorist attack, military records indicate that large explosions near the columns create ground craters that can cause foundation instability, column failure, and bridge collapse. As a result, these military records state that it may be easier to "shake down the columns" than to "shoot up the superstructure" (Bulson, 1997).

2.2.3 Dynamic Material Strength and Strain-Rate Effects

The materials used in reinforced concrete construction have response characteristics that depend on the rate of loading. Most of the data supporting this topic are experimental; therefore, the physical cause is not completely understood.

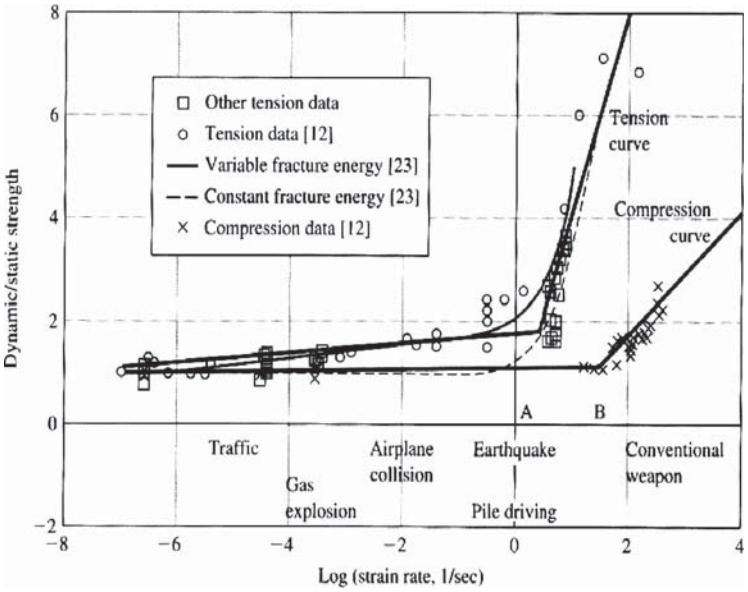

Figure 9. Concrete strain-rate effects on strength (Tedesco, 1999).

The widely held belief is that crack propagation occurs at a limiting velocity and cannot crack fast enough to keep up with a high rate of loading, and thus concrete exhibits a strain-rate threshold where concrete strength increases significantly above that value (Tedesco, 1999). Figure 9 shows the relationship between strain rate and concrete strength for tension and compression. The strain-rate threshold for concrete response in tension is approximately 1 to 10 per second, and the strain-rate threshold for compression is approximately 50 to 80 per second. Above these threshold values, concrete demonstrates significantly higher strengths than under static loading conditions. The elastic modulus is not as strain-rate sensitive as strength, and as a result, the strain rate can easily be converted to a stress rate (Tedesco, 1999).

High rates of loading also affect the mechanical properties of ductile metals, as they also cannot deform fast enough to keep up with extreme loads. Therefore, ductile metals, like steel, have a limiting deformation velocity that results in material strength increases with increasing strain rates. This limiting velocity occurs at a much higher strain rate than concrete, and various relationships between strain rate and strength for unspecified metals are shown in Figure 10 (Tedesco, 1999). The yield strength and ultimate tensile strength increase substantially, while the modulus and the elongation at rupture largely do not change (Tedesco, 1999).

Techniques exist to calculate the strength increase for both concrete and steel at a given strain rate. Dynamic increase factors (DIFs), which are defined as the ratio of dynamic material strength to static material strength, are used to account for the high strain rates present in blast events. Table 1 lists DIFs for reinforced concrete design, which are dependent on the type of stress (i.e., flexure or shear). These dynamic increase factors are used to increase material strengths over those that are measured under standard static testing protocols to account for the actual strength expected to be present under various blast scenarios. These values have been derived empirically from blast-test experiments (Department of the Army,

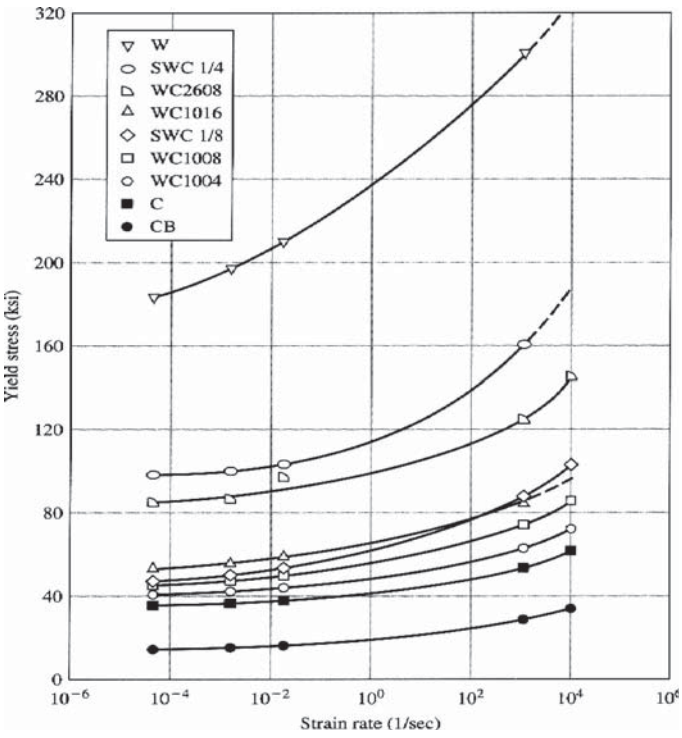

Figure 10. Effects of strain rate on yield stress for various metals (Tedesco, 1999).

Table 1. Dynamic increase factors.

Stress Type	Far Design Range*			Close-in Design Range†		
	Reinforcing Bars		Concrete	Reinforcing Bars		Concrete
	f_{dy}/f_y	f_{du}/f_u	f'_{dc}/f'_c	f_{dy}/f_y	f_{du}/f_u	f'_{dc}/f'_c
Flexure	1.17	1.05	1.19	1.23	1.05	1.25
Diagonal Tension	1.00	1.00	1.00	1.10	1.00	1.00
Direct Shear	1.10	1.00	1.10	1.10	1.00	1.10
Bond	1.17	1.05	1.00	1.23	1.05	1.00
Compression	1.10	1.00	1.12	1.13	1.00	1.16

*Far Design Range: $Z \geq 2.5$ ft/lb$^{1/3}$

†Close-in Design Range: $Z < 1.0$ ft/lb$^{1/3}$

Source: *Department of the Army, 1990*

1990). For design, DIFs are typically assumed to be constant, even though they vary with strain rate.

Strength and age increase factors are used to determine realistic material properties under dynamic loads if the actual material strengths are unknown. Strength increase factors (SIFs) are used to account for actual material (concrete and steel) strengths in excess of the specified design values, as shown in Table 2. In addition, age increase factors are used with concrete to account for strength gains beyond 28 days. From empirical data collected by the Department of the Army (1986), an age increase factor of 1.1 is specified for concrete less than six months old, and a value of 1.15 is specified otherwise.

2.2.4 Application of Seismic Design to Blast-Loaded Bridges

Seismic loads are similar to blast loads in that both produce dynamic structural response and often lead to large deformations with inelastic material response. The subsections below compare blast and seismic loads and response characteristics to determine relevant design concepts. A summary of current seismic design practice and research to investigate whether or not seismic design principles can provide adequate structural resistance for blast-loaded structures is also provided.

Table 2. Strength increase factors.

Material	SIF
Structural ($f_y \leq 50$ ksi)	1.10
Reinforcing Steel ($f_y \leq 60$ ksi)	1.10
Cold-Formed Steel	1.21
Concrete*	1.00

* The results of compression tests are usually well above the specified concrete strengths and may be used in lieu of the above factor. Some conservatism may be warranted because concrete strengths have more influence on shear design than bending capacity. TM 5-1300 specifies a SIF of 1.10.

Source: *American Society of Civil Engineers, 1997*

2.2.4.1 Comparison of Blast and Seismic Designs

Seismic and blast loads are both time dependent, and both induce a dynamic structural response that generally results in inelastic behavior. While the allowable damage to both structural and nonstructural components depends on the structure's purpose for both blast and seismic loads, life safety is usually more important than the prevention of structural damage for most designs. Designs for both seismic and blast loads allow large inelastic deformations to help dissipate energy, and improving strength, ductility, redundancy, and connection capacity in any structure can improve the performance under both seismic and blast loads.

Blast and seismic loads, however, have fundamental differences that prohibit the direct application of all seismic detailing and design requirements to blast-loaded structures. Blast loads have a higher amplitude and shorter duration than seismic events. Blast-load duration is measured in milliseconds, approximately one thousand times shorter than that of an earthquake (Conrath et al., 1999). Due to the uncertainty associated with selecting an appropriate design threat, the magnitude of a blast load is more difficult to predict than seismic loads and is independent of geographical location, unlike earthquakes, as shown in Figure 11. A blast load radiates in all directions from the source, creating a complex pressure–time history that varies according to the location of a structure, while lateral load effects will dominate a structure experiencing a seismic event. Also, an earthquake is a widespread event, while blast effects typically remain local. Therefore, seismic design and detailing should not be assumed to provide adequate protection for blast-loaded structures. According to the National Research Council report *ISC Security Design Criteria for New Federal Office Buildings and Major Renovations* (2003), "Although design for seismic resistance and design for blast resistance share some common principles, the two types of design must not be mistakenly viewed as redundant." The report also states, "Attempts to link seismic and blast design requirements by simply comparing the lateral or shear forces on a structure produced by these events (an equivalent seis-

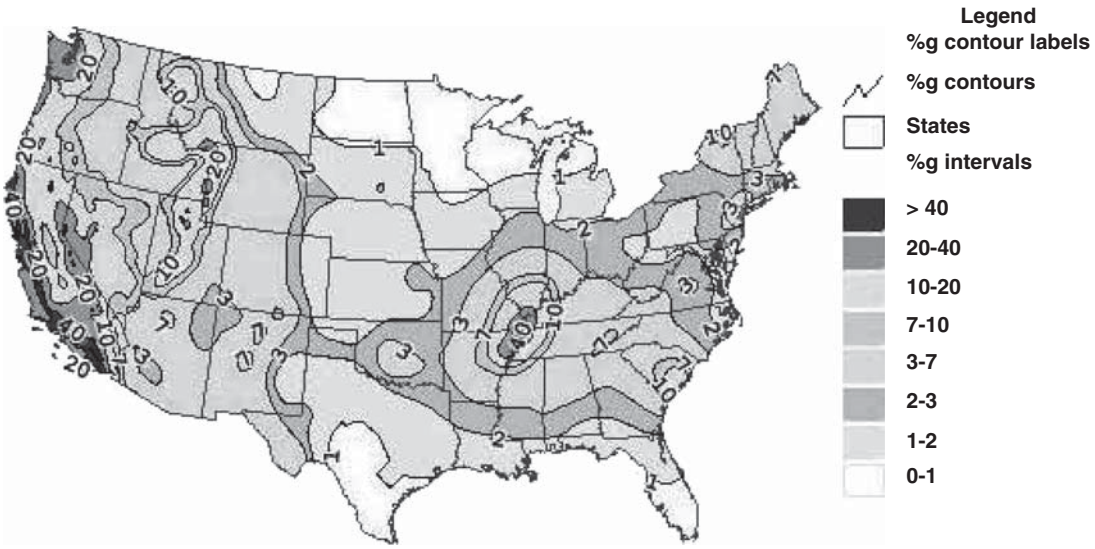

Figure 11. Seismic hazard map: peak ground acceleration (USGS, 2008).

mic base shear) perpetuate the erroneous impression that seismic design is an umbrella for blast resistance."

2.2.4.2 Seismic Design Guidelines

The *AASHTO LRFD Bridge Design Specifications* (AASHTO, 2007) specify seismic design and detailing provisions for bridges. The *Caltrans Seismic Design Criteria* (Caltrans, 2003) and *Bridge Design Specifications* (Caltrans, 2006) are additional resources for design and detailing requirements. The essential requirement for a reinforced concrete column subjected to a strong ground motion is that it retain a substantial portion of its strength as it experiences severe loading reversals into the nonlinear range of response (Pujol et al., 2000). Current seismic design procedures specify a "performance-based" or "limit-state" design. In general, structural performance criteria are available for not only the traditional life-safety level but also for more restrictive design levels, such as serviceability and damage control. Quantitatively, "serviceability" implies that a structure will not need repair after an earthquake, while "damage control" implies that only repairable damage occurs (Kowalsky, 2000). In general, "it is uneconomical to design structures to withstand lateral forces corresponding to full elastic response to design-level earthquakes. The alternative, and widely accepted approach, is to design for a lower force level and detail structure for ductility" to ensure that it can sustain the inelastic displacements associated with seismic loads without significant strength degradation (Priestley and Park, 1987).

Recognizing the difficulty in determining the actual maximum shear that a critical column may experience during an earthquake, AASHTO LRFD recommends a plastic hinge analysis for seismic design. A plastic hinge analysis considers all potential plastic hinge locations to determine the maximum possible shear demand. A typical seismic column with fixed supports and a displacement at one end due to a laterally applied force will form two plastic hinges, as shown in Figure 12. This concept, which ensures that a member will have sufficient shear capacity to allow a ductile flexural failure mechanism to form, is one that applies equally well to structures subjected to blast loads. Therefore, a plastic hinge analysis using a blast-load distribution is an ideal method to determine the maximum shear demand in blast-resistant design.

2.2.4.3 Seismic Detailing Guidelines

The ACI Building Code (2005) and AASHTO LRFD Specifications (2007) provide extensive detailing guidelines for seismically loaded concrete members in buildings and bridges. According to Sezen and Moehle (2006), "surveys of reinforced concrete building collapses in past earthquakes identify column failures as the primary cause. Such failures are commonly attributed to widely spaced and poorly anchored transverse reinforcement." Therefore, the amount and anchorage of transverse reinforcement in seismically loaded columns requires further research to determine their applicability to blast-resistant design.

"Earthquakes and laboratory experience show that columns with inadequate transverse reinforcement are vulnerable to damage including shear and axial load failure" (Sezen and Moehle, 2006). Sezen tested four full-scale reinforced concrete columns with light transverse reinforcement to collapse under a simulated seismic loading. Figure 13 shows the crack pattern of one of the specimens, which illustrates the formation of plastic hinges at the top and bottom of the column as load increased. After the flexural strength was reached, deterioration of the cross-section due to a lack of sufficient transverse re-

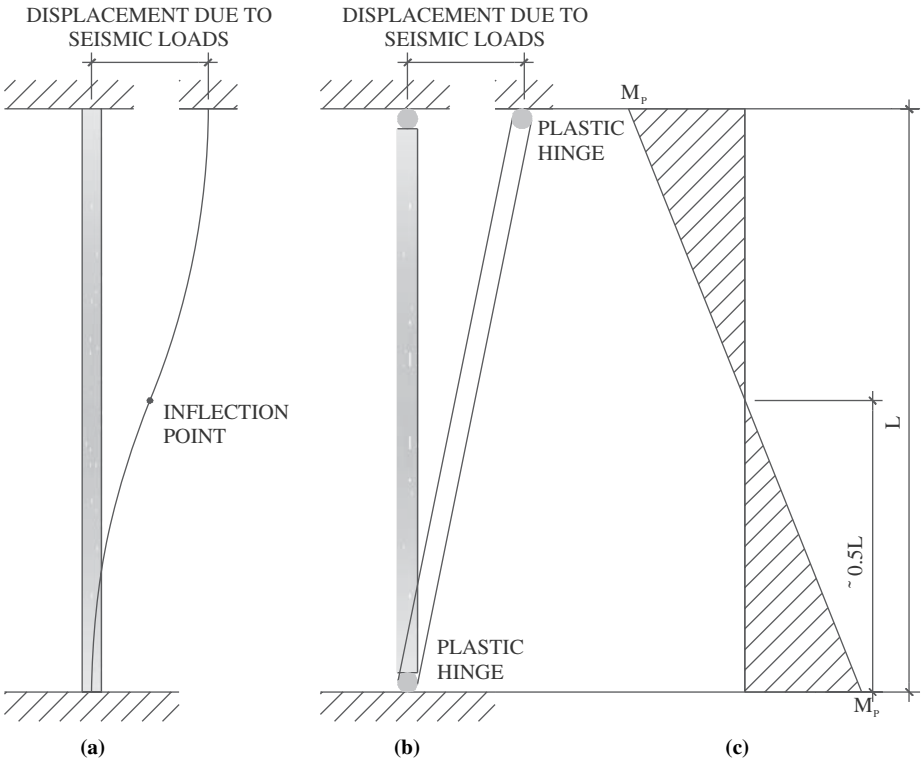

Figure 12. Plastic hinge analysis for seismic column: a) deflected shape, b) plastic hinge locations, c) plastic moment.

inforcement triggered a shear failure, as shown in Figure 14. Equations 3, 4, and 5, from the AASHTO LRFD Specifications (2007) seismic provisions, specify a minimum volumetric reinforcement ratio and minimum area of transverse reinforcement to help provide adequate core confinement for circular and rectangular columns, respectively.

$$\rho_s \geq 0.12 \frac{f'_c}{f_y} \tag{3}$$

$$A_{sh} \geq 0.12 s h_c \frac{f'_c}{f_y} \tag{4}$$

$$A_{sh} \geq 0.30 s h_c \frac{f'_c}{f_y}\left(\frac{A_g}{A_c} - 1\right) \tag{5}$$

where:

f'_c = specified compressive strength of concrete at 28 days (psi)
f_y = yield strength of reinforcing bars (psi)
s = vertical spacing of hoops, not exceeding 4 in. (in.)
h_c = core dimension of column in the direction under consideration (in.)
A_g = gross cross-sectional area (in.^{2})
A_c = area of concrete core (in.^{2})

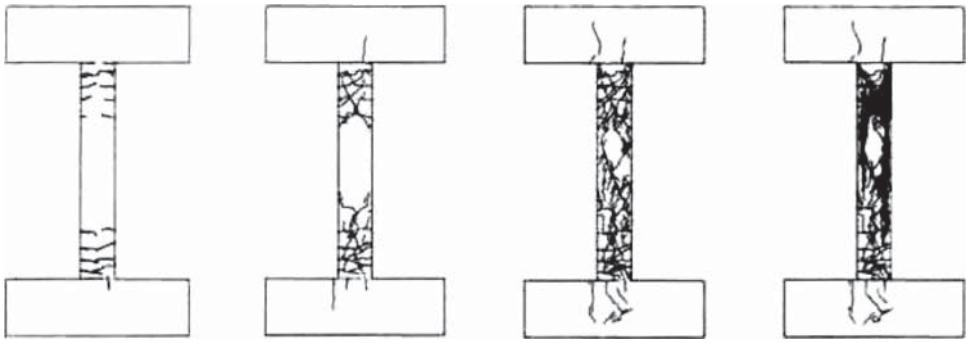

Figure 13. Crack pattern for specimen 1 (Sezen and Moehle, 2006).

(a) (b)

Figure 14. Damage after failure: a) specimen 1, b) specimen 3 (Sezen and Moehle, 2006).

The seismic provisions require more transverse reinforcement than a typical gravity-loaded column "to ensure that the axial load carried by the column after spalling of the concrete cover will at least equal the load carried before spalling and to ensure that buckling of the longitudinal reinforcement is prevented" (AASHTO, 2007). Thus, the spacing of transverse reinforcement is important for shear resistance and core confinement in the plastic hinge regions of a seismically loaded column. Likewise, blast-loaded columns may require increased transverse reinforcement to ensure ductile behavior.

Recent work by Bae and Bayrak (2008) on the seismic performance of full-scale, reinforced concrete columns is the first to demonstrate the opening of seismic discrete ties using hooks with a 135°-bend, plus an extension of 8.0 d_b, as shown in Figure 15. AASHTO LRFD Section 5.10.2.2 defines seismic hooks as a "135°-bend, plus an extension of not less than the larger of 6.0 d_b or 3 in." According to the researchers, "unlike the full-scale concrete columns, the hooked anchorages often reach close to the center of the core concrete in scaled column specimens." The remaining specimens in the research study used a minimum hook length of 15.0 d_b to prevent the opening of hoops. The larger "hook length proved to be very effective, and opening of the 135° hooked anchorages of the ties was not observed in the other tests." To avoid anchorage pullouts and to improve the performance of seismically loaded (and blast-loaded) columns with discrete hoops or ties, longer hook lengths than currently specified should be used.

2.2.5 Design Issues

The structural engineering community has gained much ground in the field of blast-resistant structural design. Despite this progress, however, the bridge engineering community still lacks design guidelines specific to blast-resistant highway bridges. The probability for a specific type of attack against a specific bridge is usually very low; however, "a low probabil-

Figure 15. Opening of discrete ties (Bae and Bayrak, 2008).

ity of occurrence does not justify minimizing our efforts to manage the potential adverse effects of a catastrophic event" (Williamson and Winget, 2005). Several papers have been written regarding the risk management, analysis, and design of critical bridges subjected to blast loads. The findings from these papers have been summarized in this section and can provide guidance for those officials considering the blast-resistant design of highway bridges.

An important aspect of designing bridges for security in an economically feasible way is to have in place plans for evaluating the criticality of any one structure on the transportation network. Thus, in deciding how to allocate resources, bridges considered more essential to the transportation infrastructure, or those thought to be at higher risk for a terrorist attack, should be given priority in the implementation of protective measures over other, less critical bridges. The references contained in this section of the review describe methods of carrying out threat and vulnerability analyses and risk assessments. Once the risks to a given bridge have been assessed, measures may need to be taken to mitigate these risks if they are deemed unacceptable. These measures generally attempt to deter an attack by increasing surveillance or limiting access, but they can also include actions to limit the effects of blast loads or procedures to aid in rescue and recovery. Usually, deterrence and prevention measures will provide the least expensive solution to mitigate risk initially. Therefore, a risk manager should consider implementing these measures for short-term risks before hardening a structure is specified. Deterrence and prevention, however, may not always provide the most cost-effective solution for long-term risks when considering lifetime costs, such as maintenance, replacement, personnel, and surveillance costs.

2.2.5.1 Risk Assessment

Designing or retrofitting all bridges to resist extreme loads is cost prohibitive, and engineers need a method to identify credible threats, prioritize assets, and manage risk. Although blast-resistant bridge design is a relatively new topic in the field of structural engineering, many state agencies and research organizations already have strategies for risk assessment and management. While each approach differs slightly in implementation, all sources provide the same general guidance. This section outlines a risk assessment strategy based on a compilation of relevant sources, and the following section provides a risk management method based on a comprehensive literature review.

Publications by Abramson et al. (1999), Rummel et al. (2002), and SAIC (2002) provide valuable information regarding risk assessment and management. A report by Williamson and Winget (2005) outlines a comprehensive approach to risk assessment, and the method they propose is a compilation of the best practices found in the literature. Step one of the risk assessment process is to identify all critical assets within a jurisdiction and determine the criticality of these assets based on function, average daily traffic, access to populated areas, access to emergency and medical facilities, military importance (Strategic Highway Network), importance to commerce, international border access, symbolic importance, availability of detours, presence of utility lines, and estimated repair time. The risk assessor should weight each criterion separately to reflect its importance within the jurisdiction, while not double counting for related criteria (e.g., average daily traffic may relate to major trade routes or availability of detours). This criticality score represents the importance of a bridge and indirectly captures the consequences of a potential attack (i.e., the consequences of an attack on a very important bridge likely will be great), and it is important to note that it should not include vulnerabilities to an attack or specific structural weaknesses because a later step considers these issues. Additionally, certain criteria may warrant a bridge's placement in a higher importance category despite its overall criticality score. Examples include signature bridges whose failure may cause great socio-economic harm and bridges with significant military importance that have no detour capable of carrying the required traffic.

Step two consists of identifying all possible internal and external threats to the critical bridges identified in step one. Internal and external threats can be a variety of actions such as the threat of earthquakes, high winds, or fire; however, the proposed risk assessment process only considers terrorist actions. Examples of potential attacks include, but are not limited to, a vehicle-delivered bomb on a superstructure, a vehicle- or maritime vessel-delivered impact and bomb against a column, hand-placed explosives between girders or inside box girders, or a series of timed events incorporating some or all of the above. As previously mentioned, designing a bridge to resist all possible threats is not feasible, and the risk manager should identify the most likely threat scenarios. Although terrorist activity is uncertain, a threat-point-of-view analysis can provide insight on the most likely terrorist threats. This analysis considers factors such as the terrorists' potential objectives, available resources, availability of targets, and the impact of a successful attack. Once all possible terrorist actions have been determined assuming that a terrorist has no limitations, each action should receive a score that indicates the relative probability of that action occurring compared to other actions. A multiplication decision matrix is best for this process, and the risk manager should conservatively assume that terrorists are experts in demolition, have structural engineering experience, and will encounter no resistance.

In step three, the risk manager formulates the potential scenarios by pairing critical assets identified in step one with potential threats identified in step two. Once scenarios are

formulated, the process includes determining the probability of each event and assessing the vulnerability of assets with each scenario. Step four consists of assessing the consequences of each attack scenario, and the risk manager should assume the worst-case consequences of an attack not considering potential mitigation measures. Potential consequences include, but are not limited to, loss of life, severe injuries, loss of bridge function due to structural damage, and financial losses. Once each scenario (i.e., combination of threat and asset) is identified, a risk manager should categorize each scenario according to the probability of successful occurrence and the severity of impact. The probability of occurrence is subjective and comes from the threat-point-of-view analysis, and the criticality score is the basis for the severity of impact. All information is then combined in tabular format to determine which scenarios have the greatest risk and therefore require the most attention. An example of this table can be seen in Figure 16. Each scenario can be placed in one of the boxes based on severity of impact and probability of successful occurrence. Those bridges that fall in the severe and high range will receive the most attention.

2.2.5.2 Risk Management

Once the risks are assessed, measures must be taken through a risk-management process to mitigate the risks to a level that is appropriate and economically feasible. The first step of risk management is to identify potential countermeasures available to mitigate the risks previously identified. Such countermeasures as deterrence, detection, or defense can reduce the probability of occurrence, while others can lessen the severity of the consequences through methods such as structural hardening, warning devices that indicate failure, or emergency operations planning. Additional considerations for selecting countermeasures include resource availability, implementation difficulty, level of inconvenience, adverse environmental effects, adverse effects on serviceability, or usefulness.

The second step of the risk-management phase is to determine the costs for each countermeasure considered. Cost considerations should include initial purchase, installation, maintenance, replacement, and service life. Step three consists of a cost–benefit analysis to determine which countermeasures would be the most effective and efficient. Williamson and Winget (2005) recommend that the benefits be in terms of risk mitigation achieved and that a countermeasure summary sheet be used. An example of a countermeasure summary sheet can be seen in Figure 17. Because some countermeasures may also reduce other risks [e.g., fiber reinforced polymer (FRP) wrapping can reduce the risk of failure due to both seismic and blast events], the countermeasure benefits should be considered during the design process for all risks associated with the bridge under consideration in order to get a complete picture. The goal of step three is to ensure the maximum pro-

Threat Scenario Categories		Severity of Impact			
		Catastrophic (Criticality > 75)	Very Serious (Criticality 51 - 75)	Moderately Serious (Criticality 26 - 50)	Not Serious (Criticality < 25)
Probability of Successful Occurrence	Highly Probable	Severe	Severe	High	Moderate
	Moderately Probable	Severe	High	Moderate	Low
	Slightly Probable	High	Moderate	Low	Low
	Improbable	Moderate	Low	Low	Low

Figure 16. Threat scenario categories (Williamson and Winget, 2005).

Countermeasure	Function/Effectiveness				Costs Per Year		
	Deterrence	Detect	Defend	Reduce Impact	Capital	Operating	Maintenance
Countermeasure 1	M	L	L		$	$	$
Countermeasure 2	M	H			$	$	$
Countermeasure 3				H	$	$	$
Countermeasure 4	L		H		$	$	$
L = Low Effectiveness M = Medium Effectiveness H = High Effectiveness	Source: Modified from SAIC *A Guide to Highway Vulnerability Assessment for Critical Asset Identification and Protection.*						

Figure 17. Countermeasure summary sheet (Williamson and Winget, 2005).

tection for all assets or the asset under consideration given the available resources. Prioritizing bridge importance may assist in allocating scarce resources among bridges. Step four consists of implementing the countermeasures and reassessing the risk with the countermeasures in place. If the countermeasures do not reduce the risk to an acceptable level, the scenario may require additional countermeasures, or senior managers will need to accept the risk to an asset until additional resources are available. It is important to note that no level of mitigation will completely eliminate all risk, and officials will need to determine the amount of risk they are willing to accept. The fifth and final step of risk management is monitoring the effectiveness of the countermeasure(s) for future decisions and using this information to guide future risk-management decisions.

2.2.5.3 Characterization of Analysis Methods for Blast-Loaded Structures

Blast prediction techniques are often separated into load determination and response determination methods, and both of these categories can be further divided into two groups: first-principle and semi-empirical methods (National Research Council, 1995). First-principle methods solve systems of equations based on the basic laws of physics. Accurate predictions of blast load and response can be obtained with these methods if the equations are solved correctly. Although first-principle programs use fundamental laws of physics and constitutive laws of materials, they have several limitations that are difficult to overcome without the use of empirical models. Blast propagation in real scenarios can be complicated by such things as atmospheric conditions, boundary effects, explosive material inhomogeneities and rates of reaction, as well as many other parameters, and first-principle methods cannot easily account for these factors (National Research Council, 1995). Additionally, the calculation of changes in blast pressure due to large structural deformations and localized failures can be quite problematic because accurate constitutive equations for materials responding in this range are not readily available. Moreover, because of the highly nonlinear nature of structural response to blast loads, an analyst using first-principle methods to compute behavior should validate any predictions with actual experimental results to ensure that the methods are being implemented correctly. It can be very difficult, however, to find validated first-principle models due to a lack of experimental data available in the public domain, and any validation applies only to the specific scenarios that were experimentally considered (National Research Council, 1995). Despite these limitations, response predictions based on first-principle results can be developed when a lack of applicable data exist, but interpretation of the results requires engineering judgment and experience.

Semi-empirical models, in contrast to first-principle models, utilize extensive data from past experiments. As a result, they require less computational effort and are generally preferable over first-principle programs. However, because a lack of experimental results for responses to blast loads exists in the public domain and because semi-empirical programs are only slowly becoming available to the general engineering community, structural engineers must often rely on first-principle methods and good engineering judgment to determine blast effects (National Research Council, 1995). In addition, semi-empirical models are often valid only for

the structural members and scenarios considered during the formulation of the model.

Weighing the relative advantages and disadvantages of each modeling approach, semi-empirical approaches are always preferable because the models include validated empirical data. In fact, because of their efficiency over first-principle models for such cases, semi-empirical models are much better for design. For those cases in which the scenario in question relies on extrapolation of test data, or for cases where data are not available, first-principle models should be used by themselves, preferably after validation against experimental data or semi-empirical models for known cases, to predict blast loading and response. While the suggestions presented throughout this document address both first-principle and semi-empirical analysis methods, semi-empirical methods should be used whenever possible.

Some methods utilize both first-principle and semi-empirical procedures (Winget, 2003). Equations first calculate blast-wave propagation and structural response, and the results are then compared to, and corrected by, empirical data from similar scenarios. These methods have wider ranging applicability than semi-empirical methods, and they require less computational effort and provide more accuracy than first-principle methods. Therefore, methods that utilize both first-principle relationships and semi-empirical data are very practical for design use. Although empirical data do not widely exist in the public domain, a few of these programs are available. The origin, accuracy, and applicability of the data used in these methods, however, may be difficult to verify. Given that possibility, the guidelines presented in this document emphasize pure first-principle structural analysis methods over combined procedures, but an analyst should understand that *legitimate* techniques based on, or corrected by, legitimate empirical data are preferable over pure first-principle methods at all times.

Most blast-analysis programs separate the calculation of blast-wave propagation effects from the determination of structural response. Thus, loads resulting from the chosen blast source are first calculated, and then they are applied to the structure using a separate response analysis method. Such separated methods are considered "uncoupled," and they typically provide conservative predictions of loads acting on structural components. Because the analysis typically assumes the structure is rigid during load calculations, structural deflections and localized member failures, which can vent and redistribute pressure, are neglected, and the analysis typically overestimates blast pressures and forces in unfailing members. Accordingly, use of uncoupled methods often provides conservative load values for designing structural members.

Coupled analysis methods, unlike uncoupled analyses, consider blast-wave propagation and structural response together as they interact over time. Thus, a structure can vent pressure through localized failure, and the forces resulting in many members will be smaller and more realistic than those predicted by uncoupled analysis approaches. For scenarios in which local failure or large deformations result, coupled analysis techniques may be necessary. Although coupled programs are expected to provide more accurate results than uncoupled ones, they do so at considerable costs due to the number of input parameters required, the time and experience needed to create a model and interpret the output, and the computational resources and time required to compute results. Because uncoupled analysis methods usually provide conservative blast propagation and structural response predictions, most design cases do not require the increased costs associated with coupled analysis methods.

Uncoupled and coupled analytical programs belong in two further subdivided groups based on the characteristics of the analytical methods employed. Uncoupled analysis methods have two categories: static analyses and dynamic analyses. Within each of those categories are single-degree-of-freedom (SDOF) models and multiple-degree-of-freedom (MDOF) models. Figure 18 and the following sections describe these divisions. It is important to note that the level of accuracy, computational time and cost, and complexity of analysis increase when moving from left to right in the figure. The next section describes further details, applications, and limitations of these methods.

2.2.5.3.1 Uncoupled Static Analyses. A static analysis for a blast scenario consists of an "equivalent wind design" (ASCE, 1997; Bounds, 1998), which is similar to the equivalent static procedure used for seismic design. Such an analysis can compute response for both single- and multiple-degree-of-freedom systems. The approximated blast pressure under consideration is a static force applied to the structure being analyzed, and the analysis does not account for inertial effects. Because this method is very general, no program specifically exists for equivalent static blast analyses; however, those programs currently used for ordinary structural analysis can be used for this purpose. Although this method is relatively simple, its main weakness is accuracy. Unlike seismic events, vehicle impact incidents, or vessel impact scenarios, blast-loading characteristics cannot be easily defined based on historical data. The loads acting on a structure for a given blast event can vary greatly depending on the type of explosive, the location of explosive, the surrounding reflecting geometry, and the geometric and material properties of the structure being investigated. Accordingly, a static blast design requires the introduction of many approximations. In addition, no general equation exists to determine a conservative static load (Bounds, 1998), which makes determining an appropriate load for design difficult (ASCE, 1997). Thus, accuracy is limited (ASCE, 1997; Bounds, 1998), and bridge

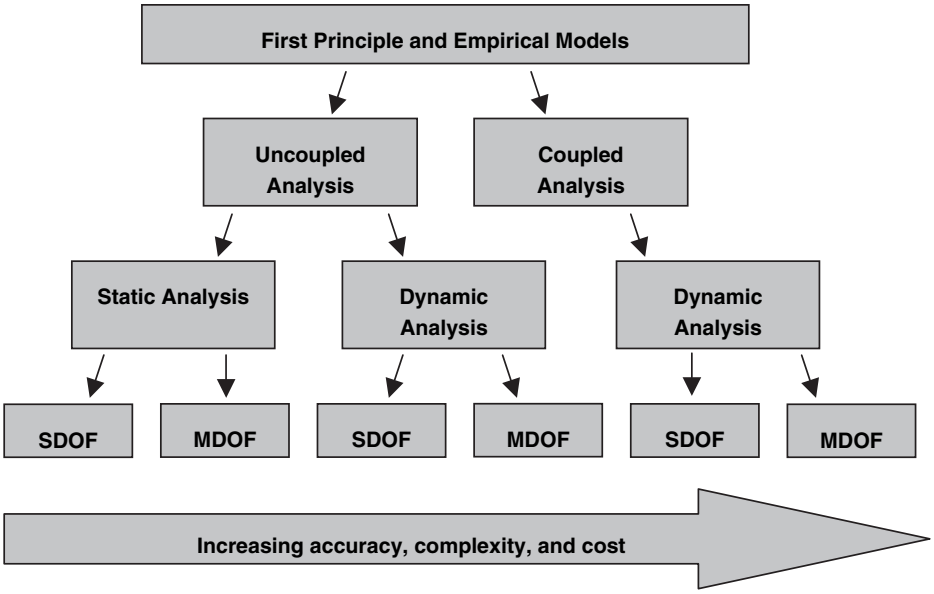

Figure 18. Flowchart of possible analysis methods (Winget, 2003).

designers should not use an equivalent static design for any purpose.

2.2.5.3.2 Uncoupled Dynamic Analyses. Dynamic uncoupled analyses vary from simple SDOF systems to more complex MDOF systems. SDOF dynamic analysis methods are relatively simple, and design engineers commonly use them to determine individual member response. The mathematical procedure required to derive the properties of the equivalent SDOF system is similar to that of a modal analysis used for seismic-resistant design. A separate load determination method can calculate the time-varying blast loading under consideration, and the SDOF analysis assumes a deflected shape for the response of the member being analyzed, often using a static loading response shape that approximates the dynamic response shape (Biggs, 1964; Department of the Army 1990). This deflected shape is then integrated along the length of the member with the actual mass and force to determine an equivalent mass and force for the dynamic system, and a simple spring-mass-damper system is then assumed and analyzed. The resistance used for the spring corresponds to the pattern of deformation for the member being analyzed. With this approach, the analysis of the SDOF model includes inelastic material behavior by noting the formation of plastic deformation mechanisms that correspond to the assumed displaced shape. For example, in a fixed–fixed beam under uniform loading, the bending moment acting at the supports will reach the plastic moment or section capacity as the magnitude of the load is increased. The analysis can include the plastic hinges that occur at the ends of a member by modifying the assumed deflected shape to account for the presence of the hinges, as shown in Figure 19. Such analyses can be solved in closed-form, but they often employ numerical solutions to allow for a wide range of loading histories and nonlinear material behavior.

Uncoupled dynamic analyses of MDOF systems can range from simple, dynamic 2-D frame analyses to very sophisticated 3-D finite element analyses. Models of the structural systems under consideration are constructed in commonly used analysis software, and the time-varying load for the analysis comes from a separate load determination method. Because a category containing uncoupled dynamic MDOF analyses can represent a wide range of methods with varying capabilities, this document considers MDOF frame analyses and detailed finite element analyses separately.

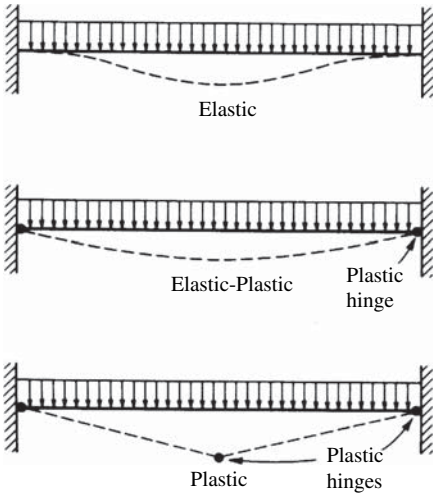

Figure 19. Stages of beam response (Biggs, 1964).

2.2.5.3.3 Coupled Dynamic Analyses. Coupled analyses are intrinsically dynamic because they "couple" blast pressures with response to consider how the loading and structure interact over time. Sophisticated software currently available can model such complex fluid–solid interaction. When modeling MDOF systems, these programs allow the engineer to investigate global changes in response due to failure or large deformations of individual components. Although these methods can provide significant increases in accuracy over uncoupled analyses, they require a considerable amount of time to input the many variables needed to define such complex systems and perform the analyses. Furthermore, these analyses require a very experienced engineer to interpret the results. In addition, many codes claim to be coupled, but only a limited number of codes truly have the capability to couple blast pressures with structural response. For the vast majority of design scenarios involving blast loads acting on bridges, this level of accuracy is usually not necessary due to uncertainties that exist with blast loadings, and simpler analytical methods can often provide conservative and reasonably accurate results at a fraction of the cost (Winget, 2003).

Although conducting coupled SDOF analyses may be technically possible, doing so would not be practical because the results would not be very useful. If a model of a structural system and blast scenario requires a coupled analysis to account for expected load changes due to events such as venting from localized failures or large deformations, more than one degree of freedom would be necessary to investigate the change in response of one component due to the behavior of another component. Therefore, for all practical purposes, coupled analyses are useful only for MDOF models.

2.3 Research Needs

Only a limited amount of information regarding blast-resistant design of bridges is available in the open literature. While it is likely that the military has extensive classified research on the topic, nearly all publicly available references on the blast response of structures focus on buildings. Bridge engineers can access design guidelines for military and petrochemical building structures when considering blast-resistant bridges, although the applicability of the principles developed for buildings to bridges is uncertain. Thus, there is a need to develop an understanding of the principles of blast-wave propagation, the potential effects of blast loads on bridges, and the resulting response and potential failure mechanisms of bridge members. The research presented in this report focuses primarily on columns because they are integral parts of most bridges. Loss of a single column could result in the collapse of multiple spans or the loss of multiple bridges in the case of multi-level interstate exchanges. In addition, bridge columns are especially vulnerable because military records show that it can be easier to destroy a bridge by shaking down the columns with large, nearby explosions than shooting up the superstructure (Bulson, 1997). While past research and currently available guidelines may not directly apply to the case of bridges, they do provide a valuable foundation for advancing the field of blast-resistant bridge design. Therefore, the following sections describe the information currently available in the literature.

2.3.1 Research Needs and Focus of Current Study

Several publications on weapons effects and structural response to blasts are available, and information included in these references provides useful information for the design of bridge components to resist blast loads. One such military document is TM 5-1300, *Structures to Resist the Effects of Accidental Explosions* (Department of the Army, 1990), which is the technical manual for design against accidental explosions. According to the introduction, "The purpose of TM 5-1300 is to present methods of design for protective construction used in facilities for development, testing, production, storage, maintenance, modification, inspection, demilitarization, and disposal of explosive materials" (Department of the Army, 1990). The manual establishes blast-resistant design procedures and construction techniques to provide protection for personnel and valuable equipment. For the purposes of the current study, TM 5-1300 provides allowable design response limits for structural elements in terms of support rotations. The manual also requires the uniform distribution of shear reinforcement throughout a member, and it provides dynamic increase factors and strength increase factors for different materials. This manual recommends Grade 60 reinforcement and a minimum of 4,000 psi concrete to provide sufficient reinforcement ductility and concrete strength for structures that need blast resistance, and it does not permit high-strength concrete unless laboratory testing can demonstrate that it has sufficient toughness.

Fundamentals of Protective Design for Conventional Weapons provides engineers with useful information regarding the design of hardened structures. Conventional weapons can range from an airblast alone to direct hits from precision-guided cased bombs, and a hardened structure's primary task is full functionality after a wartime attack. As it relates to the current study, this manual provides response limit criteria based on support rotations. UFC 3-340-01 (Departments of the Army, Air Force, Navy, and the Defense Special Weapons Agency, 2002) supersedes TM 5-855-1 and carries the title *Design and Analysis of Hardened Structures to Conventional Weapon Effects.* Both of these manuals are available only to federal contractors and are not approved for general public release.

Structural Design for Physical Security: State of Practice (Conrath et al., 1999) is a commonly used non-governmental blast-resistant design guideline for buildings. The purpose of this reference is to "provide methods, guidance, and references for structural engineers challenged with a physical security problem" for a civilian facility. This book introduces general concepts of structural response and behavior under the effects of severe short-duration dynamic loads and a design philosophy that can be adopted to enhance safety. This design philosophy is "simpler is better," recommending the use of simple geometries with minimal ornamentation, which can become airborne during explosions. Ductility and redundancy are two important considerations when trying to provide designs that localize and isolate failures. Specific information that may be relevant for the current research is the specified ductility limits based on typical structural members' observed level of damage under blast loads for a given deformation, as shown in Table 3. In flexure, the formation of a plastic hinge requires that the hinge size be approximately equal to a member's depth. Detailing plays an important role in achieving these levels of ductility, and the book recommends design approaches that improve the bending and shear strength of columns under blast loads. For reinforced concrete, this philosophy includes using adequate confining steel to ensure ductile behavior and sufficient development of reinforcement.

Design of Blast Resistant Buildings in Petrochemical Facilities (ASCE, 1997) contains civilian blast-resistant design guidelines primarily intended for petrochemical facilities. The book focuses on the structural aspects of designing buildings for blast resistance, and it details equations for several parameters needed to define the blast wave shown in Figure 4. Additionally, the text also recommends modifications to the current concrete and steel design codes (ACI, 2005 and AISC, 2006, respectively) to increase structural blast resistance. Designs for structures needing full functionality after a blast event should provide for elastic response under the predicted loads. In most cases, however, inelastic structural response is allowed and provides a means to dissipate the energy of a blast. This document also provides a design approach based on evaluating the ductility and hinge rotations of each member. Much of the information in this book is relevant to the current research.

2.3.2 Blast-Resistant Design: Buildings versus Bridges

The design approach and guidelines presented in the previous section are primarily for the blast-resistant design of buildings. There are several main differences between the designs of buildings and bridges to resist blast loads. Figure 20 illustrates a typical building and a highway overpass in Austin, Texas. Buildings, such as the UT Performing Arts Center, are able to create a large standoff to structural members through landscaping and site layout. In contrast, a highway overpass is a bridge that crosses over another road or railway, and these structures commonly have extensive access below the deck and near columns via parking areas, traffic lanes, sidewalks, or other general unobstructed areas. Therefore, gaining access to structural members is much easier for bridges than buildings, creating the possibility of a design threat with a significantly smaller standoff distance. Also, structural members in buildings, such as columns and beams, are usually behind a façade and are only indirectly loaded by a blast wave, while bridge supports, such as columns, are directly exposed to blast waves. Additionally, blast loads on flat walls and their resulting response have been experimentally verified and are well understood. However, very little is known about shock-wave interaction with slender structural members. Therefore, additional research should determine if current design guidelines for buildings are directly applicable to bridges.

Table 3. Typical failure criteria for structural elements (Conrath et al., 1999).

Element Type‡	Type of Failure	Criteria*†	Damage Level (%)		
			Light	Moderate	Severe
Beams	Global Bending/ Membrane Response	δ/L	4	8	15
	Shear	γ_v	1	2	3
Slabs	Bending/Membrane	δ/L	4	8	15
	Shear	γ_v	1	2	3
Columns	Compression	Shortening/Height	1	2	4
Load-Bearing Walls	Compression	Shortening/Height	1	2	4
Shear Walls	Shear	γ_v	1	2	3

*δ/L = Ratio of Centerline Deflection to Span

†γ_v = Average Shear Strain Across Section

‡ For Reinforced Concrete with $\rho > 0.5\%$ per face

Source: *Conrath, 1999*

(a) (b)

Figure 20. Differences between blast-resistant building and bridge design: a) UT Performing Arts Center, b) I-35 bridge near Town Lake.

2.3.3 Current and Past Research on Highway Bridges

Although the field of bridges subjected to blast loads is relatively new, some past and current research focuses on the development of design guidelines and analytical models for various bridge components subjected to these types of loads. While this effort within the open structural engineering community is in its infancy, these studies provide a good foundation on which to base the work presented in this report. This section summarizes the findings from these studies to illustrate the progress made in the field of blast-resistant bridge design.

Researchers at Florida State University analyzed the response of typical AASHTO girder bridges using STAAD.Pro, a commonly used finite element program. The researchers applied the peak pressures computed from the defined threat to the bridge as a static load. The model bridge failed under the applied loads above and below the bridge deck. The authors specifically claim that the AASHTO girders, pier caps, and columns were not resistant to typical blast loads (Islam, 2005). While these results may be quite alarming, they are extremely conservative and unrepresentative of the expected behavior of a bridge to dynamic blast loads. The study utilized a static analysis, and analysis of a structure subjected to blast loads should always be conducted dynamically. Peak pressures produced by a shock wave are often very high, but they dissipate within milliseconds. As a result, the impulse governs the response of most structures for a typical blast load. Additionally, this study did not use material increase factors in the analysis, which is not representative of real blast scenarios.

Researchers at the University of California at Berkeley studied the response of single-cell and multi-cell steel and composite bridge columns loaded with "simulated effects of car bomb explosions" using finite element analyses (Rutner et al., 2005). While the conclusions included general observations about response mechanisms of these columns based on analytical results, they did not provide any design guidelines. Researchers at the New York State Department of Transportation and City College of New York plan to develop high-precision analytical models and design guidelines for blast effects on highway bridge components based on existing seismic guidelines (Agrawal, 2007). This study is currently ongoing, and limited information is available in the literature.

Winget et al. (2004) carried out parameter studies with SDOF analyses to "evaluate the effectiveness of structural retrofits, refine the performance-based standards, and develop general blast-resistant guidelines specifically for bridges." The researchers analyzed a reinforced concrete bridge with three-column bents, changing the pier diameter, pier shape, and concrete strength. The study considered two terrorist threat scenarios: a vehicle bomb below the deck and hand-placed charges in contact with the pier. "It was expected that the vehicle bomb possesses the potential to produce large lateral blast pressures, resulting in localized breaching damage of the concrete and causing a flexural failure of the pier" (Winget et al., 2004). The contact charge was thought to "possess the potential to breach enough of the pier to render it incapable of supporting the dead loads" (Winget et al., 2004).

The researchers used BlastX version 4.2.3.0 (SAIC, 2001) to generate loads for all cases considered, and ConWep V. 2.0.6.0 (U.S. Army Corps of Engineers, 2001) provided predictions

for the reduced area of the piers due to breaching from local blast damage. Winget et al. (2004) state that "the pressure distribution varied significantly along the height of the pier at any given time. This phenomenon was due to the reflected pressures off the ground and the reflected pressure buildup between the girders under the deck." Calculations for loads on the curved column surface included a reduction of the reflected pressure based on the changing angle of incidence. Additionally, recent parameter studies conducted by Winget et al. (2005) assumed blast loads to be directed laterally for column design, and that work provided a preliminary approach for estimating blast loads on slender square and circular members; however, the design loads for these scenarios are still unclear, and additional work is needed to develop a method to predict accurate blast loads on bridge columns.

Winget et al. (2004) utilized SPAn32 (U.S. Army Corps of Engineers, 2002) to calculate the flexural response of the piers subjected to the vehicle blast loads. A plastic analysis yielded the ultimate resistance, which was adjusted during the response predictions using dynamic increase factors to modify material strengths based on the instantaneously calculated strain rate. The analyses modeled the pier as an SDOF flexural member fixed at both ends and considered the effects of nonlinearity due to material behavior. Winget et al. (2004) reported that, for simplicity, "when determining the flexural response of the piers due to the blast pressure and reduced cross-sectional area from local damage, it was conservatively assumed that the cross-sectional area along the entire height of the pier was reduced to its minimum predicted diameter at the location of maximum breaching." Winget et al. (2004) then predicted damage levels using deformation-based empirical data derived primarily from building members for concrete beam elements in flexure. For the piers, the maximum support rotation corresponded to 1.3 degrees for slight to moderate damage and 2 degrees for moderate to heavy damage. The analysis assumed that the pier lost structural integrity at 3 degrees of rotation. Significant for the current study, Winget et al. (2004) also noted that the support rotation values used in this study may require adjustment based on future experimental data specifically for bridge piers.

Research completed by Bruneau et al. (2006) at the University of Buffalo aimed to develop "a multi-hazard bridge pier concept capable of providing adequate protection against collapse under both seismic and blast loading." Quarter-scale concrete-filled circular steel columns (CFCSC) linked by a fiber-reinforced concrete cap beam and foundation beam were subjected to blast loads. The assumed threat was a small vehicle bomb below the deck at a close standoff distance. "The CFCSC exhibited a ductile behavior under blast loads and no significant damage was suffered by the fiber reinforced concrete cap-beam" (Bruneau et al., 2006). Observations included permanent deformations halfway up the height of the column and shear at the column base, including fracture of the steel tube halfway around the perimeter from the front, as illustrated in Figure 21.

Current experimental research on blast-resistant bridges includes an FHWA and state pool-funded project consisting of analytical studies and large-scale experimental blast tests on steel bridge towers subjected to blast loads (Ray, 2006). The University of Washington is also performing experimental blast tests on two full-scale prestressed girders and two full-scale girder and deck structures. These studies are cur-

(a) (b)

Figure 21. Concrete-filled steel tube subjected to blast loads: a) ductile response, b) shear response (Bruneau et al., 2007).

rently under way, and limited or no information is available in the literature.

2.3.4 Summary

This literature review provides an overview of the principles of shock propagation in free-field and reflected conditions, the computation of blast loads, general observations of blast effects on structures, and basic analytical procedures for predicting the response of structures to dynamic loads. Although this review does not provide a comprehensive discussion of every available source related to explosive effects on bridges, it does provide the basic design knowledge a bridge engineer needs to predict blast loads and the resulting response of structures, and it outlines the background for the current research. The information discussed above, along with more in-depth coverage, can be found in numerous additional sources in the open literature that exists on the topics of munitions and blast effects on structures.

2.4 Focus of Current Work

Recent increases in the frequency and intensity of terrorist attacks on transportation infrastructure highlight the need for blast-resistant design guidelines for bridges. Most currently available blast-resistant design and detailing requirements focus only on buildings, and additional research should determine if these methods and requirements, as well as seismic guidelines, are applicable to blast-resistant bridge design. "Signature" bridges (suspension bridges, cable-stay bridges, tied arches, etc.) sometimes receive priority over other bridge types for blast-resistant research and design for two reasons. First, many in the bridge engineering community believe that an attack against a signature bridge is more likely than an attack against a regular highway bridge, and second, an attack against a high-profile bridge target seems to carry a greater perceived socio-economic impact than an attack on a regular highway bridge. However, past experience does not necessarily support either of these beliefs as historical data show that terrorists desire to attack ordinary bridges even in industrialized nations that have high-profile signature bridges, and recent bridge collapses in the U.S. have shown that the failure of a typical highway structure can have a devastating socio-economic impact. A report from the Mineta Transportation Institute (Jenkins and Gersten, 2001) includes the analysis of 53 terrorist attacks that specifically targeted bridges between 1980 and 2006, and the report notes that 58% of bridges targeted worldwide and 35% of bridges targeted in industrialized nations during that time were highway bridges other than signature bridges. Considering that 60% of attacks on all transportation targets during that same time were bombings, a bombing of an ordinary highway bridge is a realistic scenario. Furthermore, the recent accidental collapses of the Oklahoma Weber Falls I-40 bridge (Blue Ribbon Panel, 2003), the Queen Isabella Causeway in Texas (Texas Office of the Governor, 2001), and the I-35 interstate bridge in Minnesota (Minnesota Department of Transportation, 2007) show the great socio-economic harm and fear that can result from the failure of one of these typical highway bridges. Moreover, an Al-Qaeda training manual specifically reinforces the threat to ordinary bridges by stating that a main goal of terrorism is "blasting and destroying bridges leading into and out of the city" to "strike terror into the enemies" ("Military Studies in the Jihad against the Tyrants," 1995), and regular attacks on ordinary bridges during the war in Iraq illustrate the success of these goals. Therefore, a bombing of a regular highway bridge in the U.S. is in fact a realistic scenario, and bridge engineers need guidelines for designing blast-resistant "ordinary" highway bridge structures.

Focusing the current research on typical highway bridge structures provides the most effective use of available project funds. Although understanding the effects of blast loads on signature bridges undoubtedly is an important research need, these structures are often complex, requiring specialized design provisions even for typical gravity and wind loads, and research on such bridges likely will provide results applicable only to the specific bridges considered. Additionally, while a significant number of existing critical bridges in the U.S. may require retrofits to resist blast loads, each of these bridges is different, with various types of structural systems in various states of disrepair. In-depth research on existing critical bridges would produce results applicable only to a limited number of scenarios. Focusing on the future design of typical highway bridge structures, however, will maximize the return on allocated research funds, as the results can guide designs for future typical highway bridges and spawn additional research on other types of bridge structures and retrofits of existing highway bridges. Therefore, the focus of the current research is on the blast-resistant design of new, typical highway bridges, and the primary objective is to develop blast-resistant design guidelines that can be easily incorporated into the AASHTO bridge design specifications.

While highway bridges have several structural components with blast resistance worthy of investigation, bridge columns are arguably the most important, and they appear to be the most vulnerable to direct attack. Most bridges intrinsically have open access to substructure members for either hand-placed or vehicle-delivered explosives in the form of traffic lanes, sidewalks, waterways, or other unrestricted areas. Although superstructure traffic also has unrestricted access to the deck, the type of superstructure can vary significantly from one bridge to another, while concrete bridge columns are integral to an overwhelming percentage of bridges. Thus, focusing on a particular superstructure type would not provide the same

comprehensive benefit as focusing on bridge columns. Moreover, while a successful attack against a superstructure likely will mean the loss of only one span, the failure of a critical bridge column likely will mean the collapse of at least two spans, and failure of a bridge column in an extensive interstate highway interchange may cause the progressive collapse of numerous spans as superstructures collapse onto one another.

Two aspects are necessary for any sound design: a thorough understanding of the load, and a good prediction of the expected response. As stated previously, most past studies of blast loads acting on structures involve flat surfaces (i.e., walls and building façades), and little is known about the interaction of a shock wave with a slender square or circular member (i.e., column). Furthermore, experts in the field of blast-resistant design are uncertain as to whether the observations regarding the response of building components to blast loads also apply to bridges. Therefore, this study includes two parts: Phase I aims to characterize the structural loads acting on square and circular bridge columns due to airblast, and Phase II investigates the response of half-scale bridge columns to blast loads, specifically focusing on various design parameters that may increase blast resistance. The following chapters provide details of both parts of this research program.

CHAPTER 3

Experimental Program

3.1 Overview

The experimental test programs for Phases I and II are presented in this chapter. Phase I included small-scale non-responding columns tested in Vicksburg, MS, by the U.S. Army Corps of Engineers. Phase II involved designing and testing half-scale reinforced concrete bridge columns. All of the instrumentation, construction, and testing for Phase II were completed at the Southwest Research Institute (SwRI) test site in Yancey, TX.

3.2 Phase I Load Characterization Study

The test program for small-scale non-responding columns tested during Phase I of this experimental research program, the data acquisition and instrumentation plan, and the experimental test setup are presented in this section. All instrumentation, construction, and testing were completed at the Big Black Test Site (BBTS) at the Engineering Research and Development Center (ERDC) of the U.S. Army Corps of Engineers in Vicksburg, MS.

The Phase I test program included eight small-scale blast tests at four sets of standoff. The objective of the small-scale tests was to characterize the structural loads on square and round bridge columns due to blast pressures. The experimental observations indicate how cross-sectional shape, standoff, and geometry between the charge and column positions influence blast pressures on the front, side, and back faces of bridge columns. The data gathered from these tests also allow the assessment of classical methods used to predict blast loads and a proposed method to modify pressures on the front face of a square column to obtain structural loads on a circular column. Although the blast loads acting on large flat panels such as walls and slabs are well characterized from past testing performed by the military and others, little is known about how blast pressures interact and engulf slender structural components such as bridge columns.

3.2.1 Experimental Setup

Classical scaling laws were used to design model tests that met the research objectives and remained within practical experimental limits of precision and accuracy. Phase I blast tests consisted of charges detonated on the ground surface to generate a regular Mach front air blast load on the columns. A scaled standoff of three was selected for each test to minimize the fireball and detonation products loading on the non-hardened pressure gauges, while a scale factor of eight allowed the explosive charge to be within the BBTS air burst safety and noise limits. The three main test variables included the charge weight, standoff, and cross-sectional shape. Thus, while the scaled standoff was held constant at three, the actual charge weight and physical standoff were varied in the test program. Table 4 lists the dimensions of each small-scale column.

The test setup for the Phase I non-responding columns is illustrated schematically in Figure 22. Figure 23 shows the test site prior to one of the detonations. The test setup foundation consisted of a 20-ft × 6-ft × 6-in. smooth-surfaced polymer-fiber reinforced concrete slab reinforced with a 2-ft × 2-ft × 1-in. replaceable steel plate at the charge location (midway between the columns). The columns were anchored by flange plates cast directly into the slab on either side of the charge.

Sensitized nitromethane was used as the high explosive material, and non-fragmenting plastic cylindrical containers with a charge diameter-to-height ratio of 1:1 approximated a spherical detonation. Two free-field pressure gauge mounts were also cast into the slab at each standoff on either side of the charge. PVC pipe cast into and underneath the slab protected the instrument cables from the blast. The test setup allowed both columns to be loaded simultaneously with the

Table 4. Phase I column design.

Column Type	Cross-Sectional Dimension (in.)	Wall Thickness (in.)	Area (in.^{2})	I_x (in.^{4})	S (in.^{3})	Z_x (in.^{3})
Round Pipe	4.5	0.674	8.1	15.3	6.79	9.97
Structural Tube*	4.5	0.500	8.0	21.7	9.63	12.1

* Shop Fabricated

same explosive charge, which increases the accuracy of the comparison between round and square column loadings.

3.2.2 Data Acquisition and Instrumentation Plan

Each non-responding column was instrumented with nine structure-mounted pressure gauges or instruments (SMI). Two free-field overpressure gauges were used during each test at the same standoff as the test column, one on either side of the charge. The locations of each gauge are shown in Table 5. The pressure gauge layout for a round and square column are illustrated in Figure 24. ERDC performed an extensive set of pre-test peak pressure analytical predictions to select pressure gauge sizes and ranges. High range Kulite HKS pressure gauges were specified.

3.3 Phase II Response Test

The design of reinforced concrete columns tested during Phase II of this experimental research program, the instrumentation and construction of each test specimen, and the experimental test setup are presented in this section. All of the instrumentation, construction, and testing were completed at the Southwest Research Institute test site in Yancey, Texas.

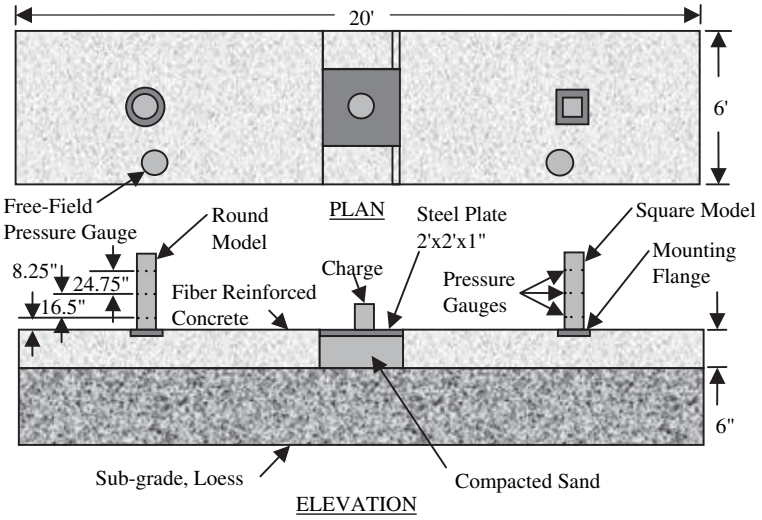

Figure 22. Phase I test setup schematic.

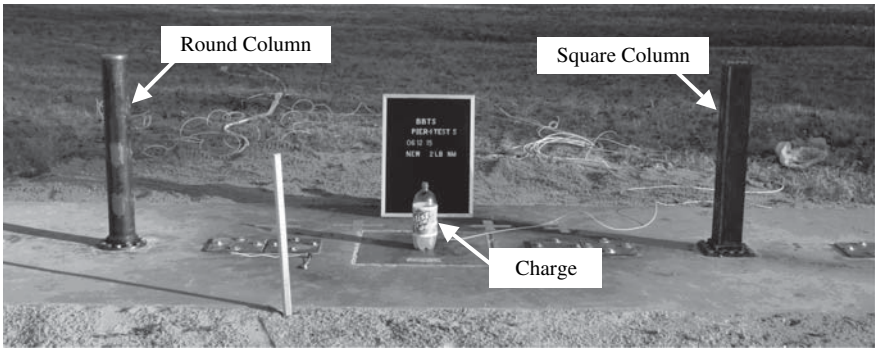

Figure 23. Phase I test setup.

Table 5. Phase I pressure gauge locations.

Type of Pressure Gauge*†	Height Above Ground (in.)			Notes
SMI Face-On, 0°	8.25	16.5	24.75	
SMI Side-On, 90°	8.25	16.5	24.75	Normal to Face
SMI Back-Side, 180°	8.25	16.5	24.75	
Free-Field‡	0	-	-	Normal to ground plane

*Pressure gauge layout for one pier
†SMI = Structure Mounted Instrument (relative to blast source)
‡Free-field pressure gauge at range of front face of pier

The test program included ten half-scale, small standoff tests and six half-scale, local damage blast tests, as shown in Table 6. The goal of the small standoff tests was to observe the mode of failure (i.e., flexure or shear) for eight different column designs. In a local damage test, charges were placed very close to or in direct contact with the test column. The objective of the local damage tests was to observe the spall and breach patterns of blast-loaded concrete columns. Experimental observations were used to evaluate the performance of several design parameters and to determine the

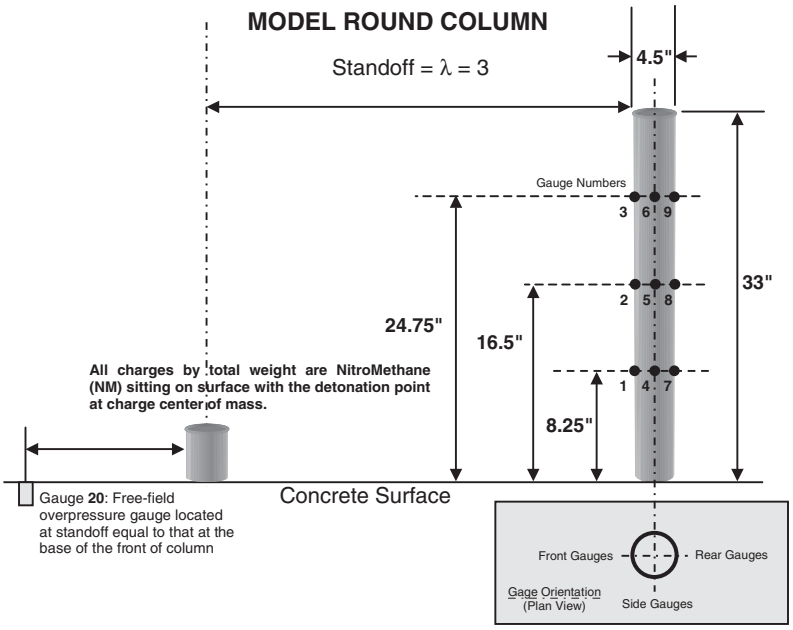

Figure 24. Phase I pressure gauge layout: a) round column, b) square column.

Table 6. Phase II test matrix.

Test No.	Column Designation	Column Design	Scaled Standoff ($ft/lb^{1/3}$)	Instrumentation	Test Objectives/Notes
Small Standoff Tests					
1	1A1	gravity	$R/W^{1/3} < 3$	3 free-field pressure gages for explosive yield validation, 6 strain gages per specimen, and high speed camera	To determine flexural response shapes and shear/flexure interaction for large round & square columns under blast loads, including seismic detailing and sections designed specifically to resist blast
2	1A2	gravity	$R/W^{1/3} < 3$		
3	2A1	gravity	$R/W^{1/3} < 3$		
4	2A2	gravity	$R/W^{1/3} < 3$		
5	1B	gravity	$R/W^{1/3} < 3$		
6	2B	gravity	$R/W^{1/3} < 3$		
7	2-seismic	seismic	$R/W^{1/3} < 3$		
8	2-blast	blast	$R/W^{1/3} < 3$		
9	3A	gravity	$R/W^{1/3} < 3$		
10	3-blast	blast	$R/W^{1/3} < 3$		
Local Damage Tests					
1	2A2	gravity	$R/W^{1/3} < 1$	High speed camera and post-test measurement only	To quantify spall/breach thresholds for round & square columns; to quantify extent of local damage
2	2A1	gravity	$R/W^{1/3} < 1$		
3	1A1	gravity	$R/W^{1/3} < 1$		
4	2B	gravity	$R/W^{1/3} < 1$		
5	2-blast	blast	$R/W^{1/3} < 1$		
6	3A	gravity	$R/W^{1/3} < 1$		

capacity and failure limit states of concrete highway bridge columns.

3.3.1 Background on Parameters Selected for Testing

The test specimens designed for this program incorporated design and detailing standards commonly used in practice in various regions of the country. A survey of several states' department of transportation (DOT) design and detailing standards is summarized below to provide the reader with a better understanding of each state's design philosophy. The national DOT design survey and background theory on blast-resistant column design were used to determine the eight different column designs with five main test variables. A summary of each column design is presented below to indicate how each design represents current national standards.

3.3.1.1 State Department of Transportation Design Survey

The goal of the state DOT design summary is to illustrate similarities and differences among states' design and detailing standards. Each state's DOT maintains a bridge and highway design manual or similar document that provides design standards for that state. The standards pertaining to concrete column design are summarized in Table 7. At a minimum, each state's standards are designed to meet the AASHTO LRFD Bridge Design Specifications. However, the state standards are commonly more stringent than the AASHTO requirements due to local design issues, such as earthquakes or highly corrosive environments.

Parameters that were not varied in this test program were found to be consistent among state DOT design standards, such as concrete strength, concrete class, concrete clear cover, and reinforcement grade. The longitudinal reinforcement ratio can be calculated according to AASHTO specifications. This value was held constant at 1.0% for the test program, which is typical for current bridge column design.

3.3.1.2 Close-in, Blast-Resistant Column Design and Detailing

Building components subjected to blast loads are designed to ensure adequate shear strength so that flexure is the controlling mode of failure. In flexure, reinforced concrete structural components that are properly detailed possess good ductility, while in shear, failures occur in a brittle manner. Thus, it is desirable to have flexure be the controlling mode of failure. A plastic hinge analysis on a blast-loaded component considers all potential plastic hinge locations to ensure the maximum possible shear demand. A basic component design includes a nonlinear SDOF analysis that considers each stage of response. Figure 19 illustrates a beam that goes through three stages of deformation: purely elastic, a combination of elastic and plastic, and purely plastic. Typically in blast-resistant design, large inelastic deformations are allowed and play an important role in a component's dissipation of energy. Due to the large uncertainty associated with determining blast loads, an SDOF analysis usually provides adequate results for design.

Table 7. State DOT column design summary.

State	Column Geometry			Concrete Standards			Col. Connection		Design Concerns
	Bent Type	Shape	Min. Diam. D (ft.)	f'_c (psi)	Class	Cover c (in.)	Footing (bottom)	Bent Cap (top)	
CA	Single	O/Re		3600		2	fixed	fixed	Seismic
CO	-	-	3	4000		2	fixed		Durability
CT	S/M	Round	3	4000	F	3	fixed		
DE	Multi	Round	3	4500	D	2	fixed	fixed	Seismic
FL	S/M	Ro/Re	3			3	fixed		
IL	Multi	Ro/Re	2.5			2	fixed	hinge	
ND	S/M	Ro/Re	2	3000	AE		fixed		
NJ	S/M	Round	3		A	2	fixed		
NY	Multi	Ro/Re			HP/ A	2	fixed	fixed	
SC	Single	O/Ro	3	4000		2	fixed	fixed	Seismic
TX	Multi	Ro/Re	1.5	3600	C	3	fixed	prop	
AASHTO				4000	A	3			

State	Long. Reinf. Standards				Shear Reinf. Standards				Splice Location
	Grade f_y (ksi)	Size Min.	Min # Long. Bars	Reinf. Ratio ρ_L %	Type	Grade f_{yh} (ksi)	Size Min.	Pitch max (in.)	
CA	60	5	6		BWH	60	5	3.75	mid height
CO	60	4			Hoops	60	4	3	
CT	60	4			Spiral	60	4		
DE	60	5			Spiral	60	5		mid height
FL	60				Hoops	60	4		
IL	60	7			S/H	60			
ND	60	5				60			
NJ	60				Spiral	60	5	3.5	mid height
NY	60				S/H	60	4	12	mid height
SC	60	8	6		BWH	60	6	12	mid height
TX	40	6	6	1	S/H	40†	3	6	
AASHTO	60	5	6		S/H	60	3	12	bottom

S/M = Single or Multi
S/H = Spiral or Hoop
BWH = butt welded hoops
O = Oblong
Ro = Round
Re = Rectangular
All fields left blank are controlled by AASHTO Specifications
† Longitudinal Bars may be designed as Gr. 40 to reduce splice lengths

While design guidance exists for blast-loaded building columns, there are currently no standards on how to design and detail a bridge column to resist blast loads. Bridge columns behave differently than building columns exposed to blast loads, preventing the direct application of current design guidelines for buildings. For example, bridge columns are easier to access than most building columns, which drastically changes the blast loads used in design. Typically, building columns are designed for the reactions from blast-loaded exterior walls or beams, while bridge columns are the primary members resisting blast loads. In addition, the applied axial load magnitude relative to the axial load capacity is usually much greater in building columns than in bridge columns, which affects the location on the axial force-bending moment interaction diagram and hence the behavior under laterally applied loads. There is little research on the blast-wave propagation around exposed structural members such as slender bridge columns. Therefore, all existing design guidelines need to be revisited for bridges specifically. However, many of the design *principles* used for blast-resistant building design should apply equally well to bridges. Current design and detailing requirements for petrochemical facilities subjected to blast loads emphasize the importance of ductility, which is similar to seismic design (ASCE, 1997). Accordingly, some general blast-resistant design concepts may still be helpful for designing blast-loaded bridge columns, and detailing requirements should focus on providing adequate reinforcement for the formation of plastic hinges.

3.3.1.3 Test Variables

For variables in Table 7 that show a range in design values depending on location within the United States, priority for the test program was given to those design details that were believed to be the most critical to reinforced concrete column performance when subjected to blast loads. The following five test program variables are discussed below: cross-sectional

shape, length-to-depth (L/D) ratio, type of transverse reinforcement, volumetric reinforcement ratio, and splice location. These design parameters were varied in the test program to provide a broad representation of current bridge column designs nationwide.

3.3.1.3.1 Cross-Sectional Shape. There are three shapes typically used in bridge column design: circular, rectangular, and oblong. Circular columns are the most economical and commonly used cross-sectional shape, as shown in Table 7. Circular columns require less formwork and provide a greater ease of construction than other shapes. Rectangular-shaped columns, however, are also regularly used in six of the eleven states listed in Table 7.

There is currently little research on how blast loads interact with bridge columns or slender members of any shape. Circular and square cross-sections were selected as test variables to better understand how blast loads interact with slender members with different reflecting surfaces because load characterization is an important step the blast-resistant design and detailing process.

3.3.1.3.2 Length-to-Depth Ratio. Another important design parameter for blast-loaded columns is the L/D ratio. The L/D ratio can be varied by changing the column cross-sectional depth while holding the length or height constant. The depth of the cross-section is directly proportional to the shear strength of a concrete column, as shown in Equation 6 (AASHTO, 2007), which is important in blast-resistant design.

$$V_N = V_c + V_s = 2\sqrt{f_c'}bd + \frac{A_v f_y d}{s} \quad (6)$$

where:

f_c' = specified compressive strength of concrete at 28 days (psi)
f_y = yield strength of reinforcing bars (psi)
d = effective depth of cross-section (in.)
b = effective width of cross-section (in.)
s = spacing of stirrups (in.)
A_v = area of shear reinforcement with a distance s (in.)

The minimum column dimension in Table 7 varies among the states depending on column type and shape. Most DOTs have adopted conservative minimum column dimension specifications to allow design redundancy and safety against vehicular collisions with substructures, which are not considered explicitly in most cases. For example, TxDOT provides a table of minimum steel requirements for round columns with diameters between 18 in. and 60 in. for designers, as shown in Figure 25.

Column Diameter	Vertical Steel Bars V			Bars T	Height
	No. of Bars	Size	%	Size & Pitch	"Y" Maximum
18"φ	6	#6	1.04	#3 @ 6"	18'
24"φ	8	#7	1.06	#3 @ 6"	24'
30"φ	8	#9	1.13	#3 @ 6"	30'
36"φ	10	#9	0.98	#3 @ 6"	36'
42"φ	14	#9	1.00	#3 @ 6"	42'
48"φ	18	#9	0.99	#3 @ 6"	48'
54"φ	18	#10	1.00	#4 @ 9"	54'
60"φ	22	#10	0.99	#4 @ 9"	60'

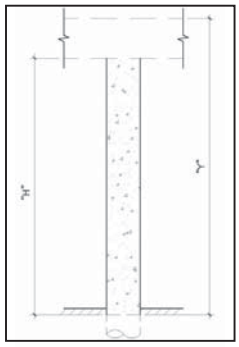

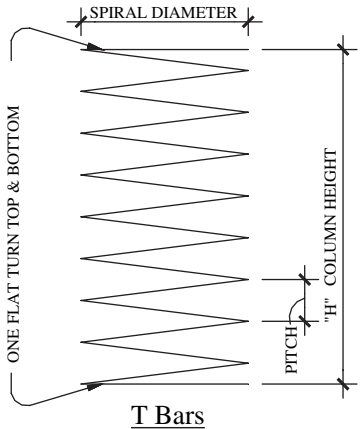

T Bars

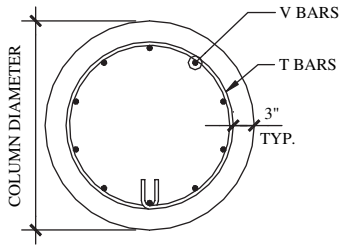

Column Section

Figure 25. Minimum column steel requirements for round columns (TxDOT, 2001).

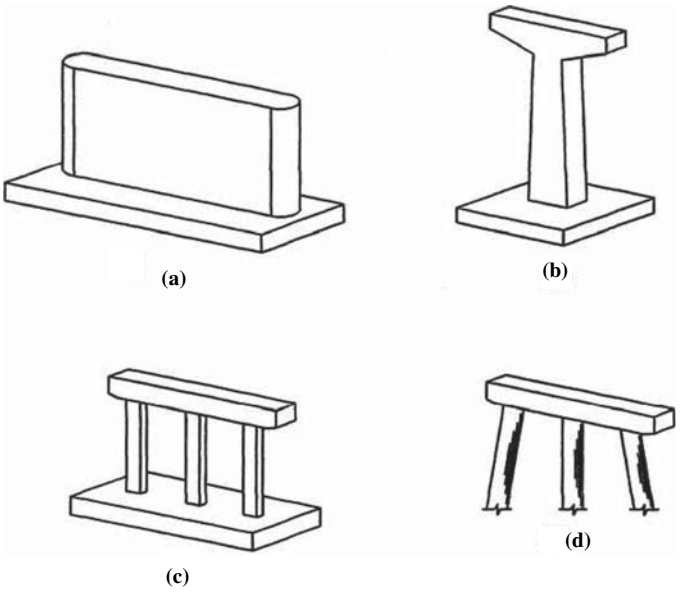

Figure 26. Typical column types: a) solid, b) single-column, c) multi-column, d) pile bent (NYSDOT, 2006).

There are four main column types: solid wall, single-column, multi-column, and pile bents, as shown in Figure 26. The two most common column configurations, single-column and multi-column, were represented in this test program with two different column dimensions. A single-column configuration consists of either a hammerhead or tee-shape capbeam overhanging each side of a large column that supports the superstructure as a whole. With increasing column height and narrow superstructures, the single-column configuration becomes more economical than the multi-column configuration by reducing the required amounts of material and formwork. Therefore, lower L/D ratios (i.e., larger column diameters) represent single-column configurations.

A multi-column configuration consists of two or more columns connected by a capbeam that supports the superstructure at points between the columns. A multi-column bent is the best choice for wide superstructures. Therefore, higher L/D ratios (smaller column diameters) represent multi-column configurations.

3.3.1.3.3 Type of Transverse Reinforcement. The type of transverse reinforcement also varies from state to state. The majority of DOT manuals prefer discrete hoop reinforcement over continuous spiral reinforcement due to ease of construction. However, spiral reinforcement increases confinement and rebar cage stability relative to the case of discrete hoops, which is critical to seismic designs that depend on this extra ductility. The use of spirals could also be helpful in blast-resistant design.

The use of continuous spiral reinforcement requires fewer anchorages than the use of discrete hoops, which minimizes the probability of pullout failures. The use of discrete hoops or ties requires proper anchorage depending on the type of loading: typical or seismic. A typical load consists of traditional gravity loads (dead and live load) plus wind load, which require the use of standard hooks. Section 5.10.2.1 of the AASHTO LRFD (2007) defines standard hooks for transverse reinforcement as one of the following:

- No. 5 bar and smaller: 90° bend, plus a 6.0 d_b extension at the free end of the bar
- No. 6, No. 7, and No. 8 bars: 90° bend, plus a 12.0 d_b extension at the free end of the bar
- No. 8 bar and larger: 135° bend, plus a 6.0 d_b extension at the free end of the bar

where:

d_b = nominal diameter of the reinforcing bar (in.)

Recent work by Bae and Bayrak (2008) on the seismic performance of full-scale, reinforced concrete columns demonstrated the opening of seismic discrete ties using hooks with a 135° bend, plus an extension of 8.0 d_b. The AASHTO LRFD Section 5.10.2.2 defines seismic hooks as a "135° bend, plus an extension of not less than the larger of 6.0 d_b or 3 in." Bae and Bayrak noted that, unlike the "full-scale concrete columns, the hooked anchorages often reach close to the center of the core concrete in small-scale column specimens." Bae and Bayrak used a minimum hook length of 15.0 d_b for the remaining tests to prevent anchorage failures. The larger "hook length proved to be very effective, and opening of the 135° hooked anchorages of the ties was not observed in the other tests." To avoid similar anchorage failures with the half-scale test columns constructed for the current research, specified hook lengths for the blast-loaded column designs were longer than those used successfully in the seismic tests by Bae and Bayrak. These "blast" hooks were specified to consist of a 135° bend with a 20.0 d_b extension at one free end of the bar, reversing directions each spacing. Additionally, for the purposes of the test program, there was a desire to represent current national practices while still taking into consideration recent research findings. Accordingly, both spiral reinforcement and discrete hoops or ties with standard and blast hooks were included as variables in the experimental program.

3.3.1.3.4 Volumetric Reinforcement Ratio. The volumetric reinforcement ratio varies depending on the governing loading condition: typical or seismic. Equation 7 (AASHTO, 2007) specifies the minimum volumetric reinforcement ratio, ρ_s, for typical, gravity-loaded columns. For the states included in Table 7, seismic loads usually govern column design and detailing requirements in California and South Carolina. Equation 8, from the AASHTO LRFD seismic provisions, specifies a more stringent minimum volumetric reinforcement ratio than for gravity-loaded columns.

$$\rho_s \geq 0.45\left(\frac{A_g}{A_c}-1\right)\frac{f'_c}{f_y} \quad (7)$$

$$\rho_s \geq 0.12\frac{f'_c}{f_y} \quad (8)$$

where:

f'_c = specified compressive strength of concrete at 28 days (psi)
f_y = yield strength of reinforcing bars (psi)
A_g = gross area of column (in.^{2})
A_c = area of concrete core (in.^{2})

The seismic provisions require sufficient transverse reinforcement "to ensure that the axial load carried by the column after spalling of the concrete cover will at least equal the load carried before spalling and to ensure that buckling of the longitudinal reinforcement is prevented" (AASHTO, 2007). Thus, the spacing of transverse reinforcement is important for shear resistance and confinement in the plastic hinge regions (typically, the top and bottom) of a seismically loaded column. Shear resistance and confinement in plastic hinge regions are also important for blast-loaded columns. The minimum volumetric reinforcement ratio shown in Equation 9 was used for blast-loaded column designs in this test program.

$$\rho_s \geq 0.18\frac{f'_c}{f_y} \quad (9)$$

where:

f'_c = specified compressive strength of concrete at 28 days (psi)
f_y = yield strength of reinforcing bars (psi)
A_g = gross area of column (in.^{2})
A_c = area of concrete core (in.^{2})

The above equations apply to circular columns. For a rectangular column, the minimum total gross sectional area, A_{sh}, of hoop reinforcement is specified in Equations 10 and 11 for seismic columns in the AASHTO LRFD seismic provisions (2007) and blast-loaded columns in this test program, respectively.

$$A_{sh} \geq 0.12 s h_c \frac{f'_c}{f_y} \quad (10)$$

$$A_{sh} \geq 0.18 s h_c \frac{f'_c}{f_y} \quad (11)$$

where:

f'_c = specified compressive strength of concrete at 28 days (psi)
f_y = yield strength of reinforcing bars (psi)
s = vertical spacing of hoops, not exceeding 4 in. (in.)
h_c = core dimension of column in the direction under consideration (in.)

Essentially, 50% more confinement steel was specified in the design of blast-loaded columns over current seismic provisions to further investigate the benefits of additional transverse reinforcement to column strength, ductility, and energy dissipation. Therefore, a different volumetric reinforcement ratio for each type of loading (typical, seismic, and blast) was considered in the test program.

3.3.1.3.5 Splice Location. Another important design parameter is the splice location of longitudinal reinforcement. Ideally, splice zones of longitudinal steel should occur at a point in a member where the bending moment is equal to zero or is very small. The moment is zero at the inflection point of the bending moment diagram; therefore, a natural place to splice longitudinal reinforcement is near that point.

The location of the inflection point depends directly on the assumed boundary conditions and load distribution, which varies for typical, seismic, and blast loads. Figure 27 illustrates the moment diagram and inflection points for each load case assuming fixed supports. Columns designed for gravity loads, including a horizontal wind load, have an inflection point near 0.2L from each column support. Wind load, however, does not typically control a gravity-loaded column design, and the typical splice near the column base allows for ease of construction. Seismic loads induce a high lateral displacement between the column supports, creating an inflection point near mid-height (0.5L). Therefore, seismic column design restricts splices within 1.5D of each support to provide sufficient rebar cage stability and column ductility within these plastic hinge regions. A column exposed to a blast wave approximated with a uniform load results in inflection points near 0.2L from each support for an elastic column response. However, a blast-loaded column is expected to behave inelastically, causing the deformed shape and effective support conditions to change as a function of time. For example, the inflection points for a uniformly loaded inelastic column that is initially fixed at both ends occur around 0.15L from each support. To investigate the effects of splice location on the performance of blast-loaded bridge columns, the test program included two different splice configurations: near the base for a typical column or no splice to represent seismic columns.

3.3.2 Column Design

The typical and seismic column designs used in the test program were based on current state DOT standards and

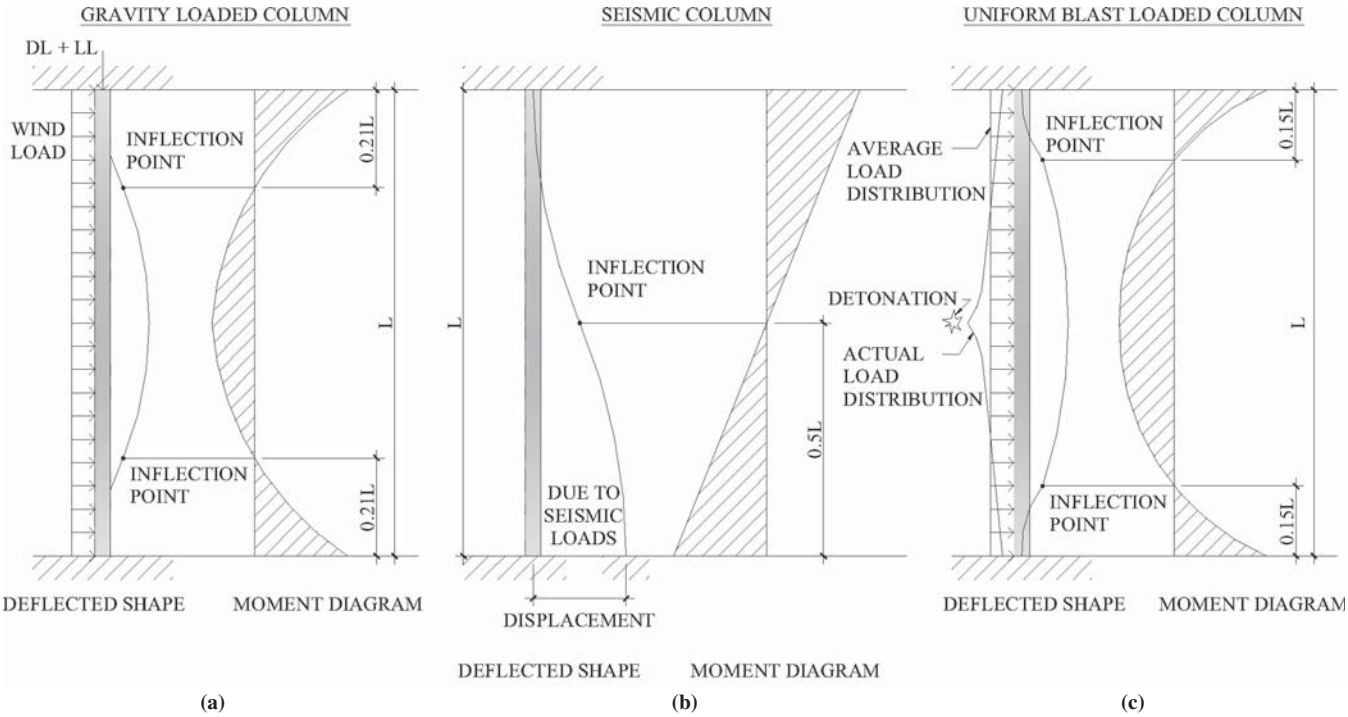

Figure 27. Moment diagram and deflected shape for each load case: a) typical, b) seismic, c) blast.

the AASHTO LRFD specifications. To reduce the chances of a potential shear failure resulting from a small standoff test, blast-loaded columns were designed using a plastic hinge analysis similarly to current seismic design provisions and as illustrated in Figure 28. The boundary conditions corresponding to a propped-cantilever condition shown in the figure are consistent with the research objectives and with the reaction structure used in the test program. Additional information on the assumed boundary conditions and reaction structure design is given in the following subsections.

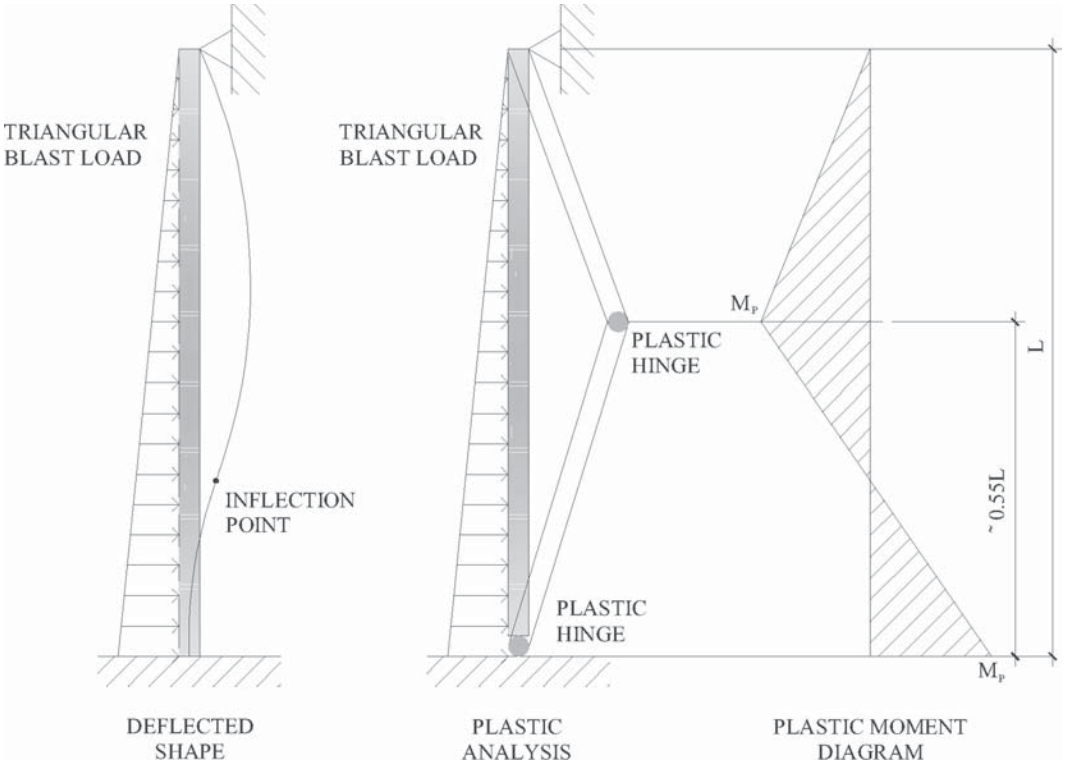

Figure 28. Plastic hinge analysis for blast-loaded column.

3.3.2.1 Blast-Column Design

A blast-loaded column design considers all potential plastic hinge locations to determine the maximum possible shear demand on the column. The maximum shear demand is a function of the boundary conditions and load distribution. Boundary conditions depend on the assumed threat scenario and the position of the center of detonation relative to the orientation of the bridge under consideration. A propped-cantilever was assumed for this test program in accordance with Table 7 for two reasons. First, this condition is consistent with the design details used by various state DOTs, and second, because this assumption will usually result in a conservative estimate of shear demand for a blast-loaded bridge column, which was expected to be the controlling mode of failure. A propped-cantilever is a conservative assumption for the experimental tests and most design scenarios because these boundary conditions lead to the largest shear demand at the base for all probable cases, except that of a cantilever, which is an unlikely configuration for a bridge column. Thus, when considering a uniformly loaded column, propped-cantilever boundary conditions produce a larger shear demand at the base of the column than that produced by the cases of simply supported and fixed–fixed columns. Accordingly, the reaction structure was designed to provide these support conditions. The reaction structure design and details are presented in Section 3.3.3.

Blast-load distribution on a column is a function of standoff. As shown in Figure 29, columns with a large standoff can be approximated by a uniform load; however, columns with a small standoff are better approximated with a varying load in most cases because, as the blast wave propagates away from the blast source, the base of the column will be loaded first (assuming the center of detonation is near the ground, which is a common assumption for blast scenarios involving a vehicle-delivered explosive). For this research, a linearly varying blast load was assumed for the plastic hinge analysis.

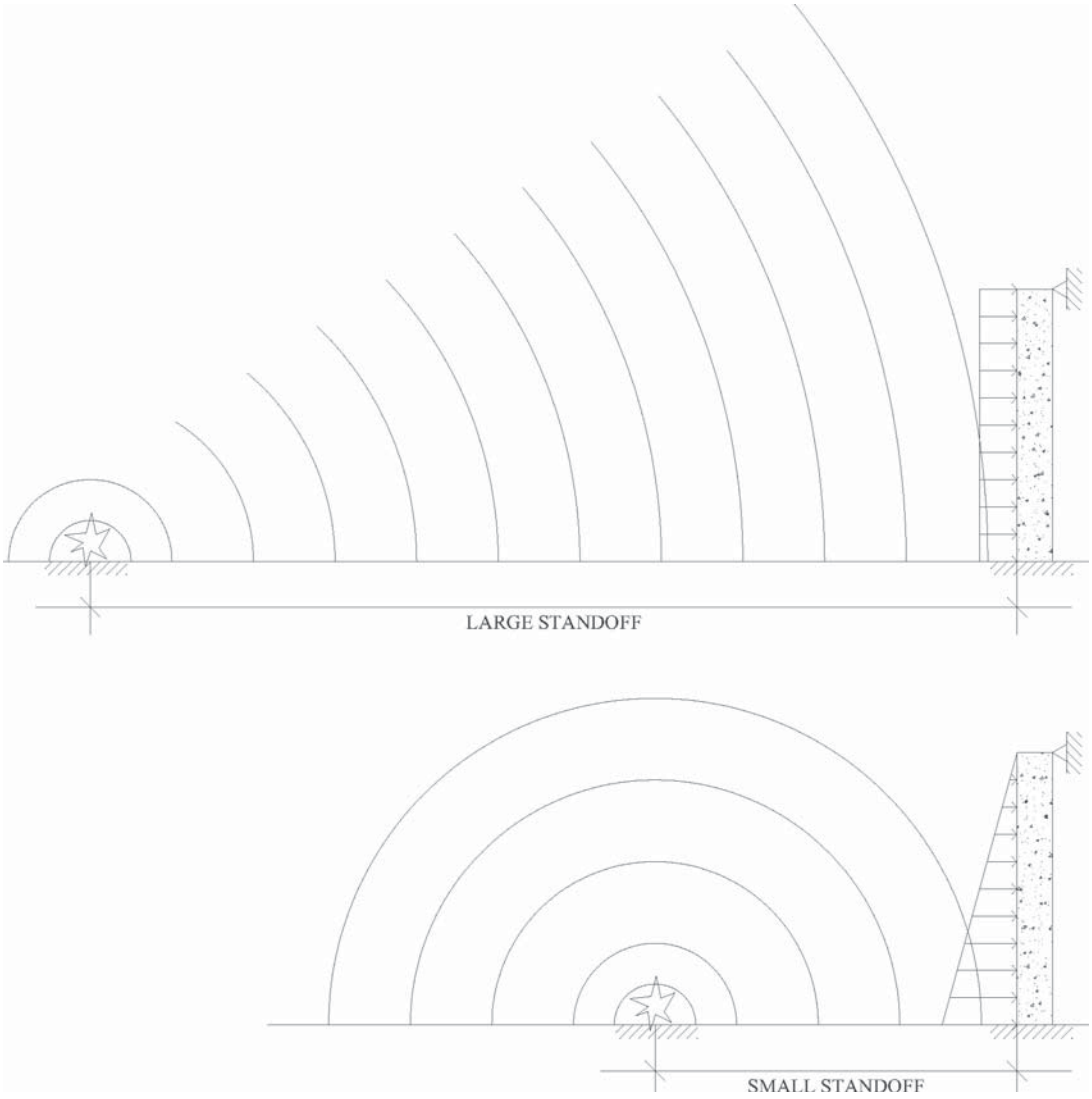

Figure 29. Blast load distribution versus standoff.

Table 8. Test variable summary.

Small Standoff Test No.	Column Designation	Column Geometry		Long. Reinf.	Transverse Reinf.		
		Shape	Size (in.)	Splice Location	Pitch/ Space (in.)	Type	Vol. Ratio ρ_s %
1	1A1	Round	18	0.25*L*	6.0	Hoops	0.82
2	1A2	Round	18	0.25*L*	6.0	Hoops	0.82
3	1B	Round	18	0.25*L*	6.0	Spiral	0.82
4	2A1	Round	30	0.25*L*	6.0	Hoops	0.47
5	2A2	Round	30	0.25*L*	6.0	Hoops	0.47
6	2B	Round	30	none	6.0	Spiral	0.47
7	2-seismic	Round	30	none	3.5	Spiral	0.80
8	2-blast	Round	30	0.25*L*	2.0	Spiral	1.40
9	3A	Square	30	0.25*L*	6.0	Ties	0.47
10	3-blast	Square	30	0.25*L*	2.0	Ties	1.40

The required pitch of transverse reinforcement can be determined by setting the maximum shear demand determined in the plastic hinge analysis equal to the shear design equations from the AASHTO LRFD, modified to account for strain rate effects (ASCE, 1997), and solving for the spacing. The plastic moment (M_p), which is equal to the flexural capacity of the cross-section (M_N), also accounts for the dynamic material strength, with dynamic increase factors for strain rate effects. Again, the maximum shear demand was used to determine the required volumetric reinforcement ratio to ensure that adequate shear capacity was provided and to force the formation of plastic hinges (a flexural failure).

3.3.2.2 Column Design Summary

Ten columns with eight different column designs were tested in Phase II of the experimental program. Typical designs for concrete columns designed in areas of high seismicity (designated Seismic) as well as those located in areas with a low seismic threat (designated A or B) were considered. In addition, two columns designed specifically for the case of blast loads (designated Blast) were also included in the test matrix. Test variables for each column design are summarized in Table 8 and illustrated in Figure 30. Constants specified in this test program include 4000 psi, Type-A concrete, 1 in. concrete

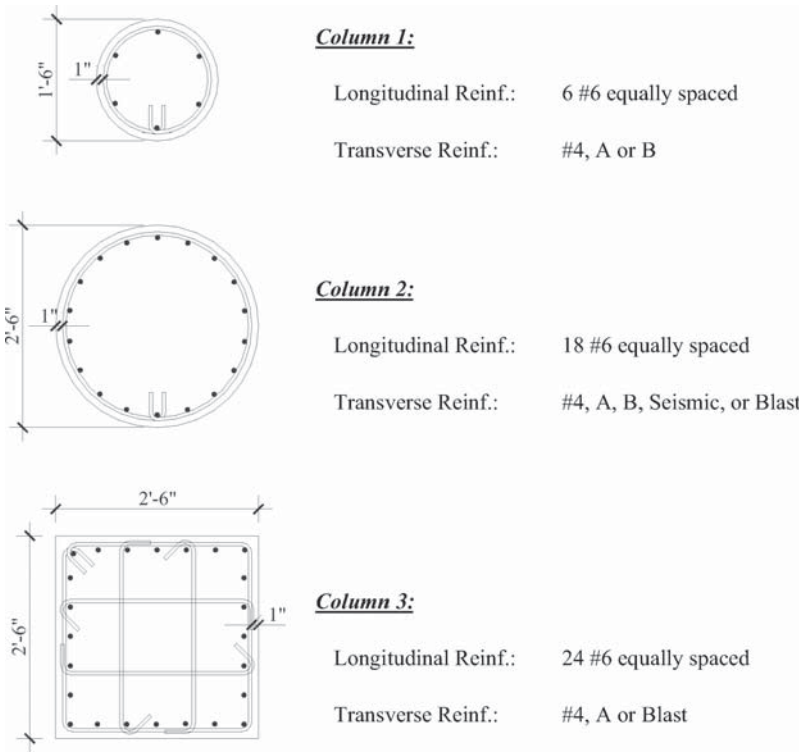

Figure 30. Column cross-sections.

clear cover (which corresponds to 2 in. of clear cover in full-scale columns), GR 60 steel reinforcing bars, 1.0% longitudinal reinforcement ratio, and propped-cantilever boundary conditions.

3.3.2.3 Material Properties

The concrete and steel specified in this project were selected to represent that which is typically used in the construction of reinforced concrete highway bridge columns. Due to the variety of concrete strengths and types used in different states, the values specified by the AASHTO LRFD were selected for the test program. Concrete of 4000 psi strength and composed of Type-A cement with a maximum aggregate size of ⅜ in. (to accommodate the small rebar spacing) was selected for this test program. Also, standard deformed, uncoated, Grade 60 reinforcing bars were specified for all reinforcement except the continuous spirals that allow the use of a smooth bar (according to the AASHTO LRFD).

3.3.2.4 Axial Load

Most bridge columns have much greater axial load capacity than axial load demand from gravity loads, and thus they typically experience service compressive loads that are well below the balance point of the column. Therefore, including a compressive axial load in the test setup would only increase both flexural and shear resistance of the specimens. Furthermore, the construction of a test frame able to maintain an axial load on column specimens while surviving multiple blast tests was impractical and cost-prohibitive given the allocated funds. Consequently, given the expected increase in capacity an axial load would contribute, coupled with the cost of developing a test setup capable of applying an axial load over the entire test program, the experimental tests conducted for this research neglected the effect of a compressive axial load.

Furthermore, while it may be possible for a scenario to exist in which a column will experience tensile forces due to uplift on the deck prior to experiencing peak flexural response, a survey of DOT design details showed that the majority of states use a configuration with the superstructure resting on a bent cap, which would not allow a column to experience tensile forces. Even for bridge configurations in which the superstructure is directly connected to a column, a column will reach its peak shear and flexural responses very early in time for the attack scenarios creating the most severe lateral loading conditions (i.e., small standoffs). The best use of allocated funds was to consider an experimental testing program that represented the most probable design threats combined with the most common bridge column configurations, and thus the Phase II experimental test program did not consider blast-loaded bridge columns with a tensile or compressive axial load.

3.3.3 Reaction Structure Design

The steel reaction structure and reinforced concrete slab for the small standoff tests were designed by Protection Engineering Consultants (PEC). The reaction structure was designed to be pre-fabricated offsite and delivered in one piece, while the slab was constructed onsite. The design and detailing of the reaction structure and slab are described below.

3.3.3.1 Steel Reaction Structure Design

The steel reaction structure was designed to resist dynamic blast loads. A single-degree-of-freedom analysis was completed for each frame member using SBEDS (U.S. Army Corps of Engineers, 2007) and assumed fixed end conditions. SBEDS (Single-degree-of-freedom Blast Effects Design Spreadsheet) is a commonly used program in the blast-resistant design community.

The reaction structure consisted of HSS 8 × 8 × ⅝ members, ½-in. φ steel rods, and W10 × 88 anchor beams, as shown in Figure 31. The HSS shapes were A500 Gr B steel, while all other steels were specified to have a minimum yield strength of 50 ksi. All connections were welded with ½-in. fillet welds at perpendicular joints or ⅝-in. flared groove welds otherwise, as shown in Figure 32.

3.3.3.2 Reinforced Concrete Slab Design

The reinforced concrete slab was also designed for dynamic blast loads. The majority of the slab was 2-ft deep, but it increased to a depth of 2 ft 6 in. around the 5-ft × 7-ft hole for the column footing, as shown in Figure 33. The slab thickness increased near the column footing to account for the large reaction forces expected there from the column and reaction structure. Figure 33 also illustrates the extensive reinforcement that is used throughout the slab. Casting of the slab took place onsite using a regular concrete truck.

3.3.4 Data Acquisition and Instrumentation Plan

The test specimen and instrumentation in a blast test are subjected to extreme loading conditions (temperature and pressure). The type and location of instrumentation must be able to endure these conditions. This test program specified the use of strain gauges on reinforcing bars, free-field pressure gauges, and high-speed video cameras to gather experimental data and observations. All wires or cables within close proximity of a test specimen were bundled and buried under-

Figure 31. Reaction structure.

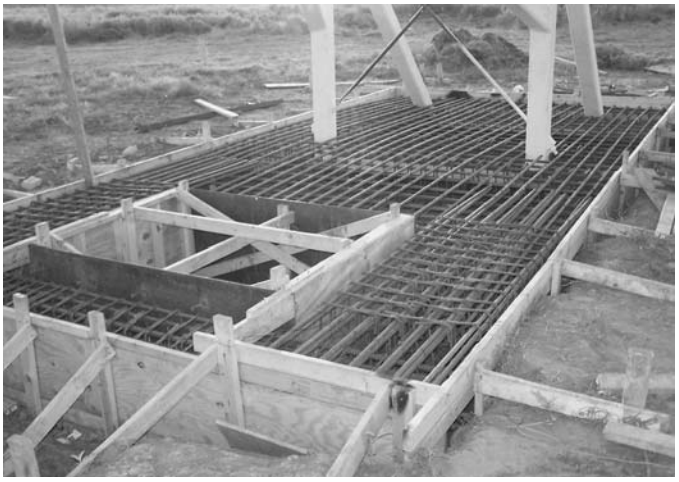

Figure 33. Slab reinforcement.

ground to prevent damage. Post-test measurements and pictures were taken to document damage conditions following each test.

3.3.4.1 Strain Gauge Installation on Reinforcing Bars

Each column was instrumented with at least eight strain gauges. Data were collected from six of the strain gauges during each small standoff test. The installation of eight strain gauges provided redundancy in case any strain gauges were damaged during construction and allowed the use of all six channels provided by the data acquisition system. As shown in Figure 34, the gauges were located on transverse and longitudinal bars to measure the strain near the base of the column, represented by triangles and circles, respectively, in the figure. (Note that the column in Figure 34 was straightened prior to casting.) The strain gauges used in this research project were TML Strain Gauges from Tokyo Sokki Kenkyujo Co., Ltd., Type FLA-5-11-15LT, with a gauge length of 5 mm.

3.3.4.2 Free-Field Pressure Gauge Locations

Three free-field pressure gauges were used during each small standoff test. Pressure gauges were located at 37 ft, 51 ft 8 in., and 76 ft from each charge. The free-field pressure gauges needed to be placed at least 30 ft from the test specimen to ensure the survival of the gauges over the ten tests. Free-field pressure gauges measure the side-on (i.e., free-field) pressure as the shock front passes the gauge. The average free-field pressure and impulse were used to calculate TNT equivalency and efficiency for each blast test.

Figure 32. Welded connections for the reaction structure.

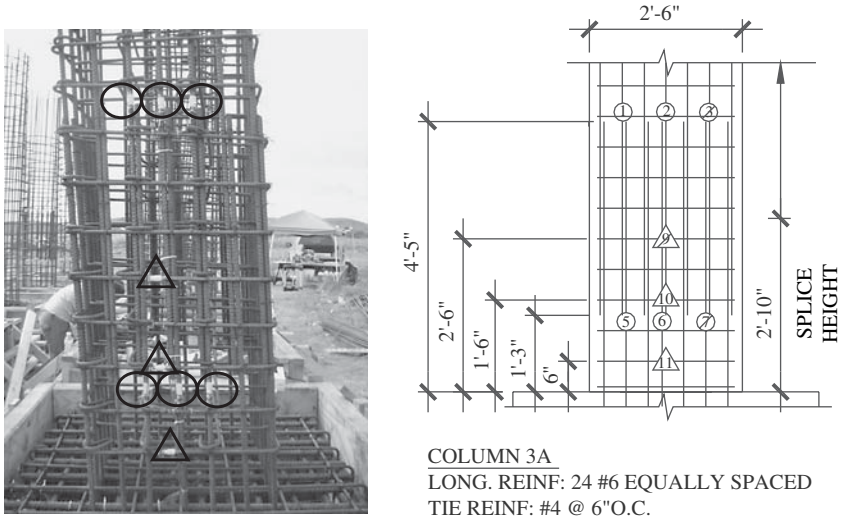

Figure 34. Strain gauge layout (Column 3A).

3.3.4.3 High-Speed Video Cameras

One or two high-speed video cameras were used for each small standoff and close-in test. Video provided by these cameras was useful in observing aspects of behavior that were difficult to discern from the strain gauge data and other instrumentation. Often, however, the "fireball" from an explosion obscured the specimen response, and the high-speed video was of limited benefit.

3.3.5 Column Construction

The construction of all columns and footings took place at the test site. A summary of the entire construction process and column fabrication is provided below.

3.3.5.1 General

The construction process began with the delivery of materials to the test site. First, the formwork and rebar cage for each column footing were constructed. Figure 35 illustrates the reinforcement used in each footing, including a mat of #8 bars top and bottom, #4 closed stirrups in each direction, and #6 longitudinal bars anchored into the bottom steel mat. Essentially, a box of steel was provided in each 5-ft square-, 2-ft 6-in.-deep concrete footing. The footings were designed with sufficient capacity to ensure that failure would occur in the column for all blast tests.

Next, the longitudinal and transverse reinforcements for each column were placed vertically into the footing cages, as shown in Figure 35. To decrease variability in the spacing of transverse reinforcement, wooden spacers were used, as shown in Figure 36. After each cage was completed, specified bars were instrumented. After instrumentation, the footings were cast and allowed to cure for several days (Figure 37) before formwork was placed around the column rebar cages. The columns were then cast in a second lift with a concrete pump truck and consolidated with a hand vibrator, as shown in Figure 38. The construction timeline allowed at least 22 days for the concrete to cure prior to testing, and concrete strength based on cylinder tests had reached 97% of the specified compressive strength at the start of the blast testing.

3.3.5.2 Column Constructability

Column constructability was not an issue for the typical gravity-loaded column designs. The construction process was considerably more difficult, however, for the seismic-loaded and blast-loaded column designs due to the increased volume of transverse reinforcement and smaller spacing or pitch. The reinforcing cage for the square blast column shown in Figure 37 was more difficult to construct than the round typical column, though clearly not impossible. Also, special care was taken when vibrating the tightly spaced rebar cages to ensure proper consolidation of the concrete.

3.3.6 Small Standoff Test Setup

As stated previously, the desired boundary conditions for the Phase II close-in blast tests were those of a propped-cantilever column. Figure 39 shows an actual column placed into the test setup to illustrate the assumed boundary conditions. To create a fixed connection at the base, the large column footing was placed into the slab opening and grouted into place to help prevent rotation. The steel collar that wrapped around the top of the concrete column was then

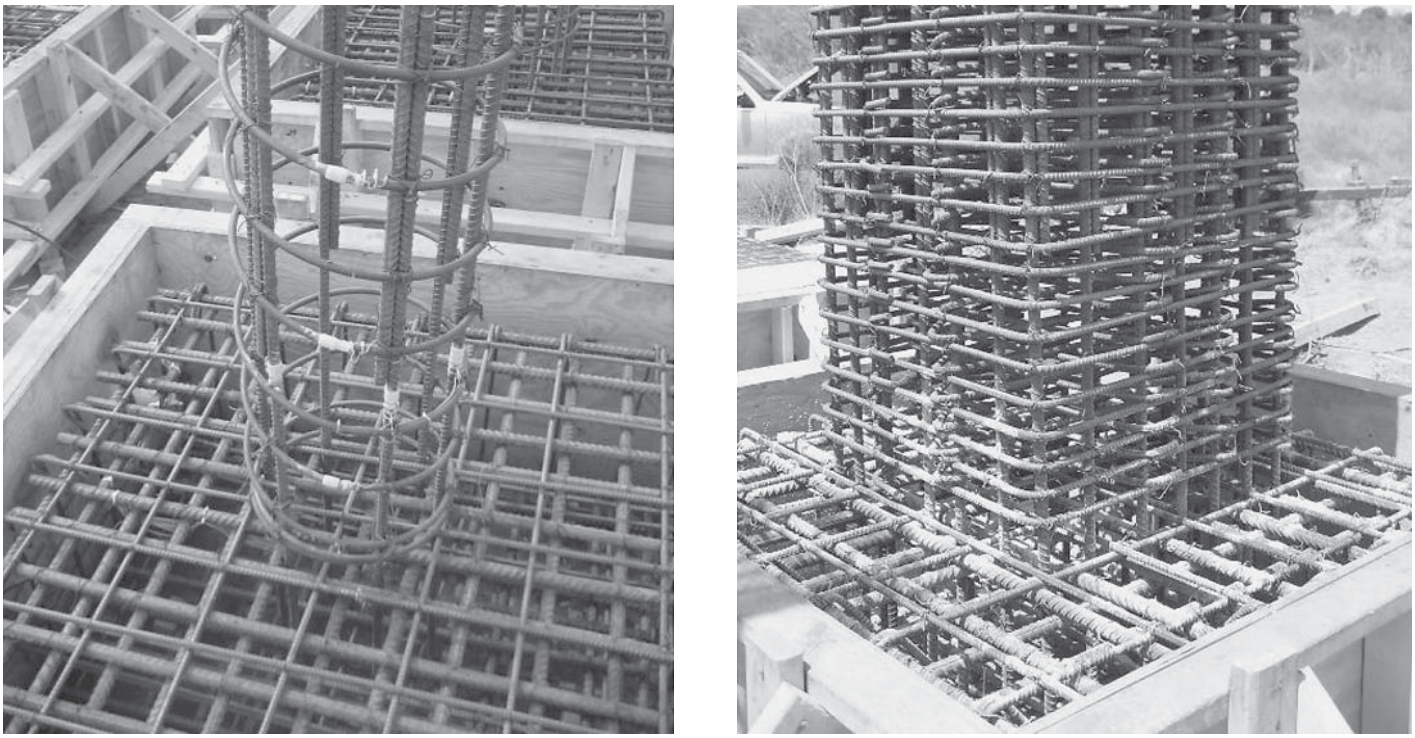

(a) (b)

Figure 35. Column footing and column rebar cage: a) column 1B, b) column 3-blast.

bolted to the reaction structure to provide the pinned connection near the top of the column. It should be noted that over the course of the test program the slab of the reaction structure experienced significant damage and may have allowed some rotation to occur at the base so that the assumed boundary conditions were not fully realized. To address this concern, the analysis of the test data and evaluation of column response considered the effect of rotation at the base. Analysis of the data and evaluation of column behavior during the test program are described in Chapter 5.

3.3.7 Spall/Breach Test Setup

The goal of the local damage tests was to observe the spall and breach patterns of columns subjected to close-in blasts. Therefore, end restraints against displacement or rotation were

Figure 36. Wooden spacers.

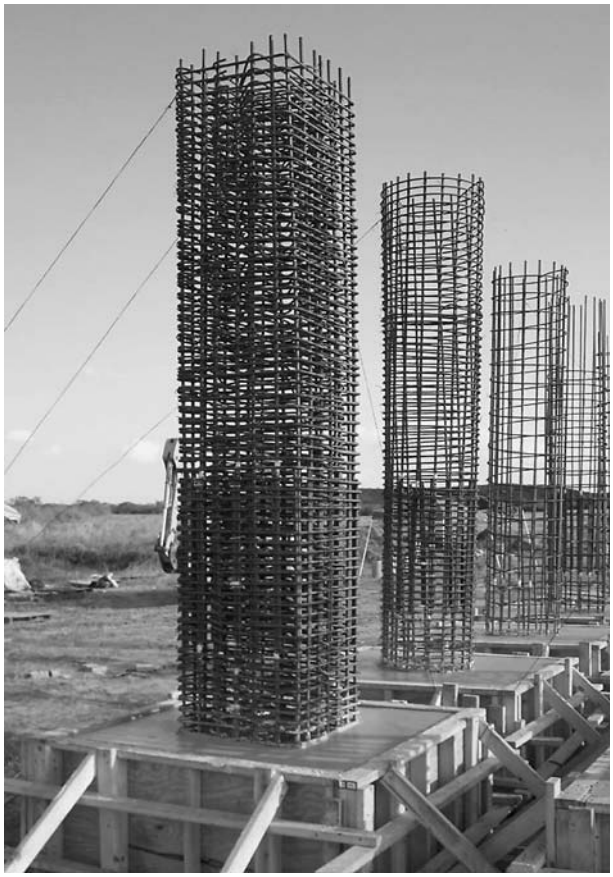

Figure 37. Column rebar cage.

Figure 38. Column casting.

not needed because only local damage was being observed. The local damage test setup consisted of a standalone column subjected to a close-in blast load in a clearing. The base and top were not supported or restrained from any rotation. Figure 40 illustrates a column just prior testing.

Figure 39. Phase II: Small standoff test setup.

Figure 40. Phase II: Local damage test setup.

3.4 Summary

This chapter presented the design and instrumentation of columns tested during Phases I and II of this experimental research program. The small-scale, non-responding blast test setup was summarized. All of the instrumentation, construction, and testing for Phase I was completed in Vicksburg, MS, by the U.S. Army Engineer Research and Development Center. The setups for the Phase II small standoff and local damage blast tests were also summarized. All Phase II instrumentation, construction, and testing was completed at the Southwest Research Institute test site in Yancey, Texas. The following chapter presents the analytical research program.

CHAPTER 4

Analytical Research Program

4.1 Overview

While bridge engineers can adapt many currently available methods to predict blast loads and the response of building components for use with bridges, there is a need for bridge-specific, simple models that provide quick and accurate results because such models facilitate an efficient design process. In addition, the most sophisticated techniques are not always necessary because these methods often require large computational demands and time commitments, while providing a level of accuracy that may not be warranted given the uncertainty associated with identifying threat scenarios and corresponding blast loads. Simple models, however, may not be appropriate for every case due to the complexity of blast loadings and associated responses. The following sections outline characteristics and capabilities of various analysis methods and software, along with guidelines for the selection of the appropriate analysis technique for a given scenario. Load determination programs and response determination programs are typically independent software packages, and thus the information in this chapter is divided accordingly. Because designers benefit from analytical methods that contribute simplicity, efficiency, and accuracy to the design process, information is provided to aid in the selection of the simplest and most appropriate analysis techniques for a particular case. Therefore, characteristics, advantages, limitations, and current uses are provided for each analysis level, and a brief description of commonly used analysis software is given.

While the capabilities of some of the software discussed have been verified by past research found in the literature, the assertions of other programs have *not* been verified. Moreover, the authors do not endorse any particular software or program, and the codes listed below are simply examples of applications one *could* use to predict loading and response. In all cases, predicting blast loads and response requires the discretion of an engineer experienced in the field of blast analysis, and analysis methods that are based on or corrected by empirical data are preferable when available due to their accuracy and efficiency. These semi-empirical programs, however, are often not available due to a lack of existing data or because they have limited distributions and are available only to government contractors.

4.2 Current State-of-Practice: SDOF

A single-degree-of-freedom analysis is standard practice for most blast-resistant designs. While an analyst *could* employ complex three-dimensional finite element analyses, the uncertainty associated with the threat size and location in blast scenarios typically does not justify such a detailed analysis. "It is a waste of time to employ methods having precision much greater than that of the input of the analysis" (Biggs, 1964). Furthermore, unlike traditional design loads, most blast designs allow significant nonlinear behavior to dissipate the energy associated with dynamic blast loads, and SDOF results compare well with experimental test data when members experience considerable plastic deformation (Department of the Army, 1990). Additionally, consideration of multi-member coupling is not necessary if the natural frequencies of connected elements differ by a factor of two or more (Biggs, 1964). Therefore, a member-by-member SDOF analysis approach is applicable for most blast design scenarios and represents the current state-of-practice for blast-resistant structural design.

Structural Dynamics: Theory and Approach by Joseph Tedesco (1999) and *Introduction to Structural Dynamics* by John Biggs (1964) both include a basic introduction to SDOF systems and the application of structural dynamics to blast-loaded structures, and this section summarizes SDOF analysis concepts pertaining to blast-loaded structures. Figure 41 illustrates an SDOF system comprised of a simply supported beam with a uniformly distributed load on half the beam and a corresponding deformed shape, $\Delta(x)$. Shown in

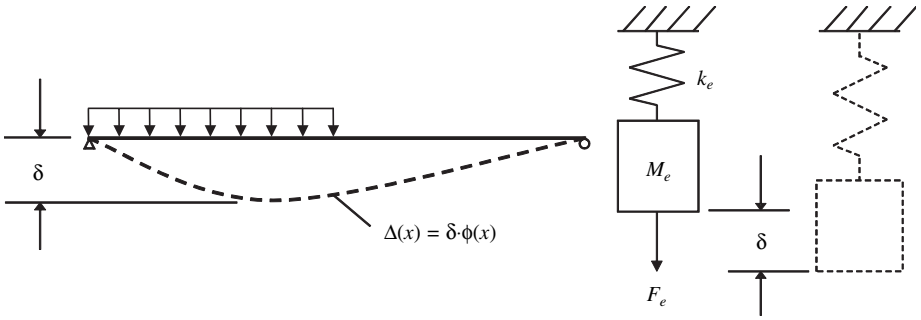

Figure 41. Idealized SDOF system.

the figure is the idealized spring-mass system with an equivalent mass, M_e, that goes through a displacement, δ, against the resistance of an equivalent stiffness, k_e, under the application of an equivalent force, F_e. An engineer can transform the real system into the idealized system and obtain equivalent system properties by applying work and energy principles to the real beam using an assumed normalized displaced shape. In the SDOF method, each stage of response has a different mode or characteristic displaced shape that requires the computation of unique equivalent beam properties. Figure 42 illustrates the deflected shapes and resistance diagrams of a fixed–fixed beam that undergoes three stages of deformation: purely elastic, a combination of elastic and plastic, and purely plastic. The accuracy of the SDOF method depends on how well the assumed deflected shapes represent each stage of response of the real structure in both space and time (ASCE, 1997). While the total response of a continuous member theoretically includes contributions from an infinite number of individual modes, the response of an SDOF system relies only on a single mode of deformation for each stage of response. This simplification is possible when one mode dominates the response, as is often the case for blast-loaded components. Most designs of structures to resist blast allow significant inelastic deformation, and the displaced shape associated with the plastic mechanism ultimately dominates the response. While the analysis could use one of the modal shapes that correspond to a vibration mode during each stage of response of the structural component, the SDOF method typically uses the displaced shape resulting from the application of a static load that has the same form as the assumed blast load. The value of δ for the real beam in Figure 41 is equal to the displacement of the equivalent SDOF system, both in magnitude and in variation with time, at the point of maximum deflection. The use of a static displaced shape as the only mode shape simplifies calculations because for many structural members it is too difficult to determine mode shapes exactly, and for most practical applications, this assumption provides more accurate results than using only the displaced shape that corresponds to the first mode of vibration (Biggs, 1964). Using the assumed normalized displaced shapes for each stage of response, an analyst may choose to derive equivalent SDOF system transformation factors based on work-equivalency

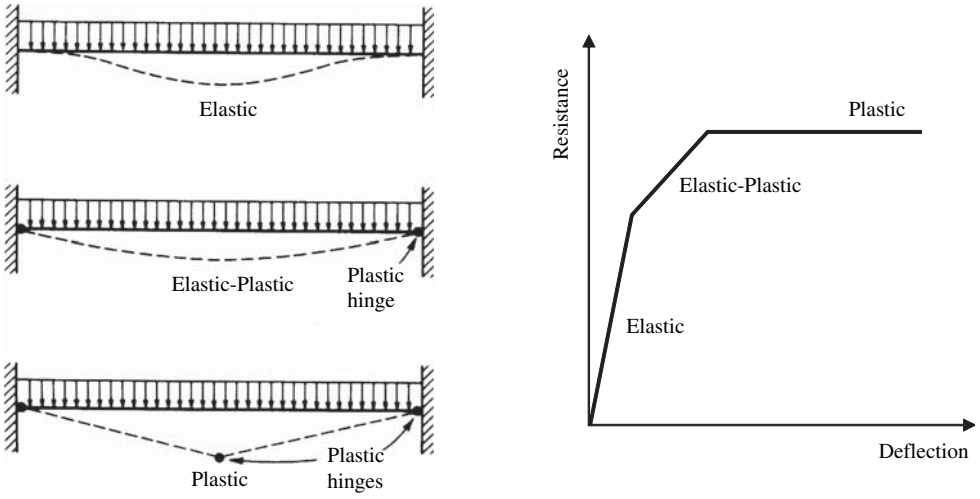

Figure 42. Stages of response for fixed–fixed beam (Biggs, 1964).

principles or use factors for known scenarios. Transformation factors for known scenarios can be found in *Introduction to Structural Dynamics* by Biggs (1964) and the U.S. Army's TM 5-1300 *Structures to Resist the Effects of Accidental Explosions* (Department of the Army, 1990).

Blast-resistant designs typically allow inelastic (i.e., permanent) deformations to dissipate energy, and SDOF analyses also include this behavior. "Although plastic behavior is not generally permissible under continuous operating conditions, it is quite appropriate for design when the structure is subjected to a severe dynamic loading only once or at most a few times during its life. Among other examples which might be cited, plastic behavior is normally anticipated in the design of blast-resistant structures and at least implied in the design of structures for earthquake" (Biggs, 1964). Plastic hinges and mechanisms can form during a blast scenario, allowing a structure to dissipate energy through large plastic deformations and rotations. This plastic deformation is important in structural design for dynamic loads because allowing a structure to dissipate energy creates the most economical design possible (ASCE, 1997).

"The primary method for evaluation of structure response is evaluation of the ductility ratio and hinge rotations" (ASCE, 1997). *Structures to Resist the Effects of Accidental Explosions* (Department of the Army, 1990) and *Design of Blast Resistant Buildings in Petrochemical Facilities* (ASCE, 1997) provide allowable rotation limits for various types of structural members. For the case of blast design, hinge rotation refers to a support rotation and indicates the degree of deformation present in critical areas of a member. Equation 12 defines a ductility ratio that measures the overall inelastic response of a structural component.

$$\mu = \frac{\Delta_{max}}{\Delta_{elastic}} \tag{12}$$

where:

μ = ductility ratio
Δ_{max} = maximum displacement of a member (in.)
$\Delta_{elastic}$ = displacement at the elastic limit (in.)

The ductility ratio and hinge rotations should not exceed allowable response limits from current blast guidelines (ASCE, 1997). Existing guidelines, however, are applicable to building components, and the limiting values will likely require adjustment as test data on the response of bridges subjected to blast loads become available (see Chapters 6 and 8). Hinge rotations are separated into three levels of response: low, medium, and high. A low level of response includes localized structure or component damage. The main structural components do not need repair, while nonstructural components require moderate repairs. A medium level of response entails extensive structure or component damage. In the case of a medium level of response, the structure cannot sustain normal loads until repairs are complete, and the total cost of those repairs is significant. A high level of response includes a structure or component that does not retain structural integrity, and this structure or member may collapse under minor loads from environmental conditions (e.g., wind, snow, rain). The total cost of repairs for a high level of response approaches the replacement cost of the structure (ASCE, 1997).

In general, the shear reinforcement detailing and the controlling stress states influence the response limits for reinforced concrete members. The allowable deformations are very low for elements with significant shear or compression demands, while large deflections are permitted when a member has adequate shear capacity. As shown in Table 9, hinge rotations alone are specified for concrete elements in flexure because the relatively stiff nature of concrete members produces very high ductility ratios for members with low maximum deformations, indicating that the use of a ductility ratio is inappropriate for these conditions. Elements responding primarily in shear are subject to brittle failures at low support rotations; therefore, the ductility ratio is the main design criterion for these elements (ASCE, 1997).

For blast-resistant structural design, shear demand is typically calculated based on the flexural capacity associated with an SDOF analysis. Both direct shear and diagonal shear are important for blast-loaded components, and structural members should contain enough capacity through a combination of transverse reinforcement and longitudinal reinforcement dowel action to prevent a shear failure and force a flexurally dominated response. While a member-by-member analysis uses the loads that result from the reaction forces and applied load of an SDOF analysis to load a supporting member, the shear design should not consider these loads because the deflected shapes assumed for those analyses do not match the actual deflected shape of a component early in time when shear dominates the response. Rather, designing a member to have enough shear capacity to prevent shear failure and allow a flexurally dominated response will provide satisfactory behavior. Thus, a designer should consider the available shear capacity of a member only after it has sufficient flexural capacity to resist the assumed blast loads, and a plastic analysis using the assumed load distribution and the plastic moment of the *final* section provides the maximum distributed load the member must sustain prior to forming a mechanism leading to flexural failure. The shear demand resulting from this analysis is the theoretical maximum shear a member will experience during an event that loads a component with the assumed load shape, and thus it is the shear demand a member must resist. The U.S. Army Technical Manual 5-1300 *Structures to Resist the Effects of Accidental Explosions* contains

Table 9. Response criteria for reinforced concrete.

Element Type	Controlling Stress	Ductility Ratio, μ_a	Support Rotation†, θ_a (degrees)		
			Low	Medium	High
Beams	Flexure	N/A	1	2	4
	Shear[1]:				
	Concrete Only	1.3			
	Concrete + Stirrups	1.6			
	Stirrups Only	3.0			
	Compression	1.3			
Slabs	Flexure	N/A	2	4	8
	Shear[1]:				
	Concrete Only	1.3			
	Concrete + Stirrups	1.6			
	Stirrups Only	3.0			
	Compression	1.3			
Beam-Columns	Flexure:		1	2	4
	Compression (C)	1.3			
	Tension (T)	-- ‡			
	Between C & T	10			
	Shear[1]	1.3			
Shear Walls, Diaphragms	Flexure	3	1	1.5	2
	Shear[1]	1.5			

[1]Shear controls when shear resistance is less than 120% of flexural resistance
†Stirrups are required for support rotations greater than 2 degrees
‡Ductility Ratio = 0.05 (ρ - ρ') < 10
Source: *American Society of Civil Engineers, 1997*

information on computing the shear demand and capacity for structural components, and the ACI and AISC design manuals contain additional information needed to calculate the shear capacity of concrete and steel members, respectively.

4.3 Simplified Modeling and Software

Blast design specialists have a large number of options when choosing a technique or software to compute blast loads and structural response, and these methods vary widely in both cost and accuracy. While an analyst may desire results from high-level finite element analyses, the exact location and magnitude of a threat typically remains unknown, and the uncertainty surrounding load prediction typically does not justify the cost of such high level analyses. As a result, several simplified methods for both blast load and response prediction are available to bridge engineers. This section describes the capabilities and limitations of several such procedures.

4.3.1 Load Prediction Techniques

Simplified load prediction techniques fall into two groups. The first group contains the methods that utilize blast phenomenology from basic equations and curves developed empirically from "ideal explosions" in free air. The second group of load determination methods, which is described in the following subsection, includes those that consider multiple reflections and pressure magnification, while not strictly employing computational fluid mechanics techniques. The following two subsections describe both types of load prediction techniques.

4.3.1.1 Free-Field Load Prediction Techniques

Ideal explosions include bare spherical charges in air or hemispherical charges on the ground. Many researchers have conducted controlled experiments using ideal explosives over many years, and several curve fits allow engineers to quickly determine basic blast load parameters, such as peak overpressure, peak reflected pressure, positive phase duration, negative phase duration, time of arrival, and impulse. From these parameters, a designer can construct an elementary pressure–time history. Several texts, military manuals, and computer programs include various forms of these equations and curves, including the U.S. Army TM 5-1300 *Structures to Resist the Effects of Accidental Explosions* (Department of the Army, 1990), the Unified Facilities Criteria (2002), and ConWep (U.S. Army Corps of Engineers, 2001), which is a widely used software application that provides an automated version of these equations and curves. These basic techniques are very useful for preliminary designs and other basic problems. As they are based on explosions in free air, these methods cannot

represent reflections off and interactions with structures, and any user must clearly understand the limitations of the selected method before applying it to a specific loading case.

While simplified analyses using available equations and curves are useful for relatively large-standoff problems (i.e., where the center of detonation is greater than a scaled range of three or more from the structure under study), they typically do not provide good results for small-standoff problems because the accuracy of the empirical data decreases at close ranges. The definition of scaled range (i.e., scaled standoff) is the actual distance from the center of an explosive to the target, divided by the equivalent TNT charge weight raised to the ⅓ power (i.e., $Z = R/W^{1/3}$). The analyst must remember that the data included in these simplified load prediction methods are from actual field measurements during detonation events, and very close-in data have been, and still remain, very difficult to measure due to extremely high temperatures and pressures in the immediate vicinity of an explosive source. Because most critical threats associated with bridge-related blast problems will likely involve very close-in detonations with scaled standoffs much less than 1 ft/lbs$^{1/3}$, analysts should consider the limitations in using simplified load prediction techniques for computing blast-load parameters for such scenarios.

Additionally, these analysis methods do not account for reflections and confinement, which can be significant for several scenarios involving explosives acting against bridges, such as a detonation inside a box girder and a detonation beneath a bridge overpass. Pressures from confined and partially confined explosions cannot dissipate as quickly as unconfined explosions, and as a result, they can produce much higher impulses on a structure (Ray et al., 2003). Magnification factors exist, though, to adjust incident blast pressures for varying levels of confinement, and one can choose values conservatively with success (Gannon, 2004).

Because of the associated limitations, methods that utilize blast phenomenology from basic equations and curves developed empirically from "ideal explosions" in free air may not be adequate for determining design blast-load parameters for many applications. They may be useful and adequate, however, for cases when only one reflection is significant (e.g., above-deck blasts). These techniques also provide a useful and expedient "sanity check" for high-level blast prediction software packages (i.e., nonlinear finite element analyses employing computational fluid dynamics). While such advanced programs can produce impressive graphical results, the analyst should always study the results to ensure against the "garbage-in-garbage-out" possibilities of large, data-intensive calculations.

4.3.1.2 Load Prediction Techniques That Consider Confinement and Reflections

The most widely used application in this group is BlastX (SAIC, 1994). The BEL code (U.S. Army Corps of Engineers, 2000) is an open-distribution version of BlastX that includes a bridge-specific graphical user interface. Although some of these load determination techniques are intended to model blast propagation through enclosed areas such as buildings, they can be adapted for use with bridges. These methods track pressure values as they radiate from an explosion source and as they reflect off surfaces through basic first-order principles of wave reflection. In addition, they can include correction factors to account for differing wave magnitudes reflecting off various surfaces. As a result, they provide higher accuracy than those load determination methods that do not consider confinement and reflections. In addition, a recent study investigated the use of BlastX for modeling a blast below a bridge deck, and the results showed that BlastX has the ability to provide conservative but reasonably accurate results for this case (Ray et al., 2003). The authors of this report caution, however, that results from these codes require additional adjustments for some scenarios. For example, software such as BlastX and BEL are not capable of modeling round geometries such as columns of bridge piers, and experimental and analytical research described in this report show that these codes significantly overestimate loads on slender square and circular members (i.e., bridge columns) subjected to blast loads.

This second group of load determination analysis methods is recommended for use in bridge design because they consider reflections and pressure magnification. For most cases, the result is an acceptably accurate but conservative loading obtained at a modest computational cost, although inaccuracies incurred when modeling explosions against slender flat or curved members (i.e., bridge columns) were overly conservative in some cases. *This method should not be employed for contact charges as it does not predict internal detonation pressures (i.e., pressures that have not gone through the explosive detonation product–air interface). Its use for very complex environments with many varied reflecting surfaces should also be carefully considered, and, if possible, a fluid-mechanics or empirically based model should be used instead.* The capabilities and limitations of load prediction methods based on fluid mechanics are discussed later in this document.

4.3.2 Response Prediction

Engineers may choose from a wide variety of methods when analyzing the responses of structures subjected to blast loads, ranging from simple and easy-to-use SDOF analyses to highly complex, 3D nonlinear finite element analyses. While advanced finite element codes are advantageous for specialized design, research, and post-event scenarios, the uncertainty in the load prediction does not usually justify this level of effort for most design problems. Additionally, simplified methods for response prediction are extremely useful for providing a baseline by which to validate the results of high-level finite element analyses. Thus, all engineers analyzing structures

subjected to blast should be familiar with the advantages, uses, and inadequacies of simplified analysis methods. This section describes two levels of analyses for predicting structural response due to blast and includes examples of commonly accepted and used software.

4.3.2.1 Single-Degree-of-Freedom Systems

The simplest response determination methods are those based on SDOF mass-spring-damper systems. The vast majority of currently available design procedures for blasts utilize these approximate systems (Conrath et al., 1999) because they provide reasonably accurate estimates of response while minimizing time and cost. Accordingly, uncoupled SDOF analyses are the most widely used methods for determining response to blast loads throughout the structural engineering community. For example, engineers frequently use these methods in the design of structural members for sensitive control rooms (Barker and Whitney, 1992), and investigators used an SDOF method to analyze the response of the blast-loaded columns and slabs in the Alfred P. Murrah federal building (Mlakar et al., 1998) that was attacked in Oklahoma City in 1995. In addition, the U.S. Army TM 5-1300 *Structures to Resist the Effects of Accidental Explosions* (Department of the Army, 1990), which is widely considered to be one of the leading references for blast-resistant design, recommends SDOF analyses for most cases.

Although it may seem that higher resolution techniques are preferable because blast loadings and the resulting responses are often very complicated, such accuracy is not necessarily warranted. Many uncertainties exist in blast loadings, including the location of the explosive, the magnitude of the explosive, and the type of explosive. Unless a very specific threat is expected, a general understanding of structural response to an assumed blast source, which can be provided by SDOF methods, is sufficient for design. John Biggs, a former MIT professor who pioneered SDOF analyses for response to blast loads and whose work provides the basis for most blast-resistant design and analysis procedures currently used (including the Army's TM 5-1300), wrote that SDOF analysis techniques "should not be regarded as merely crude approximations, to be used for rough or preliminary analysis, nor should they be regarded as methods to be used only by engineers who lack the training or intellect to employ more sophisticated techniques. Problems in structural dynamics typically involve significant uncertainties, particularly with regard to loading characteristics. It is a waste of time to employ methods having precision much greater than that of the input of the analysis" (Biggs, 1964).

If desired, an analyst can combine an SDOF analysis with a continuously updated sectional analysis when varied localized changes in material behavior through the depth of a cross-section may significantly affect member resistance. Because this approach considers composite material behavior and changes in constitutive properties through the depth of a cross-section, it may be useful when a member does not have an easily identifiable single value for the yield moment, such as with prestressed concrete girders, or when the assumption of idealized hinging may not be appropriate, such as when loads vary considerably over the length of a member. Examples of sectional analysis programs include RCCOLA (Farahany, 1983), RESPONSE-2000 (Bentz, 2001), and RECONASANCE (Alaoui, 2004). Although this procedure will provide more accurate representations of cross-sectional behavior, little is known about the accuracy of the resulting response compared to responses determined by ordinary SDOF analyses, and engineers should study the results carefully before implementing this procedure as common design practice.

It is possible to use hand calculations with simple formulas for SDOF response determination, and charts are also available in Bigg's *Introduction to Structural Dynamics* (Biggs, 1964) and the U.S. Army's TM 5-1300 *Structures to Resist the Effects of Accidental Explosions* (Department of the Army, 1990) to establish the SDOF nonlinear response of structural elements. In addition, many easy-to-use programs, such as SBEDS (U.S. Army Corps of Engineers, 2007) and SPAn32 (U.S. Army Corps of Engineers, 2002), exist for this purpose. Some SDOF response determination techniques, such as the "Israeli Method," incorporate empirical data to improve the accuracy of SDOF analysis results (Eytan, 1992). In the "Israeli Method," a load determination program called Car Bomb (Eytan, 1992) first independently produces the load on a structure, and then SDOF models determine the response of structural members. The models, however, include input coefficients that relate to the specific design scenario. These values come from extensive data and adjust the response obtained by the SDOF analysis to provide more accurate results than might be computed without such adjustments. As indicated earlier, *any model that is accurately adjusted or has been accurately validated using empirical data should be used when available.*

Even if an engineer feels it is necessary to use higher level analysis techniques to compute structural response to blast loads, SDOF analyses are extremely useful for the preliminary design and sizing of members (American Society of Civil Engineers, 1997; Biggs, 1964; Conrath et al., 1999; Department of the Army et al., 2002). Parameter studies with high-level models, such as with MDOF models, may not be practical due to the large number of input requirements. Moreover, 3D nonlinear general-purpose finite element analyses are not conducive to parameter studies due to the large amount of time needed to build, mesh, refine, and run a model. The limited number of input values needed to define an SDOF model, however, facilitates extensive parameter studies. Therefore, if an analyst desires results from high-level analyses, SDOF meth-

ods may be useful to size individual members before using a high-level model to verify the global response of the structural system. Practicing blast engineers sometimes use this type of procedure involving a progression of analyses (Hinman, 1998).

SDOF models are valuable because they can provide reasonably accurate predictions of response for a wide range of structural components. This accuracy is in large part attributed to the use of complex spring resistance (i.e., load-deformation) functions that are based on empirical data. Such resistance functions can account for complex modes of behavior, including tensile and compression membrane effects and member instabilities. Because blast scenarios are unpredictable, detailed response analyses of attack scenarios are often not necessary. Rather, understanding the response of a member due to a general threat is sufficient for designing blast-resistant structural components. Many components, whose end restraints can be readily determined or conservatively estimated, can be analyzed by such methods. Examples include beams, slabs, columns, and walls. Bridge applications include the analysis of individual girders, piers, and truss members as well as individual wall sections of towers and box girders. In some cases, as is often done for the analysis of bridges subjected to seismic events (BERGER/ABAM Engineers Inc., 1996), composite sections can be modeled as responding as a single element so that bridge decks and entire superstructures may also be analyzed using SDOF techniques. Such an approach may not always be appropriate, however, and guidance concerning the limitations of SDOF analyses is provided below.

When appropriate assumptions for end restraints are unclear, boundary conditions can be assumed and then varied to maximize the response quantity of interest. For example, a propped-cantilever or two fixed ends can be conservatively assumed for shear calculations because design criteria are based on maximum forces at the supports, and the stiff end restraints associated with the fixed support condition will lead to conservative estimates of the required shear capacity. For flexural calculations, because maximum deformation controls the design, simply supported ends can be conservatively assumed (the cantilever case should also be verified not to control the design). Moment capacities can be adjusted to include the effects of axial loads by using interaction diagrams, and resistance diagrams can be approximated by straight lines.

For the reasons mentioned above, use of an SDOF analysis is the most appropriate choice for the design of most individual bridge components and systems, including those often designed for non-blast loads using MDOF frame analysis procedures. Although SDOF analyses can only consider one component at a time, the interaction between two structural components can be considered by determining the reaction forces as a function of time that must be transferred from one component to another (American Society of Civil Engineers, 1997; Conrath et al., 1999; Department of the Army et al., 2002). This approach has been shown to provide acceptably accurate predictions of structural performance when the ratio of the natural period of the connected components is larger than or equal to two (American Society of Civil Engineers, 1997; Conrath et al., 1999; Department of the Army et al., 2002).

Although SDOF methods can be used for most structural members, discretion should be used when choosing the most appropriate analysis method. For example, the designs of some bridges, including suspension and cable-stayed bridges, do not ordinarily receive guidance from AASHTO specifications because they require extensive experience or high-level analyses even for "ordinary" loadings, such as dead loads, live loads, wind loads, and seismic loads. The designs of the systems and components of these bridges often require specialized engineering firms that use high-level finite element analysis software such as that described in Section 4.3.3. For those bridges, the choice of analysis methods when designing for blast loads should reflect the same considerations that require advanced analysis procedures or experience to design for "ordinary" loads. As mentioned above, it is important to remember that, although some structures require sophisticated analysis procedures, SDOF methods are well-suited for the preliminary sizing of most components and the complete design of many bridge members, including those bridges often designed using MDOF frame analysis codes.

Because SDOF analyses provide acceptable results while minimizing costs, they should be used whenever possible. Some limitations for their use do exist, however, and such methods should not be used for all purposes. In general, SDOF analyses can and should be used for any and all structural components that are not included in the following cases:

- **Cases when conservative load values are not acceptable.** Because SDOF procedures are uncoupled, blast loads computed from load determination methods may be inaccurate if significant localized failure and venting occurs, such as when trying to use only an SDOF analysis to model an entire bridge superstructure that may experience load relief if part of the deck fails and vents pressure. If the use of conservative loads that do not account for pressure relief due to localized structural failure within the component being analyzed is not acceptable, the analyst should use an alternate modeling approach in which connected components (e.g., bridge deck and girders) are treated as individual SDOF systems where the reactions from the directly loaded component act as the load input to the supporting component. The vast majority of cases do not require coupled analyses. SDOF analyses typically can account for the effects of localized failure and venting through modification of system properties much more readily than performing a coupled analysis.
- **Cases when localized failure may occur.** Examples of such localized failures include spall and breach for concrete

members and local buckling and fracture for steel members. These failures often result from close-in or contact blasts, but they are not necessarily limited to such attacks. Although it is possible to use reduced cross-sections, especially for concrete members, to alter existing SDOF methods to account for such events, it requires extensive experience and knowledge of the failure mode. Some empirical methods exist for concrete members to determine response involving localized failure, but they are often not publicly available and are applicable only to specific cases. Because such failures often can be unpredictable, varying widely according to both blast and component characteristics, scenarios with the potential for localized failure should be analyzed with care, and SDOF methods should not be used for all members and all standoffs.

- **Cases when the failure mode is uncertain.** Although SDOF methods may be able to determine structural response up to failure for individual members within a system, they cannot predict global response when the failure mode is uncertain, such as with highly confined blasts, when potential structural instabilities exist, or when localized material or member failure may occur. Examples potentially include blasts at abutments, within double-decked bridges, within or close to hollow piers, within or close to segmental box sections, in contact with a structure, and with significant fragmentation.
- **Cases when P-Δ effects may contribute to failure.** Although axial-flexural interaction diagrams can be used to alter member resistance to account for changes in moment capacity due to axial loads, typical SDOF analyses generally do not consider P-Δ effects. It may be possible, however, to incorporate an iterative technique that accounts for geometric nonlinearity within SDOF calculations. Such techniques are not common, and inexperienced analysts should not use SDOF methods to analyze long, slender, axially loaded members that may experience P-Δ effects. Tall bridge piers loaded by large surface blasts are examples of such members. The terms "tall bridge piers" and "large surface blasts" are intentionally vague because each design scenario will be unique, and an experienced engineer will need to determine whether or not P-Δ effects will be significant.
- **Cases when the member under consideration is not sufficiently slender.** Most currently available SDOF methods neglect rotational inertia and shear effects by default. Therefore, analysts should be careful when using SDOF methods to analyze deep members. Examples of such non-slender members include concrete anchors for suspension bridge cables, short columns, most pier caps, and deep beams. It is important to point out, however, that the resistance function and stiffness can be modified to account for shear deformation and rotational inertia if these effects are considered to be important for the problem under consideration.
- **Cases when loading exists on more than one principal axis.** Loading on more than one principal axis may result in biaxial bending or torsion. Current SDOF methods cannot determine such responses, and constructing a new code for such purposes would be difficult due to the essentially infinite number of various structural members that can respond in any direction. An example is a bridge superstructure loaded by a vehicle bomb detonating at an angle to the superstructure.
- **Cases when the loading is not centered on the primary axis (i.e., not centered along the width) of the member considered.** Off-centered loading can create biaxial bending and torsion, and, as mentioned previously, SDOF methods cannot easily determine these types of responses. An example is a bridge superstructure loaded by a vehicle bomb at a widthwise edge of a bridge (i.e., near the railing).
- **Cases when more than one mode shape may contribute to the response.** Although a distributed-mass modal analysis can accurately determine such responses, pure SDOF methods cannot because they assume the response to be characterized by a single mode shape, which is approximated by a characteristic deflected shape. Examples in which SDOF methods may not be accurate include cables and very long superstructures as well as structures in which the response is primarily elastic.
- **Cases when the blast load cannot be easily approximated over the entire affected area as a function of time.** If significant load variations occur over the length of the structure being analyzed (i.e., blast pressures arrive at significantly different times or structural geometry prevents easy approximation of the pressure distribution), the load will not be adequately represented by a simple time function, and a more substantial analysis may be required. Examples may include close-in blasts and blasts against unusual structural geometries involving multiple corners and steps.
- **Cases when the rebound response will be significant, possibly causing failure in the reverse direction.** Although SDOF analyses can predict rebound of members, the accuracy of these calculations is uncertain. Damage incurred during the initial response may alter the resistance capacity for the rebound response. No specific examples of these cases are available because the significance of the rebound phase depends solely on the characteristics of each member and loading considered.
- **Cases when more than one member contributes to the response.** SDOF methods intrinsically lend themselves to the analysis of only one member or component. Thus, any component that receives significant structural contributions from an attached system should not be analyzed using SDOF models. Examples include entire superstructures when the determination of individual member failure is desired and piers when knowledge of the contribution of

the superstructure is desired. In most cases, however, assumptions can be made for the end restraints in order to use SDOF analyses to obtain conservative results.

- **Cases when changes in material behavior that varies through the depth of a cross-section may influence response, preventing easy approximation of an effective resistance diagram based on static loading.** Examples of such localized material behavior that may affect response include local plastic deformation, failure of extreme fibers, strain-hardening, localized strain-rate effects, or strain-hardening induced material changes. Because typical SDOF analyses use approximate resistance diagrams based on a static load-deflection curve, they typically do not include the effects of localized changes in material behavior. Assuming a direct transition from linear response to a plastic hinge for cross-sectional behavior may not adequately represent material behavior. In addition, when the loading varies significantly across the length of a member, idealized hinging may not be appropriate. In these cases, MDOF frame analyses may be necessary

4.3.2.2 Multiple-Degree-of-Freedom Systems

In some cases, engineers may need to use response techniques consisting of 2D or 3D MDOF structural analysis software when simplified response analysis procedures cannot adequately analyze a structural component. Examples of these programs include ETABS (Computers and Structures Inc., 2006a), SAP 2000 (Computers and Structures Inc., 2006b), and RISA 3-D (RISA Technologies, 2005). These techniques have several advantages that, for many cases, provide more accurate and reliable results than simplified response determination methods such as SDOF analyses. For example, MDOF 2D and 3D structural analysis software can determine the interaction among the individual responses of multiple members within a structural system, providing a better understanding of global behavior than can a combination of individual SDOF analyses. In addition, MDOF frame analysis methods can investigate member response that is governed by more than one mode shape, and they can also predict response due to P-Δ effects. Furthermore, while MDOF systems provide these advantages over SDOF analyses, MDOF frame analysis software packages are easier to use than general-purpose finite element analysis procedures.

As with any analysis method that provides an increase in accuracy, however, MDOF systems have additional costs over SDOF models due to the additional time needed to build and analyze models. Additionally, MDOF analysis methods exchange increased accuracy of response calculations with more complex loading input demands. Because a blast may load multiple members within a structural system, the analyst may need to calculate and output several complex load histories with differing pressure magnitudes and time variations for a large number of targets and then input these values into the analysis model. Because of the given structural geometry and the need to account for interaction among various structural components that lead to the need for an MDOF analysis, it is expected that at least a load determination method that considers reflections and confinement, which may be difficult to obtain without proper authorization, would be necessary in order to track and record blast pressures at this level of detail. Even with such methods, the initial geometry of the structure would provide the framework for the loading, and, because the loading would not reflect localized failure of members that may occur within a model, an inaccurate prediction of behavior may still result. On the contrary, when SDOF analysis methods are used individually on members within a structural system, the reaction forces of the first member loaded become the loading on the members supporting the first member. Thus, the reaction forces that pass from one member to another reflect the load reduction observed in some members due to the occurrence of individual member failure.

Although the increased accuracy provided by MDOF frame analysis methods can be very useful for some design situations, it is important to understand that this level of accuracy is not always warranted. For example, the interaction of structural members is only important when the natural periods of the interacting members differ by a factor less than two (American Society of Civil Engineers, 1997; Biggs, 1964; Conrath et al.; Department of the Army et al., 2002). For all other cases, SDOF systems yield sufficiently accurate results, and the reaction forces of one member can be used to accurately load another member. Also, in comparison to SDOF analytical methods, which have minimal input requirements, MDOF frame analysis methods require greater time and effort for conducting parameter studies. Thus, the analyst may desire SDOF methods for the initial sizing of members.

It is important to note that MDOF analyses may not be sufficient for all purposes. While SDOF analyses can provide accurate representations of blast-loaded components because spring resistance functions can account for complex modes of deformation, incorporating such features as large deformations and membrane effects, MDOF frame analysis models cannot typically rely on the same empirical data to compute results with the same degree of accuracy as the SDOF analyses. The ability of MDOF models to provide reasonable predictions of structural response to blast loads will depend on the ability of the software to account for nonlinear dynamic behavior, including both large deformations and inelastic material response. Furthermore, the results will also depend on the methods used to model a structure, including the number of elements selected to represent a particular structural component, location of the nodes, and so on. As mentioned above, SDOF analyses may reveal the effects of individual

member failure on response that MDOF frame analysis methods may fail to capture. Moreover, because MDOF analysis methods are not coupled (at least in the context in which they are being described in this section), they cannot determine load changes due to structural response, and, accordingly, they incorporate overestimated blast loads, which can result in structural members being overdesigned. In addition, MDOF methods cannot predict spall and breach without significant adjustments that require a very experienced engineer. Thus, a high-level model and a specialist are required for such predictions (Conrath et al., 1999).

Although MDOF frame analysis methods can be very useful for determining the response of complex structural systems involving the interaction of multiple members, contributions from multiple modes, and the influence of P-Δ *effects, they are not appropriate for the following cases:*

- **Cases when localized failure or large localized deformations may affect response.** Although MDOF frame analysis methods can determine the effect of individual member response on the global response of structural systems, they cannot take into account the effects of member material loss due to localized failure such as breaching or spalling. If such damage is likely, the problem will require a more sophisticated analysis and a very experienced analyst. Examples of such cases include blasts against hollow piers and close-in or contact blasts against any member.
- **Cases when localized failure is expected to affect loading.** Because MDOF frame analysis methods are uncoupled, they cannot determine changes in loading due to localized failure or large deformations, which can result in venting. In some cases, such as with blast pressure on a bridge deck, venting can reduce loads on other structural members (e.g., the girders), affecting global response and reducing the required resistance of structural components in the system. In other cases, such as with blast pressure against hollow piers, failure of a wall can cause blast pressures to vent into the interior of the pier. Neglecting the effects of venting by using MDOF frame analysis methods may greatly affect both loading and response. Examples of cases when the design may be significantly influenced by localized failure include blasts at abutments, within or close to hollow piers, within or close to box-like sections (e.g., box girders, towers of cable-stayed bridges), in contact with a structure, and with significant fragmentation.

4.3.3 Advanced Modeling Methods and Software

While simplified methods for load and response prediction are appropriate for most design cases, some situations require an advanced understanding of blast loading and structural response that SDOF and MDOF frame analysis methods do not provide. Examples include blasts against slender or curved members, explosions within confined regions, venting due to localized failure, and cases in which localized large deformation or member failure may affect response. These analysis problems require 3D computational fluid dynamics models to determine loads and 3D nonlinear general-purpose finite element analyses to predict response. While these methods can produce more accurate results than simplified models and depict behavior not captured by SDOF and MDOF systems, they can also generate highly misleading and erroneous results, and only analysts experienced with both blast phenomena and advanced modeling techniques should conduct and interpret the results of these simulations. This section describes the characteristics, limitations, and uses of various advanced modeling techniques.

4.3.3.1 Explicit versus Implicit Analysis Methods

All computationally based analysis methods employ either an implicit solution technique or an explicit solution technique to solve the governing equations of motion for the system under consideration. Both procedures have unique advantages and disadvantages that make each appropriate for different cases. An implicit method calculates a solution at a given time step based on the equilibrium of the external, internal, and inertial forces in the system at that time step. As a result, depending on the constants used, implicit solutions can be unconditionally stable and can provide accurate predictions of structural response at time steps that are larger than those used with explicit methods. A drawback with implicit methods, however, is that they require the factorization of the stiffness matrix (i.e., inverting the stiffness matrix) for each time step, and this requirement greatly increases computation time for problems in which the stiffness of elements in the structural model change due to nonlinear response, which is often the case with blast loads. The increased computation time is the result of a costly iteration at each time step to determine equilibrium, and each iteration step requires the reformulation and refactorization of a new stiffness matrix that reflects adjustments based on the nonlinearity of the system at that iteration step.

An explicit solution technique, unlike an implicit method, determines response values at each time step based on equilibrium at the previous time step. One outcome of such a formulation is that explicit methods do not require factorization of the stiffness matrix for each time step. Because equilibrium is not satisfied precisely at each time step, however, explicit solutions can become numerically unstable if appropriately small time steps are not chosen. As a result, explicit methods require more time steps than implicit methods to converge to the same solution. Depending on the case being considered,

this fact may make explicit solutions less efficient than implicit solutions.

It is important to note that the solution technique employed by an analysis method varies with each individual program, even within the levels of analysis defined within this document. Thus, it is the responsibility of the analyst to understand how the solution procedure employed by the selected software will influence the computed results. Although many factors must be considered when choosing an appropriate solution technique, most analysts choose an explicit method for complex analyses of structural response to blast because the benefit gained by not having to factorize the stiffness matrix during each time step typically outweighs having to use small time steps. Furthermore, allowing for failure and removal of elements from an analysis model is readily achieved with an explicit code, while such a scenario poses a significant computational challenge for implicit codes. Alternatively, for simple analyses, involving only one member or a system experiencing only elastic response, an implicit analysis may be appropriate.

4.3.3.2 Load Prediction

The most sophisticated level of load determination is defined as one that employs fluid mechanics computations. Examples include SHAMRC (Applied Research Associates Inc., 2005), which is available only to government contractors, and LS-DYNA (LSTC, 2007). These load determination methods are "high resolution" models that use the mechanics and characteristics of fluids (i.e., air in the case of blast) and fluid flow to calculate variations in pressure, density, velocity, and so on as a function of time and position. As a result, they have the ability to consider multiple reflections, pressure magnification, turbulence, pressure buildups, and "hot spots" (i.e., localized areas of large pressure buildup). Thus, very accurate predictions of blast loads can be obtained using these methods. Due to the increased resolution, however, these methods are very computationally intensive, and significantly more personnel time and experience is needed to correctly input required analysis parameters over that required for lower level analyses. In addition, close-in blasts require response calculation (i.e., coupling) to determine the influence of material failure and breach on load variation. Because lower resolution tools have the ability to provide reasonable and conservative results (Ray et al., 2003) and because the specifics of future attacks are generally uncertain, the level of accuracy provided by high resolution models is not warranted for most design cases. The decision to use a highly accurate and likewise expensive computational procedure must be on the basis of a cost–benefit analysis. The expense may be well warranted on a large project where the removal of even small degrees of conservatism could potentially save large amounts of money. In general, however, analyses employing computational fluid dynamics are primarily suggested for research environments and for analyzing past events when a specific attack scenario is known.

4.3.3.3 Response Prediction

Advanced design scenarios, research problems, and post-event evaluations often require general-purpose, uncoupled, nonlinear finite element software packages. The primary distinction that differentiates these analyses from MDOF frame analyses is that the higher level of analysis allows for the discretization of general-shaped geometries using a large number of small elements consisting of solids, plates, shells, beams, and so on. Examples of analysis software with these capabilities include ABAQUS (ABAQUS Inc., 2004), ANSYS (ANSYS Inc., 2004), and LS-DYNA3D (FEA Information Inc., 2006). Among these software packages, LS-DYNA3D is frequently used for predicting the response of structures subjected to blast loads. Finite element analyses make use of a large number of degrees of freedom that interact together, and the model is then analyzed using structural analysis techniques similar to those employed for the MDOF frame analysis methods. Thus, increased accuracy is possible by dividing the system into small, discrete "finite elements." These models are often very complex, however, involving large personnel time requirements to construct a model and input system parameters. In addition, significantly more time is often necessary to analyze a model and to ensure that the results converge to a stable and accurate solution. Because engineers with limited experience can easily input and analyze details of a physical system, unsubstantiated confidence can often be obtained in the validity of the results. Some programs are so complex that they are accurately used only by the developing organization (National Research Council, 1995). Hence, only highly trained personnel should use 3D nonlinear general-purpose finite element methods when absolutely necessary.

Additionally, as analysis techniques become more sophisticated, they move further away from the quantities desired for design. For example, rather than providing bending moment acting at a given cross-section in a beam, nonlinear general-purpose finite element methods typically only give stress, strain, and displacement values at discrete locations. The analyst must take this information and determine bending moment through post-processing of the results. Furthermore, the input and time requirements of this level of analysis are not conducive to the parameter studies often used to size members. Therefore, these methods have limited usefulness for the design of most members. If nonlinear general-purpose finite element techniques are desired for design, the process may be expedited by using lower level analysis methods to size members initially before using these higher level response determination techniques to verify the final design.

Despite the increase in cost, nonlinear general-purpose finite element methods can be valuable because they can provide detailed information regarding failure modes and the effects of localized failure. "Meshes," or grids containing the "finite elements," model the physical system and allow computation of localized effects. Accordingly, these models can be very useful for predicting structural response for scenarios that lower resolution techniques do not easily model. Examples include examining local deformation and failure of walls in hollow piers, finding the onset of deck failure for blast-loaded superstructures, calculating the global response of post-tensioned segmental box girders due to localized failure, and predicting response to blasts at abutments.

Although nonlinear general-purpose finite element methods do have concrete constitutive models that can provide spall and breach predictions, the results should be used with caution. These detailed analyses are very complex, and existing concrete constitutive models struggle to capture complex dynamic material behavior and failure due to uncertainties involving rebar bond, rebar buckling, variable strength and modulus, strain-rate effects, complex crack propagations, and variations in mix design and workmanship (Department of the Army et al., 2002). Such predictions require very sophisticated models developed by a specialist with significant experience to correctly build a model and interpret the results of such an analysis (Conrath et al., 1999).

It is also important to note that uncoupled nonlinear general-purpose finite element methods may be very useful for predicting a response that involves localized failure and large deformations, but they cannot include the effect local failure has on loading, nor can they determine how the resulting loading and response interact over time. This "coupling" of the response is usually not necessary because neglecting venting and pressure redistribution results in conservative load values, and the uncertainties that exist in the determination of design blast loads do not warrant such accuracy. Thus, for most practical design applications, uncoupled nonlinear general-purpose finite element methods provide the highest level of resolution needed. In some situations, however, it may be appropriate to consider coupling, and those cases are as follows:

- **Cases when localized failure is expected to affect loading.** Uncoupled nonlinear general-purpose finite element method response techniques cannot determine changes in loading resulting from venting due to localized failures or large deformations. In some cases, such as blast pressure on a bridge deck, venting can reduce loads on other structural members, affecting global response and reducing the required resistance of some components. In other cases, such as with blast pressure against a hollow pier, failure of a wall can allow pressure to vent into the interior of the pier, complicating both loading and response. For an optimum design, the analysis assumptions should not neglect the effects of venting, thus requiring a coupled analysis.

4.3.3.4 Coupled Analyses

The highest level of response computation techniques consists of coupled 3D nonlinear general-purpose finite element procedures. These programs can provide the most accurate predictions of both loading and response because, unlike lower-level methods, they account for the interaction of loading and response over time. Thus, this highest level of analysis can consider pressure release and redistribution resulting from localized failure or large deformations, providing the most accurate representations of actual structural performance. Although any level of analysis has limitations concerning applicability, coupled 3D nonlinear general-purpose finite element techniques are valid for any purpose because they are the highest resolution procedures currently available. It is important to remember, however, that use of such methods is not typically necessary because lower resolution methods usually provide acceptable results, and it is important to note applicable limitations for proper use of these programs.

Although some programs may advertise the ability to couple loads and response, the coupling is often very limited, and AUTODYN (Century Dynamics, 2004), DYSMAS (U.S. Army Corps of Engineers, 2006), and LS-DYNA (LSTC, 2007) are three of the few programs that are truly capable of coupling blast pressures with structural response. In addition, ensuring the accuracy of results can be very difficult due to the large number of inputs needed. Successful operation requires extensive experience and time to properly model structural systems, achieve the correct failure modes, and interpret the results. Response predictions are usually applicable only for the specific case under consideration. Furthermore, as with uncoupled general-purpose finite element analysis methods, coupled general-purpose finite element methods do not directly generate the quantities needed for design, and the input and time requirements of this level of analysis are not conducive to the parameter studies often used to size members. It is also important to note that, as with uncoupled general-purpose finite element methods, coupled general-purpose finite element methods do have concrete constitutive material models that can provide spall and breach predictions. An analyst should review the results with discretion, however, because such models often struggle to accurately predict dynamic behavior and failure due to the many uncertainties intrinsically characteristic to concrete (Department of the Army et al., 2002). Only a specialist with significant experience should perform these simulations (Conrath et al., 1999).

Because of the extensive issues associated with such methods and because uncoupled analyses provide conservative results, most research and design problems only need uncoupled

analyses (National Research Council, 1995). *Thus, coupled 3D nonlinear general-purpose finite element analysis methods are useful only for specialized cases to conduct research, to analyze past attacks when the specifics of the blast and structural response are known, and to investigate specific design concerns for which uncoupled methods have been deemed unsuitable.* Design scenarios that may benefit from this highest level of response prediction include optimizing walls of hollow towers for blast loads and sizing superstructure members to allow for the failure of bridge decks to vent blast loads. In general, as stated earlier, the decision to use a highly accurate and likewise expensive computational procedure must be on the basis of a cost–benefit analysis. The expense may be well warranted on a large project where the removal of even small degrees of conservatism could potentially save large amounts of money. Nonetheless, increasingly complex analyses often can produce highly erroneous results, and only analysts experienced with predicting blast loading and response should undertake this option.

4.3.3.5 Combining Load Prediction Techniques with Response Prediction Techniques

Most response determination programs are uncoupled, meaning that load determination is separate from response determination. As such, an engineer must first predict structural loads due to blast, output the results, and then input the load data into the response analysis model. The combination of load determination and response determination techniques for a given scenario is the choice of the designer, and practical limitations for the combinations of load and response methods are important factors in that decision. Low-level load analyses do not easily provide information needed for high-level response analyses, and low-level response determination methods do not warrant the increased accuracy and expense associated with high-level load determination methods. In order to maximize efficiency and accuracy, a designer must choose appropriate analysis combinations based on the output limitations of load determination techniques and the input requirements of response determination techniques.

Although the outputs obtained from different load analyses vary even within the analysis levels described in this document, the analyst should note some general observations. Typically, load prediction methods based on blast phenomenology from basic equations and curves developed empirically from "ideal explosions" in free air are able to provide, for example, a time–pressure history acting over a given target area or a time-varying equivalent uniform load acting on a single structural component. As noted earlier, however, the loads computed by those methods do not account for the effects of multiple reflections, confinement, and other important factors that influence the actual blast loads that can act on bridges. The load prediction methods account for confinement and reflections typically produce a time-dependent load history for a user-specified number of "targets." The targets are defined within a three-dimensional space and are defined as individual points on planar surfaces. Load analyses that employ computational fluid dynamics have the capability to calculate time-varying pressure histories on various planes in three dimensions.

The input requirements of response determination techniques also vary within a given level of analysis, but, as with load analyses, some general observations can provide guidance when choosing an appropriate combination of load and response analyses. SDOF response analyses need one-dimensional loading data for a single member, such as an equivalent uniform load, a pressure distribution along a member, or a pressure history for selected points. In contrast, MDOF frame analysis methods and 3D nonlinear general-purpose finite element methods require that the analyst input load histories for a variety of points on a structure. This loading data must usually be specified in three dimensions. For example, to utilize a load analysis that adjusts blast phenomenology based on empirical data to consider reflections and confinement in conjunction with an MDOF frame analysis, the analyst must input loading data that acts over various faces and members of an individual bridge. Thus, considering the case of a below-deck blast scenario against a girder bridge, the analyst would need to specify individual loads acting at a suitable number of points to accurately capture its variation in time and space on the columns in the pier, the girders, and the deck.

The discussion above does not address all possible scenarios, but it illustrates the important fact that, although it may be possible to combine all levels of load analyses with all levels of response analyses, it is not appropriate to do so. Based on the characteristics of available analysis methods, some general guidance can be developed to aid in the selection of appropriate load and response analysis combinations. For example, depending on the level of accuracy desired and the geometric properties of the structure under consideration, load data required for an SDOF analysis is easily extractable from the output of a load analysis that uses blast phenomenology based on empirical data with or without consideration of confinement and reflections, and it is appropriate to use at least a load analysis that considers reflections and confinement to predict loads for an MDOF frame analysis or a 3D nonlinear general-purpose finite element analysis.

4.3.3.6 Summary

This chapter outlines the capabilities and limitations of several levels of analysis programs available to blast engineers. Not all levels of load and response prediction techniques

are appropriate for all cases, and similarly not all levels of load prediction techniques are compatible with all levels of response prediction methods. An engineer should take care to select analysis methods that are suitable for the resources available, the goals of the project team, and the specific scenario being considered. Use of inappropriate methods may produce results that are not conservative enough or are overly conservative, or may be a waste of resources. The information provided in the previous subsections provides guidelines to assist engineers in selecting the most appropriate combination of load and response analyses for the scenario under consideration.

CHAPTER 5

Observations and Research Findings

5.1 Overview

Observations from analytical research and experimental test programs are presented in this chapter. The experimental research was divided into two phases. The first phase focused on determining the blast-load variation as a function of time and position for scaled round and square non-responding columns. In the second phase of experimental testing, half-scale reinforced concrete columns were tested under close-in blast loads. Both Phase I and Phase II test programs are described below.

5.1.1 Phase I Tests

The observations from each blast test on the small-scale, non-responding columns tested in Phase I of this experimental research program are summarized in this section. The entire Phase I test program and all data processing were completed in December 2006 at the U.S. Army Corps of Engineers' Engineering Research and Development Center in Vicksburg, MS.

The Phase I test program included eight small-scale blast tests at four sets of standoff distances. The same scaled standoff was used for all tests. The objective of the small-scale tests was to characterize the structural loads on square and round bridge columns due to blast pressures. The experimental observations indicate how cross-sectional shape, standoff, and geometry between the charge and column positions influence blast pressures on the front, side, and back faces of bridge columns. The data gathered from these tests also allow the assessment of the accuracy of classical methods used to predict blast loads on slender structural components such as bridge columns. Prior to these tests, the majority of the data used to develop empirical blast-load models came from free-field blast tests as well as blasts against large, flat panels. Thus, the focus of the Phase I tests was to study blast-load variation as a function of time and position on slender components for which there were limited data available.

5.1.1.1 Characterization of Blast Loads on Columns

ERDC recorded 160 channels of pressure–time history data during the Phase I blast tests. Figure 43 shows an example of the pressure–time and impulse–time history for one of the test series. For each test, the results from a free-field pressure gauge on each side of the charge were compared to ensure that a similar amount of blast energy was directed toward each specimen. The percent difference in free-field impulse ranged from 6% to 35% and were very reasonable for tests at such a small scale. For any given test, the data show that the pressures and impulses at the bottom of a column are significantly higher and arrive much earlier in time than those at the top of the same column. Figure 44 shows the difference in pressure and arrival time along the height of a column. This difference becomes significantly more prominent as the physical standoff decreases, and this finding suggests that shear will likely be the dominating mode of response for blast scenarios with similar scaled standoffs and heights-of-burst as those considered in the Phase I tests. Furthermore, given that pressures and impulses at the bottom of a column are greater and arrive sooner than those at the top of the column, shock waves reflecting off the deck will not likely control the response of a typical bridge column because a typical column will reach its peak response very early in time for the most serious design threats.

Scenarios with smaller standoff distances tend to produce lower pressures and impulses at the top of columns than do scenarios of the same scaled standoff but with larger physical standoff distances. For a series of blast tests having the same scaled standoff, cases with smaller actual standoff distances have larger scaled distances to elevated gauges on the column than do cases with larger standoff distances. Additionally, for a given scaled standoff, the angle at which the shock front strikes elevated gauges on a column increases as the standoff decreases. For the geometries considered in the Phase I test program, the reflected pressure decreases as the angle at which

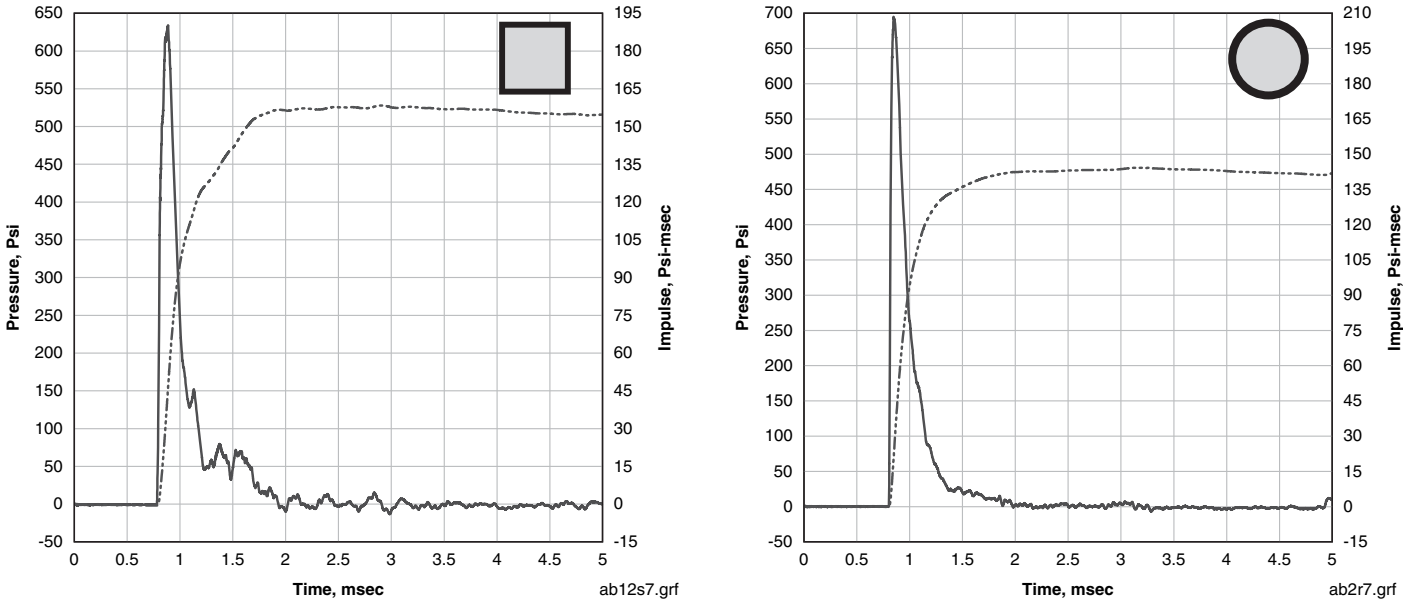

Figure 43. Example plots of pressure and impulse for the middle front gauge.

the shock front strikes the column increases, resulting in significantly decreased pressure and impulse near the top of the column as the standoff distance decreases. Figure 45 shows the difference in geometry for two different standoff distances with the same scaled standoff, and one can see that the ratio R'_2/R'_1 is significantly greater than the ratio R'_2/R'_1.

Bridge Explosive Loading (BEL) (U.S. Army Corps of Engineers, 2000) and BlastX (SAIC, 2001) are two programs that can predict blast effects on flat surfaces. Comparisons between computed values and experimental data show that these programs routinely over-predict pressures and impulses, especially at locations near the top of a column. Figures 46 and 47 show comparisons between the predictions obtained using BEL and experimental pressures and impulses for the front gauges of the square columns for a representative test in the Phase I program. The BEL predictions overestimate the

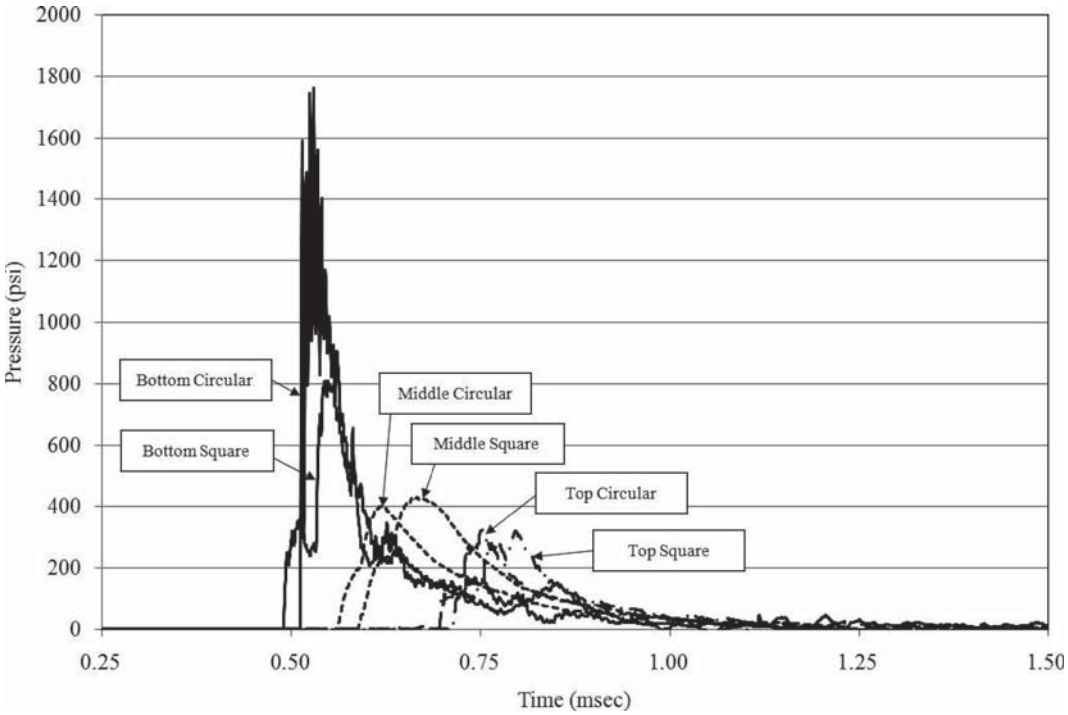

Figure 44. Front gauge pressure–time histories.

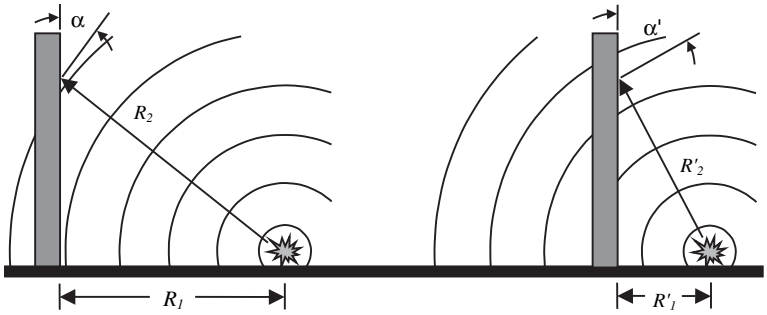

Figure 45. Schematic of geometry differences between two scenarios with the same scaled standoff but different actual standoff distances.

peak pressure and impulse for all three of the front gauges, and the overestimation increases along the height of the column.

Initially, the case of a shock wave striking a column may seem similar to that of a shock wave striking a wall; however, the fact that BEL and BlastX increasingly over-predict pressure and impulse as the distance from the column base increases may be evidence that clearing for a column is more complex than previously thought. Because columns are significantly more slender than walls, the empirically derived three-transits-to-the-edge rule, defined in Section 2.2.1 (Departments of the Army, Air Force, and Navy and the Defense Special Weapons Agency, 2002), may prove to be inaccurate for such slender members. Moreover, additional clearing at the free surfaces at the tops of these columns may contribute to the fact that BEL and BlastX increasingly over-predict pressures and impulses as the location along the height of the column increases.

The data gathered during the Phase I non-responding column tests also show the importance of considering cross-sectional shape and standoff geometry when determining structural loads on columns. Figure 48 shows a plot of the net impulses on the circular and square columns for one of the tests, and the differences between the pressures and impulses along the height of the columns in these tests are clear. In general, the pressures and impulses acting on the circular column are less than those acting on the square column. This difference can be 3%–34% for a series of cases with the same scaled

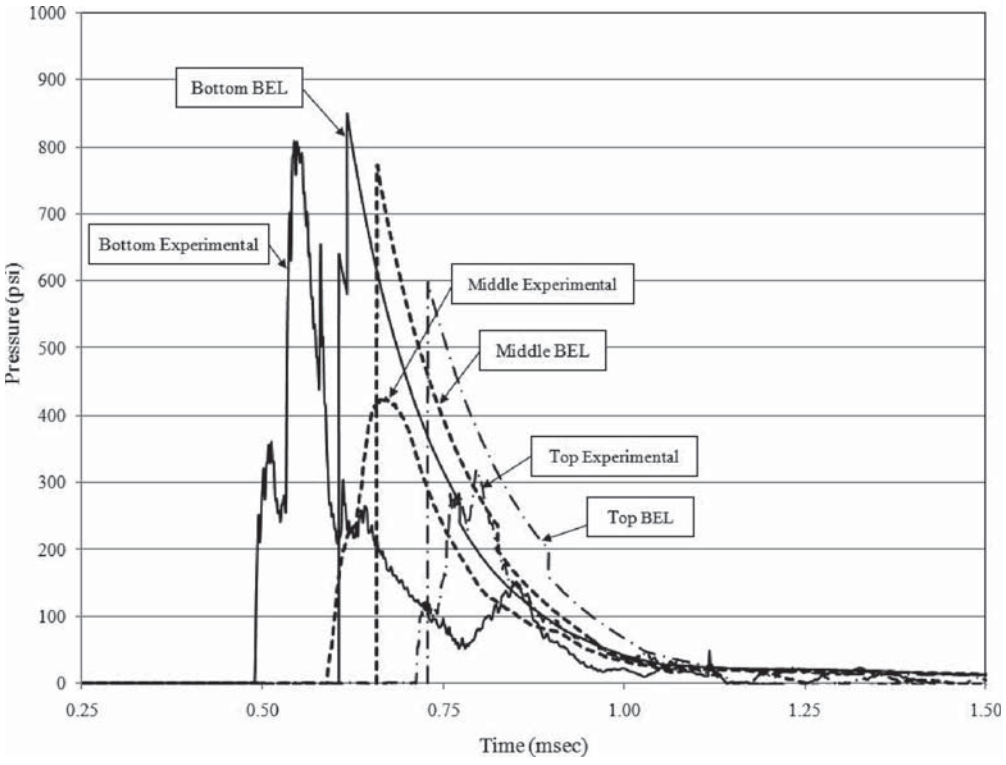

Figure 46. Front-gauge experimental and BEL-predicted pressure comparison.

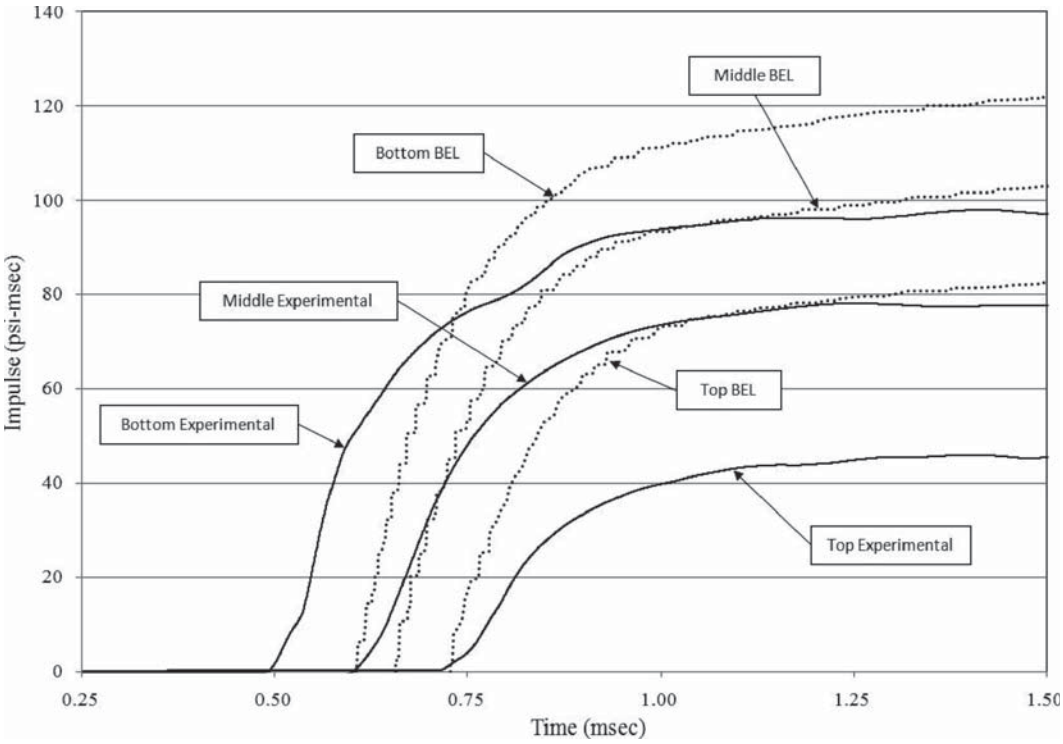

Figure 47. Front-gauge experimental and BEL-predicted impulse comparison.

standoff, and this difference depends on the actual standoff distance and the location of interest along the height of the column. In some cases, the pressures and impulses at the bottom gauge of the circular column are equal to or greater than their corresponding values for the square column. Caution must be exercised, however, when examining the Phase I data because small-scale tests can have a large relative error that makes direct comparisons between data sets difficult, and the small scale of the Phase I tests may have magnified very small inaccuracies in measurements to gauge locations and stand-

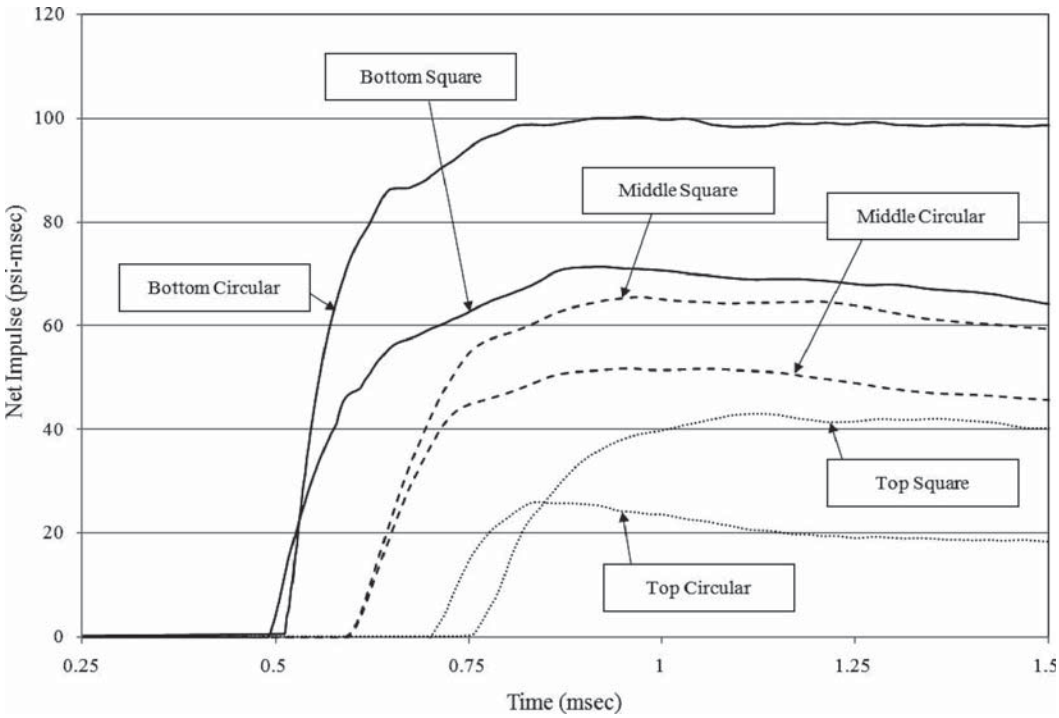

Figure 48. Net impulse comparison.

off distances, resulting in pressure–time histories that are difficult to compare directly. Nevertheless, these observations are interesting and merit additional investigation, and future work should address these issues.

Interestingly, the back-face pressures and impulses on the circular columns in the Phase I tests are typically equal to or larger than the corresponding pressures on the square columns. Figure 48 shows a comparison between the net impulses for the circular and square columns of a representative test, where the net impulse is defined as the difference between the front- and back-face impulses at a given elevation.

Typically, the net pressures and impulses on the circular columns of the Phase I tests are less than those on the corresponding square columns; however, as was the case with front-face pressure–time histories, the results of some tests show that the net pressures and net impulses at the bottom gauges are greater for the circular columns than the square columns. Ultimately, based on a study of the collected test data and detailed analytical models, the researchers believe that several factors influence the pressure–time and impulse–time histories experienced by square and circular columns for a given charge weight and standoff distance. These factors include the difference between the standoff distances to the center of a column and to the edge of the same column, the diameter of a column, the angle of the reflected pressure around the circumference of a circular column, and the difference in the clearing times for circular and square columns.

In general, circular columns will experience less net load than square columns with the same projected area (i.e., when the edge width of the square column equals the diameter of the circular column). Several factors may influence the difference in pressures and impulses along the heights of square and circular columns that contribute to this difference in net loads. Reflected pressures, and more importantly reflected impulses, are functions of the angle of incidence and peak incident overpressure. The angle of incidence at a given location around the front face of a circular column is greater than that of a similar position along the front face of a square column (i.e., locations with the same horizontal distance perpendicular to the column centerline). Furthermore, the peak incident overpressure is less at a given location around the circumference of a circular column than at a similar position along the face of a square column. This reduction in peak incident overpressure is due to the increased standoff distance to the position on the circular column as compared to that on a square column. Both an increase in angle of incidence and a decrease in peak incident overpressure individually produce reduced reflected pressure and impulse. Therefore, a circular column will experience less load than a square column because the summation of the resulting reflected impulses around the front face of a circular column is less than that along the face of a square column. Additionally, the physics of clearing for circular columns is not well understood, and researchers do not know whether the shock wave clears from or simply flows around the front face of a circular column. Considering that circular columns do not have a flat edge to directly reflect a shock wave, one can safely assume that the reduction in load due to clearing will be greater for circular columns than for square columns, and the three-transits-to-the edge rule (Departments of the Army, Air Force, and Navy and the Defense Special Weapons Agency, 2002) may not be applicable to the case of a circular column. Finally, a shock wave will engulf a circular column more easily than a square column, making the resultant impulse on the back face of a circular column greater than that of a square column, further reducing the net resultant load a circular column must resist relative to a square column. While the exact relative contribution of all these factors is still unknown, experimental tests and fluid dynamics analyses confirm that the reflected pressures and impulses are less for circular cross-sections than for square cross-sections.

5.1.1.2 Methods to Predict Loads on Square and Circular Columns

The data obtained during the Phase I blast tests provide a basis on which to evaluate a proposed method for predicting structural loads on square and circular columns. This method is outlined in a 2005 paper by Winget et al. The experimental data from Phase I of this research show that the method proposed by Winget et al. (2005) to adapt blast pressures on flat surfaces to predict blast pressures on circular columns is reasonably accurate in some cases; however, the method often yields erratic and erroneous results because it is very sensitive to several parameters that are difficult to define. For example, the current data show that pressures near the top of a column are significantly lower than those predicted by the proposed method. Furthermore, the current data also show that pressures at the bottom of a column are much higher and arrive earlier in time than pressures at the top of a column. This observation is expected due to the previously explained cross-sectional properties of a column and the geometry of the column location relative to the explosive charge. The proposed method, however, does not capture this behavior.

Several factors may contribute to the inaccuracies introduced by the previously proposed method to predict structural blast loads. The method proposed by Winget et al. (2005) uses the pressure predicted by BEL for several points along the height of a column to create a pressure–time history that varies with *position* along the height of a column but does not vary with *time* along the height of a column. The loading produced by this method would most likely result in a

flexural response of the column, whereas the loading due to the pressures recorded during the Phase I tests would most likely result in a shear-dominated behavior early in time. Moreover, because BEL increasingly over-predicts pressures as the height of the location of interest on a column increases, the error of the proposed method will also increase with the height of the location of interest on a column. Additionally, the method is very sensitive to the positive phase duration, which can be difficult to accurately define. The proposed method also relies on the three-transits-to-the-edge rule, which is likely not valid for circular and very slender members. Reflections along the front face of a circular column are not directly perpendicular to the blast source, and it is not yet clear how to calculate the clearing time for a circular column. Also, unlike square columns, the effective standoff distance and angle of incidence to positions along the circumference of a circular column varies. This difference is likely to be important for large columns subjected to explosive charges at small standoff distances. Although the previously outlined method can provide a good first approximation of structural loads on bridge columns, the current data do not support the accuracy of that method for the cases investigated in this study.

5.1.2 Phase II Tests

The observations from each blast test on the half-scale, reinforced concrete bridge columns tested in Phase II of this experimental research program are summarized in this section. The entire Phase II test program was completed in October 2007 at the Southwest Research Institute test site in Yancey, Texas, and data processing was done by researchers at Protection Engineering Consultants and the University of Texas at Austin.

The Phase II test program included ten half-scale, small standoff and six half-scale, local damage blast tests. Actual material properties for concrete and steel were determined from standard laboratory tests. Pressure and impulse data were used to determine equivalent TNT charge weights for consistent comparisons among the tests. The experimental observations were used to develop design and detailing guidelines for concrete highway bridge columns and analytical tools to predict blast-load distribution and resulting column response.

5.1.2.1 Material Properties

The concrete and steel specified in this project were selected to represent that which is typically used in the construction of reinforced concrete highway bridge columns. Actual material properties were measured to improve calculations and analyses of the experimental test data.

5.1.2.1.1 Concrete Properties. Due to the variety of concrete strengths and types used in different states, the values specified by the AASHTO LRFD were selected for the test program. Concrete with a strength of 4000 psi composed of Type-A cement and a maximum aggregate size of ⅜ in. was specified to accommodate the small rebar spacing used in several of the specimens.

To verify that the concrete columns attained the specified strength, cylinder tests were conducted at various times to determine the compressive strength. The cylinder tests were performed using the Forney universal cylinder test machine according to ASTM C39 Standard Test Method for Compressive Strength of Cylindrical Concrete Specimens. Standard 4-in. × 8-in. cylinders were capped with neoprene bearing pads and steel retaining rings before testing. For each age, a minimum of three compressive capacities were recorded and averaged, and the compressive strength was calculated using Equation 13. Table 10 lists the average compressive strength for the concrete columns, footings, and slab.

$$f'_c = \frac{4P}{\pi D^2} \tag{13}$$

where:

f'_c = cylinder compressive strength (psi)
P = applied load (lbs)
D = diameter of cylinder (in.)

5.1.2.1.2. Mechanical Properties of Steel Reinforcement. This section presents the measured stress–strain properties of the reinforcing steel (rebar) used in this test program. All reinforcement specified and used was uncoated steel bar. Standard deformed, Grade 60 reinforcing bars were specified for all reinforcement except the continuous spirals that allowed the use of a smooth bar (AASHTO LRFD, 2007).

To verify the actual yield strength, tension tests were performed in a 600-kip, hydraulically actuated, universal testing machine. Three different types of reinforcing bars were tested: #6 deformed longitudinal bars, #4 smooth spiral reinforce-

Table 10. Concrete compressive strength.

Days	Compressive Strength (psi)		
	Column	Footing	Slab
0	0	0	0
14	3550	3600	4000
22	3900	**4650**	**5250**
23	3850		
28	**4150**		
35	4050		
36	4100		
38	4100		
Specified	4000	4000	5000

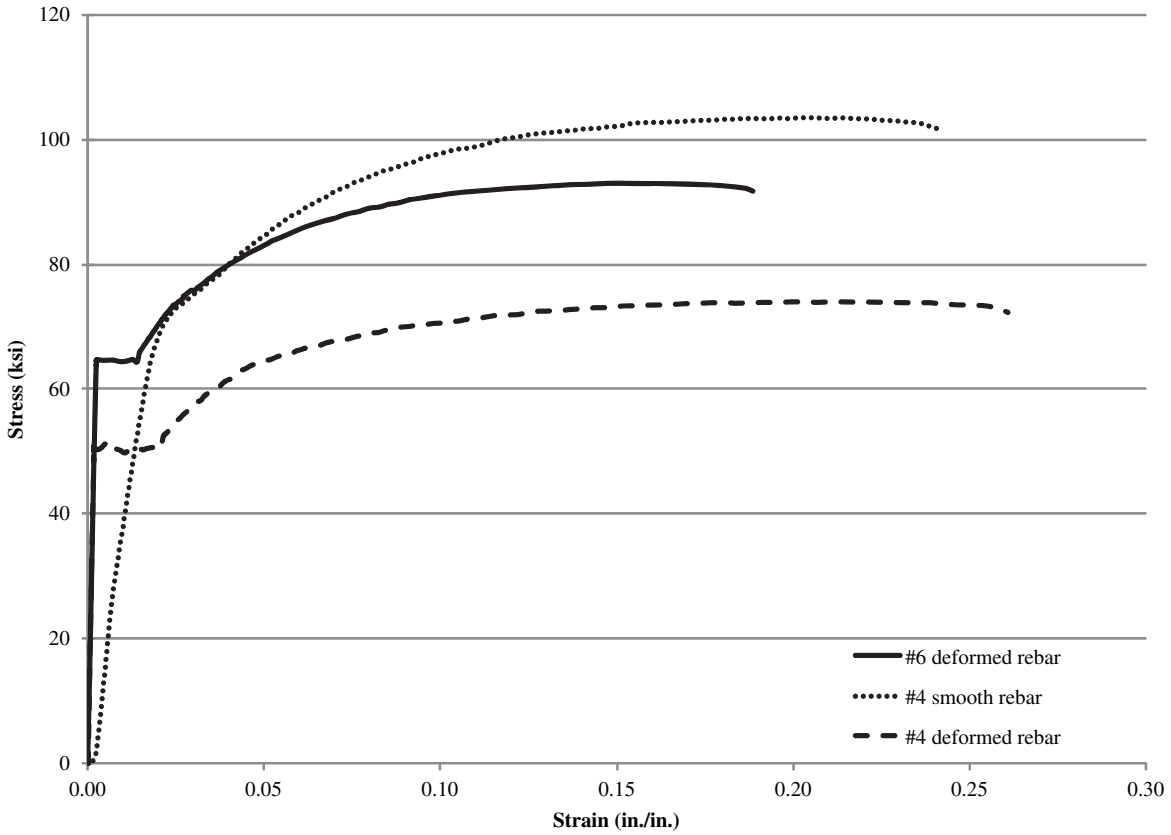

Figure 49. Tensile strength of reinforcing bars.

ment, and #4 deformed discrete ties and hoops. The stress–strain plot for each bar type is illustrated in Figure 49. The average yield strength for the deformed #6 reinforcement was 65 ksi, with an ultimate strength of 90 ksi. Testing of the smooth reinforcement was performed on straight pieces of the spiral reinforcement sent directly from the steel distributor. The smooth reinforcement had an average yield strength of 70 ksi and an ultimate strength of 98 ksi. The discrete hoops and ties consisting of #4 deformed rebar had an average yield strength of 50 ksi and an ultimate strength of 72 ksi. Thus, the #4 deformed bars had a lower strength than specified. For all subsequent calculations, the actual material properties were used. On average, all bars had a modulus of elasticity of 29,000 ksi. While Figure 49 shows a modulus for the smooth rebar that is slightly lower than the deformed bars, past tests have shown that it is not uncommon for the modulus to change slightly when a bar that was initially curved is straightened for the purposes of carrying out tension tests. Thus, it was assumed to have the same modulus as the other reinforcing bars.

5.1.2.1.3 Dynamic Strength Increase. The material properties described above were determined from standard laboratory tests using very slow loading rates, which are appropriate for typical loads. Concrete and steel subjected to rapidly applied blast loads, however, exhibit an increase in strength under the short duration loading. According to the ASCE (1997) document *Design of Blast Resistant Buildings in Petrochemical Facilities,* "These materials cannot respond at the same rate at which the load is applied. Thus, the yield strength increases and less plastic deformation will occur. At a fast strain rate, a greater load is required to produce the same deformation than at a lower rate." Therefore, to account for this increase in strength, material properties were multiplied by the dynamic increase factors, as discussed in Section 2.2.3. The *DIF* amplifies the measured static material strength to account for high strain rates present in blast loading.

5.1.2.2 TNT Equivalency

TNT equivalency is the ratio of the weight of an explosive to an equivalent weight of TNT. TNT equivalencies are used in the majority of research on blast effects to relate the energy output of common explosives to that of TNT. Table 11 summarizes the averaged free-air equivalent weights for different explosives based on peak pressure and impulse (Tedesco, 1999; Department of the Army, 1990).

In this research program, a combination of ammonium nitrate and fuel oil (ANFO) was used as the explosive, and it

Table 11. Averaged free-air equivalent weights.

Explosive	Equivalent Weight, Pressure (lbm*)	Equivalent Weight, Impulse (lbm*)	Pressure Range (psi†)
ANFO	0.82	--	1 - 100
Composition A-3	1.09	1.067	5 - 50
Composition B	1.11	0.98	5 - 50
	1.20	1.30	100 - 1000
Composition C-4	1.37	1.19	10 - 100
Cyclotol (70/30)	1.14	1.09	5 - 50
HBX-1	1.17	1.16	5 - 20
HBX-3	1.14	0.97	5 - 25
H-6	1.38	1.15	5 - 100
Minol II	1.20	1.11	3 - 20
Octol (70/30, 75,25)	1.06	--	E
PBX - 9404	1.13	--	5 - 30
	1.70	1.20	100 - 1000
PBX - 9010	1.29	--	5 - 30
PETN	1.27	--	5 - 100
Pentolite	1.42	1.00	5 - 100
	1.38	1.14	5 - 600
	1.50	1.00	100 - 1000
Picratol	0.90	0.93	--
Tetryl	1.07	--	3 - 20
Tetrytol (Tetryl/TNT) (75/25, 70/30, 65/35)	1.06	--	E
TNETB	1.36	1.10	5 - 100
TNT	1.00	1.00	Standard
TRITONAL	1.07	0.96	5 - 100

*To Convert pounds (mass) to kilograms, multiply by 0.454
†To Convert pounds (force) per square inch to kilopascals, multiply by 6.89
Source: *Department of the Army, 1990*

required a booster (a small quantity of C-4) to ensure reliable detonation. ANFO is commonly used in improvised explosive devices (IEDs) known as fertilizer bombs. Table 11 shows that ANFO is on average 82% as efficient as TNT.

The actual TNT equivalency for each small standoff blast test was determined using the recorded free-field pressure and impulse data. While the equivalency factors listed in Table 11 are average values that are suitable for design, the actual equivalency varies as a function of explosive geometry, target orientation, and atmospheric conditions. Accordingly, to accurately capture the effective TNT equivalency from each blast test, a detailed investigation of the measured pressures and impulses was needed. Available literature and methods for predicting loads are based on TNT equivalency; therefore, TNT equivalency is used to ensure comparability of results with previous data and research projects.

Each small standoff test employed three free-field pressure gauges at known distances away from the charge to determine the TNT equivalency for each test. First, the maximum side-on pressure, P_{so}, and impulse, i_s, were recorded from each pressure gauge. The impulse was calculated from the pressure data as the area under the pressure–time history curve. Next, knowing the standoff, R (distance between the blast source and each gauge), the "spaghetti" charts and corresponding equations from the U.S. Army's TM 5-1300 *Structures to Resist the Effects of Accidental Explosions* were used to determine the charge weight, W, in pounds of TNT. Figure 5 illustrates the "spaghetti" chart for a hemispherical surface burst used in this test program. This chart, which is based on experimental data, provides valuable information about blast loading parameters in a convenient, non-dimensional format. The ratio of the weight of ANFO to TNT was then calculated for each pressure and impulse to determine the efficiency, as shown in Table 12. The efficiencies at each free-field gauge location were then averaged together to determine the average efficiency of each blast test. The average efficiencies ranged from 72% to 94% for pressure and 40% to 66% for impulse. This wide range in efficiencies among different tests with the same explosive can be accounted for by considering the variability in the composition of the ANFO, the exact location of the booster, the atmospheric conditions, and so on.

Due to the lack of pressure gauges during the local damage tests, it was difficult to determine the efficiency for each of those tests. Atmospheric conditions should not have played a major role in the local damage tests because of the close

Table 12. Efficiency of ANFO.

Column	Efficiency							
	Gauge 1		Gauge 2		Gauge 3		Average %	
	Pressure	Impulse	Pressure	Impulse	Pressure	Impulse	Pressure	Impulse
1A1	--	--	--	--	0.84	0.43	84	43
1A2	0.93	0.38	0.76	0.54	0.78	0.48	82	47
1B	0.90	0.41	0.86	0.63	0.81	0.94	86	**66**
2A1	0.87	0.31	0.78	0.55	0.77	0.52	81	46
2A2	1.00	0.40	0.87	0.64	0.86	0.66	91	57
2B	1.00	0.39	0.84	0.66	0.98	0.67	**94**	57
2-Seismic	0.95	0.41	0.94	0.64	0.91	0.62	93	56
2-Blast	0.83	0.25	0.78	0.59	0.92	0.68	84	51
3A	0.93	0.37	0.76	0.65	--	--	85	51
3-Blast	0.75	0.26	0.69	0.54	--	--	**72**	**40**
Average %	91	35	81	60	86	62	85	51

proximity of the charge to the specimen. Also, the data in Table 12 suggests that as the charge gets closer to the target, efficiency increases in terms of pressure and decreases in terms of impulse. Therefore, due to the lack of pressure gauges and conflicting Gauge 1 efficiencies in terms of pressure and impulse, the ANFO efficiency for the local damage tests was assumed to be 82% as specified in Table 11. A constant efficiency is consistent with the decrease in variability due to atmospheric conditions.

The average equivalent weight of TNT and standoff was then used to determine the scaled standoff, *Z,* with Equation 1. The scaled standoff is an indication of the intensity of the blast loading and enabled the comparison of different blast test results with previous testing on the response of structures subjected to blast effects.

5.1.2.3 Small Standoff Test Results

The goal of the small standoff tests was to observe the mode of failure (i.e., flexure or shear) for ten columns with eight different column designs to aide in the development of blast-resistant design and detailing guidelines. The scaled standoff, *Z,* was varied depending on the column type to ensure that a failure was observed. Observations from each small standoff test are presented below. The high-speed video cameras were extremely helpful in capturing the blast front caused by each explosion, as shown in Figure 50. However, column response was hard to observe directly from the video due to the explosive "fireball" and large dust and smoke clouds caused by each test. Therefore, to record the column response after each test, pictures and post-test measurements were taken of each column.

Overall, seven of the ten columns experienced a combination of shear and flexural cracking, while three columns sustained severe shear damage. Table 13 summarizes the column design, scaled standoff, and damage level for each small standoff test.

Figure 50. Blast-wave propagation during small standoff test.

Table 13. Small standoff tests.

Column	Design	Charge Weight*, W	Standoff†, R	Level of Damage
1A1	gravity	2.8 w	5.8 z	superficial
1A2	gravity	2.9 w	3.2 z	failure
1B	gravity w/ spiral	3.4 w	2.6 z	minor
2A1	gravity	2.8 w	3.9 z	superficial
2A2	gravity	3.3 w	2.4 z	minor
2B	gravity w/ spiral	3.4 w	2.4 z	superficial
2-Seismic	seismic	3.3 w	2.4 z	superficial
2-Blast	blast	9.0 w	3.4 z	minor
3A	gravity	9.1 w	3.4 z	extensive
3-Blast	blast	8.5 w	2.6 z	extensive

*w = charge weight parameter
†z = standoff distance parameter

Superficial damage entails surface cracking. Minor damage includes widespread surface cracking and some spall of concrete cover. Extensive damage is defined as significant deformation and spalling of concrete cover, though the majority of the concrete core is still intact and able to carry some axial load. Failure, in this case, means that a shear failure occurred at the base. Specific charge weights and standoffs are not provided for security reasons. Therefore, the charge weight and standoff are shown in terms of the parameters w and z, respectively.

5.1.2.3.1 Column 1A1. The first small standoff test was completed on October 10, 2007. Column 1A1, an 18-in. diameter gravity design column with discrete hoops at 6 in. on center, was tested at a charge weight of 2.8w and the largest standoff, 5.8z, to determine the damage threshold for an 18-in. diameter column. Figure 51 illustrates the combination of shear and flexural cracking experienced by Column 1A1. Flexural cracking was observed at mid-height, while diagonal shear cracking was seen near the column base. Cracking due to rebound of the specimen responding dynamically was expected for the blast loads; however, no cracks were noted on the front face of the column. Therefore, the column did not rebound far enough to produce tension and cracking on the front face. Overall, the column performed well at this scaled standoff and sustained only superficial damage (surface cracking).

5.1.2.3.2 Column 1A2. Column 1A2, with an identical design as Column 1A1, was the second column tested in the experimental research program. The previous test was used as a guide to determine the onset of inelastic deformation. Based on this analysis and due to a desire to understand column response with large inelastic deformations, a 45% smaller standoff than on Column 1A1 was used for Column 1A2. During this test, a similar size charge at a location close to the column, 3.2z, was used to exceed the elastic response limit. The blast resulted in a direct shear failure at the base of

Figure 51. Small standoff blast damage: Column 1A1.

Column 1A2, as seen in Figure 52. A permanent deflection of 5 in. at a height of 21 in. above the ground was noted. Also, spall of the concrete cover was observed on the bottom 16 in. of the column. The brittle shear failure occurred due to the opening of three discrete hoops with standard hooks within the bottom 16 in. After the loss of concrete cover, the standard hooks experienced an anchorage failure, resulting in the loss of core confinement and overall column integrity. The development of the failure zone prevented the column from fully rebounding and forming tensile cracks on the front face.

5.1.2.3.3 Column 1B. Column 1B, an 18-in. diameter gravity design column with a continuous spiral at a 6-in. pitch, was tested at a 17% larger charge weight, 3.4*w*, and 19% smaller standoff, 2.6*z*, than Column 1A2. A more intense loading than Column 1A2 was used to evaluate the benefit of spiral reinforcement over discrete ties. A combination of shear and flexural cracking is illustrated in Figure 53. Flexural cracking at mid-height was observed around the entire column, and shear cracking was observed at the base. The flexural cracking at mid-height on the front face of the column is most likely attributable to full rebound of the column due to the intense blast load. Spall of the concrete cover at the base on the side closest to the blast was also noted. Overall, Column 1B performed well with minor damage noted, including widely distributed cracking and some spall.

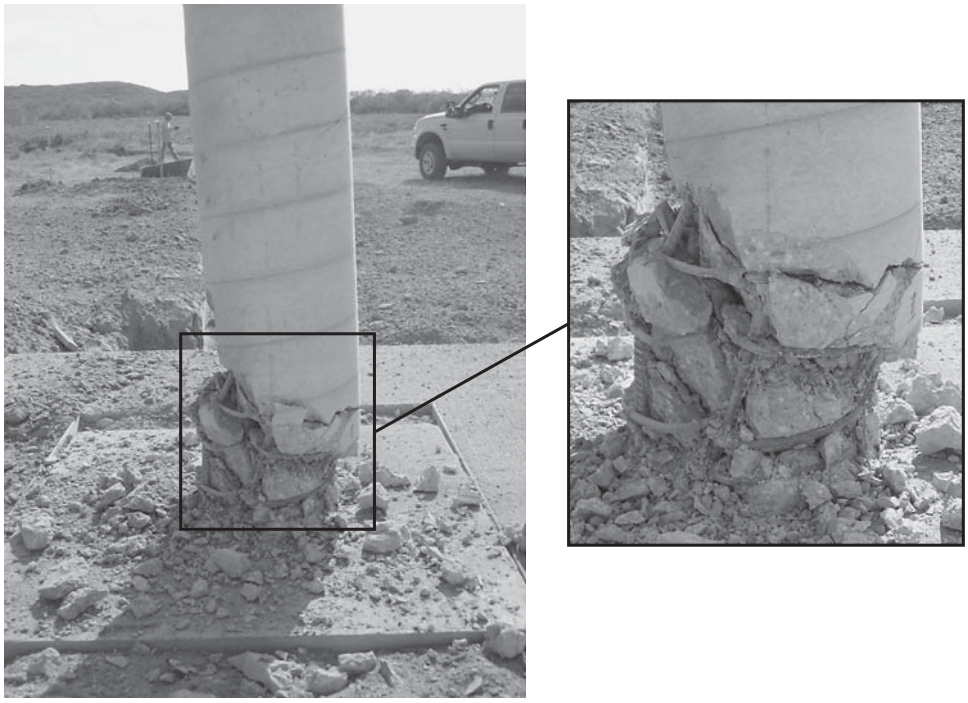

Figure 52. Small standoff blast damage: Column 1A2.

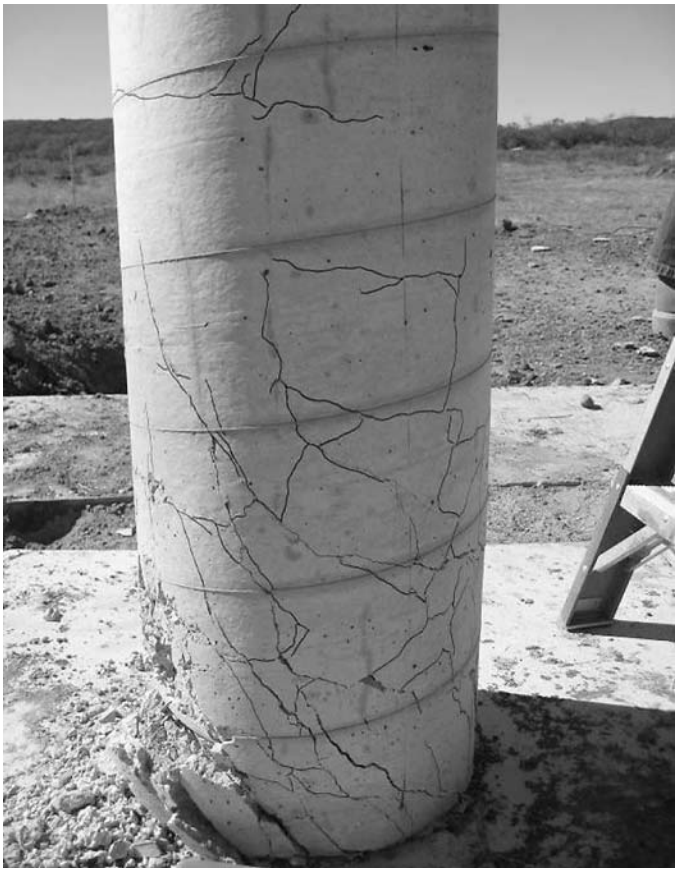

Figure 53. Small standoff blast damage: Column 1B.

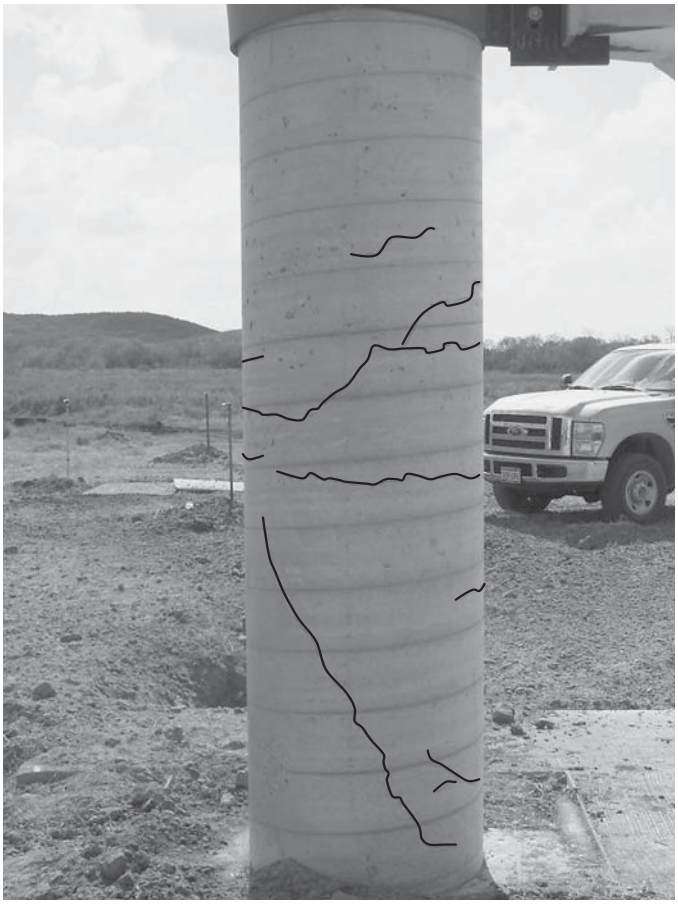

Figure 54. Small standoff blast damage: Column 2A1.

5.1.2.3.4 Column 2A1. The first 30-in. diameter column was tested on October 15, 2007. Column 2A1, a gravity design column with discrete hoops at 6 in. on-center, was tested with a charge size of 2.8*w* at a large standoff, 3.9*z,* to determine the inelastic response threshold for a 30-in. diameter column. The standoff was 32% smaller than the standoff used on Column 1A1. Figure 54 illustrates the combination of shear and flexural cracking experienced by Column 2A1. Flexural cracking was observed at mid-height, while diagonal shear cracking was seen near the column base. Rebound was illustrated by flexural cracking at mid-height on the front face of the column. Overall, the column performed well at this scaled standoff and only sustained superficial damage with cracking limited to the cover concrete.

5.1.2.3.5 Column 2A2. Column 2A2, with an identical design as Column 2A1, was tested with a 20% larger charge weight at a 38% smaller standoff than Column 2A1 to study the inelastic behavior of the column. A 3.3*w* size charge at a standoff of 2.4*z* was used. The column response was similar to that of Column 2A1, illustrating the robustness of the larger diameter columns exposed to a more intense blast loading. Flexural cracking was observed at mid-height, and diagonal shear cracking was observed at the column base, as seen in Figure 55. Rebound response was noted with flexural cracks on the front face of the column. Spall of the concrete cover closest to the blast at the column base was also observed. Overall, the column sustained minor damage, including widespread cracking and some spall.

5.1.2.3.6 Column 2B. Column 2B, a 30-in. diameter gravity design column with continuous spiral reinforcement at a 6-in. pitch, was tested at a similar size charge and standoff as Column 2A2. A 3.4*w* size charge was placed close to the column at a standoff of 2.4*z.* A combination of shear and flexural cracking was noted, as shown in Figure 56. Flexural cracking at mid-height was observed on the front and back face of the column, indicating that significant rebound had occurred. Diagonal shear cracks were also observed at the base. Overall, Column 2B performed well with only superficial damage noted, including cracking of the concrete cover.

5.1.2.3.7 Column 2-Seismic. Column 2-Seismic, a 30-in. diameter seismic design column with a continuous spiral at a 3.5-in. pitch, was tested at the same charge weight and

Figure 55. Small standoff blast damage: Column 2A2.

Figure 56. Small standoff blast damage: Column 2B.

standoff as Column 2A2. Again, a 3.3*w* size charge was placed near the column at a standoff of 2.4*z*. A combination of shear and flexural cracking was noted, as shown in Figure 57. Flexural cracking at mid-height was observed on the front and back face of the column, indicating that rebound had occurred. Diagonal shear cracks were also noted at the base. Overall, Column 2-Seismic performed well, with only superficial damage noted, primarily cracking of the concrete cover.

5.1.2.3.8 Column 2-Blast. Column 2-Blast, a 30-in. diameter blast design column with a continuous spiral at a 2-in. pitch, was tested with a 2.7-times larger size charge and 1.4-times larger standoff than Column 2-Seismic. During this test, a 9.0*w* size charge at a physical standoff of 3.4*z* was used to create the large blast load. Thus, despite having a similar scaled standoff as Column 2-Seismic, the actual loading scenario involved a much higher quantity of explosives than the previous tests, thereby allowing for an evaluation of the use of scaled standoff as a design parameter for close-in blast tests on bridge columns. A combination of shear and flexural cracking was noted, as shown in Figure 58. Flexural cracking at mid-height was observed, as well as diagonal shear cracks at the base. Spall of the concrete cover occurred at the column base and at mid-height on the blast side of the column, indicating rebound of the column. Overall, Column 2-Blast performed well with minor damage noted, including widespread cracking and some spall.

Figure 57. Small standoff blast damage: Column 2-Seismic.

5.1.2.3.9 Column 3A. Column 3A, a 30-in. square gravity design column with discrete ties at 6 in. on-center, was tested at a charge weight and standoff similar to Column 2-Blast. The column was tested with a 9.1*w* size charge at a standoff of 3.4*z*. The blast resulted in significant deformation due to shear at the base of Column 3A, as seen in Figure 59. A permanent deflection of 3 in. at a height of 9 in. above the ground was noted. Observations included complete spall of the bottom 17 in. of concrete cover and flexural cracking at mid-height on the front and back face of the column. Overall, the concrete core was still intact even though the column sustained extensive damage at the base.

5.1.2.3.10 Column 3-Blast. Column 3-Blast, a 30-in. square blast design column with discrete ties at 2 in. on-center, was tested at a 7% smaller charge weight and 24% smaller standoff than Column 3A. The small scaled standoff was comprised of a charge size of 8.5*w* placed very close to the column at a standoff of 2.6*z*. Accounting for the actual charge weight and standoff distance, Column 3-Blast was subjected to the most severe loading of all the columns tested in the small standoff tests. The blast resulted in significant deformation due to shear at the base of Column 3-Blast, as seen in Figure 60. A permanent deflection of 6.5 in. at a height of 13 in. above the ground was noted. Also, complete spall of the bottom 16 in. of concrete cover and flexural cracking at mid-height was observed. Overall, the concrete core was still intact even though the column sustained extensive damage at the base, including significant deformation and spalling of cover concrete.

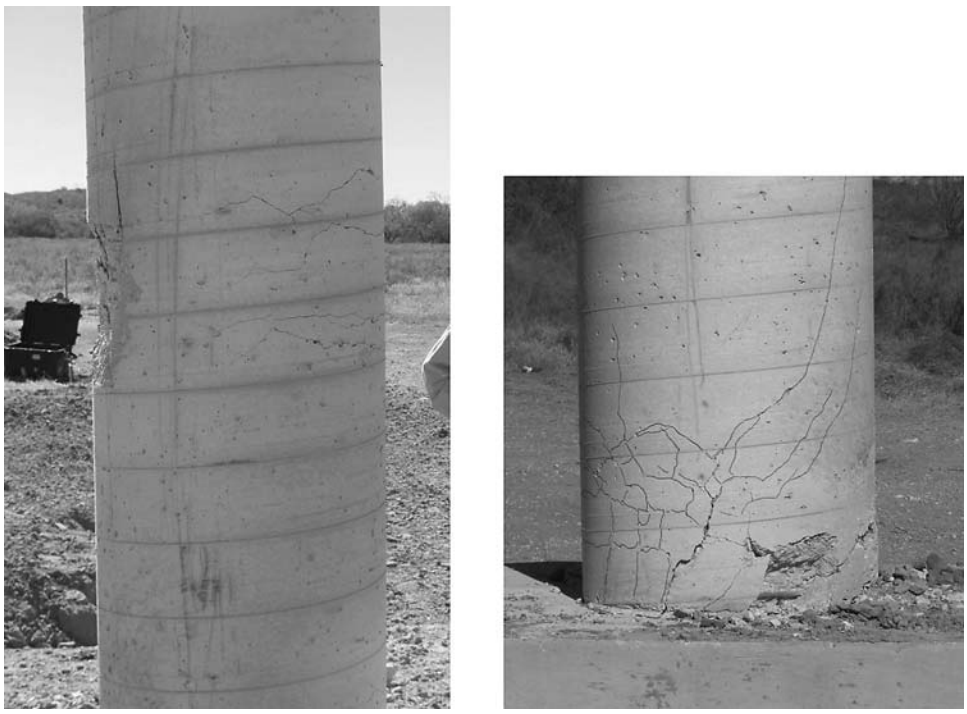

Figure 58. Small standoff blast damage: Column 2-Blast.

Figure 59. Small standoff blast damage: Column 3A.

Figure 60. Small standoff blast damage: Column 3-Blast.

5.1.2.3.11 Summary of Column Failures. The small standoff tests enabled the observation of the mode of failure for ten concrete columns with eight different column designs over a range of different scaled standoffs (i.e., blast scenarios). During the small standoff testing, three columns exhibited significant shear deformations at the base, including Columns 1A2, 3A, and 3-Blast, as the result of severe blast loadings. The other seven columns experienced a combination of shear and flexural cracking and an overall less brittle response than the other three columns. The column design, standoff, charge weight, and damage level for each column are summarized in Table 13. The most common mode of failure was shear; however, the majority of columns had adequate shear capacity to resist the applied loads, experienced limited spall of concrete cover and essentially no column breach, and were very robust. The blast columns were exposed to a more intense loading than their less reinforced counterparts while experiencing similar responses. Thus, given the same blast loading scenario, the blast columns are expected to perform better than the respective gravity or seismic columns.

5.1.2.4 Local Damage Test Results

In a local damage test, charges were placed very close to or in contact with the test column. The objective of the local damage tests was to observe the spall and breach patterns of blast-loaded concrete columns. Breach is defined as the complete loss of concrete through the depth of a given cross-section along the height of a column (i.e., a localized loss of cross-section). In most cases, columns with superficial or minor damage from the small standoff tests were re-used in the local damage tests. Table 14 summarizes the column design, blast load, and damage level of each local damage test. Pictures of each column illustrate the damage incurred by each blast.

5.1.2.4.1 Test 1. The first local damage test was conducted on October 17, 2007, on Column 2A2. Column 2A2 was a 30-in. diameter gravity design column with discrete hoops at 6 in. on-center that sustained minor damage from the small standoff tests. For the local damage experiment, the column was tested with a $3.7w$ size charge at a standoff of $0.4z$.

Table 14. Local damage test summary.

Column	Design	Charge Weight*, *W*	Standoff†, *R*	Level of Breach
2A2	gravity	0.0 *w*	0.0 *x*	complete
2A1	gravity	2.8 *w*	5.8 *x*	partial
1A1	gravity	2.9 *w*	3.2 *x*	complete
2B	gravity w/ spiral	3.4 *w*	2.6 *x*	partial
2-Blast	blast	2.8 *w*	3.9 *x*	cover spall
3A	gravity	3.3 *w*	2.4 *x*	cover spall

*w = charge weight parameter
†x = standoff distance parameter
‡Assuming 82% efficiency of ANFO

Figure 61 illustrates the complete breach of Column 2A2. The complete breach occurred in a very brittle manner. Loss of 100% of the concrete core at least one column diameter above and below the splice location resulted in the column failure. Therefore, Test 1 on Column 2A2 illustrates that a large charge placed sufficiently close will fail the column, reinforcing the idea that not all columns can be protected for all possible threat scenarios (Winget, 2003).

5.1.2.4.2 Test 2. The second local damage test was on Column 2A1, a 30-in. diameter gravity design column with discrete hoops at 6 in. on-center that sustained superficial damage from the small standoff tests. Noting the failure of Column 2A2 in the first local damage test, Column 2A1 was tested with a much smaller charge weight to determine the onset of localized damage or breaching. Figure 62 illustrates the partial breach of Column 2A1. A combination of three severed discrete hoops and the loss of approximately 70% of the concrete core at least one column diameter above and below the blast location resulted in significant permanent deformation and imminent failure of the column.

5.1.2.4.3 Test 3. The third local damage test was on Column 1A1, an 18-in. diameter gravity design column with discrete hoops at 6 in. on-center that sustained superficial damage from the small standoff tests. Column 1A1 was tested at the same charge weight and standoff as Test 2. Figure 63 illustrates the complete breach of Column 1A1. A 100% loss of the concrete core at least one column diameter above and below the blast location resulted in column failure. The concrete core within the splice overlap was completely rubblized, which led to the loss of column (concrete or steel) continuity in that region.

5.1.2.4.4 Test 4. The fourth local damage test was on Column 2B, a 30-in. diameter gravity design column with continuous spiral reinforcement at a 6-in. pitch that sustained superficial damage from the small standoff tests. For the local damage test, the column was tested with a 1.1*w* size charge at a standoff of 0.4*z,* identical to Tests 2 and 3. Figure 64 illustrates the partial breach of Column 2B. The spiral was severed in two locations near the blast source, and the column lost approximately 90% of the concrete core at least one column diameter above the blast location. The continuous longitudinal reinforcement used in Column 2B remained in one piece; however, the longitudinal reinforcement sustained permanent deformation at the location of the blast.

5.1.2.4.5 Test 5. The last local damage test was conducted on Column 2-Blast and Column 3A simultaneously. Column 2-Blast was a 30-in. diameter blast design column with a continuous spiral at a 2-in. pitch that sustained minor damage after the small standoff tests. Column 3A was a 30-in. square

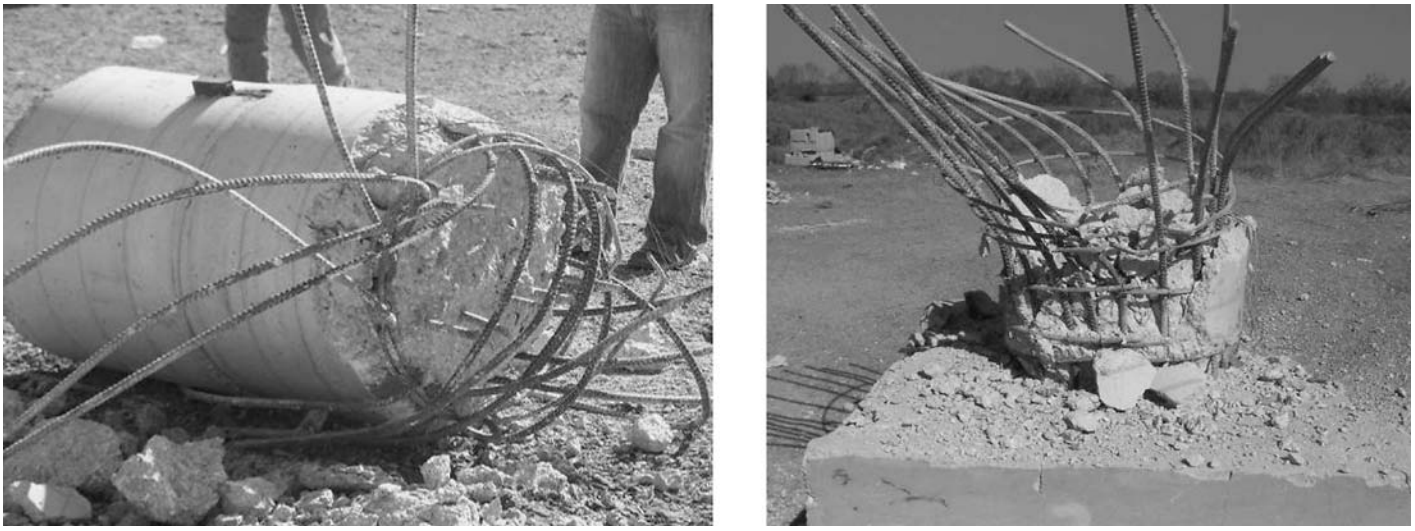

Figure 61. Local damage Test 1: Column 2A2.

Figure 62. Local damage Test 2: Column 2A1.

gravity design column with discrete ties at 6 in. on-center that sustained extensive damage from the small standoff tests. Column 3A was chosen to allow the evaluation of column geometry during the local damage tests. The columns were tested with a 0.7*w* size charge at a standoff of 0.7*z*.

Figure 63. Local damage Test 3: Column 1A1.

Figure 64. Local damage Test 4: Column 2B.

Figure 65 illustrates the local blast damage on Column 2-Blast. The spall of concrete cover was noted on the column sides only, enabling the concrete core to stay intact. Widening of previous cracks from the small standoff test was also observed.

Figure 66 illustrates the local blast damage and final position of Column 3A. Additional spalling of concrete cover in the vicinity of the blast location was noted on the column sides only, while the back cover remained intact, enabling the concrete core to stay intact. Widening of previous cracks from the small standoff test was also observed. It is important to note that Column 3A would likely not have toppled over if the base was restrained.

5.1.2.4.6 Summary of Column Failures. The local damage tests allowed the observation of spall and breach patterns for blast-loaded concrete columns. Only two of the six columns (1A1 and 2A2) experienced a complete breach. Columns 2A1 and 2B experienced a significant loss of the concrete core, while the remaining two columns stayed intact. Column 2-Blast and 3A exhibited spalling of the side concrete cover. Table 14 summarizes the observations made during the local damage tests.

Figure 65. Local damage Test 5: Column 2-Blast.

5.1.2.5 Discussion of Test Variables

The test program included ten half-scale, small standoff and six half-scale, local damage blast tests on eight different column designs. Column specimens were constructed with consideration given to five main test variables, including scaled standoff, column geometry, amount of transverse reinforcement, type of transverse reinforcement, and splice location. This section relates each test variable to the experimental observations and data to determine design and detailing recommendations for concrete highway bridge columns.

Figure 66. Local damage Test 6: Column 3A.

5.1.2.5.1 Scaled Standoff. One of the best ways to improve the performance of blast-loaded reinforced concrete highway bridge columns is to increase the standoff distance. Increasing the design scaled standoff will decrease the effects of blast loads on columns. Figure 67 compares two identical 18-in. columns tested at different standoffs. The gravity-designed columns used standard hooks, which are a poor detail for blast-loaded columns (see Section 5.1.2.5.4); however, when the standoff is sufficiently increased, detailing becomes less significant in controlling response.

If only vehicle standoff is limited, small charges may still be placed in direct contact with a column, potentially causing localized damage or breaching of the concrete core. Results from local damage tests, shown in Figure 68, illustrate that increasing the standoff from the face of the structural column by a small amount (on the order of inches) can increase a column's chance of survival substantially in a situation involving close-in blast loads. Aside from physical barriers, standoff from a structural member can be increased by adding an architectural feature around the structural column.

5.1.2.5.2 Column Geometry. Column cross-sectional shape affects how a blast load interacts with a column. The use of a circular column is an effective way of decreasing the blast pressure and impulse on a column relative to a square column of the same size. Therefore, the use of a circular column cross-section over a square cross-section is recommended. A square column provides a flat surface that reflects the overpressure directly back toward the source, creating a large reflected pressure. The increase of reflected pressure on a circular column is not as significant as on a square column because the pressure around the perimeter of a circular column is reflected at an angle (with the exception of the centerline position) relative to the direction of shock wave propagation from the blast source. Also, pressures do not clear around the edges of a square column as quickly as they wrap around and fill in behind a circular column. Therefore, a blast load interacting with a circular column will produce a less severe loading than one acting on a similarly sized rectangular or square column. Figure 69 illustrates the results of a blast wave propagating around a circular and square column with the same cross-sectional dimension at the same scaled standoff. The square column was pushed over by the blast load, while the circular column remained standing, demonstrating the decrease in load on a circular column due to clearing. Clearing is the process by which a high reflected

(a) (b)

Figure 67. Importance of scaled standoff: a) large standoff (Column 1A1), b) small standoff (Column 1A2).

pressure seeks relief toward lower pressure regions (free edges) through a rarefaction (or relief) wave that propagates from the low to the high-pressure region.

Using a circular column cross-section over a square cross-section can lead to a decrease in the net resultant impulse the column must resist, as shown in Figure 70. Section 5.1.1.1 discusses the physical phenomena that contribute to the reduction in impulse experienced by a circular column as compared to that of a square column, and limited test data suggest that the reduction in impulse can be as much as 34% at certain locations for small standoffs. Although additional testing is needed to validate these findings, a circular column with the same design and detailing requirements as a square column is expected to have less damage for a threat with the same scaled standoff.

If the standoff distance cannot be increased to sufficiently decrease the effects of blast loads on columns, then the following design and detailing provisions are recommended:

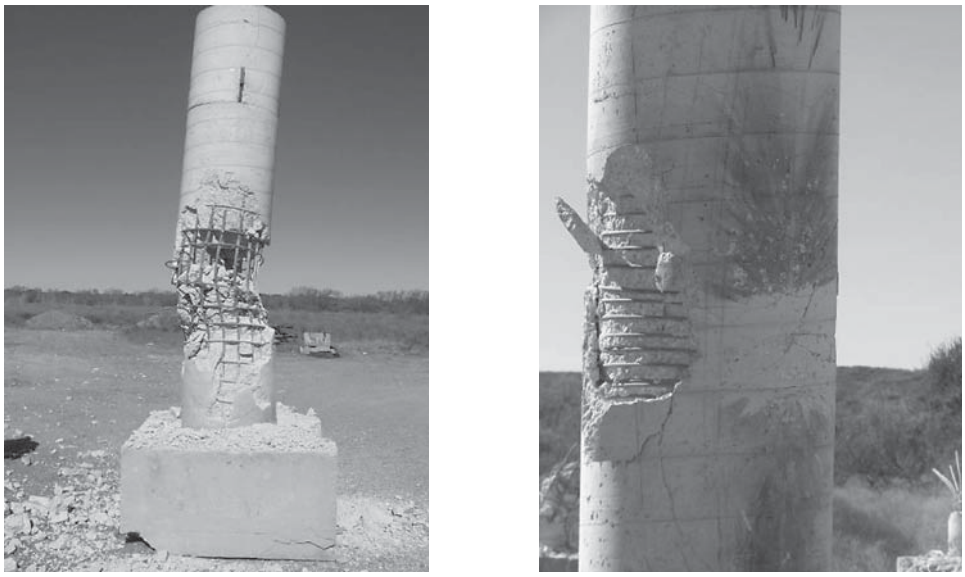

(a) (b)

Figure 68. Effectiveness of small-scaled standoff: a) Test 4, b) Test 5.

Figure 69. Clearing around a square and circular column (side view).

increasing the amount of transverse reinforcement, requiring continuous spiral reinforcement or discrete hoops with sufficient anchorage, and avoiding splices. These design provisions are covered in detail in the following sections.

5.1.2.5.3 Amount of Transverse Reinforcement. Experimental observations show that increasing the volumetric reinforcement ratio is beneficial to the response of blast-loaded columns because it increases the column ductility and shear capacity. Direct shear is a major concern for blast-loaded columns, as shown in Figure 71. To reduce the chances of a potential shear failure, the "blast" columns (specimens 2-Blast and 3-Blast) were designed to force the formation of plastic hinges (a flexural failure). Similarly to seismic design, all potential plastic hinge locations were considered to ensure the maximum possible shear demand. During the design process, a propped-cantilever column with a triangular load,

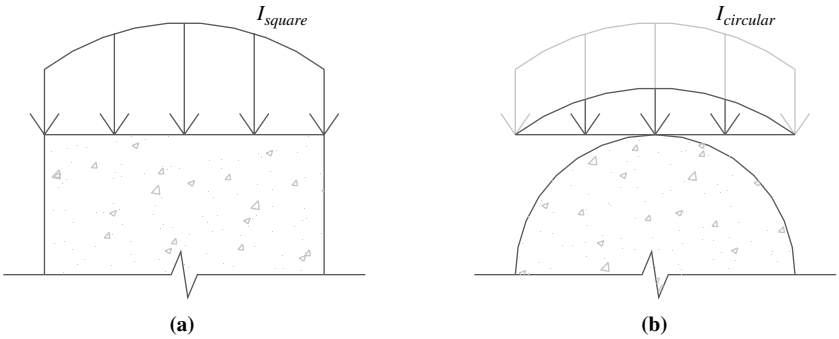

Figure 70. Relative net impulse on column cross-section: a) square column, b) circular column.

Figure 71. Shear deformation of blast-loaded columns: a) 18-in. round column (1A1), b) 30-in. square column (3A).

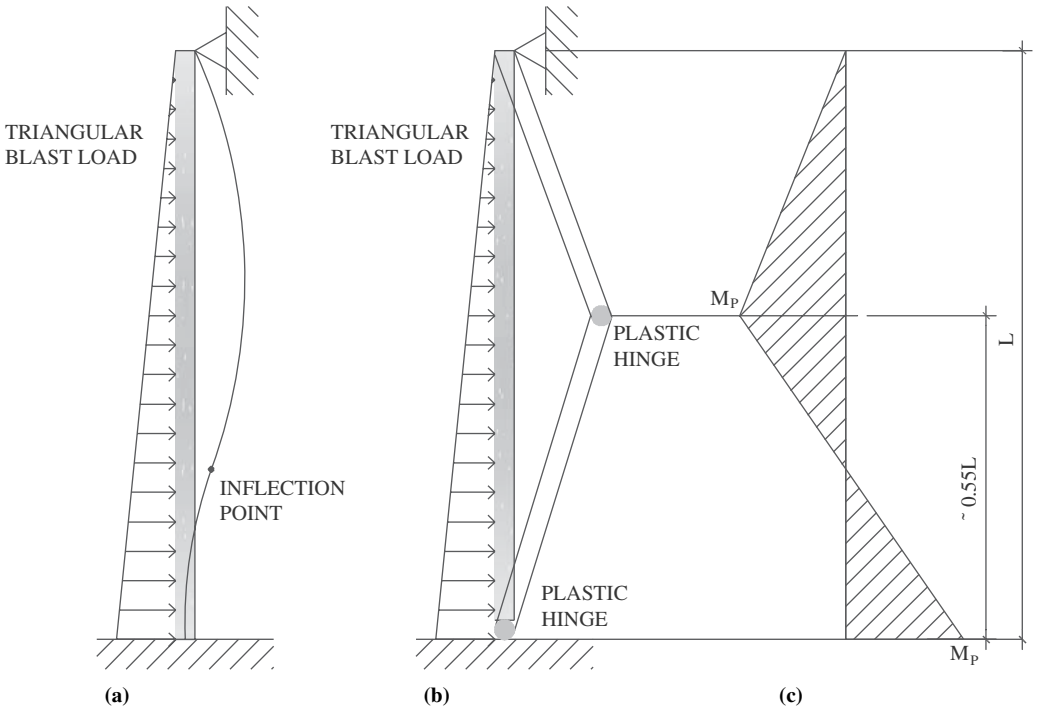

Figure 72. Plastic hinge analysis for blast-loaded column: a) deflected shape, b) plastic hinge locations, c) plastic moment.

shown in Figure 72, was assumed to form two hinges before failure. The plastic hinge analysis determined a maximum shear of:

$$V_{base} = \frac{9M_P}{L} \tag{14}$$

where:

M_P = plastic moment capacity (kip-ft)
L = height of column (ft)

In comparison, a typical seismic column (shown in Figure 73) that is fixed–fixed with a displacement at one end due to a laterally applied force will also form two plastic hinges. The maximum shear from a plastic hinge analysis is:

$$V_{base} = \frac{2M_P}{L} \tag{15}$$

where:

M_P = plastic moment capacity (kip-ft)
L = height of column (ft)

These plastic hinge analyses clearly demonstrate the large shear demand on blast-loaded columns, which can be greater than four times the shear demand from seismic loads.

Using the shear equations given above, a required pitch of transverse reinforcement was determined by setting Equations 14 and 15 equal to the shear design equations from the AASHTO LRFD (2007), modified to account for strain rate effects (ASCE, 1997), and solving for the spacing (Table 15). The plastic moment (M_P), which is equal to the flexural capacity of the cross-section (M_n), should also account for the dynamic material strength, with dynamic increase factors for strain rate effects.

Section 5.7.4.6 of the AASHTO LRFD (2007) requires a minimum transverse reinforcement ratio for a circular gravity-loaded column of:

$$\rho_s \geq 0.45\left(\frac{A_g}{A_c} - 1\right)\frac{f'_c}{f_y} \tag{16}$$

where:

f'_c = specified compressive strength of concrete at 28 days (psi)
f_y = yield strength of reinforcing bars (psi)
A_g = gross area of column (in.^{2})
A_c = area of concrete core (in.^{2})

Section 5.10.11.4.1(d) of the AASHTO LRFD (2007) requires a minimum transverse reinforcement ratio for a circular seismic column and minimum area of transverse

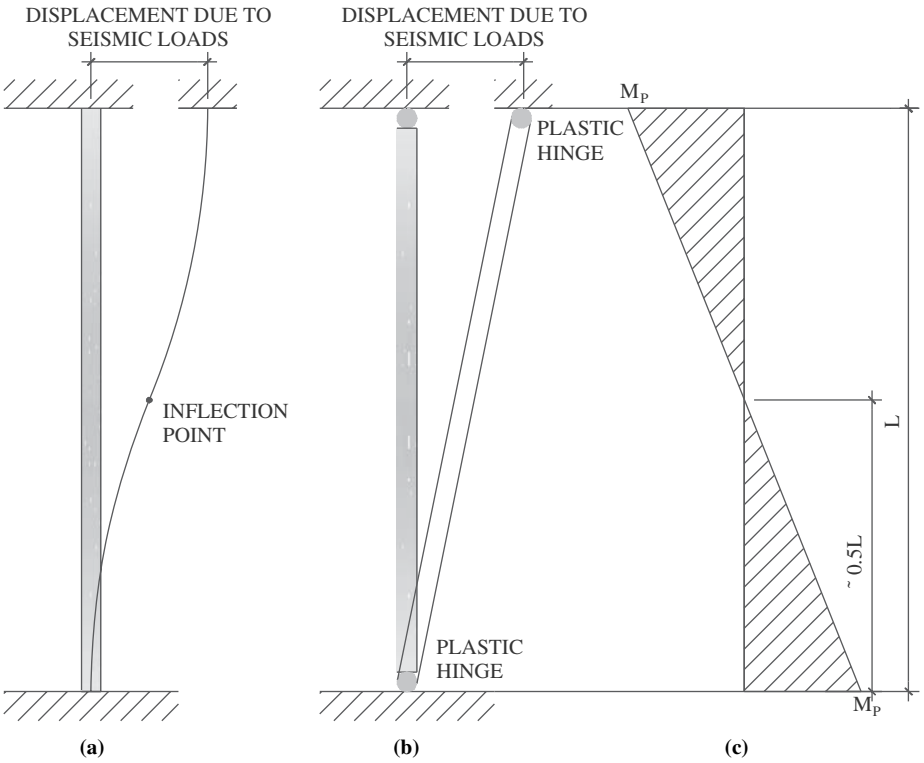

Figure 73. Plastic hinge analysis for seismic column: a) deflected shape, b) plastic hinge locations, c) plastic moment.

reinforcement for a rectangular seismic column, respectively, of:

$$\rho_s \geq 0.12 \frac{f'_c}{f_y} \tag{17}$$

$$A_{sh} \geq 0.12 s h_c \frac{f'_c}{f_y} \tag{18}$$

where:

f'_c = specified compressive strength of concrete at 28 days (psi)
f_y = yield strength of reinforcing bars (psi)
s = vertical spacing of hoops, not exceeding 4 in. (in.)
h_c = core dimension of column in the direction under consideration (in.)

Table 15. Pitch of transverse reinforcement.

Seismic Column Capacity					Pitch (in.)	
End Condition	**Scale**	$M_N = M_P$ **(kip-ft)**	$V_{u,base}$ **(kip)**	V_c **(kip)**	$V_c = 0$	$V_c > 0$
Pin-Fixed (blast)	1 : 2	584	592	90	0.9	1.0
Fixed-Fixed (seismic)	1 : 2	584	104	90	5.0	37.8

Equation 16 controlled the transverse reinforcement design of all gravity-designed columns (Type-A and Type-B), while Equations 17 and 18 controlled the design of all seismic- and blast-designed columns. Though not initially anticipated, it is important to note that the Type-A columns did not meet the requirements of the AASHTO LRFD (2007) Article 5.7.4.6 as they were constructed because the actual steel strength (f_y = 50ksi) was lower than the specified strength used for design, 60 ksi.

Equation 17, with a coefficient of 0.18, is recommended as the minimum transverse reinforcement ratio for all circular blast-designed columns, while Equation 18, with a coefficient of 0.18, is recommended as the minimum area of transverse reinforcement for all rectangular blast-designed columns. Columns meeting these minimums tested at a small standoff sustained minor and extensive damage (see Figure 74); however, the core still remained intact and the column could still carry load. Essentially, 50% more confinement is recommended for blast-designed columns over current seismic provisions to improve the ductility, energy absorption, and dissipation capacity of the cross-section.

Using the experimental test observations and data, a new minimum transverse reinforcement ratio and area of transverse reinforcement is recommended, with the following equations for a circular and rectangular blast-loaded column, respectively.

(a) (b)

Figure 74. Columns meeting minimum transverse reinforcement requirements: a) minor damage (2-Blast), b) extensive damage (3-Blast).

$$\rho_s \geq 0.18 \frac{f'_c}{f_y} \tag{19}$$

$$A_{sh} \geq 0.18 s h_c \frac{f'_c}{f_y} s \tag{20}$$

where:

f'_c = specified compressive strength of concrete at 28 days (psi)
f_y = yield strength of reinforcing bars (psi)
s = vertical spacing of hoops, not exceeding 4 in. (in.)
h_c = core dimension of column in the direction under consideration (in.)

5.1.2.5.4 Type of Transverse Reinforcement and Discrete Tie Anchorage. Experimental observations show that continuous spiral reinforcement performs better than discrete hoops for small standoff tests. Figure 75 compares two 18-in. columns tested at a similar standoff, with the only variable being the type of transverse reinforcement. Figure 75 illustrates the benefit of spiral reinforcement in the response of blast-loaded columns. The continuous reinforcement better confines the core at the base where a shear failure is most likely to occur. Therefore, continuous spiral reinforcement is recommended for blast-loaded columns.

Performance of discrete hoops can be improved to a level equivalent to that of the continuous spiral reinforcement

(a) (b)

Figure 75. Importance of continuous transverse reinforcement: a) discrete hoops (Column 1A2), b) continuous spiral (Column 1B).

with better anchorage into the concrete core. The column with discrete hoops in Figure 75 experienced a shear failure at the column base because the bottom three hoops were pulled open. The discrete hoop anchorage was designed in accordance with Section 5.10.2.1 of the AASHTO LRFD Bridge Design Specifications (2007) and used standard hooks with a "90° bend, plus a 6.0 d_b extension at the free end of the bar." Section 5.10.2.1 defines standard hooks for transverse reinforcement as one of the following:

a) No. 5 bar and smaller: 90° bend, plus a 6.0 d_b extension at the free end of the bar
b) No. 6, No. 7, and No. 8 bars: 90° bend, plus a 12.0 d_b extension at the free end of the bar
c) No. 8 bar and smaller: 135° bend, plus a 6.0 d_b extension at the free end of the bar

where:

d_b = nominal diameter of the reinforcing bar (in.)

The standard hooks shown in Figure 76 do not sufficiently anchor the discrete hoops into the concrete core of a half-scale, blast-loaded column. Recent work by Bae and Bayrak (2008) on the seismic performance of full-scale, reinforced concrete columns demonstrated the opening of seismic discrete ties using hooks with a 135° bend, plus an extension of 8.0 d_b. The AASHTO LRFD (2007) Section 5.10.2 defines seismic hooks as a "135°-bend, plus an extension of not less than the larger of 6.0 d_b or 3 in." Bae and Bayrak (2008) noted that, "unlike the full-scale concrete columns, the hooked anchorages often reach close to the center of the core concrete in scaled column specimens." Similar observations apply to the half-scale specimens used in this research program. Bae and Bayrak (2008) used a minimum hook length of 15.0 d_b for the remaining full-scale tests to prevent the opening of hoops. The researchers stated that the larger "hook length proved to be very effective, and opening of the 135° hooked anchorages of the ties was not observed in the other tests." The blast-loaded column in Figure 77 also used discrete ties with a larger hook length than required by the current AASHTO provisions and did not experience any anchorage issues; however, construction of the specimen was challenging. The square column in the figure utilized sufficient transverse reinforcement and hooks with a 135° bend, plus a 20.0 d_b extension at one free end of the bar, reversing directions each spacing. To avoid anchorage pullouts and to improve the performance of blast-loaded (and seismically loaded) columns with discrete hoops or ties, longer hook lengths than currently specified are recommended. Properly anchored hooks for blast loads should

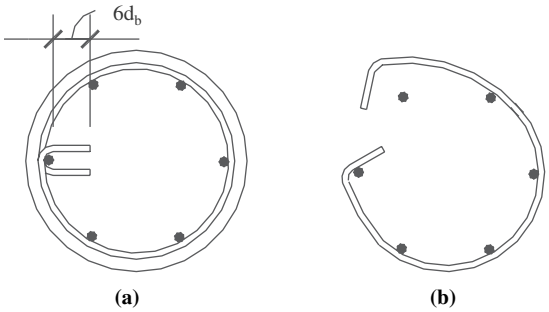

Figure 76. Discrete hoop with standard hook (Column 1A2): a) before test, b) anchorage pullout.

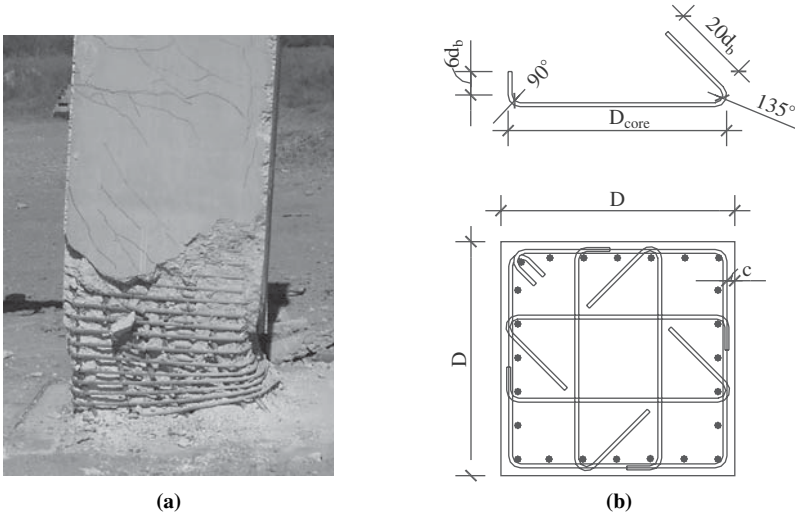

Figure 77. Sufficiently anchored discrete ties (Column 3-Blast): a) discrete ties, b) discrete tie diagram.

consist of a 135° bend, plus an extension of not less than the larger of 20.0 d_b or 10 in.

5.1.2.5.5 Location of Longitudinal Splices. If the splice location is at or near the blast location, there is a possibility of breaching at the splice for cases of very small scaled standoffs. Breach is defined as the complete loss of concrete through the depth of a cross-section. Specific observations regarding the performance of longitudinal splices are not provided due to the limited data collected from these tests during the test program. Additional research is needed to fully characterize splice behavior at locations very close to applied blasts.

5.2 Observations from Analytical Programs

Analytical models for load and response were used to simulate the tests carried out during the Phase I and Phase II test programs and to carry out parametric studies. Results from these efforts are described in this section.

Experimental observations show that direct shear early in time is a prominent failure mode for columns without adequate shear reinforcement, as seen in Figure 78. A simplified SDOF analysis was used to determine the shear reinforcement needed for each column to force a flexural mode of response. Strain data from the small standoff tests and data processing are presented below. The strain data were used to determine the actual boundary conditions and load distribution of each small standoff test.

5.2.1 Strain Data

Strain gauge data were collected from each small standoff test at six different locations. The strain gauge data were filtered manually by removing all outliers from the data set to determine the maximum strain and time of occurrence. An outlier was defined in two ways: as a strain value exceeding the strain gauge capacity (30,000 μStrain) or as a maximum or minimum strain value with less than two points leading up to it. Other filtration methods, such as a low pass filter in Matlab (Mathworks, 2008) and DPLOT (HydeSoft, 2008), were evaluated to help smooth the data; however, these methods altered the data too significantly, cutting out multiple peaks. Therefore, the data were manually filtered as illustrated in Figure 79, which was more appropriate when focusing on the maximum strain values of the strain–time history.

Figure 78. Direct shear failure.

To check the maximum values obtained in the manual filter process, project researchers calculated likely times at which the maximum flexural response would occur, and it was apparent by the lack of data at those times that many of the gauges failed prior to a flexural response, indicating an early gauge failure. Tests on Columns 1A1, 2A1, 2A2 and 2B survived long enough and had readings that lasted through the calculated flexural response time to provide sufficient data for the evaluation of flexural response. Large early time responses were also noted near the time of arrival of the blast wave, before the pier had enough time to react to the impulse load. These early time responses were most likely gauge wire responses to the initial shock transmission through the columns. The early peak strain times were practically identical for all gauge locations because the strain gauge wires were bundled as they ran through the column base and were all excited at the same time as the shock crossed the bundle. Thus, the early time responses were essentially an indication of the time of arrival for the direct shock transmission and were not used in determining the peak strain.

Flexural strain data from four of the small standoff tests (1A1, 2A1, 2A2, 2B) were used to evaluate the actual boundary conditions and load distribution. Filtered flexural strain data are shown in Figure 80; to better show the data trend, the rolling average over five points is also shown. The other six tests experienced early gauge failure and typically recorded a peak in less than one millisecond of starting data collection, as illustrated by Figure 81. The majority of the columns with early gauge failures experienced a shear failure at the base. Thus, a flexural response was not able to be developed within this millisecond time period of data collection before the shear failure occurred.

5.2.2 Actual Boundary Conditions

Before completing the SDOF analyses to determine the shear capacity of each column, the experimental data were used to assess the actual boundary conditions experienced by each column during the blast tests. For design, a propped-cantilever was assumed as the boundary conditions for each column. To verify the actual boundary conditions developed

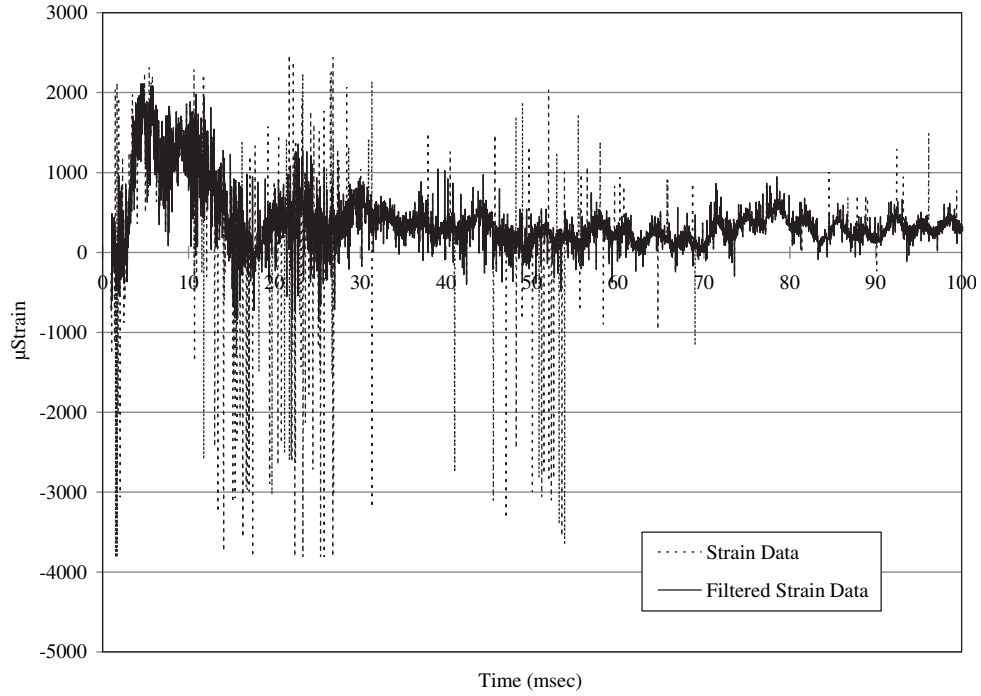

Figure 79. Filtered longitudinal reinforcement (flexural) strain data.

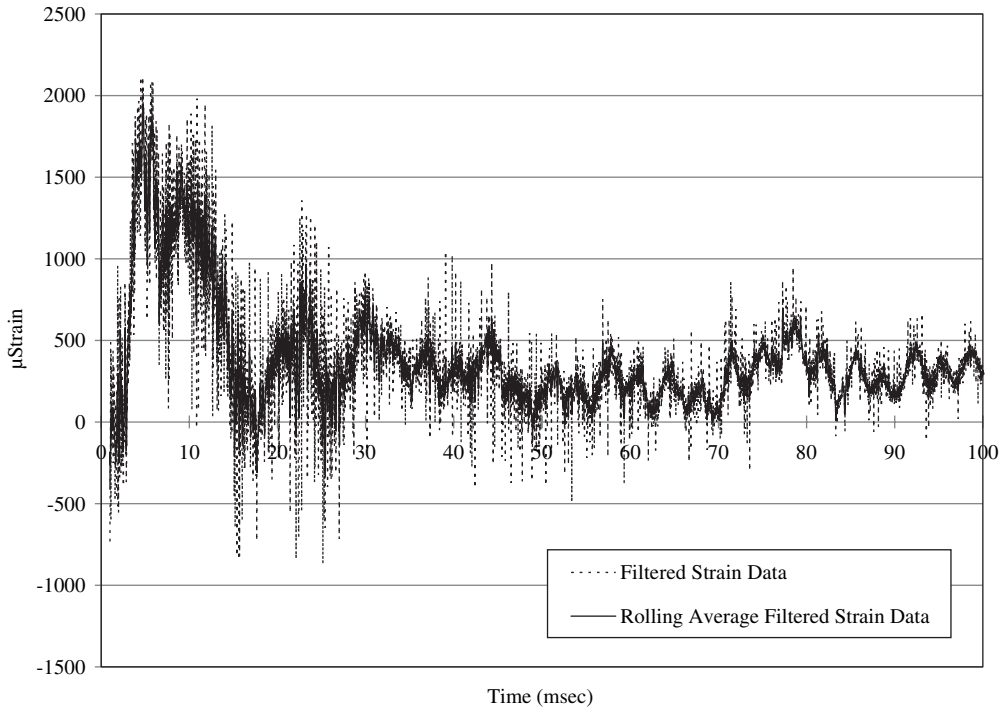

Figure 80. Longitudinal reinforcement (flexural) strain data.

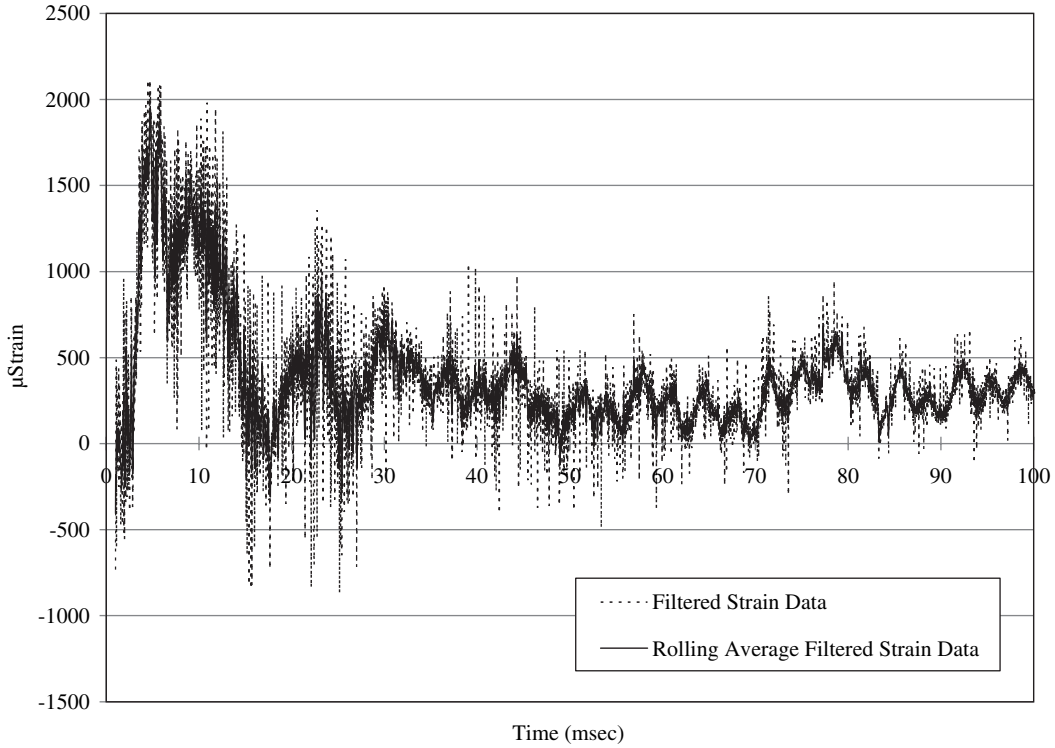

Figure 81. Longitudinal reinforcement (flexural) strain data: early gauge failure.

by the test frame, flexural strain data from four of the small standoff tests (1A1, 2A1, 2A2, 2B) were used.

The peak flexural strain was recorded for each strain gauge on the longitudinal reinforcement. At the same time, a moment–curvature plot for each column, which depends upon the column shape, the cross-sectional dimension, and the amount of transverse reinforcement, was calculated using Response 1990 (Collins and Bentz, 1990). Actual material properties multiplied by dynamic increase factors for strain rate effects were used to develop each moment–curvature diagram. From the moment–curvature plots, the moment corresponding to the peak flexure strain data and the plastic moment capacity were determined.

The columns were originally designed as propped-cantilevers; however, the measured strain data did not support this assumption. Figure 82 illustrates the moment diagram corresponding to a linear load distribution acting on a propped-cantilever and a simply supported column. All of the measured flexural peak strain data were positive, resulting in only positive moments. A propped-cantilever column, however, creates a negative moment at the fixed end (i.e., compression on the back face of the column). From these data, it can be concluded that insufficient fixity was provided at the base to provide the propped-cantilever boundary conditions assumed for design. While some partial fixity was likely, it has been assumed for the purposes of analysis that the column behaved as though it were simply supported because rotation could occur at the base. This assumption greatly simplifies the response analyses and agrees well with the recorded data. For each column, the shape of the moment diagram was approximated using the location of the strain gauges and moments corresponding to the measured strains from the moment–curvature plots.

5.2.3 Actual Load Distribution

The experimental data were also used to determine the actual load distribution experienced by each column during the blast tests. As indicated in the previous section, the boundary conditions for each column can be reasonably approximated with simple supports. Flexural strain data from four of the small standoff tests (1A1, 2A1, 2A2, 2B) were used to determine the approximate load distribution. The deformed shape from the static application of the assumed load profile is the primary deflected shape that the column is expected to experience during its dynamic response (Biggs, 1964). According to Biggs (1964), the mode shape corresponding to the static application of the load is expected to be the dominant one for members that experience an inelastic response, which was true for all the columns tested during this project.

To verify the actual load distribution developed by the blast-wave propagation, each column was analyzed using a uniform and triangular load distribution. Figure 83 illustrates the deflected shape and maximum moment for a simply supported column with each load distribution. The type of load distribution affects the location of maximum moment.

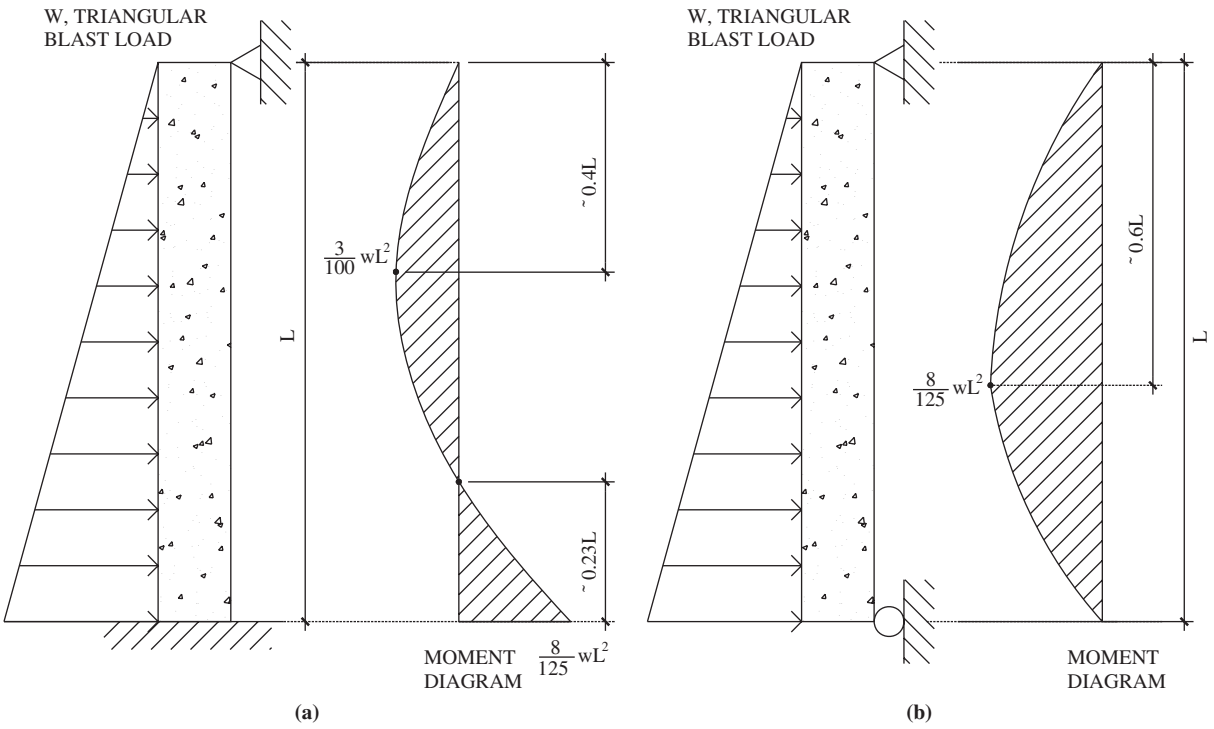

Figure 82. Moment diagram vs. boundary condition: a) propped-cantilever, b) simply supported.

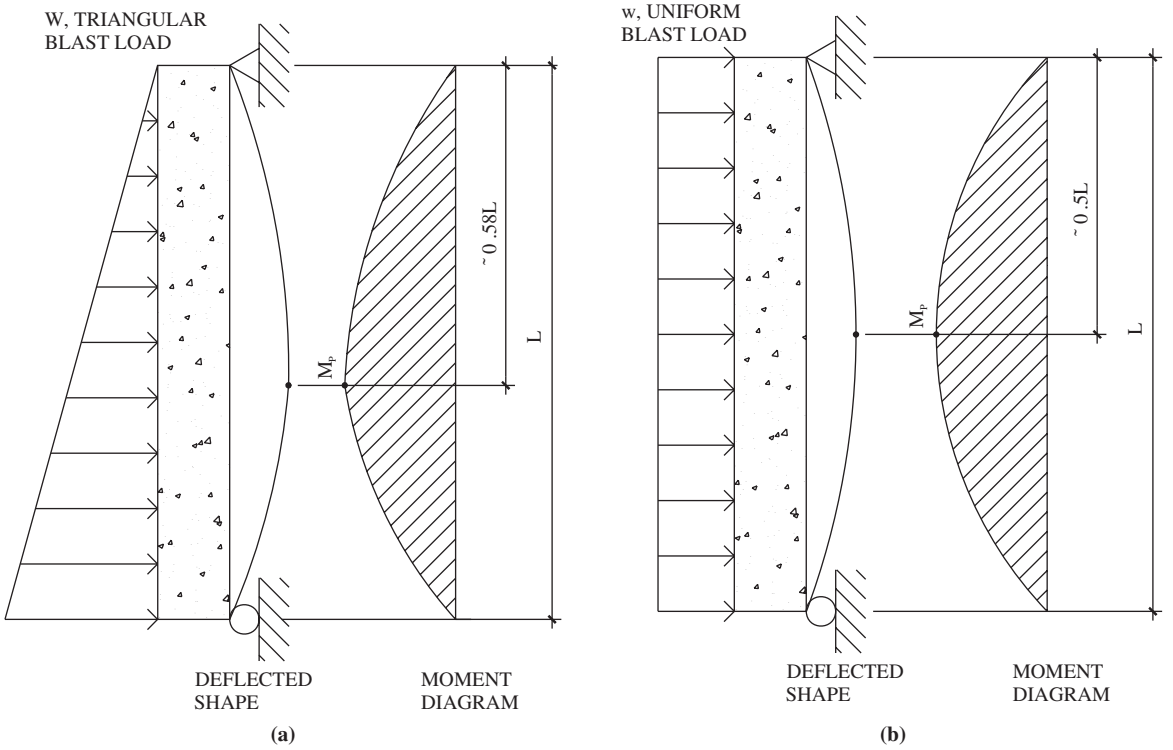

Figure 83. Blast-load distribution: a) triangular, b) uniform.

The magnitude of the maximum moment was assumed to be equal to the plastic moment or column capacity from the moment–curvature plots. The moment at each strain gauge was then calculated using the gauge location and assumed moment diagram. The percent difference between the experimental moment and calculated moment for each support condition and load distribution were compared to determine the best match.

Overall, a simply supported column best represents the boundary conditions in this test program. The load distribution depends on the scaled standoff. For a large scaled standoff ($Z \geq 2.0$ ft/lb$^{1/3}$, Column 1A1), a uniform load best approximates the blast load distribution; however, for a small scaled standoff (Column 2A1, 2A2, and 2B), a load that varies linearly from zero to w_o, the maximum magnitude of an assumed load curve, along the height of the column is a better approximation than the uniform case.

5.3 Summary

In this chapter, primary observations made from analytical studies and the experimental test programs were presented. The variation in blast loads on square and circular bridge columns were described and compared with predictions developed from empirical relationships and available software. In general, it was found that the actual pressures and impulses experienced by blast-loaded columns were less than those predicted by available methods, particularly near the top of the columns studied. Furthermore, the test data suggest that the clearing of shock waves around slender components is a complicated process, and additional research is needed to better characterize these effects.

Results from the Phase II experimental program were also presented in this chapter. The significance of each test variable, based on results from each small standoff and local damage blast test, was presented, and a description of damage observed from each test was given. The flexural strain data from the small standoff tests was presented and used to determine the actual boundary conditions and blast-load distributions that occurred during the test program. Based on the observations from the testing and analytical research, blast-resistant design and detailing guidelines for reinforced concrete highway bridge columns are presented in the next chapter.

CHAPTER 6

Design and Detailing Guidelines

6.1 Overview

The Phase I test program included eight small-scale blast tests at four sets of standoff. The experimental observations and analytical models indicate how cross-sectional shape, standoff, and geometry between the charge and column positions influence blast pressures on the front, side, and back faces of bridge columns. Phase II of the experimental testing program included ten half-scale, small standoff and six half-scale, local damage blast tests on eight different column designs. Column specimens were constructed with consideration given to five main test variables, including scaled standoff, column geometry, amount of transverse reinforcement, type of transverse reinforcement, and splice location. The following design and detailing recommendations have been developed from the experimental observations, test data, and corresponding analytical models.

6.2 Risk Assessment Guidelines for Bridges

Section 2.7 of the AASHTO LRFD guidelines, given below, focuses on risk assessment and design demand. Type, geometry, and importance of a bridge should be considered when completing a vulnerability assessment.

2.7 BRIDGE SECURITY

2.7.1 General

An assessment of the importance of a bridge should be conducted during the planning of new bridges and/or during rehabilitation of existing bridges. This should take into account the social/economic impact of the loss of the bridge, the availability of alternate routes, and the effect of closing the bridge on the security/defense of the region.

For bridges deemed important, a formal vulnerability study should be conducted, and measures to mitigate the vulnerabilities should be considered for incorporation into the design.

C2.7.1

At the time of this writing (Winter 2008), there are no uniform procedures for assessing the importance of a bridge to the social/economic and defense/security of a region. Work is being done to produce a uniform procedure to prioritize bridges for security.

In the absence of uniform procedures, some states have developed procedures that incorporate their own security prioritization methods which, while similar, differ in details. In addition, procedures to assess bridge importance were developed by departments of transportation in some states to assist in prioritizing seismic rehabilitation. The procedures established for assessing bridge importance may also be used in conjunction with security considerations.

Guidance on security strategies and risk reduction may be found in the following documents: Science Applications International Corporation (*2002*), The Blue Ribbon Panel on Bridge and Tunnel Security (*2003*), Winget (*2003*), Jenkins (*2001*), Abramson (*1999*), and Williamson (*2009*).

2.7.2 Design Demand

Bridge owners should establish criteria for the size and location of the threats to be considered in the analysis of bridges for security. These criteria should take into account the type, geometry, and importance of the structure being considered. The criteria should also consider multi-tier threat sizes and define the associated level of structural performance for each tier.

Design demands should be determined from analysis of a given size design threat, taking into account the associated performance levels. Given the demands, a design strategy should be developed and approved by the bridge owner.

C2.7.2

It is not possible to protect a bridge from every conceivable threat. The most likely threat scenarios should be determined based on the bridge structural system and geometry and the identified vulnerabilities. The most likely attack scenarios will minimize the attacker's required time on target, possess simplicity in planning and execution, and have a high probability of achieving maximum damage.

The level of acceptable damage should be proportionate to the size of the attack. For example, linear behavior and/or local damage should be expected under a small-size attack, while significant permanent deformations and significant damage and/or partial failure of some components should be acceptable under larger size attacks.

The level of threat and the importance of the bridge should be taken into account when determining the level of analysis to be used in determining the demands. Approximate methods may be used for low-force, low-importance bridges, while more sophisticated analyses should be used for high-force threats to important bridges.

6.3 Blast-Load Guidelines

After the completion of a risk and vulnerability assessment, a bridge component should be designed for the appropriate blast load. The following section defines important blast load variables.

3.15 BLAST LOADING

3.15.1 Introduction

Where it has been determined that a bridge or a bridge component should be designed for intentional or unintentional blast force, the following should be considered:

- Size of explosive charge,
- Shape of explosive charge,
- Type of explosive,
- Standoff distance,
- Location of the charge,
- Possible modes of delivery and associated capacities (e.g., maximum charge weight will depend upon vehicle type and can include cars, trucks, ships, etc.), and
- Fragmentation associated with vehicle-delivered explosives.

C3.15.1

The size, shape, location, and type of an explosive charge determine the intensity of the blast force produced by an explosion. For comparison purposes, all explosive charges are typically converted to their equivalent TNT charge weights.

Standoff refers to the distance between the center of an explosive charge and a target. Due to the dispersion of blast waves in the atmosphere, increasing standoff causes the peak pressure on a target to drop as a cubic function of the distance (i.e., for a given quantity of explosives, doubling the standoff distance causes the peak pressure to drop by a factor of eight). The location of the charge determines the amplifying effects of the blast wave reflecting from the ground surface or from the surfaces of surrounding structural elements. The location of the charge also determines the severity of damage caused by fragments from the components closest to the blast traveling away from the blast center.

Information on the analysis of blast loads and their effects on structures may be found in Biggs (*1964*), Baker et al. (*1983*), Department of the Army (*1990*), Bulson (*1997*), and Department of the Army (*1986*).

Section 3.4.1 of the AASHTO LRFD considers blast loading as an extreme event. Bridge scour associated with normal flow only needs to be considered in combination with blast loads.

2.6.4.4.2 Bridge Scour

As required by Article 3.7.5, scour at bridge foundations is investigated for two conditions . . .

When combined with blast loading, only the scour associated with normal flow should be considered.

C2.6.4.4.2

A majority of bridge failures in the United States and elsewhere are the result of scour . . .

The probability of blast loading taking place at the time the scour associated with the design or check floods exists is assumed to be quite small. For this reason, only the scour associated with normal flow needs to be considered when investigating the effects of blast loading.

6.4 Design and Detailing Guidelines for Columns

After the completion of a risk assessment, the design category for a blast-loaded, reinforced concrete bridge column can be established. Recommended guidelines for Section 4.7.6.2 of the AASHTO LRFD given below define each blast design category as a function of the scaled standoff, *Z*. Design and detailing guidelines for each category are further described below.

4.7.6.2 Substructure Blast Design Categories

For the purpose of designing substructure components for blast loads, the substructures shall be classified as Blast Design Category A, B or C based on the value of the scaled standoff, *Z*, as follows:

- For Blast Design Category A:
  $Z > 3$
- For Blast Design Category B:
  $3 \geq Z > 1.5$
- For Blast Design Category C:
  $Z \leq 1.5$

in which:

$$Z = \frac{R}{W^{1/3}} \qquad (4.7.6.2\text{-}1)$$

where:

Z = Scaled standoff (ft/lb$^{1/3}$)
R = Owner-specified standoff distance (ft)
W = Owner-specified charge Weight (lbs TNT equivalent)

Detailing of the transverse reinforcement for blast loading shall satisfy:

- For Blast Design Category A: No additional requirements beyond those for other applicable loads.
- For Blast Design Category B: All requirements for Seismic Zones 3 and 4 as specified in Articles 5.10.11.4.1c, 5.10.11.4.1d and 5.10.11.4.1e. The provisions of Article 5.10.2.3 shall also apply.
- For Blast Design Category C: All requirements for Seismic Zones 3 and 4 as specified in Articles 5.10.11.4.1c,

C4.7.6.2

The value of the scaled standoff, *Z*, is an indication of the intensity of the blast loading. In general, the higher the value of this parameter, the lower the expected intensity of blast loading and the less stringent the detailing requirements need to be for concrete columns.

Physical measures to increase the standoff distance are good design practice.

Bridge owners should establish criteria for the size and location of the threats to be considered in the analysis of bridges for security as specified in Article 2.7.2. These criteria should take into account the type, geometry, and importance of the structure being considered.

TNT equivalency is the ratio of the weight of an explosive to an equivalent weight of TNT. TNT equivalencies are used in the majority of research on blast effects to relate the energy output of common explosives to that of TNT. A table of averaged free-air equivalent weights for different explosives is provided in Tedesco (1999) or the U.S. Army's *Structures to Resist the Effects of Accidental Explosions* (Department of the Army, 1990).

Columns tested in Design Category C experienced a range of damage levels depending on the scaled standoff, *Z* (Williamson, 2009). Columns with a small scaled standoff were exposed to a severe blast load that resulted in the formation of plastic hinges, spalling of concrete cover, and, in some cases, total breach of the column (breach is defined as complete loss of concrete through the depth of the cross-section). Typically for $Z < 0.5$, local damage failures such as breaching control (Williamson, 2009). Columns with a large scaled standoff within Design Category C experienced a combination of shear and flexural cracking. Columns in Design Categories A

5.10.11.4.1d and 5.10.11.4.1e and as modified by Article 5.10.12.3. The provisions of Article 5.10.2.3 shall also apply.

and B will be required to withstand less intense loadings than those in Category C, and the design requirements for blast are reduced accordingly. Under these conditions, less stringent detailing requirements are needed to achieve acceptable performance.

4.7.6.3 Substructure Columns Blast Design
Shear Force

Where substructure columns satisfy the requirements for Blast Design Categories A and B, as specified in Article 4.7.6.2, specific blast loading magnitudes and distributions need not be considered in the design and detailing. Detailing requirements of Article 5.10.12 shall apply.

Where the transverse reinforcement of substructure columns is designed and detailed for Blast Design Category C, as specified in Article 4.7.6.2, they shall be designed and detailed to resist the shear force and moment resulting from a plastic analysis of the substructure column. Sufficient shear capacity shall be provided to assure that flexure controls.

C4.7.6.3

Substructure columns subjected to significant blast loads are expected to develop a plastic failure mechanism and, hence, plastic analysis of the substructure units is appropriate.

Using the base shear force from the static application of the load, the required pitch of transverse reinforcement can be determined by modifying the shear design equations to account for strain rate effects (ASCE, 1997), and solving for the spacing. The plastic moment, M_p, which is equal to the flexural resistance of the cross-section, M_n, should also account for the dynamic material strength, with dynamic increase factors for strain rate effects. Dynamic increase factors can be found in the U.S. Army's *Structures to Resist the Effects of Accidental Explosions* (Department of the Army, 1990) and ASCE (*1997*).

The maximum shear demand on a substructure column is a function of the boundary conditions and load distribution. Boundary conditions should be determined to correspond to the geometry of the column in question and its connections to adjacent components. Blast load distribution is a function of the standoff distance and the cross section of the column.

The expected failure mechanism and the estimated load distribution shall be taken into account when determining the shear demand on substructure columns.

The intent of the design categories is to provide adequate detailing for bridge columns as the structural demand and design threat increases. Decreasing the design threat by providing sufficient standoff distance from bridge columns is a safe alternative to increasing the design category and detailing requirements. In general, a higher scaled standoff requires less stringent detailing requirements because of the lower intensity of the blast loading.

All columns tested during the experimental program fell into Design Category C and experienced a range of damage levels depending on the scaled standoff. Columns with a small scaled standoff were exposed to a severe blast load that resulted in the formation of plastic hinges, spalling of concrete cover, and in some cases total breach of the column. Columns with a large scaled standoff but still within Design Category C experienced a combination of shear and flexural cracking. Columns in Design Categories A and B will be exposed to less intense loadings than those in Category C; thus, the design requirements for blast are reduced accordingly.

6.4.1 Design Category A

Highway bridge columns in Design Category A do not require any design modifications for blast resistance and should follow the design and detailing provisions required by the AASHTO *LRFD Bridge Design Specifications* (2007) for the normally anticipated loading conditions. Therefore, Category A columns should be designed ignoring blast loads.

5.10.12.2 Blast Design Category A

Blast loads should not be considered in the design and detailing of substructure columns designed for Blast Design Category A, as specified in Article 4.7.6.2.

C5.10.12.2

Due to the low intensity of the blast loading on substructure columns classified as Blast Design Category A, such columns are expected to perform satisfactorily when designed and detailed for other applicable loads without direct consideration of blast effects.

6.4.2 Design Category B

The design of highway bridge columns in Category B is based on the seismic design and detailing provisions of the AASHTO *LRFD Bridge Design Specifications* (2007), though there are some notable differences. The Caltrans *Seismic Design Criteria* (Caltrans, 2006) and *Bridge Design Specifications* (Caltrans, 2003) are additional resources for design and detailing requirements. There are only two exceptions to the above documents. First, a more stringent extension length of hooks when using discrete ties or hoops (see Chapter 5) is recommended. Hooks should consist of a 135° bend, plus an extension of not less than the larger of 15.0 d_b or 7.5 in. Second, transverse reinforcement detailing for the plastic hinge region should be applied over the entire column height. The additional transverse reinforcement over the entire column height results from the uncertainty associated with potential blast locations. Both of these exceptions are noted in Section 5.10.2.3 of the proposed design guidelines.

The more stringent hook length requirement performed satisfactorily when tested for seismic loading by Bae and Bayrak (2008) on full-scale concrete columns, where the opening of seismic discrete ties using hooks with a 135° bend, plus an extension of 8.0 d_b, was first demonstrated. Blast and seismic loads are both dynamic loads that induce dynamic structural responses and inelastic behavior. To allow the formation of plastic hinges and achieve a favorable mode of failure (flexure), adequate anchorage into the core concrete must be provided over the entire column height.

6.4.3 Design Category C

Highway bridge columns in Category C should, as a minimum, meet the design requirements for Category B columns. The following requirements place more stringent design and detailing guidelines on blast-loaded columns to further improve column survivability. The guidelines should be implemented in the following order of effectiveness: standoff, column geometry, amount of transverse reinforcement, type of transverse reinforcement and anchorage, and splice location.

6.4.3.1 Increase Standoff

One of the best ways to improve the performance of blast-loaded, reinforced concrete highway bridge columns is to increase the standoff distance with physical deterrents such as bollards, security fences, and vehicle barriers. If access to the columns is sufficiently limited, the design standoff distance can be increased, which will decrease the effects of blast loads on columns and the associated design category.

If only vehicle standoff is limited, small charges may still be placed in direct contact with a column, potentially causing localized damage or breaching of the concrete core. Results from local damage tests illustrate that increasing the standoff from the face of the structural column by as little as a few inches can increase a column's chance of survival substantially in a situation involving close-in blast loads. Aside from physical barriers, standoff from a structural member can be increased by adding a sacrificial cover or architectural feature around the structural column.

6.4.3.2 Column Geometry

The following recommendations regarding cross-sectional shape and dimension can improve the response of reinforced concrete columns subjected to blast loads.

6.4.3.2.1 Cross-Sectional Shape. To the extent practical, the cross-sectional shape of a blast-loaded column should be selected to minimize the intensity of the blast load. Cross-sectional shape affects how a blast load interacts with a column. The

use of a circular column is an effective way of decreasing the blast pressure and impulse on a column relative to a square or rectangular column of the same size, and the decrease in impulse can be up to 34% for small scaled standoffs (see Chapter 5). Therefore, the use of a circular column cross-section over a square cross-section is recommended, as stated in Section 2.7.3 of the AASHTO LRFD recommended guidelines.

2.7.3 Selection of Component Geometry

To the extent practical, the cross-sectional shape of the components subjected to blast loading should be selected to minimize the effects of the blast load.

C2.7.3

For components of the same width exposed to the same blast conditions, i.e., same charge weight and standoff distance, the intensity of blast loading may differ depending on the cross-sectional shape of the component (Williamson, 2009). For example, the blast pressure on square and rectangular columns is higher than on circular columns of the same width. The decrease in impulse on circular columns relative to square columns can be up to 34% for small scaled standoffs. Selecting shapes that result in reduced blast load will minimize the damage.

6.4.3.2.2 Cross-Sectional Dimension. Cross-sectional dimension also affects blast-wave propagation and the resulting spall patterns. Figure 84 illustrates two identically detailed columns with the only variables being column diameter and standoff. Column 2A2 was tested with a similar charge weight at a smaller standoff distance than Column 1A2, and despite the smaller scaled standoff, it sustained less damage. Therefore, increasing the column diameter improves the shear capacity of the column, minimizing the effects of detailing. A minimum cross-sectional dimension of 30 in. is recommended to improve the response of columns subjected to close-in blast loads.

(a) (b)

Figure 84. Importance of cross-sectional dimension: a) 18-in. diameter (Column 1A2), b) 30-in. diameter (Column 2A2).

6.4.3.3 Detailing and Design

If the standoff distance cannot be increased to decrease the effects of blast loads on columns sufficiently, the following design and detailing provisions are recommended: increasing the amount of transverse reinforcement, requiring continuous spiral reinforcement or discrete hoops with sufficient anchorage, and avoiding splices. Additional details for these design provisions are given below.

6.4.3.3.1 Amount of Transverse Reinforcement. Experimental observations show that increasing the volumetric reinforcement ratio is beneficial to the response of blast-loaded columns because it increases the column ductility and shear capacity. Direct shear is a major concern for blast-loaded columns, and adequate shear capacity is needed to ensure that columns fail in a ductile manner (see Chapter 5). Accordingly, to meet the high shear demands placed on a blast-loaded column in Category C, more stringent transverse reinforcement requirements than those used for seismic design are needed (see Chapter 5).

Equation 21 is recommended as the minimum transverse reinforcement ratio for all circular blast-designed columns, while Equation 22 is recommended as the minimum area of transverse reinforcement for all rectangular blast-designed columns. Columns meeting these minimums tested at a small standoff sustained minor and extensive damage; however, the core still remained intact and the column could still carry load. Essentially, 50% more confinement is recommended for blast-designed columns over current seismic provisions to improve the ductility and energy dissipation capacity of the cross-section.

$$\rho_s \geq 0.18 \frac{f'_c}{f_y} \tag{21}$$

$$A_{sh} \geq 0.18 s h_c \frac{f'_c}{f_y} \tag{22}$$

where:

f'_c = specified compressive strength of concrete at 28 days (psi)
f_y = yield strength of reinforcing bars (psi)
s = vertical spacing of hoops, not exceeding 4 in. (in.)
h_c = core dimension of column in the direction under consideration (in.)

This new minimum amount of transverse reinforcement should be applied over the entire column height to account for the uncertainty associated with potential blast locations. The proposed Section 5.10.12.3 of the AASHTO LRFD specifies these new minimum transverse reinforcement ratios.

5.10.12.3 Blast Design Category B and C

Where columns are designed and detailed for Blast Design Categories B and C, as specified in Article 4.7.6.2, transverse reinforcement shall be designed to satisfy all detailing requirements for Seismic Zones 3 and 4 as specified in Articles 5.10.11.4.1c, 5.10.11.4.1d and 5.10.11.4.1e except that:

- the requirements of Article 5.10.2.3 shall also apply
- the length of the intermediate plastic hinges shall be taken equal to twice the length of the end region specified in Article 5.10.11.4.1c

In addition, for substructure columns designed for Blast Design Category C:

- the volumetric ratio of spiral or seismic hoop reinforcement, ρ_s, for circular columns specified in Equation 5.10.11.4.1d-1 shall be increased by 50%, and

C5.10.12.3

In Seismic Zones 3 and 4, it is assumed that plastic hinges will form directly above the footing and, in multi column bents, directly below the cap beam. The length of the end region in Article 5.10.11.4.1c is based on these assumed locations.

For bridges subjected to blast loading, the column may develop intermediate plastic hinges. It is assumed that the plastic hinge region will extend for a distance equal to the length of the end region on either side of the intermediate plastic hinge location. This assumes that the length from the point of maximum moment to the end of the plastic hinge is independent of the type of loading and the location of the plastic hinge. The theoretical location of the intermediate plastic hinge can be computed from a plastic analysis.

The determination of an intermediate plastic hinge location can be uncertain because the blast loads vary significantly with both time and position along the height of a column. Accordingly, in most cases, the increased transverse reinforcement

- the total gross sectional area, A_{sh}, of rectangular hoop reinforcement specified for rectangular columns in Equations 5.10.11.4.1d-2 and 5.10.11.4.1d-3 shall be increased by 50%

specified by Article 5.10.12.3 should be placed throughout the entire height of the column.

The minimum amount of confinement reinforcement is increased to improve ductility and energy dissipation capacity of potential plastic hinges.

6.4.3.3.2 Type of Transverse Reinforcement and Sufficient Discrete Tie Anchorage. Experimental observations show that continuous spiral reinforcement performs better than discrete hoops for small standoff tests. The continuous reinforcement better confines the core at the base where a shear failure is most likely to occur. Therefore, continuous spiral reinforcement is recommended for blast-loaded columns.

Performance of discrete hoops can be improved by providing adequate anchorage into the concrete core. To avoid anchorage pullouts and to improve the performance of blast-loaded (and seismically loaded) columns with discrete hoops or ties, longer hook lengths than currently specified are recommended. Properly anchored hooks for blast loads should consist of a 135° bend, plus an extension of not less than the larger of 20.0 d_b or 10 in. Figure 85 illustrates the proper anchorage for each design category.

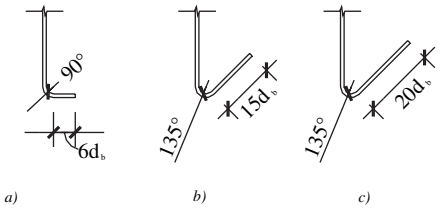

Figure 85. Discrete tie anchorage: a) Design Category A, b) Design Category B, c) Design Category C.

5.10.2.3 Hooks for Blast-Resistant Columns

Where columns are designed and detailed for Blast Design Categories B and C, as specified in Article 4.7.6.2, hooks in the transverse reinforcement specified in Articles 5.10.11.4.1c and 5.10.12.3 shall consist of a 135°-bend, plus an extension of not less than:

- For columns designed and detailed for Design Category B: the larger of 15 d_b or 7.5 in.
- For columns designed and detailed for Design Category C: the larger of 20 d_b or 10 in.

C5.10.2.3

Half-scale models of bridge substructure columns subject to blast loading indicated that columns constructed using transverse reinforcement utilizing 90 degree standard hooks with an extension length equal to 6 d_b did not perform satisfactorily. The deformation of the hooks caused the loss of core confinement and resulted in severe damage to the columns as shown in Figure C1.

Bae and Bayrak (2008) demonstrated the opening of seismic discrete ties using hooks with a 135°-bend, plus an extension of 8.0 d_b on full-scale concrete columns. Blast and seismic

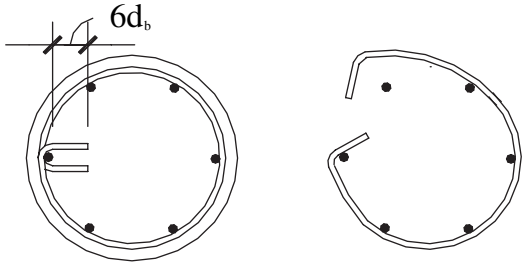

(a) Before Test (b) Anchorage Pullout

Figure C1. Unacceptable failure of discrete hoops with Standard Hooks when subjected to severe blast loading.

Where columns are designed and detailed for Blast Design Categories B and C, hooks in the transverse reinforcement and their required locations shall be detailed in the contract documents.

loads are both dynamic loads that induce dynamic structural responses and inelastic behavior. To allow the formation of plastic hinges and achieve a favorable mode of failure (flexure), adequate anchorage into the core concrete must be provided. Full-scale columns constructed using the 135°-bend with an extension equal to the larger of 15 d_b or 7.5 in. performed satisfactorily when tested for seismic loading (Bae and Bayrak, 2008). Such hooks are specified herein for columns designed and detailed for Design Category B.

Square columns constructed using the 135°-bend with an extension equal to the larger of 20 d_b or 10 in. performed satisfactorily during severe blast testing (Williamson, 2009). The core of such columns remained intact, and the column could still carry load even after sustaining extensive blast damage. This article extends the use of the longer extensions to all columns in Design Category C.

For all columns in Design Categories B and C, the increased level of detailing should be provided over the entire column height as recommended in Article C5.10.12.3

Further research is needed to evaluate the performance of welded hoops and other transverse reinforcement layouts.

6.4.3.3.3 Location of Longitudinal Splices. If the splice location is at or near the blast location, there is a possibility of breaching at the splice. Breach is defined as the complete loss of concrete through the depth of a cross-section. Local damage tests demonstrated that columns with a splice can experience significant damage over the majority of the column height and column failure due to lack of member continuity (concrete and steel) if breach occurs in the splice region. Columns without a splice contained the localized damage to about one column diameter above and below the blast location. Therefore, locating splices away from contact charges helps minimize localized blast damage. However, column survivability also depends on the amount and type of transverse reinforcement, cover depth, and cross-section size. Experimental data are lacking to determine column capacity in a blast-damaged state.

To improve the blast performance of columns that fall into Design Category C, splicing of longitudinal reinforcement should be avoided when feasible. If the use of a splice is necessary, the splice location should follow Section 5.12.13.4 from the AASHTO LRFD proposed guidelines.

5.12.13.4 Splices in longitudinal Reinforcement of columns in Design Category B and C

The provisions of Article 5.10.11.4.1f shall apply.

Where columns are designed and detailed for Blast Design Categories B and C, as specified in Article 4.7.6.2, the entire length of splices in longitudinal bars of substructure columns subject to blast loading shall be located:

- outside the end plastic hinge region specified in Article 5.10.11.4.1c,
- outside the column region that extends for a distance equal to the length of the end region, as specified in Article 5.10.11.4.1c, on either side of the expected location of intermediate plastic hinges, and;
- no less than 12 ft above the ground surface (or the lower deck in the case of a double-deck bridge) in the vicinity of the column.

C5.12.13.4

There is a possibility of breaching at the splice, if the splice location is at or near the blast location. The local damage tests on half-scale bridge columns (Williamson, 2009) illustrated that a column with a splice at a quarter of the column height from the base (0.25L) can experience significant local damage over the majority of the column height and column failure due to lack of member continuity (concrete and steel) in the splice region. Columns without a splice contained the localized damage to about one column diameter above and below the blast location. The intent of the requirements of this article is to locate splices away from plastic hinge locations and away from contact charges to help minimize localized blast damage. Locating the entire length of the splices at least 12 ft above the ground surface (or lower deck in the case of a double-deck bridge) is based on considering truck bombs to be located 6 ft above the ground (deck) surface.

At the time of this writing (winter 2008), experimental data to determine the column load resistance in the damaged state are not available.

Locating the entire length of the splices at least 12 ft above the ground surface (or the lower deck surface in the case of a double-deck bridge) is based on considering truck bombs to be located 6 ft above the ground (deck) surface. The intent of the above guidelines is to locate splices away from contact charges to help minimize localized blast damage. Additional research is needed to fully characterize splice behavior at locations very close to applied blasts.

6.5 Analysis Guidelines for Columns

To design for blast loads in Design Category C, a dynamic analysis should be completed.

4.7.6 Analysis of Blast Effects

4.7.6.1 General

As a minimum, bridge components analyzed for blast forces should be designed for the dynamic effects resulting from the blast pressure on the structure. The results of an equivalent static analysis shall not be used for this purpose.

C4.7.6.1

Localized spall and breach damage should be accounted for when designing bridge components for blast forces. Data available at the time these provisions were developed (winter 2008) are not sufficient to develop expressions for estimating the extent of spall/breach in concrete columns; however, spall and breach damage can be estimated for other types of components using guidelines found in Department of the Army (1990).

Due to the uncertainties that exist when considering likely attack scenarios and associated blast loads, an appropriate equivalent static load cannot be used for design. Moreover, the highly impulsive nature of blast loads warrants the consideration of inertial effects during the analysis of a structural component. Therefore, an equivalent static analysis is not acceptable for the design of any structural member subjected to blast loads. Information on designing structures to resist blast loads may be found in ASCE (*1997*), Department of the Army (*1990*), Conrath et al. (*1999*), Biggs (*1964*), and Bounds (*1998*).

Section 4.7.6.3 outlines a procedure that checks the flexural capacity of a column exposed to a close-in blast load using a single-degree-of-freedom analysis.

4.7.6.3 Blast Analysis Procedure for Highway Bridge Columns

To evaluate the capacity of a blast-loaded column, a flexural analysis that calculates rotation and flexural ductility shall be completed.

In lieu of a refined analysis of blast loading, an equivalent blast load based on the scaled standoff is adequate. Software such as BEL or BlastX can be used to determine the equivalent blast load in terms of uniform pressure and impulse. A single-degree-of-freedom analysis using the equivalent loads shall be completed to calculate rotation and flexural ductility. The design limits are specified as follows:

$$\theta \leq 1.0^\circ$$
$$\mu \leq 15$$

C4.7.6.3

This analysis uses flexural response as an indicator for shear response, and shear is not directly calculated. Direct shear capacity, per UFC 3-340-01, is not necessarily indicative of shear performance (Williamson, 2009). Shear checks are directly built into the design limits of the flexural analysis.

The design limits, rotation and flexural ductility, are based on large-scale test data (Williamson, 2009). Columns tested with slight to moderate damage without significant shear damage were used to select these limits. These limits help ensure that a shear mechanism does not form as a result of the large shear demand caused by close-in blast loads (Williamson, 2009). The flexural performance of a column can be improved by increasing the column cross-sectional size and the amount of longitudinal reinforcement.

where:
θ = Rotation (degrees)
μ = Flexural Ductility

These limits ensure that column damage is limited to allow continued service following an extreme event.

In general, the blast analysis procedure for highway bridge columns includes the following steps.

1) First, determine the design threat in terms of standoff and charge weight (reference Articles 2.7.2 and 3.15.1) to calculate the scaled standoff and design category (reference Article 4.7.6.2).
2) Detail the column according to the design category required by the design charge weight and standoff distance specified in step 1), and conduct a dynamic analysis using steps 3)-5) if required. Article 4.7.6.2 provides references to the detailing and design guidelines required for each design category.
3) Using the charge weight and standoff distance specified in step 1), use an acceptable load prediction method to determine an equivalent uniform pressure and impulse. At a minimum, the load prediction technique employed for this purpose should account for the increase in pressure and impulse due to reflections off the front face of the column and ground/deck surface. BEL and BlastX are two examples of load prediction software that are acceptable for this purpose.
4) Determine the mass of the column, and using a uniform load shape, calculate the maximum flexural resistance and stiffness for each stage of response of the column to create a resistance diagram. The boundary conditions used to determine the resistance diagram should correspond to those in the actual structure. If the exact boundary conditions in the actual structure are uncertain (i.e., if a boundary is neither pinned nor fixed but has some unknown restraint), two analyses assuming an upper and lower bound for the unknown boundary conditions will provide an adequate range of response prediction for design purposes.
5) Using appropriate load-mass factors to compute the equivalent load, mass, and stiffness of the column, employ a single-degree-of-freedom analysis method of choice to determine the peak displacement and support rotation of the column The load-mass factors for a uniformly-loaded column are as follows:

Simply-Supported

$K_{LM.elastic} = 0.78$
$K_{LM.plastic} = 0.66$

Propped-Cantilever

$K_{LM.elastic} = 0.77$
$K_{LM.elastic\text{-}plastic} = 0.79$
$K_{LM.plastic} = 0.67$

Fixed-Fixed

$K_{LM.elastic} = 0.77$
$K_{LM.elastic\text{-}plastic} = 0.79$
$K_{LM.plastic} = 0.66$

The time varying load should be a triangular load with a magnitude equal to the peak pressure calculated in step 3), and the triangular load curve should preserve the total impulse. Therefore, the duration of the triangular load should be equal to 0.5 × impulse / peak pressure.

6) Compare the computed peak displacement and support rotations to the allowable limits for member ductility and support rotation specified in section 4.7.6.3, and redesign if necessary

Further details of the single-degree-of-freedom analysis procedure can be found in Bigg's *Introduction to Structural Dynamics* (1964), Tedesco's *Structural Dynamics: Theory and Application* (1999), and the Department of the Army's *Structures to Resist the Effects of Accidental Explosions* (TM 5-1300) (1990). Note that load factors are not specified in blast-resistant design due to the inherent uncertainty associated with blast loads; however, dynamic increase factors and strength increase factors are used to better estimate actual design strength and reduce design conservatism for an extreme load event. Dynamic and strength increase factors can be found in ASCE (*1997*) and Department of the Army (*1990*). Additionally, the single-degree-of-freedom procedure does not necessarily require the use of an equivalent uniform load. If the results of an acceptable load prediction technique produce the data necessary to develop and apply a non-uniform load distribution to the column, a designer may elect to use this more refined load distribution in lieu of an equivalent uniform load. If this option is selected, however, the designer is required to use this more refined load distribution to calculate the appropriate stiffness, maximum resistance, and load-mass factors for each stage of response. The three references cited above provide the information necessary to compute these values using the applied load distribution.

Design examples in Chapter 8 provide detailed calculations required to evaluate performance of bridge columns subjected to blast.

6.6 Summary

Blast-resistant design and detailing guidelines for reinforced concrete highway bridge columns, based on experimental observations and data, were proposed in this chapter. This information was provided in a manner that is consistent with the AASHTO LRFD Specifications (2007) so that bridge engineers can readily use the results of this research. The following chapter summarizes guidelines for analytical modeling of blast-loaded bridge columns.

CHAPTER 7

Analysis Guidelines

7.1 Overview

The advantages, capabilities, limitations, and uses of several levels of load and response analysis techniques have been outlined in previous sections of this report. In the sections below, application of both simplified analysis techniques and detailed finite element modeling for the case of blast-loaded bridge columns are illustrated. Although the procedures described below provide a starting point for engineers who wish to learn the intricacies of modeling blasts acting on bridge columns, they should not be taken as a comprehensive lesson in analytical modeling of structures subjected to blast loads, and it is recommended that only analysts experienced in both blast phenomenology and analytical modeling predict structural response to blast loads.

7.2 Simplified Analyses Guidelines

Design procedures based on the results of a single-degree-of-freedom analysis are those most commonly used for blast-resistant design. Although engineers increasingly feel the need to use highly complex finite element analyses for design, the majority of design cases do not warrant such highly detailed analyses due to the many uncertainties associated with blast loads, such as the exact charge weight, shape of the charge, type of explosive material, and standoff distance. Additionally, blast-resistant designs typically allow significant nonlinear behavior to expend the energy associated with dynamic blast loads, and SDOF analyses have been shown to provide acceptable results when structural components undergo large inelastic deformations (Department of the Army, 1990). The theory behind and justification for the SDOF design procedure is presented in Section 4.2 of this report and several publicly available texts, such as *Structural Dynamics: Theory and Application* by Joseph Tedesco (1999) and *Introduction to Structural Dynamics* by John Biggs (1964). Additionally, the U.S. Army Technical Manual TM 5-1300, *Structures to Resist the Effects of Accidental Explosions* (Department of the Army, 1990), contains the procedure most commonly applied to the blast-resistant design of building components. The design procedure for reinforced concrete bridge columns outlined in this section closely adheres to the widely accepted and trusted procedure from TM 5-1300 with special considerations for bridge columns derived from the experimental portion of this research.

Bridge columns should be designed using an SDOF analysis procedure, which initially requires the computation of a few basic column properties such as the plastic moment capacity, M_p, the total mass of the member, M, and the moment of inertia, I_z. The material strengths used in the calculation of the plastic moment capacity should include a strength increase factor to account for the presumed actual material strengths and dynamic increase factors to account for strength increases due to strain-rate effects. The dynamic increase factors are material specific, and they should be applied to the material properties prior to calculating the section capacity. Table 16 shows common strength increase factors for concrete, and Table 17 shows common dynamic increase factors for concrete and steel. Increasing material strengths for design may seem counter-intuitive relative to normal design procedures; however, a typical bridge structure is not expected to experience repeated blast loadings over its lifespan, and typical design objectives are to sacrifice the structure to protect life, provide egress, and, in the case of bridge columns, allow motorists and pedestrians to flee the bridge. Therefore, the blast-resistant design of bridge columns should use the entire available capacity of a column to resist these extreme loads.

The SDOF-based design procedure also requires an engineer to predict the magnitude, distribution, and time-history of the blast load applied to a member. Available load prediction techniques, such as the charts or empirical equations provided in the U.S. Army's TM 5-1300 or software developed to predict loads on structures based on first-principal or empirical data, such as ConWep, BlastX, or BEL, are valuable tools for this purpose. Although load cases for typical design

Table 16. Strength increase factors.

Material	SIF
Structural ($f_y \leq 50$ ksi)	1.10
Reinforcing Steel ($f_y \leq 60$ ksi)	1.10
Cold-Formed Steel	1.21
Concrete*	1.00

* The results of compression tests are usually well above the specified concrete strengths and may be used in lieu of the above factor. Some conservatism may be warranted because concrete strengths have more influence on shear design than bending capacity. TM 5-1300 specifies a SIF of 1.10.

Source: *American Society of Civil Engineers, 1997*

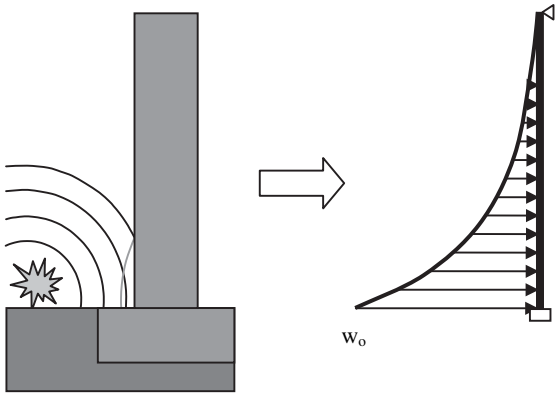

Figure 86. Example of hypothetical assumed load shape for an SDOF analysis.

scenarios include load factors that conservatively account for uncertainties in the assumed loads, these factors should not be used when designing bridge columns to resist blast loads. Regardless of the load prediction technique selected, the result should be a distributed load that varies only with time and approximates the predicted load as it varies in both time and position. Figure 86 shows an example load shape for a hypothetical bridge column and blast scenario. This assumed load distribution is necessary to conduct a plastic collapse analysis of a member to calculate the maximum resistances and hinge locations for each stage of response. Figure 19 shows the three stages of response for a beam with two fixed ends and a uniformly distributed blast load. The hinge locations will provide the boundary conditions needed to determine the normalized deflected shapes that result during each stage of response from the application of the assumed load shape. These normalized deflected shapes allow the computation of the equivalent load, equivalent mass, and system stiffness that equate the single-degree-of-freedom system to the real system for each stage of response. The visual relationship between the single-degree-of-freedom system and the real system is shown for the elastic stage of response for a simply supported beam in Figure 87. The calculation for the equivalent load is based on the work done by the assumed distributed load as the member undergoes a unit deflection at the point of maximum deflection, and the equivalent mass represents the inertia contributed to the system by the mass distributed along the length of the member as the member undergoes a unit deflection at the point of maximum deflection. While the intent of this section is to describe the blast-resistant design process for bridge columns, it is not meant to provide a tutorial on developing the SDOF analysis procedure, and Bigg's *Introduction to Structural Dynamics* (1964) and the U.S. Army's TM 5-1300 *Structures to Resist the Effects of Accidental Explosions* (Department of the Army, 1990) provide charts that contain factors to quickly convert the total load and total mass into SDOF-equivalent values for common loading scenarios and boundary conditions and the equations needed to calculate these equivalent properties for other cases. The determination of equivalent system properties for this analysis and design procedure should assume a single load distribution that does not vary with position along the member. Real structural systems do not experience loads in this manner, as the shock wave will propagate along the length of a member, applying the load at different locations along the member at different points in time. While it technically may be possible to vary the load distribution along the length of the member during an SDOF analysis by updating the equivalent load and mass

Table 17. Dynamic increase factors.

Stress Type	Far Design Range*			Close-in Design Range†		
	Reinforcing Bars		Concrete	Reinforcing Bars		Concrete
	f_{dy}/f_y	f_{du}/f_u	f'_{dc}/f'_c	f_{dy}/f_y	f_{du}/f_u	f'_{dc}/f'_c
Flexure	1.17	1.05	1.19	1.23	1.05	1.25
Diagonal Tension	1.00	1.00	1.00	1.10	1.00	1.00
Direct Shear	1.10	1.00	1.10	1.10	1.00	1.10
Bond	1.17	1.05	1.00	1.23	1.05	1.00
Compression	1.10	1.00	1.12	1.13	1.00	1.16

*Far Design Range: $Z \geq 2.5$ ft/lb$^{1/3}$

†Close-in Design Range: $Z < 1.0$ ft/lb$^{1/3}$

Source: *Department of the Army, 1990*

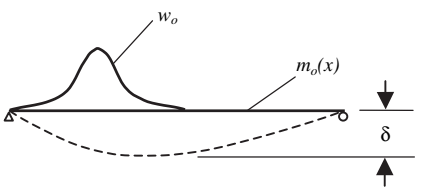

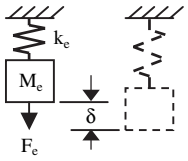

$w_o(x)$	assumed distributed load	F_e	equivalent load
$m_o(x)$	mass per unit length	M_e	equivalent mass
δ	maximum deflection of member	k_e	equivalent stiffness
		δ	maximum deflection of member

Figure 87. Relationship between real system and equivalent SDOF system.

factors with each time step, most analyses should not include this additional complexity because the uncertainty in the loads does not justify this effort, and to the knowledge of the authors, no currently available SDOF software has this capability. Additionally, as mentioned above, the current procedure for building components has shown good correlation to experimental results with the selection of appropriate assumed load distributions.

Once the equivalent SDOF system properties are known, an SDOF analysis should be used to determine the peak deflection and maximum support rotations of the bridge column being analyzed. User-friendly software packages are available for this purpose, or the bridge designer may wish to create an SDOF analysis tool using the basic mechanics of structural dynamics. In either case, the results of an SDOF analysis should be compared to allowable ductility ratios and rotation limits. Based on the results of the experimental portion of this research program, acceptability criteria for blast-resistant concrete bridge columns are a maximum support rotation of 1.0 degree and a maximum ductility ratio of 15.0, and the U.S. Army TM 5-1300 *Structures to Resist the Effects of Accidental Explosions* (Department of the Army, 1990) contains similar values for building components. A designer should resize a member and repeat the analysis process if the SDOF analysis results in a ductility ratio or support rotation that exceeds the allowable limits.

Both direct shear and diagonal shear are important for blast-resistant design, and a bridge column design should contain enough capacity through a combination of transverse reinforcement and longitudinal reinforcement dowel action to prevent a shear failure and force a flexurally dominated response. An important and notable difference between the design of blast-loaded bridge columns and blast-loaded building columns that is captured in the design procedure developed under this research project is the manner in which diagonal shear and direct shear at the base of a bridge column are handled. In the design procedure proposed for bridge columns, transverse steel detailing requirements and flexural response limits have been selected to ensure that corresponding shear deformations remain within acceptable limits. Accordingly, design for direct shear at the base of a blast-loaded bridge column is inherently included in the SDOF design procedure and is not checked using the same procedure as is used for blast-loaded building columns. Furthermore, the design guidelines presented in the previous chapter outline prescriptive requirements for the minimum allowable volumetric reinforcement ratio. Additional details and a demonstration of how the design procedure is implemented can be found in Chapters 6 and 8, which provide specification-ready design guidelines and detailed design examples, respectively. As described above for the calculations for flexural capacity, the shear design should consider strength and dynamic increase factors and no load factors.

The simplified design and analysis procedure described in this section is based on the widely accepted and trusted procedure presented in the U.S. Army's TM 5-1300 *Structures to Resist the Effects of Accidental Explosions* (Department of the Army, 1990) with specific modifications for bridge columns based on the results of the experimental portion of this research. As such, this procedure should provide a reasonable yet conservative design at a minimal cost, and it is recommended for bridge columns when a simplified analysis procedure is appropriate, as described in Chapter 5. Additional information regarding this procedure and its applicability to building components can be found in various sources, including *Structural Dynamics: Theory and Application* (Tedesco, 1999) and *Introduction to Structural Dynamics* (Biggs, 1964).

7.3 Airblast Modeling Using Computation Fluid Dynamics

Finite element codes employing computational fluid dynamics are valuable tools for predicting blast loads for situations involving complex designs, research problems, and post-event evaluations because they can include phenomena not captured by simplified analysis procedures, such as multiple reflections off complicated geometries, localized member failure, and blast loads coupled with structural response.

While some finite element implementations of high-explosive modeling have user-friendly graphical user interfaces (GUIs), many general-purpose finite element codes require a user to manually specify a wide range of parameters, including the geometry, material properties, and mesh characteristics. While these codes can produce reliable results for a wide range of complex airblast scenarios, they also can generate highly misleading and erroneous solutions. These models are highly mesh-dependent, and several variables greatly influence the resulting load predictions, such as the explosive and air material properties, the size and shape of the elements in the explosive region, and the density and shape of the air mesh. Successful airblast modeling using computational fluid dynamics codes requires an analyst experienced in theoretical shock physics, realistic physical behavior of high-explosive detonations, and the capabilities and limitations of the selected finite element code.

Various general-purpose finite element codes with computational fluid dynamics capabilities implement the detonation of high explosives differently, and multiple methods exist even within the same finite element code. It is important to refer to the user's manual of the selected software to determine the most appropriate method for the scenario under consideration. Most implementations require separate definitions for the explosive and the air, and this separation can be defined in at least two ways. One way to separate the explosive and air is to have regions of elements that represent both materials. In this case, the elements in each region have the property definitions of the material they represent, and the regions share common nodes on their boundaries. The other approach to separate the explosive and the air is a volume fraction technique, which requires the user to create a single mesh and then define the volumes within that mesh that contain the individual materials. Both of these methods will produce similar results if implemented correctly because the Arbitrary-Lagrangian-Eulerian (ALE) elements that define both the explosive and the air allow multiple materials within each element over the duration of an analysis. Using this analysis technique, general-purpose finite element codes generally require the user to allow the ALE mesh to contain multiple fluid definitions within the same elements. Regardless of the approach selected to separate the materials, efficient and reliable analyses have different mesh requirements for the explosive and air regions. These requirements are described further below.

As with any finite element analysis, the mesh shape and size greatly influence the fidelity of the results. The literature documents the influence of mesh size on analytical results, and the work completed for this research reinforces its importance. Pressure and impulse predictions improve significantly as the air mesh becomes progressively finer (Cendon et al., 2004; Knight et al., 2004; Luccioni et al., 2006), and airblast models lacking sufficiently small elements throughout the mesh will generate inaccurately low pressures and impulses. Therefore, the analyst should always conduct a thorough sensitivity study comparing analytical results with known empirical results to determine the minimum mesh density required for the scenario under consideration. Additionally, the mesh size specifically in the explosive region is very important. The explosive mesh should be as uniform as possible, with elements of roughly the same dimensions, and no less than 16 elements along each edge of the explosive region is sufficient to allow the explosive to burn completely (Alia and Souli, 2006). Accordingly, the analyst should avoid using cylindrical or spherical meshes in the explosive region (i.e., a combination of wedge or conical elements with quadrilateral elements). The elements closest to the origin in these meshes will have disproportional edge lengths, and the analyses will produce lower peak pressures and impulses at a much larger computational cost than a model with only quadrilateral elements in the explosive region.

Computational fluid dynamics analyses often employ "tracers," which are the analytical equivalent of pressure gauges, to track variations in pressure over the duration of an analysis, and the mesh dimensions and fineness around these tracers greatly influence the computed results. Thus, in addition to mesh requirements for the explosive region and for the model as a whole, the region around a target demands a sufficiently fine mesh to capture clearing effects and reflections. If the mesh is too coarse in an area where the blast wave will reflect off a target, the tracers in this region may detect very inaccurate pressure–time histories because the mesh will not be able to adequately capture pressure differentials from one location to another. For example, if the mesh is too coarse around tracers located on a target, two different tracers at different locations on the same target with different clearing times and angles of incidence may record identical pressure–time histories because they reside within the same element. In fact, a simulation may not be able to detect the difference between, for example, a square column and a circular column at the same standoff when the element edge length at the face of the columns is greater than the width of the columns (i.e., the front faces of the columns completely reside within the width of one element). Thus, an airblast model needs a very fine mesh in the target region when tracers are present, with several elements across the width and along the length of a target, to accurately capture clearing effects and the differences in pressure along the face of a target.

While the mesh size is a well-established and documented variable that influences the accuracy of an explosion simulation, the mesh shape alone also plays an important role. A uniform mesh with the shape of the expected shock front propagation is preferable to other discretizations, as it allows the pressure perpendicular to the direction of propagation to remain in equilibrium. As such, a spherical mesh is most

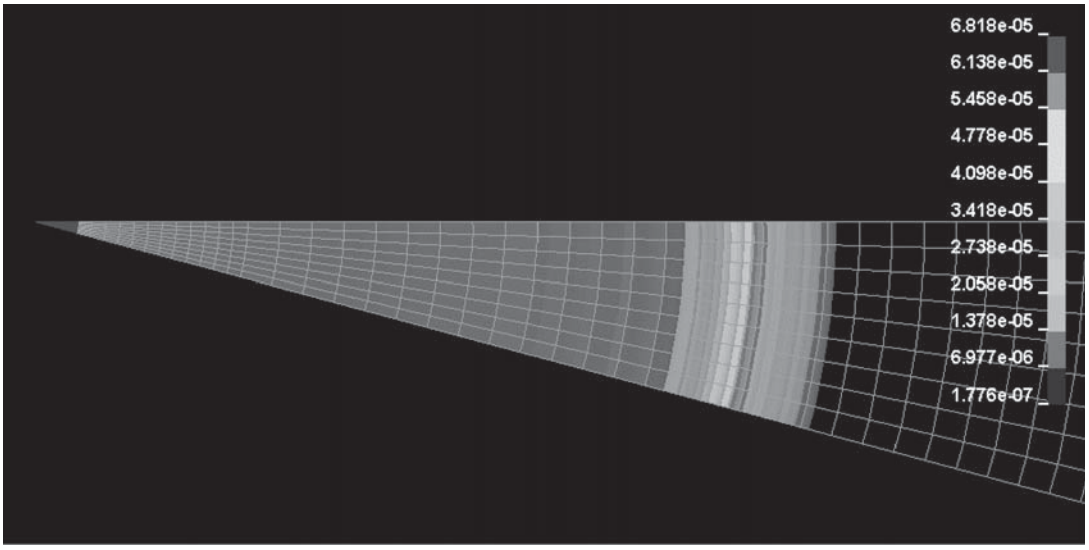

Figure 88. Isosurfaces of blast pressures in a uniform mesh.

appropriate for a spherical burst, and likewise, a cylindrical mesh is most appropriate for a cylindrical burst. A non-uniform mesh may not allow the pressure to equilibrate perpendicular to the shock front, and a pressure differential can occur between elements as shown in Figures 88 and 89. These two simulations represent similar explosions while using two different meshes. The mesh in Figure 88 is a symmetrical wedge from a uniform cylindrical mesh, and the mesh in Figure 89 is a symmetrical wedge with a mesh that has a transition to maintain a finer mesh in the region around a target. (The target is not shown in the figure.) The different shades represent pressure levels, similar to a topographical map, and the pressure values in the scales in the upper right of the figures are in Mbar units. Figure 88 shows a uniform spherical blast wave, and the pressure in this model is in equilibrium perpendicular to the direction of flow. Figure 89 shows distortion in the blast wave perpendicular to the direction of flow, and this distortion is evident in the variation in shading seen in the shock front. The concentration of darker shading in the fine mesh region indicates a concentration of higher pressure in the denser element region. This pressure differential is an inherent result of a non-uniform mesh because the uniformly expanding shock front has to distribute fluid among uneven element widths, and as a result, coarse mesh regions lose pressure and do not have accurate results. Thus, as illustrated by these figures, distortion in the blast wave can occur in models that do not use uniform meshes, and a mesh with elements of varying sizes may lose accuracy in computing pressure and energy

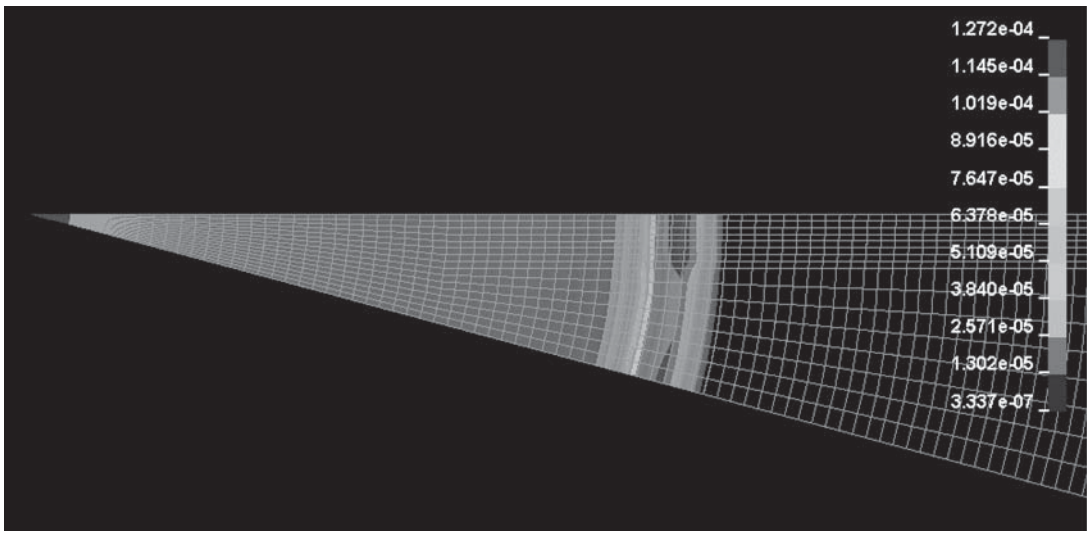

Figure 89. Isosurfaces of blast pressures in a non-uniform mesh.

relative to a model with a uniform mesh. At the very least, a model with elements of varying sizes will contain relative inaccuracies from one location of interest to another, and in some cases, the entire model will give deficient results. While the geometry of the air mesh outside the explosive region should conform to these rules, the elements within the explosive region should adhere to the guidelines presented above. Thus, the explosive region should employ only quadrilateral elements with similar proportions, even if the air mesh is cylindrical or spherical.

The selected time step is another important parameter that the analyst must specify. While the results of this research do not necessarily show that continually decreasing the time step will always increase the accuracy of a model, the literature states that smaller time steps generally lead to more accurate results than models with larger time steps, albeit while compromising computational efficiency (Knight et al., 2004). The analyst should always conduct a study to determine the sensitivity of an analysis to the time step, and the optimum time step should be used.

Strategies do exist to achieve adequate mesh fineness while eliminating the need to construct cost-prohibitive model geometries. One such method is an adaptive mesh, which automatically contracts in regions of high pressure gradients, such as around a shock front. While this method can prevent costly mesh geometries by allowing a coarse mesh to automatically subdivide into a fine mesh in regions where calculations are important, the adaptive mesh algorithm can significantly increase the computational time of the analysis. Accordingly, there is a trade-off in efficiency between using an adequately fine mesh that is uniform with one that employs an initially coarse mesh and mesh refinement. The appropriate alternative will depend on the specifics of the model being solved. Symmetry is another strategy to achieve adequate mesh fineness without compromising cost. Symmetry in an airblast model can mean cubic, cylindrical, or spherical fractions as appropriate, and an example of cylindrical symmetry is shown in Figure 88. Regardless of the mesh shape and size chosen for a given application, the analyst should always consider symmetry as a useful resource to reduce computational cost. While employing symmetry is commonly used whenever possible, perfect reflecting surfaces do not exist in real scenarios, and an analysis that employs symmetry may produce results that do not compare well to high-explosive detonations on or near deformable surfaces (e.g., the earth).

The term "explosive burn" commonly refers to the procedure of analytically simulating the burning of a high-explosive material to produce high-pressure gaseous detonation products. While the explosive burn modeling technique varies depending on the finite element code of choice, a common implementation involves one or more mathematical equations that essentially expand the explosive material at a high rate to the pressure, volume, and density of the gaseous detonation products. The explosive burn is the most computationally demanding aspect of a free-field airblast simulation because the mesh in the explosive region needs to be very fine for suitably accurate results, and a strategy to reduce the computational demand of a model is to eliminate the need to repetitively burn the explosive material during an analysis. To that end, it is possible in some cases to burn the explosive with one model and then remap the shock front onto a separate mesh. While this approach may cost the analyst some additional preparation time, it can prevent the analyst from rerunning computationally demanding detonation simulations.

While these guidelines will improve the efficiency and accuracy of modeling high-explosive detonations in finite element codes, obtaining reliable load predictions from high-level analyses is challenging. Reproducing experimental results can be especially challenging, as in many cases it is difficult to know the exact atmospheric conditions, explosive material properties, and locations of pressure gauges. Moreover, some codes may have inherent deficiencies and simplifying assumptions built into their calculations, and these deficiencies can compound during repetitive calculations over numerous time steps. Thus, prior to endorsing any structural loads obtained from a finite element analysis, the analyst should always verify the accuracy of the computational fluid dynamics (CFD) capabilities within the code of choice by checking free-field overpressures at a few locations in a model against verifiable empirical results. The analyst should adjust model variables to reflect reality as needed, and as a last resort, one can overcome certain deficiencies and inaccuracies by artificially adjusting the explosive properties and specifically calibrating the model to match experimental results. Only analysts with a firm grasp of high-explosive theory and realistic behavior should attempt this approach, and those interpreting the results should exercise extreme caution. While adjusted explosive properties may reproduce accurately part or all aspects of a pressure–time history at a given point in space and time, altering model input can compromise the results at other locations within a model, and the net load throughout the structure being modeled may not represent reality nor satisfy the intent of the analysis being performed.

7.4 Concrete Modeling

Several options exist in most finite element codes for modeling concrete material behavior, and the performance of each varies depending on the accuracy of the material model, the implementation within the finite element code, and the experience of the analyst. Concrete constitutive models used in finite element analyses should employ at least a two-invariant formulation and a nonlinear equation-of-state to capture the nonlinear hardening and softening behavior characteristic of

concrete, and three-invariant formulations are preferable when available to correctly model volumetric expansion (Magallanes, 2008). Additionally, past research shows that constant-stress solid elements produce good results for both static and impact analyses (Schwer and Malvar, 2005; Gokani, 2006). Regardless of the concrete model and element formulation chosen, however, an analyst should verify the fidelity of that model by comparing the results of a single element stress analysis to known theoretical or experimental behavior of the selected concrete (Magallanes, 2008), and the results from a model of a complete reinforced concrete structure should show good correlation with known experimental results prior to trusting analytical results.

Most concrete structures contain reinforcement, and finite element models should include the concrete and reinforcing steel explicitly. Models should employ solid and beam elements that have displacement functions of the same order. For example, truss elements are best for rebar when a model employs constant-stress solid elements for concrete because both element formulations have linear displacement functions, thereby guaranteeing displacement compatibility along the shared element edges. The simplest approach to modeling rebar is to connect the rebar elements to the concrete elements at common nodes. Although this method is a simplification of reality in which potential slip between rebar elements and concrete elements is ignored, analysts typically choose this approach because it provides reasonable results for the preparation time required. This simplification may not be appropriate in some cases, and models can incorporate additional aspects of concrete behavior, such as bar slip and rebar buckling, by using beam element formulations for rebar or connecting rebar elements to concrete elements using springs. While including such features may be more representative of actual behavior, this increase in accuracy comes at a large preparation and computational cost. In some cases, however, the flexural resistance of rebar can contribute significantly to structural response, as when significant spall and breach degrades a member cross-section. Finite element models should include rebar elements with a beam element formulation rather than a truss element formulation for these cases. In general, the analyst should first try an analysis with truss elements to determine if section loss and the flexural resistance of the reinforcing steel are important.

As with concrete, all steel material property definitions should consider strain-rate dependent properties when predicting response to airblast, and two procedures are available for this purpose. As outlined in Section 2.2.4, the first method to consider the effect of strain rate on reinforcement properties involves increasing the yield and ultimate strengths of the reinforcing steel by applying constant dynamic increase factors such as those shown in Table 17. While this method is often acceptable for design because it quickly and easily allows the computation of conservative material properties for most airblast cases, it does not allow an accurate comparison between member stresses at a given time step and material properties computed using the strain rate from the same time step. Therefore, simply applying constant dynamic increase factors may not be appropriate for some analysis cases. Experimental studies show that actual material properties vary significantly with strain rate and continue to increase as the strain rate increases (Department of the Army, 1990; Tedesco, 1999), and finite element analyses that include erosion (i.e., removal of failed elements) need accurate material properties during each time step to assess the adequacy of each element. Because both member stresses and actual material properties vary significantly during an analysis, the application of constant dynamic increase factors could result in premature or delayed erosion of some elements. Most general-purpose finite element software includes strain-rate dependent material definitions that are applicable to reinforcing steel, and two of these are the Johnson-Cook and Cowper-Symonds relationships (LSTC, 2007). Several recent and past studies illustrate the use of these relationships for scenarios involving structures subjected to blast and impact loads (Karagiozova and Jones, 2000; Raftenberg, 1997; Rusinek, 2008; Rushton et al., 2008; Turhan et al., 2008).

7.5 Coupled Analyses

Coupled analyses are very complex, involving the interaction of an Eulerian mesh and a Lagrangian mesh, and the results can vary widely depending on the user-selected inputs. To run a coupled analysis, the user must build a model with a Lagrangian mesh (i.e., typically the structure) overlapping (but not connected to) an Eulerian mesh (i.e., typically the fluid) before evacuating the fluid from the Lagrangian mesh. When the fluid in the Eulerian mesh (i.e., the shock front as it travels through air in the case of airblast) penetrates the surface of a Lagrangian structure during a simulation, the finite element code will move the fluid back to the surface of the Lagrangian structure and apply a reaction force to the fluid normal to the surface of the Lagrangian structure. Because some codes allow modeling of porous surfaces, a user-defined penalty factor or penalty curve typically governs the amount of fluid that will leak through the surface of the Lagrangian mesh, and it also defines the relationship between the depth of fluid penetration and the resulting force applied to the fluid. This concept is similar to Hooke's Law, where the force is equal to the stiffness multiplied by the displacement. The stiffness of the coupled surface can be constant or vary linearly, and a user can increase or decrease the "stiffness" of the coupled surface by adjusting the penalty factor or penalty curve; therefore, the solution can vary widely depending on the user selected inputs. For example, if the analyst sets the penalty

factor too high, the coupled surface can be too "stiff," and the shock front will bounce off the Lagrangian surface with too much momentum (Knight et al., 2004). A penalty factor set too "low" can result in a large amount of fluid leaking through the coupled surface. The analyst bears the responsibility of defining an appropriate penalty factor or penalty curve, and many models may require calibration with experimental data. As a result, these problems can be very complex, requiring a very experienced analyst and reliable empirical data. Thus, using these models is not advisable unless structural response will significantly change the flow of the shock front. Detailed information on coupled analyses is beyond the scope of this report, as the intention of this chapter is not to provide a tutorial on finite element modeling for such cases. If more detailed information is desired, the reader should consult the research literature and the user's manual of the software being used.

7.6 Summary

This chapter outlines available methods to predict blast loads on and the resulting response of bridge columns. Methods that employ single-degree-of-freedom analyses, such as the one described in this chapter, are valuable for design scenarios because they yield acceptable accuracy given the uncertainty of the loads. As a result, they are commonly used by blast engineers. While these simplified methods are often useful and desirable, they may not always be appropriate, and the analyst may wish to use a more advanced procedure. As described above, several general-purpose finite element software packages have the ability to conduct high-level airblast and structural response analyses, and the implementation of explosive modeling, the availability of material constitutive models, and the analysis procedure employed are different for each. Thus, while the above sections give general principles for modeling high-explosive detonation, shock propagation, and structural response using these codes, the analyst should be familiar with the capabilities, requirements, and limitations of the selected software. With proper knowledge and experience, general-purpose finite element software is a valuable tool for predicting blast loads and response in advanced design or research environments. Such load scenarios include cases with complex geometries, structures for which venting due to localized failure may drastically reduce loads, and situations for which the charge weight, explosive properties, and structure parameters are known or can be reasonably well estimated. Applicable response scenarios include cases in which localized failure (i.e., spall or breach) may affect the loading or the global response of a structure.

CHAPTER 8

Design Examples

8.1 Overview

This chapter aims to illustrate the design process for reinforced concrete highway bridge columns subjected to blast loads. Each design example combines the prescriptive design guidelines presented in Chapter 6 and the simplified analysis guidelines presented in Chapter 7. A design example for a column in each design category is provided.

8.2 Design Examples

Standard column designs and material properties were selected for the design examples to illustrate the recommended analysis and design requirements for typical highway bridge columns exposed to blast loads. The requirements vary depending on the given threat scenario (scaled standoff) and associated Design Category A, B, or C.

Columns within Design Category A have a small enough threat scenario that no additional design checks are required to withstand the associated blast loads. For columns in Design Categories B and C, the additional prescriptive design requirements include checks on the minimum transverse reinforcement ratio, the location of longitudinal splices, and the type of anchorage for transverse reinforcement. Additionally, columns with a threat scenario within Design Category C require a flexural capacity check using a single-degree-of-freedom analysis. The flexural analysis specifies ductility and flexural rotation design limits based on the large-scale columns tested during Phase II of this research program. Specifically, columns with slight to moderate damage without significant shear damage were used to select these design limits. Assuming the columns are at the onset of shear-dominated response, they should have significant reserve shear capacity beyond these limits. If these design limits are not met, column performance can be improved by increasing the column size (diameter or width) and the amount of longitudinal reinforcement.

The analysis procedure for Category C columns uses flexural response as an indicator of shear response, and shear is not directly calculated. The Phase II tests found that direct shear capacity (per current codes, i.e., UFC 3-340-01) are not necessarily indicative of shear performance. Therefore, the shear check is directly built into the prescriptive design requirements and flexural analysis by the minimum transverse reinforcement ratio and flexural design limits, respectively. These limits help ensure that a shear mechanism does not form at the column base as a result of the large shear demand caused by close-in blast loads.

For the examples that follow, columns are assumed to behave as propped-cantilevers. Actual boundary conditions will depend on how a column is detailed and connected to the cap beam or superstructure. Accordingly, expected boundary conditions should be used for design, and design threat scenarios should account for the orientation of the blast relative to the bridge. If appropriate assumptions for boundary conditions are unclear, end restraints should be assumed and varied to maximize the response of interest. For the flexural calculations in the design examples, simple supports can be conservatively assumed because maximum deformation controls the design.

8.2.1 Design Example 1: Design Category C Column

Design Example 1 illustrates the design process for a reinforced concrete bridge column in Design Category C. This example shows a column that must meet all of the proposed analysis and design requirements. It details the design procedure for concrete highway bridge columns exposed to close-in blast loads according to the AASHTO LRFD guidelines recommended in this report. When a threat is given for a column in a non-seismic region, design the column accordingly.

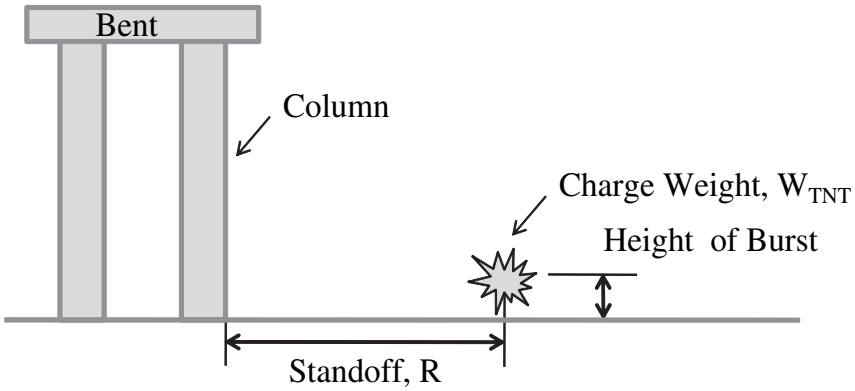

Given:

Design Threat: (AASHTO LRFD Sections 2.7.2 and 3.15.1)

Hemispherical burst near the ground

Standoff:	$R_x = 6$ ft
Charge Weight (lb TNT):	$W_{TNT} = 160$ lb TNT

Column Parameters:

Non-seismic region

Exterior column of multi-column bent

Support Conditions:	Propped Cantilever	
Column Cross-Sectional Shape:	Shape = "circular"	(AASHTO LRFD Section 2.7.3)
Column Height (between supports):	$L_o = 18$ ft	

Material Properties:

Concrete Strength: $f'_c = 4000$ psi

Concrete Unit weight: $\gamma_c = 150$ pcf

Concrete Age: $C_{age} = 2$ months

Grade 60 Reinforcement

Rebar Modulus of Elasticity: $E_s = 29000$ ksi

Yield Strength: $f_y = 60$ ksi

Dynamic and Material Increase Factors:
(AASHTO LRFD C4.7.6.3)

Strength Increase Factor: $K_E = 1.10$ for concrete and rebar

Age Increase Factor:

$$K_A = \begin{cases} 1.15 \text{ if } C_{age} \geq 6 \\ 1.10 \text{ if } 6 > C_{age} \geq 0 \end{cases} \qquad K_A = 1.1$$

Dynamic Increase Factors:

Stress Type	Reinforcing Bars	Concrete
Flexure	$DIF_{fl.st} = 1.17$	$DIF_{fl.con} = 1.19$

Dynamic Ultimate Compressive Stress for Flexure:

Concrete: $f'_{dc.fl} = f'_c \, K_A \, K_E \, DIF_{fl.con}$ $\qquad f'_{dc.fl} = 5759.6$ psi

Steel: $f_{dy.fl} = f_y \, K_E \, DIF_{fl.st}$ $\qquad f_{dy.fl} = 77.2$ ksi

Determine Design Category for design requirements. (AASHTO LRFD Section 4.7.6.2)

Scaled Standoff:
(Eqn 4.7.6.2-1)

$$Z = \frac{R_x}{W_{TNT}^{\frac{1}{3}}} \qquad Z = 1.1 \text{ ft/lb}^{1/3}$$

$$\text{DesignCategory} = \begin{cases} \text{“A” if } Z > 3 \\ \text{“B” if } 1.5 < Z \leq 3 \\ \text{“C” if } 0.5 < Z \leq 1.5 \\ \text{“not recommended” if } Z \leq 0.5 \end{cases} \qquad \text{DesignCategory} = \text{“C”}$$

According to the Section 4.7.6.2 of the design guidelines, columns in Design Category C need to follow the prescriptive detailing and design requirements in Sections 5.10.11.4.1c - e, 5.10.12.3, and 5.10.2.3.

Column Parameters:

Column Diameter:	$D = 36$ in.	
Concrete Clear Cover:	cover $= 2$ in.	
Area of Longitudinal Reinf.:	10 #9 bars	$d_{l.b} = 1.128$ in.
	$A_s = 10\ 1.00$ in.^{2}	$A_s = 10$ in.^{2}
Type of Transverse Reinf.:	#6 bars	$d_{v.b} = 0.75$ in.
	Type = "hoops"	
Spacing/pitch of Transverse Reinf.:	$s_{cc} = 4$ in.	
Area of Shear Reinf. Bar:	$A_{v.bar} = 0.44$ in.^{2}	

Cross-Section Properties:

Gross Column Area:	$A_g = \pi \left(\frac{D}{2}\right)^2$	$A_g = 1017.9$ in.^{2}
Area of Column Core:	$A_c = \pi \left(\frac{D - 2\ \text{cover}}{2}\right)^2$	$A_c = 804.2$ in.^{2}
Effective depth:	$d_{eff} = 0.8\ D$	$d_{eff} = 28.8$ in.
Longitudinal Reinforcement Ratio:	$\rho_L = \frac{A_s}{A_g}$	$\rho_L = 0.982\%$
Volumetric Reinforcement Ratio:	$\rho_s = \frac{4\ A_{v.bar}}{s_{cc}\ (D - 2\ \text{cover})}$	$\rho_s = 1.375\%$

Determine Moment Capacity of Column:
(AASHTO LRFD 5.8.2.9)

Diameter of circle passing through longitudinal reinforcement:

	$D_r = D - 2\ \text{cover} - 2\ d_{v.b} - d_{l.b}$	$D_r = 29.4$ in.
Effective moment arm:	$d_v = \max\left[0.72\ D,\ 0.9\left(\frac{D}{2} + \frac{D_r}{\pi}\right)\right]$	$d_v = 25.9$ in.
Moment Capacity:	$M_n = \left(\frac{A_s}{2}\right) f_{dy.fl}\ d_v$	$M_n = 834$ kip ft

Check AASHTO LRFD Design and Detailing Requirements:

Minimum Transverse Reinforcement Ratio:
(AASHTO LRFD 5.10.12.3)

$$\rho_{s.min} = \begin{cases} 0.45\left(\frac{A_g}{A_c} - 1\right)\frac{f'_c}{f_y} & \text{if DesignCategory = “A”} \\ 0.12\frac{f'_c}{f_y} & \text{if DesignCategory = “B”} \\ \left[1.5\left(0.12\frac{f'_c}{f_y}\right)\right] & \text{if DesignCategory = “C”} \end{cases} \qquad \rho_{s.min} = 1.2\%$$

$$\text{RatioCheck} = \begin{cases} \text{“Transverse Reinf. okay” if } \rho_s \geq \rho_{s.min} \\ \text{“increase amount transverse reinf.” if } \rho_s < \rho_{s.min} \end{cases}$$

RatioCheck = “Transverse Reinf. okay”

Longitudinal Splice Location:
(AASHTO LRFD 5.12.13.4)

End Region:
(AASHTO LRFD 5.10.11.4.1c) $\text{EndRegion} = \max\left(D, \frac{1}{6}L_o, 18\text{ in.}\right)$ EndRegion = 36 in.

Minimum Height of Longitudinal Splices above the ground or lower deck:

$$\text{SpliceHeight} = \begin{cases} \text{“no requirements” if DesignCategory = “A”} \\ \text{EndRegion if DesignCategory = “B”} \\ \text{max (12 ft, EndRegion) if DesignCategory = “C”} \end{cases} \qquad \text{SpliceHeight} = 12\text{ ft}$$

Type of Transverse Reinforcement:

According to AASHTO LRFD 5.10.2.3, transverse reinforcement should consist of continuous spiral reinforcement or discrete hoops with adequate anchorage.

$$\text{Anchorage} = \begin{cases} \text{“Typical Hook” if DesignCategory = “A”} \\ \text{“Seismic Hook” if DesignCategory = “B”} \\ \text{“Blast Hook” if DesignCategory = “C”} \end{cases} \qquad \text{Anchorage} = \text{“Blast Hook”}$$

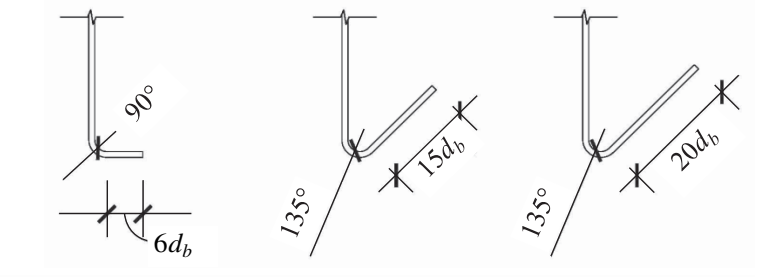

Typical Hook Seismic Hook Blast Hook

Flexural Capacity Check: (AASHTO LRFD 4.7.6.3)

Use BEL to determine equivalent uniform pressure, equivalent impulse and duration for given threat scenario.

Assumptions for BEL analysis:

- Airblast on Columns
- Do not use BlastX
- Target size equal column size
- Charge is on the ground
- Target is supported on Top & Bottom

BEL Equivalent Pressure: $P_{BEL} = 1784$ psi

BEL Equivalent Impulse: $I_{BEL} = 466.5$ psi ms

BEL Duration: $t_{BEL} = \frac{2I_{BEL}}{P_{BEL}}$ $t_{BEL} = 0.523$ ms

Use Single-Degree-of-Freedom Analysis (SBEDS) to determine rotation and ductility.

The column will be designed as an independent uncoupled member.

SBED assumptions:

- Concrete Beam-Column Analysis
- Propped Cantilever Supports, uniform load, flexure only
- Column Spacing = effective diameter
- Use equivalent pressure and duration from BEL
- 2% damping
- use dynamic material strengths

SBEDS Rotation: $\theta_{SBEDS} = 0.14$ deg

SBEDS Ductility: $\mu_{SBEDS} = 1.6$

RotationCheck = “rotation okay” if $\theta_{SBEDS} \le 1.0$ deg; “increase column size” if $\theta_{SBEDS} > 1.0$ deg

DuctilityCheck = “ductility okay” if $\mu_{SBEDS} \le 15$; “increase area of long. reinf.” if $\mu_{SBEDS} > 15$

RotationCheck = “rotation okay”

DuctilityCheck = “ductility okay”

Example 1 Design Summary:

Design Threat:

Standoff:	$R_x = 6$ ft
Charge Weight (lb TNT):	$W_{TNT} = 160$ lb TNT
Scaled Standoff:	$Z = 1.1$ ft/lb$^{1/3}$
DesignCategory = “C”	

Column Parameters:

Non-seismic region	
Support Conditions:	Propped Cantilever
Column Cross-Sectional Shape:	Shape = “circular”
Column Height (between supports):	$L_O = 18$ ft
Column Diameter:	$D = 36$ in.
Concrete Clear Cover:	cover = 2 in.

Material Properties:

Concrete Strength:	$f'_c = 4000$ psi
Yield Strength:	$f_y = 60$ ksi

Longitudinal Reinforcement:

Area of Longitudinal Reinf.:	10 #9 bars
Longitudinal Reinforcement Ratio:	$\rho_L = 0.982\%$
Minimum Height Long. Splice:	SpliceHeight = 12 ft

Transverse Reinforcement:

Type of Transverse Reinf.:	#6 bars Type = “hoops”
	Anchorage = “Blast Hook”
Spacing/pitch of Transverse Reinf.:	$s_{cc} = 4$ in.
Volumetric Reinforcement Ratio:	$\rho_s = 1.375\%$
	RatioCheck = “Transverse Reinf. okay”

Flexural Capacity Check:

RotationCheck = “rotation okay”

DuctilityCheck = “ductility okay”

8.2.2 Design Example 2: Design Category C Column

Design Example 2 takes into consideration the response of the reinforced concrete bridge column in Design Example 1 for a larger threat within Design Category C. For the conditions assumed, the column must be redesigned to meet all applicable criteria. This example illustrates a column that must meet all of the proposed analysis and design requirements for a large charge weight. It details the design procedure for concrete highway bridge columns exposed to close-in blast loads according to the AASHTO LRFD guidelines recommended in this report. Redesign the column in Design Example 1 for a larger threat.

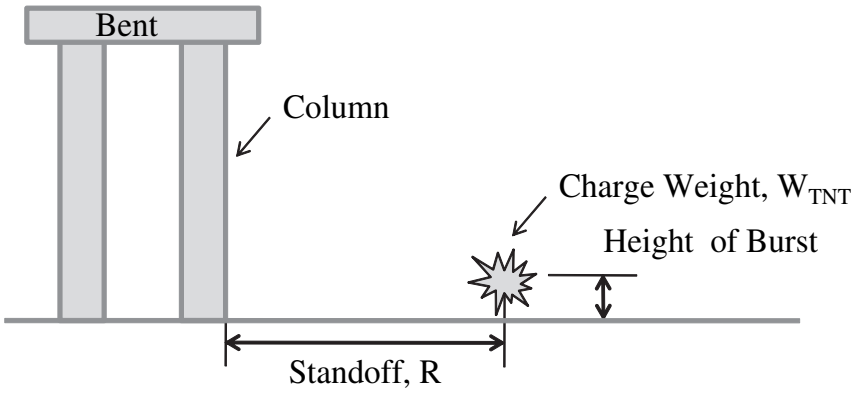

Given:

Design Threat: (AASHTO LRFD Sections 2.7.2 and 3.15.1)

Hemispherical burst near the ground

Standoff: $R_x = 15$ ft

Charge Weight (lb TNT): $W_{TNT} = 5000$ lb TNT

Column Parameters:

Non-seismic region

Exterior column of multi-column bent

Support Conditions: Propped Cantilever

Column Cross-Sectional Shape: Shape = "circular" (AASHTO LRFD Section 2.7.3)

Column Height (between supports): $L_o = 18$ ft

Material Properties:

Concrete Strength: $f'_c = 4000$ psi

Concrete Unit weight: $\gamma_c = 150$ pcf

Concrete Age: $C_{age} = 2$ months

Grade 60 Reinforcement

Rebar Modulus of Elasticity: $E_s = 29000$ ksi

Yield Strength: $f_y = 60$ ksi

Dynamic and Material Increase Factors:
(AASHTO LRFD C4.7.6.3)

Strength Increase Factor: $K_E = 1.10$ for concrete and rebar

Age Increase Factor:

$$K_A = \begin{cases} 1.15 \text{ if } C_{age} \geq 6 \\ 1.10 \text{ if } 6 > C_{age} \geq 0 \end{cases} \qquad K_A = 1.1$$

Dynamic Increase Factors:

Stress Type	Reinforcing Bars	Concrete
Flexure	$DIF_{fl.st} = 1.17$	$DIF_{fl.con} = 1.19$

Dynamic Ultimate Compressive Stress for Flexure:

Concrete: $f'_{dc.fl} = f'_c \, K_A \, K_E \, DIF_{fl.con}$ $\qquad f'_{dc.fl} = 5759.6$ psi

Steel: $f_{dy.fl} = f_y \, K_E \, DIF_{fl.st}$ $\qquad f_{dy.fl} = 77.2$ ksi

Determine Design Category for design requirements. (AASHTO LRFD Section 4.7.6.2)

Scaled Standoff:
(Eqn 4.7.6.2-1)

$$Z = \frac{R_x}{W_{TNT}^{\frac{1}{3}}} \qquad Z = 1.1 \text{ ft/lb}^{1/3}$$

$$\text{DesignCategory} = \begin{cases} \text{“A” if } Z > 3 \\ \text{“B” if } 1.5 < Z \leq 3 \\ \text{“C” if } 0.5 < Z \leq 1.5 \\ \text{“not recommended” if } Z \leq 0.5 \end{cases} \qquad \text{DesignCategory} = \text{“C”}$$

According to the Section 4.7.6.2 of the design guidelines, columns in Design Category C need to follow the prescriptive detailing and design requirements in Sections 5.10.11.4.1c - e, 5.10.12.3, and 5.10.2.3.

Column Parameters:

Column Diameter: $D = 36$ in.

Concrete Clear Cover: $cover = 2$ in.

Area of Longitudinal Reinf.: 10 #9 bars $d_{l.b} = 1.128$ in.

$A_s = 10\ 1.00\ in.^2$ $A_s = 10\ in.^2$

Type of Transverse Reinf.: #6 bars $d_{v.b} = 0.75$ in.

Type = "hoops"

Spacing/pitch of Transverse Reinf.: $s_{cc} = 4$ in.

Area of Shear Reinf. Bar: $A_{v.bar} = 0.44\ in.^2$

Cross-Section Properties:

Gross Column Area: $A_g = \pi \left(\frac{D}{2} \right)^2$ $A_g = 1017.9\ in.^2$

Area of Column Core: $A_c = \pi \left(\frac{D - 2\ cover}{2} \right)^2$ $A_c = 804.2\ in.^2$

Effective depth: $d_{eff} = 0.8\ D$ $d_{eff} = 28.8$ in.

Longitudinal Reinforcement Ratio: $\rho_L = \frac{A_s}{A_g}$ $\rho_L = 0.982\%$

Volumetric Reinforcement Ratio: $\rho_s = \frac{4\ A_{v.bar}}{s_{cc}\ (D - 2\ cover)}$ $\rho_s = 1.375\%$

Determine Moment Capacity of Column:
(AASHTO LRFD 5.8.2.9)

Diameter of circle passing through longitudinal reinforcement:

$D_r = D - 2\ cover - 2\ d_{v.b} - d_{l.b}$ $D_r = 29.4$ in.

Effective moment arm: $d_v = \max \left[0.72\ D, 0.9 \left(\frac{D}{2} + \frac{D_r}{\pi} \right) \right]$ $d_v = 25.9$ in.

Moment Capacity: $M_n = \left(\frac{A_s}{2} \right) f_{dy.fl}\ d_v$ $M_n = 834$ kip ft

Check AASHTO LRFD Design and Detailing Requirements:

Minimum Transverse Reinforcement Ratio:
(AASHTO LRFD 5.10.12.3)

$$\rho_{s.min} = \begin{cases} 0.45\left(\frac{A_g}{A_c} - 1\right)\frac{f'_c}{f_y} & \text{if DesignCategory = “A”} \\ 0.12\,\frac{f'_c}{f_y} & \text{if DesignCategory = “B”} \\ \left[1.5\left(0.12\,\frac{f'_c}{f_y}\right)\right] & \text{if DesignCategory = “C”} \end{cases} \qquad \rho_{s.min} = 1.2\%$$

$$\text{RatioCheck} = \begin{cases} \text{“Transverse Reinf. okay” if } \rho_s \geq \rho_{s.min} \\ \text{“increase amount transverse reinf.” if } \rho_s < \rho_{s.min} \end{cases}$$

RatioCheck = “Transverse Reinf. okay”

Longitudinal Splice Location:
(AASHTO LRFD 5.12.13.4)

End Region:
(AASHTO LRFD 5.10.11.4.1c) $\text{EndRegion} = \max\left(D, \frac{1}{6}L_o, 18\text{ in.}\right)$ EndRegion = 36 in.

Minimum Height of Longitudinal Splices above the ground or lower deck:

$$\text{SpliceHeight} = \begin{cases} \text{“no requirements” if DesignCategory = “A”} \\ \text{EndRegion if DesignCategory = “B”} \\ \max(12\text{ ft, EndRegion}) \text{ if DesignCategory = “C”} \end{cases} \qquad \text{SpliceHeight} = 12\text{ ft}$$

Type of Transverse Reinforcement:

According to AASHTO LRFD 5.10.2.3, transverse reinforcement should consist of continuous spiral reinforcement or discrete hoops with adequate anchorage.

$$\text{Anchorage} = \begin{cases} \text{“Typical Hook” if DesignCategory = “A”} \\ \text{“Seismic Hook” if DesignCategory = “B”} \\ \text{“Blast Hook” if DesignCategory = “C”} \end{cases} \qquad \text{Anchorage} = \text{“Blast Hook”}$$

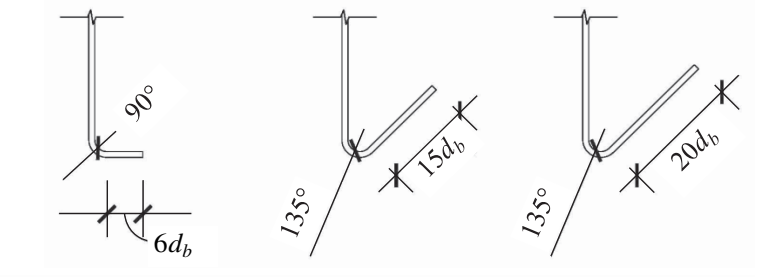

Typical Hook Seismic Hook Blast Hook

Flexural Capacity Check: (AASHTO LRFD 4.7.6.3)

Use BEL to determine equivalent uniform pressure, equivalent impulse and duration for given threat scenario.

Assumptions for BEL analysis:

- Airblast on Columns
- Do not use BlastX
- Target size equal column size
- Charge is on the ground
- Target is supported on Top & Bottom

BEL Equivalent Pressure: $P_{BEL} = 6816$ psi

BEL Equivalent Impulse: $I_{BEL} = 4789$ psi ms

BEL Duration: $t_{BEL} = \frac{2I_{BEL}}{P_{BEL}}$ $t_{BEL} = 1.405$ ms

Use Single-Degree-of-Freedom Analysis (SBEDS) to determine rotation and ductility.

The column will be designed as an independent uncoupled member.

SBED assumptions:

- Concrete Beam-Column Analysis
- Propped Cantilever Supports, uniform load, flexure only
- Column Spacing = effective diameter
- Use equivalent pressure and duration from BEL
- 2% damping
- use dynamic material strengths

SBEDS Rotation: $\theta_{SBEDS} = 9.71$ deg

SBEDS Ductility: $\mu_{SBEDS} = 108$

RotationCheck = “rotation okay” if $\theta_{SBEDS} \le 1.0$ deg; “increase column size” if $\theta_{SBEDS} > 1.0$ deg

DuctilityCheck = “ductility okay” if $\mu_{SBEDS} \le 15$; “increase area of long. reinf.” if $\mu_{SBEDS} > 15$

RotationCheck = “rotation okay”

DuctilityCheck = “ductility okay”

Try new column: Note: Only redefined variables are shown below.

Column Parameters:

Column Diameter: $D = 60$ in.

Area of Longitudinal Reinf.: 26 #14 bars $d_{l.b} = 1.693$ in.

$A_s = 26\ 2.25\ \text{in.}^2$ $A_s = 58.5\ \text{in.}^2$

Cross-Section Properties:

Gross Column Area: $A_g = \pi \left(\frac{D}{2} \right)^2$ $A_g = 2827.4\ \text{in.}^2$

Area of Column Core: $A_c = \pi \left(\frac{D - 2\ \text{cover}}{2} \right)^2$ $A_c = 2463\ \text{in.}^2$

Effective depth: $d_{eff} = 0.8\ D$ $d_{eff} = 48$ in.

Longitudinal Reinforcement Ratio: $\rho_L = \frac{A_s}{A_g}$ $\rho_L = 2.07\ \%$

Determine Moment Capacity of Column:
(AASHTO LRFD 5.8.2.9)

Diameter of circle passing through longitudinal reinforcement:

$D_r = D - 2\ \text{cover} - 2\ d_{v.b} - d_{l.b}$ $D_r = 52.8$ in.

Effective moment arm: $d_v = \max \left[0.72\ D,\ 0.9 \left(\frac{D}{2} + \frac{D_r}{\pi} \right) \right]$ $d_v = 43.2$ in.

Moment Capacity: $M_n = \left(\frac{A_s}{2} \right) f_{dy.fl}\ d_v$ $M_n = 8131$ kip ft

Flexural Capacity Check: (AASHTO LRFD 4.7.6.3)

Use BEL to determine equivalent uniform pressure, equivalent impulse and duration for given threat scenario.

BEL Equivalent Pressure: $P_{BEL} = 6774$ psi

BEL Equivalent Impulse: $I_{BEL} = 4752$ psi ms

BEL Duration: $t_{BEL} = \frac{2 I_{BEL}}{P_{BEL}}$ $t_{BEL} = 1.403$ ms

Use Single-Degree-of-Freedom Analysis (SBEDS) to determine rotation and ductility.

SBEDS Rotation: $\theta_{SBEDS} = 1.0$ deg

SBEDS Ductility: $\mu_{SBEDS} = 10.51$

$$\text{RotationCheck} = \begin{cases} \text{“rotation okay” if } \theta_{SBEDS} \le 1.0 \text{ deg} \\ \text{“increase column size” if } \theta_{SBEDS} > 1.0 \text{ deg} \end{cases}$$

$$\text{DuctilityCheck} = \begin{cases} \text{“ductility okay” if } \mu_{SBEDS} \le 15 \\ \text{“increase area of long. reinf.” if } \mu_{SBEDS} > 15 \end{cases}$$

RotationCheck = “rotation okay”

DuctilityCheck = “ductility okay”

Recheck Transverse Reinforcement:

Type of Transverse Reinf.: #7 bars, $d_{v.b} = 0.875$ in.

Type = “spiral”

Spacing/pitch of Transverse Reinf.: $s_{cc} = 3.5$ in.

Area of Shear Reinf. Bar: $A_{v.bar} = 0.6 \text{ in.}^2$

Volumetric Reinforcement Ratio: $\rho_s = \dfrac{4\,A_{v.bar}}{s_{cc}\,(D - 2 \text{ cover})}$, $\rho_s = 1.22\%$

Check AASHTO LRFD Design and Detailing Requirements:

Minimum Transverse Reinforcement Ratio:
(AASHTO LRFD 5.10.12.3)

$$\rho_{s.min} = \begin{cases} 0.45\left(\dfrac{A_g}{A_c} - 1\right)\dfrac{f'_c}{f_y} & \text{if DesignCategory = “A”} \\ 0.12\,\dfrac{f'_c}{f_y} & \text{if DesignCategory = “B”} \\ \left[1.5\left(0.12\,\dfrac{f'_c}{f_y}\right)\right] & \text{if DesignCategory = “C”} \end{cases}$$

$\rho_{s.min} = 1.2\%$

$$\text{RatioCheck} = \begin{cases} \text{“Transverse Reinf. okay” if } \rho_s \ge \rho_{s.min} \\ \text{“increase amount transverse reinf.” if } \rho_s < \rho_{s.min} \end{cases}$$

RatioCheck = “Transverse Reinf. okay”

Design Summary:

Design Threat:

Standoff: $R_x = 15$ ft

Charge Weight (lb TNT): $W_{TNT} = 5000$ lb TNT

Scaled Standoff: $Z = 0.88$ ft/lb$^{1/3}$

DesignCategory = “C”

Column Parameters:

Non-seismic region

Support Conditions: Propped Cantilever

Column Cross-Sectional Shape: Shape = “circular”

Column Height (between supports): $L_O = 18$ ft

Column Diameter: $D = 60$ in.

Concrete Clear Cover: cover = 2 in.

Material Properties:

Concrete Strength: $f'_c = 4000$ psi

Yield Strength: $f_y = 60$ ksi

Longitudinal Reinforcement:

Area of Longitudinal Reinf.: 26 #14 bars

Longitudinal Reinforcement Ratio: $\rho_L = 2.07\%$

Minimum Height Long. Splice: SpliceHeight = 12 ft

Transverse Reinforcement:

Type of Transverse Reinf.: #7 bars Type = “spiral”

Anchorage = “Blast Hook”

Spacing/pitch of Transverse Reinf.: $s_{cc} = 3.5$ in.

Volumetric Reinforcement Ratio: $\rho_s = 1.224\%$

RatioCheck = “Transverse Reinf. okay”

Flexural Capacity Check:

RotationCheck = “rotation okay”

DuctilityCheck = “ductility okay”

8.2.3 Design Example 3: Design Category B Column

Design Example 3 illustrates the design changes required for a column in Design Category B. In this case, the column design must meet current seismic AASHTO LRFD design requirements as well as the prescriptive blast design requirements shown. Only the portion of the column design dealing with blast loads is provided below. Seismic design requirements need to be checked separately. A single-degree-of-freedom analysis does not need to be performed for blast-loaded columns in Category B. Note that the column moment capacity is computed accounting for dynamic and material increase factors. While this value would be appropriate for estimating column capacity for blast loads, it should *not* be used to design columns for the controlling seismic loads. It details the design procedure for concrete highway bridge columns exposed to close-in blast loads according to the AASHTO LRFD guidelines recommended in this report. When a threat is given for a column in a high-seismic region, design the column accordingly.

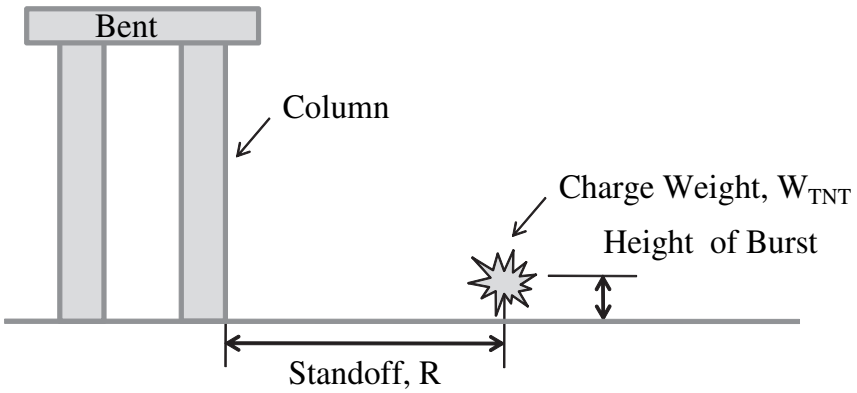

Given:

Design Threat: (AASHTO LRFD Sections 2.7.2 and 3.15.1)

Hemispherical burst near the ground

Standoff: $R_x = 10$ ft

Charge Weight (lb TNT): $W_{TNT} = 275$ lb TNT

Column Parameters:

High-seismic region

Exterior column of multi-column bent

Support Conditions: Propped Cantilever

Column Cross-Sectional Shape: Shape = "circular" (AASHTO LRFD Section 2.7.3)

Column Height (between supports): $L_o = 24$ ft

Material Properties:

Concrete Strength: $f'_c = 4000$ psi

Concrete Unit weight: $\gamma_c = 150$ pcf

Concrete Age: $C_{age} = 2$ months

Grade 60 Reinforcement

Rebar Modulus of Elasticity: $E_s = 29000$ ksi

Yield Strength: $f_y = 60$ ksi

Dynamic and Material Increase Factors:
(AASHTO LRFD C4.7.6.3)

Strength Increase Factor: $K_E = 1.10$ for concrete and rebar

Age Increase Factor:

$$K_A = \begin{cases} 1.15 \text{ if } C_{age} \geq 6 \\ 1.10 \text{ if } 6 > C_{age} \geq 0 \end{cases} \qquad K_A = 1.1$$

Dynamic Increase Factors:

Stress Type	Reinforcing Bars	Concrete
Flexure	$DIF_{fl.st} = 1.17$	$DIF_{fl.con} = 1.19$

Dynamic Ultimate Compressive Stress for Flexure:

Concrete: $f'_{dc.fl} = f'_c K_A K_E DIF_{fl.con}$ $f'_{dc.fl} = 5759.6$ psi

Steel: $f_{dy.fl} = f_y K_E DIF_{fl.st}$ $f_{dy.fl} = 77.2$ ksi

Determine Design Category for design requirements. (AASHTO LRFD Section 4.7.6.2)

Scaled Standoff: (Eqn 4.7.6.2-1)

$$Z = \frac{R_x}{W_{TNT}^{\frac{1}{3}}} \qquad Z = 1.54 \text{ ft/lb}^{1/3}$$

$$\text{DesignCategory} = \begin{cases} \text{“A” if } Z > 3 \\ \text{“B” if } 1.5 < Z \le 3 \\ \text{“C” if } 0.5 < Z \le 1.5 \\ \text{“not recommended” if } Z \le 0.5 \end{cases} \qquad \text{DesignCategory} = \text{“B”}$$

According to the Section 4.7.6.2 of the design guidelines, columns in Design Category C need to follow the prescriptive detailing and design requirements in Sections 5.10.11.4.1c - e, and 5.10.2.3.

Column Parameters:

Column Diameter:	$D = 36$ in.	
Concrete Clear Cover:	cover = 2 in.	
Area of Longitudinal Reinf.:	12 #9 bars	$d_{l.b} = 1.128$ in.
	$A_s = 12\ 1.00$ in.^{2}	$A_s = 12$ in.^{2}
Type of Transverse Reinf.:	#6 bars	$d_{v.b} = 0.75$ in.
	Type = “spiral”	
Spacing/pitch of Transverse Reinf.:	$s_{cc} = 6$ in.	
Area of Shear Reinf. Bar:	$A_{v.bar} = 0.44$ in.^{2}	

Cross-Section Properties:

Gross Column Area: $A_g = \pi \left(\frac{D}{2}\right)^2$ $A_g = 1017.9 \text{ in.}^2$

Area of Column Core: $A_c = \pi \left(\frac{D - 2 \text{ cover}}{2}\right)^2$ $A_c = 804.2 \text{ in.}^2$

Effective depth: $d_{eff} = 0.8 D$ $d_{eff} = 28.8 \text{ in.}$

Longitudinal Reinforcement Ratio: $\rho_L = \frac{A_s}{A_g}$ $\rho_L = 1.18 \%$

Volumetric Reinforcement Ratio: $\rho_s = \frac{4 A_{v.bar}}{s_{cc} (D - 2 \text{ cover})}$ $\rho_s = 0.917\%$

Determine Moment Capacity of Column:
(AASHTO LRFD 5.8.2.9)

Diameter of circle passing through longitudinal reinforcement:

$D_r = D - 2 \text{ cover} - 2 d_{v.b} - d_{l.b}$ $D_r = 29.4 \text{ in.}$

Effective moment arm: $d_v = \max\left[0.72 D, 0.9 \left(\frac{D}{2} + \frac{D_r}{\pi}\right)\right]$ $d_v = 25.9 \text{ in.}$

Moment Capacity: $M_n = \left(\frac{A_s}{2}\right) f_{dy.fl} d_v$ $M_n = 1001 \text{ kip ft}$

Check AASHTO LRFD Design and Detailing Requirements:

Minimum Transverse Reinforcement Ratio:
(AASHTO LRFD 5.10.12.3)

$$\rho_{s.min} = \begin{cases} 0.45\left(\frac{A_g}{A_c} - 1\right)\frac{f'_c}{f_y} & \text{if DesignCategory = “A”} \\ 0.12\frac{f'_c}{f_y} & \text{if DesignCategory = “B”} \\ \left[1.5\left(0.12\frac{f'_c}{f_y}\right)\right] & \text{if DesignCategory = “C”} \end{cases} \qquad \rho_{s.min} = 0.8\%$$

$$\text{RatioCheck} = \begin{cases} \text{“Transverse Reinf. okay” if } \rho_s \geq \rho_{s.min} \\ \text{“increase amount transverse reinf.” if } \rho_s < \rho_{s.min} \end{cases}$$

RatioCheck = “Transverse Reinf. okay”

Longitudinal Splice Location:
(AASHTO LRFD 5.12.13.4)

End Region:
(AASHTO LRFD 5.10.11.4.1c) $\text{EndRegion} = \max\left(D, \frac{1}{6}L_o, 18\text{ in.}\right)$ EndRegion = 48 in.

Minimum Height of Longitudinal Splices above the ground or lower deck:

$$\text{SpliceHeight} = \begin{cases} \text{“no requirements” if DesignCategory = “A”} \\ \text{EndRegion if DesignCategory = “B”} \\ \text{max (12 ft, EndRegion) if DesignCategory = “C”} \end{cases} \qquad \text{SpliceHeight} = 4\text{ ft}$$

Type of Transverse Reinforcement:

According to AASHTO LRFD 5.10.2.3, transverse reinforcement should consist of continuous spiral reinforcement or discrete hoops with adequate anchorage.

$$\text{Anchorage} = \begin{cases} \text{“Typical Hook” if DesignCategory = “A”} \\ \text{“Seismic Hook” if DesignCategory = “B”} \\ \text{“Blast Hook” if DesignCategory = “C”} \end{cases} \qquad \text{Anchorage} = \text{“Blast Hook”}$$

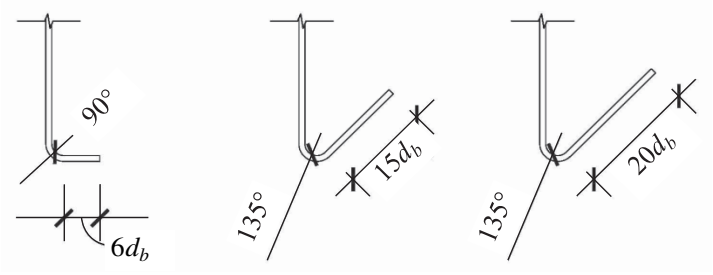

Typical Hook Seismic Hook Blast Hook

Example 3 Design Summary:

Design Threat:

Standoff:	$R_x = 10$ ft
Charge Weight (lb TNT):	$W_{TNT} = 275$ lb TNT
Scaled Standoff:	$Z = 1.54$ ft/lb$^{1/3}$
DesignCategory = “B”	

Column Parameters:

Non-seismic region	
Support Conditions:	Propped Cantilever
Column Cross-Sectional Shape:	Shape = “circular”
Column Height (between supports):	$L_O = 24$ ft
Column Diameter:	$D = 36$ in.
Concrete Clear Cover:	cover = 2 in.

Material Properties:

Concrete Strength:	$f'_c = 4000$ psi
Yield Strength:	$f_y = 60$ ksi

Longitudinal Reinforcement:

Area of Longitudinal Reinf.:	12 #9 bars
Longitudinal Reinforcement Ratio:	$\rho_L = 1.18\%$
Minimum Height Long. Splice:	SpliceHeight = 4 ft

Transverse Reinforcement:

Type of Transverse Reinf.:	#6 bars Type = “spiral”
	Anchorage = “Seismic Hook”
Spacing/pitch of Transverse Reinf.:	$s_{cc} = 6$ in.
Volumetric Reinforcement Ratio:	$\rho_s = 0.917\%$
	RatioCheck = “Transverse Reinf. okay”

Flexural Capacity Check:

SDOF Analysis is not required for Design Category B

8.2.4 Design Example 4: Design Category A Column

Design Example 4 illustrates a column in Design Category A; therefore, no special design or analysis guidelines are required. A column designed for the current AASHTO LRFD (2007) is sufficient for the given threat scenario. It details the design procedure for concrete highway bridge columns exposed to close-in blast loads according to the AASHTO LRFD guidelines recommended in this report. When a threat is given for a column in a non-seismic region, design the column accordingly.

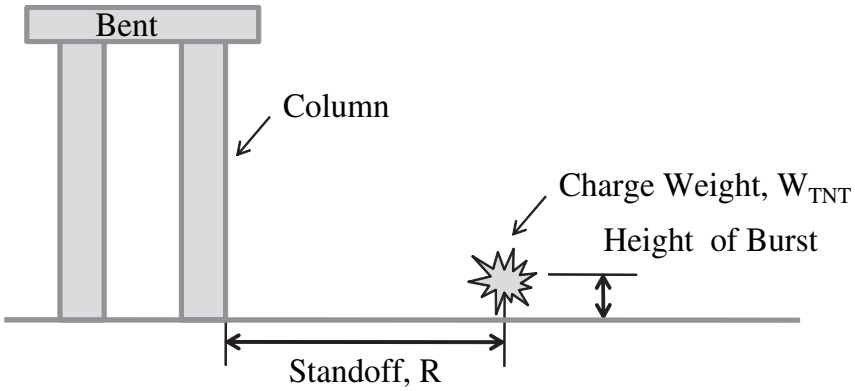

Given:

Design Threat: (AASHTO LRFD Sections 2.7.2 and 3.15.1)

Hemispherical burst near the ground

Standoff: $R_x = 15$ ft

Charge Weight (lb TNT): $W_{TNT} = 100$ lb TNT

Column Parameters:

Non-seismic region

Exterior column of multi-column bent

Support Conditions: Propped Cantilever

Column Cross-Sectional Shape: Shape = "circular" (AASHTO LRFD Section 2.7.3)

Column Height (between supports): $L_o = 18$ ft

Material Properties:

Concrete Strength: $f'_c = 4000$ psi

Concrete Unit weight: $\gamma_c = 150$ pcf

Concrete Age: $C_{age} = 2$ months

Grade 60 Reinforcement

Rebar Modulus of Elasticity: $E_s = 29000$ ksi

Yield Strength: $f_y = 60$ ksi

Dynamic and Material Increase Factors:
(AASHTO LRFD C4.7.6.3)

Strength Increase Factor: $K_E = 1.10$ for concrete and rebar

Age Increase Factor:

$$K_A = \begin{cases} 1.15 \text{ if } C_{age} \geq 6 \\ 1.10 \text{ if } 6 > C_{age} \geq 0 \end{cases} \qquad K_A = 1.1$$

Dynamic Increase Factors:

Stress Type	Reinforcing Bars	Concrete
Flexure	$DIF_{fl.st} = 1.17$	$DIF_{fl.con} = 1.19$

Dynamic Ultimate Compressive Stress for Flexure:

Concrete: $f'_{dc.fl} = f'_c \, K_A \, K_E \, DIF_{fl.con}$ $\qquad f'_{dc.fl} = 5759.6$ psi

Steel: $f_{dy.fl} = f_y \, K_E \, DIF_{fl.st}$ $\qquad f_{dy.fl} = 77.2$ ksi

Determine Design Category for design requirements. (AASHTO LRFD Section 4.7.6.2)

Scaled Standoff:
(Eqn 4.7.6.2-1)

$$Z = \frac{R_x}{W_{TNT}^{\frac{1}{3}}} \qquad Z = 3.23 \text{ ft/lb}^{1/3}$$

$$\text{DesignCategory} = \begin{cases} \text{“A” if } Z > 3 \\ \text{“B” if } 1.5 < Z \leq 3 \\ \text{“C” if } 0.5 < Z \leq 1.5 \\ \text{“not recommended” if } Z \leq 0.5 \end{cases} \qquad \text{DesignCategory} = \text{“A”}$$

According to the Section 4.7.6.2 of the design guidelines, columns in Design Category A do not need to follow any additional guidelines for blast.

Column Parameters:

Column Diameter:	$D = 36$ in.	
Concrete Clear Cover:	cover $= 2$ in.	
Area of Longitudinal Reinf.:	10 #9 bars	$d_{l.b} = 1.128$ in.
	$A_s = 10\ 1.00$ in.^{2}	$A_s = 10$ in.^{2}
Type of Transverse Reinf.:	#6 bars	$d_{v.b} = 0.75$ in.
	Type = "hoops"	
Spacing/pitch of Transverse Reinf.:	$s_{cc} = 6$ in.	
Area of Shear Reinf. Bar:	$A_{v.bar} = 0.44$ in.^{2}	$A_{v.bar} = 0.44$ in.^{2}

Cross-Section Properties:

Gross Column Area:	$A_g = \pi \left(\frac{D}{2}\right)^2$	$A_g = 1017.9$ in.^{2}
Area of Column Core:	$A_c = \pi \left(\frac{D - 2\ \text{cover}}{2}\right)^2$	$A_c = 804.2$ in.^{2}
Effective depth:	$d_{eff} = 0.8\ D$	$d_{eff} = 28.8$ in.
Longitudinal Reinforcement Ratio:	$\rho_L = \frac{A_s}{A_g}$	$\rho_L = 0.98\%$
Volumetric Reinforcement Ratio:	$\rho_s = \frac{4\ A_{v.bar}}{s_{cc}\ (D - 2\ \text{cover})}$	$\rho_s = 0.917\%$

Determine Moment Capacity of Column:
(AASHTO LRFD 5.8.2.9)

Diameter of circle passing through longitudinal reinforcement:

	$D_r = D - 2\ \text{cover} - 2\ d_{v.b} - d_{l.b}$	$D_r = 29.4$ in.
Effective moment arm:	$d_v = \max\left[0.72\ D,\ 0.9\left(\frac{D}{2} + \frac{D_r}{\pi}\right)\right]$	$d_v = 25.9$ in.
Moment Capacity:	$M_n = \left(\frac{A_s}{2}\right) f_{dy.fl}\ d_v$	$M_n = 834$ kip ft

Check AASHTO LRFD Design and Detailing Requirements:

Minimum Transverse Reinforcement Ratio:
(AASHTO LRFD 5.10.12.3)

$$\rho_{s.min} = \begin{cases} 0.45\left(\frac{A_g}{A_c} - 1\right)\frac{f'_c}{f_y} & \text{if DesignCategory = “A”} \\ 0.12\,\frac{f'_c}{f_y} & \text{if DesignCategory = “B”} \\ \left[1.5\left(0.12\,\frac{f'_c}{f_y}\right)\right] & \text{if DesignCategory = “C”} \end{cases} \qquad \rho_{s.min} = 0.797\%$$

$$\text{RatioCheck} = \begin{cases} \text{“Transverse Reinf. okay” if } \rho_s \geq \rho_{s.min} \\ \text{“increase amount transverse reinf.” if } \rho_s < \rho_{s.min} \end{cases}$$

RatioCheck = “Transverse Reinf. okay”

Longitudinal Splice Location:
(AASHTO LRFD 5.12.13.4)

End Region:
(AASHTO LRFD 5.10.11.4.1c) $\text{EndRegion} = \max\left(D, \frac{1}{6}L_o, 18\text{ in.}\right)$ EndRegion = 36 in.

Minimum Height of Longitudinal Splices above the ground or lower deck:

$$\text{SpliceHeight} = \begin{cases} \text{“no requirements” if DesignCategory = “A”} \\ \text{EndRegion if DesignCategory = “B”} \\ \text{max (12 ft, EndRegion) if DesignCategory = “C”} \end{cases}$$

SpliceHeight = “no requirements”

Type of Transverse Reinforcement:

According to AASHTO LRFD 5.10.2.3, transverse reinforcement should consist of continuous spiral reinforcement or discrete hoops with adequate anchorage.

$$\text{Anchorage} = \begin{cases} \text{“Typical Hook” if DesignCategory = “A”} \\ \text{“Seismic Hook” if DesignCategory = “B”} \\ \text{“Blast Hook” if DesignCategory = “C”} \end{cases} \qquad \text{Anchorage = “Blast Hook”}$$

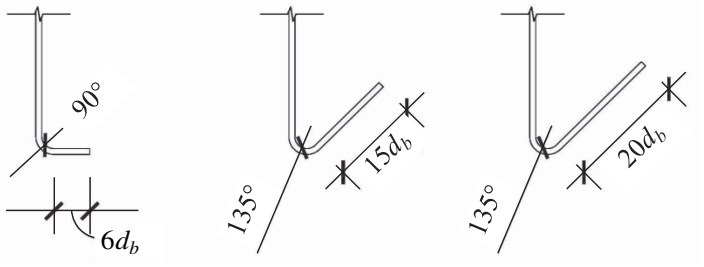

Typical Hook Seismic Hook Blast Hook

Design Summary:

Design Threat:

Standoff:	R_x = 15 ft
Charge Weight (lb TNT):	W_{TNT} = 100 lb TNT
Scaled Standoff:	Z = 3.23 ft/lb$^{1/3}$
DesignCategory = "A"	

Column Parameters:

Non-seismic region	
Support Conditions:	Propped Cantilever
Column Cross-Sectional Shape:	Shape = "circular"
Column Height (between supports):	L_O = 18 ft
Column Diameter:	D = 36 in.
Concrete Clear Cover:	cover = 2 in.

Material Properties:

Concrete Strength:	f'_c = 4000 psi
Yield Strength:	f_y = 60 ksi

Longitudinal Reinforcement:

Area of Longitudinal Reinf.:	12 #9 bars
Longitudinal Reinforcement Ratio:	ρ_L = 0.98%
Minimum Height Long. Splice:	SpliceHeight = "no requirements"

Transverse Reinforcement:

Type of Transverse Reinf.:	#6 bars Type = "hoops"
	Anchorage = "Typical Hook"
Spacing/pitch of Transverse Reinf.:	s_{cc} = 6 in.
Volumetric Reinforcement Ratio:	ρ_s = 0.917%
	RatioCheck = "Transverse Reinf. okay"

Flexural Capacity Check:

SDOF Analysis is not required for Design Category A

8.3 Summary

A total of four design examples were presented in this chapter. The primary purpose of these examples was to illustrate the use of the analysis and design provisions developed during the course of the research conducted under NCHRP Project 12-72. A summary of the work completed on this project and recommendations for future research are provided in the next chapter.

CHAPTER 9

Summary, Conclusions, and Recommendations

9.1 Summary of Research Program

Past terrorist events consisting primarily of explosive attacks, including 60% of those against highway infrastructure between 1920 and 2000 (Jenkins and Gersten, 2001), highlight the need for blast-resistant structures. Although the chances of a terrorist attack against most structures are typically assumed to be very small, the economic and socio-economic consequences can be extremely high. Therefore, the National Cooperative Highway Research Program funded NCHRP Project 12-72 (*Blast-Resistant Highway Bridges: Design and Detailing Guidelines*) to address this concern. The results of this research program are described in this report.

Columns provide the main support for nearly all bridges independent of the type of superstructure, and as such they play a major role in the response of bridges to explosions. The loss of a column will most likely lead to the loss of a bridge's integrity. Thus, to implement the design of bridges for security, there was a need for experimental and analytical research on blast-loaded bridge columns to evaluate the effectiveness of current blast-resistant design guidelines for buildings applied to bridges and to assess whether or not bridge seismic detailing can provide adequate protection for blast-loaded bridges. Furthermore, there was a need to develop new design and detailing guidelines tailored specifically for bridges subjected to explosions, and the main goals of this research were as follows:

- Investigate the response of concrete bridge columns subjected to blast loads,
- Develop blast-resistant design and detailing guidelines for highway bridge columns, and
- Develop analytical models of blast-load distribution and the resulting column response that are validated by experimental data.

The research program included two different phases of testing. In Phase I, small-scale blast tests on square and round non-responding columns were carried out near Vicksburg, MS, with support provided by the Engineering Research and Development Center of the U.S. Army Corps of Engineers. These tests were critical for determining how loads interact with slender structural components, and they provided valuable data on how blast pressures vary with time and position at various locations on the tested columns under a variety of blast scenarios. In Phase II, large-scale blast tests were performed at a remote testing site in central Texas by the University of Texas at Austin with the help of Protection Engineering Consultants and the Southwest Research Institute.

The Phase II test program included the fabrication of ten half-scale columns with five main test variables, designed to represent a national survey of current bridge column specifications and the AASHTO LRFD Bridge Design Specifications (2007). Seismic design and detailing provisions were used in designing one column, while two columns included new blast-resistant design details.

Ten half-scale, small standoff and six half-scale, local damage blast tests were completed in this phase of the experimental program (six columns were tested twice). The goal of the small standoff tests was to observe the mode of failure (i.e., flexure or shear) for eight different column designs. The objective of the local damage tests was to observe the spall and breach patterns of blast-loaded concrete columns. Each blast test evaluated the relative importance of the five main test variables, including scaled standoff, column geometry, amount of transverse reinforcement, type of transverse reinforcement, and splice location. The columns were instrumented with six strain gauges that collected data during the small standoff tests. Strain data were used to verify boundary conditions and blast-load distribution for each small standoff test. The experimental observations and strain data were used to develop design and detailing guidelines for blast-loaded reinforced concrete highway bridge columns.

Complementing the experimental testing program, analytical research to model the response of blast-loaded bridge columns was carried out at various levels of fidelity throughout the research program. Models included simplified methods for predicting loads, such as design charts and equations, as well as software provided by the U.S. Army Corps of Engineers (BEL). Simplified methods of response modeling consisted primarily of single-degree-of-freedom dynamic analyses. These simplified load and response models established the foundation for the recommended design procedure. Aside from these models, detailed finite element models were utilized to represent specific tests within the experimental program. Once these high-fidelity models were validated, parametric studies were carried out to extend the results beyond the range of parameters that could be tested physically. Finally, compiling the results of the analytical models and collected test data, design and detailing provisions were proposed.

9.2 Conclusions and Recommendations

The conclusions and recommendations presented herein are based on the experimental evidence and numerical simulation results gathered during the course of this research study. The primary conclusions leading to the proposed blast-resistant design and detailing guidelines for highway bridge columns are summarized in the subsections below.

9.2.1 Summary of Small Standoff Blast Tests

The small standoff tests enabled the observation of the mode of failure for eight different concrete column designs for various blast-load scenarios. During the small standoff tests, three columns exhibited significant shear deformations at the base, including Columns 1A2, 3A, and 3-Blast. The other seven columns experienced a combination of shear and flexural cracking and exhibited less significant shear deformations at the base. The most common mode of failure was shear; however, the majority of columns had adequate shear capacity, experienced essentially no spall or breach, and were very robust.

Column 1A2, an 18-in. circular gravity column, experienced a shear failure at the base; however, by increasing the standoff (1A1) or using continuous spiral reinforcement (1B), the column's response to close-in blast loads improved. Column 1A1, identical to Column 1A2, was tested at a larger standoff distance than Column 1A2 and experienced only minor damage. Continuous spiral reinforcement also improved the column response to close-in blast loads as demonstrated by the performance of Column 1B. One finding from the experimental test program is that, in cases where spiral reinforcement is not used, discrete ties can be made to perform well if adequate anchorage is provided.

The 30-in. diameter blast-detailed column (2-Blast) was exposed to a more intense loading than its less reinforced counterparts while experiencing a similar response. Thus, given the same blast loading scenario, the circular blast-detailed column would be expected to perform better than the respective gravity or seismic columns. The 30-in. square blast-detailed column (3-Blast) experienced extensive shear deformation at the base; however, it required very large loads to achieve this level of damage. Therefore, the square column with blast-resistant reinforcing details would be expected to perform better than other columns that had less reinforcement when tested at similar loads.

9.2.2 Summary of Local Damage Tests

The local damage tests allowed the observation of spall and breach patterns of blast-loaded concrete columns. Only two of the six columns (1A1 and 2A2) experienced a complete breach. Columns 2A1 and 2B experienced a significant loss of the concrete core, while the remaining two columns stayed intact. Column 2-Blast and 3A exhibited spalling of the side concrete cover, which was not initially expected.

9.2.3 Summary of Design Guidelines

The intent of the design categories proposed under this research is to provide adequate detailing for bridge columns as the structural demand and design threat increase. All columns tested in this experimental program fell into Design Category C (i.e., significant threat scenario) and experienced a range of damage levels depending on the scaled standoff. Columns with a small scaled standoff were exposed to a severe blast load that resulted in the formation of plastic hinges, spalling of concrete cover, and in some cases, total breach of the column. Decreasing the design threat by providing sufficient standoff distance from bridge columns is a safe alternative to increasing the design category and detailing requirements. In general, a higher scaled standoff requires less stringent detailing requirements because of the lower intensity of the blast loading.

One of the best ways to decrease the design loads (and hence the design category) is to increase the standoff distance with physical deterrents such as bollards, security fences, and vehicle barriers. Maximizing the standoff distance is the easiest and often the least costly method to achieve the appropriate level of protection for a bridge. Therefore, if access to the columns is sufficiently limited, the design standoff distance can be increased, which will decrease the effects of blast loads on the columns and the associated design category. When standoff distance is not available to avoid Design Category C, the design and detailing provisions described below should be met.

To the extent practical, the cross-sectional shape of a blast-loaded column should be selected to minimize the intensity of the blast load. Cross-sectional shape affects how a blast load interacts with a column. The use of a circular column is an effective way of decreasing the blast pressure and impulse relative to a square or rectangular column of the same size, and the decrease in impulse can be up to 34% for small scaled standoffs. Therefore, the use of a circular column cross-section over a square cross-section is recommended. With proper detailing, however, columns with rectangular and square cross-sections can be made to be blast resistant.

The cross-sectional dimensions of a column also have a major impact on column capacity in the case of a close-in blast, and this parameter controls the onset of a breaching failure. Consequently, a minimum column diameter of 30 in. is recommended for columns subjected to close-in blast loads.

Experimental observations show that continuous spiral reinforcement performs better than discrete hoops with standard hooks for small standoff threats. To avoid anchorage pullouts and to improve the performance of blast-loaded columns with discrete hoops or ties, longer hook lengths than currently specified should be used. Also, to improve the energy absorption and dissipation capacity of potential plastic hinges, the minimum amount of confinement reinforcement should be increased by 50% over that which is currently specified for seismic designs in the current AASHTO LRFD (2007). This increased level of detailing should extend over the entire column height to help account for the variability associated with different threat scenarios.

The splicing of longitudinal reinforcement should be avoided when feasible. Locating splices away from contact charges can help minimize localized blast damage. As stated previously in the report, it is not possible to design all bridge columns to resist all possible threats. An acceptable level of risk must be accepted for these extreme load cases. If a large enough quantity of explosive is placed close enough to a bridge column, failure is to be expected.

9.3 Recommendations for Future Work

The recommendations for blast-resistant design and detailing of reinforced concrete highway bridge columns proposed in this research were based on experimental data gathered during a two-phase testing program and detailed analytical studies. It is desirable to obtain additional experimental data that can be used to further validate the proposed recommendations. Also, more research is needed to better understand the spall and breach patterns for concrete columns subjected to close-in blasts. Spalling on the column sides was noted in this experimental program with six half-scale blast tests. Prior to these tests, columns subjected to close-in blast loads were assumed to perform similarly to walls, with spalling on the front and back face.

According to Winget et al. (2004), "Retrofit techniques should enhance concrete confinement, increase bending resistance and ductility, add protection against breaching, or a combination of these effects." To improve a column's response to blast loads, increasing the amount of transverse steel is a viable option that will increase a column's ductility and confinement. This added ductility and confinement allows for the concrete core to stay intact and continue providing support to the superstructure once plastic hinging starts to occur. As the amount of transverse steel increases, however, the ease of construction decreases. Placement of reinforcing steel becomes problematic, which increases the probability of voids in the concrete. To avoid such problems, other blast-resistant design alternatives that should be considered include the use of concrete-filled tubes, fiber-reinforced concrete, mechanical couplers at splice locations, and external retrofits.

Concrete-filled steel tubes would eliminate the difficulties in construction seen with regular reinforced concrete columns. More research is needed, however, to better understand connections of these members to the foundation and superstructure. Bruneau et al. (2006) successfully demonstrated the applicability of this design approach for blast-loaded columns tested at a small scale, but additional study is needed to determine how feasible this approach is for large-diameter columns for which typical steel shapes are not available. A concrete-filled tube may be an economical solution if labor is expensive and steel prices are low. Fiber-reinforced concrete, in combination with a typical gravity-reinforced column design, may be a viable alternative to a heavily reinforced concrete column. Fiber-reinforced concrete aides in the prevention of concrete spall by reinforcing concrete away from the location of reinforcing bars. Additional research is needed, however, to validate the performance of fiber-reinforced concrete columns subjected to blast loads and to determine if they provide a cost-effective option for such load cases.

Mechanical couplers at splice locations in reinforced concrete columns subjected to close-in blasts may reduce the chances of column failure associated with discontinuous longitudinal reinforcement. According to Zehrt et al. (1998), "Mechanical splices must be capable of developing the ultimate dynamic strength of the reinforcement without reducing its ductility before they can be used in blast resistant concrete elements." Therefore, additional blast testing of large-scale concrete columns with mechanical couplers is recommended. External retrofits can also be employed to improve the response of reinforced concrete columns to close-in blasts. The use of fiber-reinforced polymer wraps and steel jacketing are two

potential solutions to improve concrete confinement and protection against spalling and breach.

The research described in this report focused primarily on the response of reinforced concrete bridge columns, but additional research on blast-resistant design is needed for other types of bridge components. It should be noted that the field of blast-resistant bridge design is relatively new to the general bridge engineering community, and while the research presented in this study is believed to advance the state of practice considerably, much additional research is needed to mature this field to the current level of the design of bridges for other types of extreme loads such as earthquakes.

References

ABAQUS Inc. (2004). ABAQUS, Version 6.5. www.abaqus.com.

ABC News. (2007). "Iraq: 2 Bridge Blasts in 2 Days." June 11, 2007. http://abcnews.go.com/International/popup?id=3265885&contentIndex=1&page=3&start=false. Accessed June 30, 2008.

Abramson, H. N., et al. (1999). *Improving Surface Transportation Security: A Research and Development Strategy.* National Academy Press: Washington, D. C.

Agrawal, A. (2007) "Blast and Seismic Effects on Highway Bridges." *NJJDOT Technology Transfer Seminar.* October 30, 2007. http://www.utrc2.org/events/events.php?viewid=172. Accessed July 3, 2008.

Alaoui, S. (2004). RECONASANCE: REinforced CONcrete Analysis Spreadsheet enhANCEnced. MS Report. Department of Civil Engineering, University of Texas: Austin, Texas.

Alia, A., and M. Souli. (2006). "High Explosive Simulation Using Multi-material Formulations." *Applied Thermal Engineering.* Vol. 26. pp. 1032–1042.

American Association of State Highway and Transportation Officials (AASHTO). (2007). *AASHTO LRFD Bridge Design Specifications,* 4th Edition. Washington, D.C.

American Concrete Institute (ACI). (2005). *Building Code Requirements for Structural Concrete (ACI 318-05).* ACI Committee 318, Farmington Hills, MI.

American Institute of Steel Construction (AISC). (2006). *Load and Resistance Factor Design Specification for Steel Buildings.* 13th Edition.

American Society of Civil Engineers (ASCE) Task Committee on Blast-Resistant Design. (1997). *Design of Blast Resistant Buildings in Petrochemical Facilities.* ASCE: Reston, VA.

ANSYS Inc. (2004). ANSYS, Version 8.1. www.ansys.com.

Applied Research Associates Inc. (2005). *Computational Physics Group: Capabilities.* http://www.ara.com/mpsp/SWD/Computational%20Physics_Group.htm?. Accessed February 12, 2006.

Bae, S., and O. Bayrak (2008). "Seismic Performance of Full-Scale Reinforced Concrete Columns." *ACI Structural Journal.* Vol. 105, No. 2. pp. 123–133.

Baker, W. E. et al. (1983). *Explosion Hazard and Evaluation.* Elsevier Scientific Publishing Co.: Amsterdam.

Barker, D. D., and M. G. Whitney. (1992). "Design of Blast Hardened Control Rooms: A Case Study." *Structures under Shock and Impact II.* Bulson, P. S., Ed. Proceedings of the 2nd International Conference on Structures under Shock and Impact. Portsmouth, UK. June 16–18. Computational Mechanics Publications.

Bentz, E. (2001). *Response-2000, Shell-2000, Traix-2000, Membrane-2000: User Manual.* Version 1.1. Department of Civil Engineering, University of Toronto: Toronto, Ontario, Canada. http://www.ecf.utoronto.ca/~bentz/manual2/final.pdf.

BERGER/ABAM Engineers Inc. (1996). *Seismic Design of Bridges Design Example No. 1: Two-Span Continuous CIP Concrete Box Bridge.* Publication No. FHWA-SA-97-006. Federal Highway Administration (FHWA). October 1996.

Biggs, J. M. (1964). *Introduction to Structural Dynamics.* McGraw-Hill, Inc.: New York.

The Blue Ribbon Panel on Bridge and Tunnel Security. (2003). *Recommendations for Bridge and Tunnel Security.* Special report prepared for FHWA and AASHTO.

Bounds, W., ed. (1998). *Concrete and Blast Effects.* Special Publication (SP-175). American Concrete Institute. Farmington Hills, MI.

Bruneau, M., D. Lopez-Garcia, and S. Fujikura. (2006). "Multihazard-Resistant Highway Bridge Bent." *ASCE Structures Congress.* St. Louis, Missouri.

Bruneau, M., S. Fujikura, and D. Lopez-Garcia. (2007). "Blast Resistant Bridge Piers." *Structure Magazine.* March, pp. 19–21.

Bulson, P. S. (1997). *Explosive Loading of Engineering Structures.* E & F N Spon. Routledge: London.

California Department of Transportation (Caltrans). (2003). *Bridge Design Specifications.* http://www.dot.ca.gov.hq/esc/techpubs/. Accessed August 10, 2006.

California Department of Transportation (Caltrans). (2006). *Seismic Design Criteria, Version 1.4.* http://www.dot.ca.gov.hq/esc/techpubs/. Accessed February 10, 2008.

Cendon, D. A., V. S. Galvez, and F. Galvez. (2004). "Modeling Explosions Using ALE Meshes: The Influence of Mesh Refinement in Pressures and in Efforts Induced by Blast/Structure Interaction." *Structures and Materials.* Vol. 15. Eighth International Conference on Structures under Shock and Impact. pp. 173–180.

Century Dynamics. (2004). AUTODYN, Version 6.0. www.century-dynamics.com.

Collins, M., and M. Bentz. (1990). Response1990. University of Toronto.

Computers and Structures Inc. (2006a). ETABS, Version 9. 1995 University Avenue, Suite 540, Berkeley, CA 94704. www.csiberkeley.com/products_ETABS.html.

Computers and Structures Inc. (2006b). SAP 2000, Version 10. 1995 University Avenue, Suite 540, Berkeley, CA 94704. www.csiberkeley.com/products_SAP.html.

Conrath, E. J., T. Krauthammer, K. A. Marchand, and P. F. Alakar. (1999). *Structural Design of Physical Security: State of Practice.* ASCE: Reston, VA.

Department of the Army. (1986). *Fundamentals of Protective Design for Conventional Weapons (TM 5-855-1).* Washington, D.C.

Department of the Army. (1990). *Structures to Resist the Effects of Accidental Explosions (TM 5-1300).* Washington, D.C.

Departments of the Army, Air Force, and Navy and the Defense Special Weapons Agency. (2002). *Design and Analysis of Hardened Structures to Conventional Weapons Effects. Unified Facilities Criteria (UFC) 3-340-01.* Washington, D.C. (for official use only).

Department of Defense. (2005). *Design of Buildings to Resist Progressive Collapse.* Unified Facilities Criteria (UFC) 4-023-03. Approved for public release January 25, 2005.

Eytan, R. (1992). "Response of Real Structures to Blast Loadings—The Israeli Experience." *Structures under Shock and Impact II.* Bulson, P. S., Ed. Proceedings of the 2nd International Conference on Structures under Shock and Impact. Portsmouth, UK. June 16–18, 1992. Computational Mechanics Publications. pp. 483–495.

Farahany, M. (1983). *User Oriented Computer Program for Flexural Behavior of General Reinforced Concrete Sections.* MS Report. Department of Civil Engineering, University of Texas: Austin, Texas. December 1983.

FEA Information Inc. (2006). *LS-DYNA: Applications.* http://www.ls-dyna.com/. Accessed March 13, 2006.

Fox News. (2004). "Terror Threat against U.S. Allies." http://www.foxnews.com/story/0,2933,117836,00.html.

Fujikura, S., M. Bruneau, and D. Lopez-Garcia. (2008). "Experimental Investigation of Multihazard Resistant Bridge Piers Having Concrete-Filled Steel Tube under Blast Loading." *Journal of Bridge Engineering.* Vol. 13, No. 6. pp. 586–594.

Gannon, J. C. (2004). *Design of Bridges for Security against Terrorist Attacks.* MS Thesis. Department of Structural Engineering, University of Texas at Austin. Fall, 2004.

General Services Administration. (2003). *GSA Progressive Collapse Analysis and Design Guidelines for New Federal Office Buildings and Major Modernization Projects.* Washington, D.C.

Glasstone, S., and P. J. Dolan. (1997). *The Effects of Nuclear Weapons,* 3rd Edition. The United States Department of Defense and the United States Department of Energy: Washington, D.C.

Gokani, V. (2006). *Design and Evaluation of Retrofit T203 and T501 Barriers with Mechanical Anchors using Experimental Testing and Finite-Element Simulation.* MS Thesis. Department of Civil, Environmental, and Architectural Engineering, University of Texas at Austin.

Hinman, E. (1998). "Approach for Designing Civilian Structures against Terrorist Attack." *Concrete and Blast Effects.* SP-175, ACI Committee 370. Bounds, W., Ed. American Concrete Institute: Farmington Hills, Michigan. pp. 1–17.

HydeSoft Computing, LCC. (2008). DPLOT 2.1.8.0. Engineer Research and Development Center: Vicksburg, MS. www.dplot.com.

Islam, A. (2005). *Performance of AASHTO Girder Bridges under Blast Loading.* Dissertation, Florida State University.

Jenkins, B. M. (1997). "Protecting Public Surface Transportation and Patrons from Terrorist Activities: Case Studies of Best Security Practices and a Chronology of Attacks." *MTI Report 97-4.* Mineta Transportation Institute: San Jose, CA.

Jenkins, B. M., and L. N. Gersten. (2001). *Protecting Public Surface Transportation against Terrorism and Serious Crime.* Mineta Transportation Institute: San Jose, California.

Karagiozova, D., and N. Jones. (2000). "Energy Absorption of a Layered Cladding under Blast Loading." *Structures under Shock and Impact VI.* WIT Press. Southampton, UK. pp. 447–456.

Knight, G., J. Mathis, and M. Barsotti. (2004). *An Investigation into the Effects of Blast Clearing Around Structures.* Final Report, ME 5653 Computational Fluid Dynamics, University of Texas at San Antonio.

Kowalsky, M. (2000). "Deformation Limit States for Circular Reinforced Bridge Columns." *Journal of Structural Engineering,* Vol. 126, No. 8. pp. 869–878.

LSTC. (2007). *LS-DYNA Keyword User's Manual, Version 971.* Livermore Software Technology Corporation.

Luccioni, B., D. Ambrosini, and R. Danesi. (2006). "Blast Load Assessment Using Hydrocodes." *Engineering Structures.* Vol. 28. pp. 1736–1744.

Magallanes, J. (2008). "Importance of Concrete Material Characterization and Modeling to Predicting the Response of Structures to Shock and Impact Loading." *Structures under Shock and Impact X.* WIT Press: Southampton, UK.

Mathworks, Inc. (2008). Matlab 7.6. www.mathworks.com.

"Military Studies in the Jihad against the Tyrants." *Al Qaeda Terrorist Training Manual* (1995). On the United States Department of Justice Website at http://www.au.af.mil/au/awc/awcgate/terrorism/alqaida_manual/. Accessed December 3, 2009.

Minnesota Department of Transportation (Mn/DOT). (2007). "Interstate 35W Bridge Collapse." http://www.dot.state.mn.us/i35wbridge/index.html. Accessed April 20, 2008.

Mlakar, P. F., W. G. Corley, M. A. Sozen, and C. H. Thornton. (1998). "The Oklahoma City Bombing: Analysis of Blast Damage to the Murrah Building." *Journal of Performance of Constructed Facilities.* Vol. 12, No. 3. pp. 113–119.

National Research Council. (1995). *Protecting Buildings from Bomb Damage: Transfer of Blast-Effects Mitigation Technologies from Military to Civilian Applications.* Committee on Feasibility of Applying Blast-Mitigating Technologies and Design Methodologies from Military Facilities to Civilian Buildings. National Academy of Sciences: Washington, D.C.

National Research Council. (2003). *ISC Security Design Criteria for New Federal Office Buildings and Major Renovations.* National Academies Press: Washington, D.C.

Priestley, M. J. N., and R. Park. (1987). "Strength and Ductility of Concrete Bridge Columns under Seismic Loading." *ACI Structural Journal.* Jan–Feb 1987. pp. 61–76.

Pujol, S., M. Sozen, and J. Rameriz. (2000). "Transverse Reinforcement for Reinforced Concrete Frames to Resist Earthquakes." *Journal of Structural Engineering,* Vol. 126, No. 4. pp. 461–466.

Raftenberg, M. N. (1997). "Close-in Blast Loading of a Steel Disc; Sensitivity to Steel Strength Modeling." *International Journal of Impact Engineering.* Elsevier Science Ltd.: Oxford, UK.

Ray, J. C. (2006). "Validation of Numerical Modeling and Analysis of Steel Bridge Towers Subjected to Blast Loadings." *Proceedings of the Structures Congress and Expositions,* p. 129.

Ray, J. C., B. J. Armstrong, and T. R. Slawson. (2003). "Airblast Environment beneath a Bridge Overpass." *Transportation Research Record,* n. 1827, pp. 63–68.

RISA Technologies. (2005). RISA 3-D, Version 5.5. www.risatech.com/risa-3d.asp.

Rummel, T., M. Hyzak, and M. L. Ralls. (2002). "Transportation Security Activities in Texas." *International Bridge Conference 2002 Presentation #IBC-02-A3.* Texas Department of Transportation: Austin, TX.

Rushton, N., G. Schleyer, and R. Cheesman. (2008). "Analysis of the Explosive Loading of Open-Ended Steel Pipes." *Structures under Shock and Impact X.* WIT Press: Southampton, UK.

Rusinek, A. (2008). "Influence of Conical Projectile Diameter on Perpendicular Impact of Steel Plate." *Engineering Fracture Mechanics.* Vol. 75, N. 10. pp. 2946–2967.

Rutner, M., A. Astaneh-Asl, and J. Son. (2005). "Protection of Bridge Piers against Blast." *ACI Structural Journal,* Vol. 103, No. 6, pp. 842–849.

Schwer, L. E., and L. J. Malvar. (2005). "Simplified Concrete Modeling with *MAT_CONCRETE_DAMAGE_REL3." *JRI LS-DYNA USER WEEK.*

Science Applications International Corporation (SAIC). (1994). *International Blast and Thermal Environment for Internal and External Explosions: A User's Guide for the BLASTX Code.* Version 3.0. (SAIC 405-94-2). https://pdc.usace.army.mil/software/blastx.

Science Applications International Corporation (SAIC). (2001). BlastX, Version 4.2.3.0. Science Applications International Corporation, San Diego, California, (distribution limited to U.S. government agencies and their contractors).

Science Applications International Corporation (SAIC), Transportation Policy and Analysis Center. (2002). *A Guide to Highway Vulnerability Assessment for Critical Asset Identification and Protection.* Report prepared for the American Association of State Highway and Transportation Officials' Security Task Force. Available at http://security.transportation.org/community/security/doc/guide-VA_FinalReport.pdf.

Sezen, H. and J. Moehle. (2006). "Seismic Tests of Concrete Columns with Light Reinforcement." *6th Japanese–German Bridge Symposium,* Munich, Germany.

Tedesco, J. (1999). *Structural Dynamics: Theory and Approach.* Addison Wesley Longman: Menlo Park, CA.

Texas Office of the Governor. (2001). "Queen Isabella Causeway to Re-Open Before Thanksgiving." http://www.governor.state.tx.us/divisions/press/pressreleases/PressRelease.2001-11-14.0443. Accessed April 20, 2008.

Transportation Pooled Fund Program (TPFP). (2008). *Blast Testing of Full-Scale, Precast, Prestressed Concrete Girder Bridges.* Project TPF-5(115). http://www.pooledfund.org/projectdetails.asp?id = 346&status=4.

Turhan, L., Ö. Eksik, E. B. Yalçin, A. Demirural, T. Baykara, and V. Günay. (2008). "Computational Simulations and Ballistic Verification Tests for 7.62 mm AP and 12.7 mm AP Bullet Impact against Ceramic Metal Composite Armours." *Structures under Shock and Impact X.* WIT Press: Southampton, UK.

United States Geological Survey (USGS). (2008). "2008 United States National Seismic Hazard Maps." http://earthquake.usgs.gov/research/hazmaps/products_data/2008. Accessed June 19, 2008.

U.S. Army Corps of Engineers. (2000). BEL, Version 1.1.0.3. U.S. Army Corps of Engineers, Engineer Research and Development Center, Vicksburg, Mississippi. (For Official Use Only).

U.S. Army Corps of Engineers. (2001). ConWep, Version 2.0.6.0. U.S. Army Engineer Research and Development Center, Vicksburg, MS.

U.S. Army Corps of Engineers. (2002). SPAn32, Version 1.2.6.9. U.S. Army Corps of Engineers Omaha District, Omaha, NE.

U.S. Army Corps of Engineers. (2006). *ERDC MSRC: Major Shared Resource Center.* http://erdc.hpc.mil/hardSoft/Software/dysmas.htm. Accessed March 3, 2006.

U.S. Army Corps of Engineers. (2007). SBEDS: Single Degree of Freedom Blast Effects Design Spreadsheet, Version 3.2. U.S. Army Corps of Engineers.

U.S. Army Engineer Research and Development Center. *Bridge and Tunnel Vulnerability Workshop: May 13–15, 2003.* Vicksburg, MS, Sponsored by the Federal Highway Administration Office of Bridge Technology, Washington, D.C. (Distribution Limited)

Wikipedia. (2008). *1993 World Trade Center Bombing.* http://en.wikipedia.org/wiki/World_Trade_ Center_bombing.

Williamson, E. B., and D. G. Winget. (2005). "Risk Management and Design of Critical Bridges for Terrorist Attacks." *Journal of Bridge Engineering,* ASCE, Vol. 10, No. 1, pp. 96–106.

Williamson, E. B. (2008). "CE 397: Blast-Resistant Structural Design" Class Notes. Department of Civil, Architectural, and Environmental Engineering, the University of Texas at Austin.

Winget, D. G. (2003). *Design of Critical Bridges for Security against Terrorist Attacks.* M.S. Thesis, the University of Texas at Austin.

Winget, D. G., K. A. Marchand, and E. B. Williamson. (2004). "Analysis of Blast Loads on Substructures." *Proceedings, Structures under Shock and Impact.* Greece.

Winget, D. G., K. A. Marchand, and E. B. Williamson. (2005). "Analysis and Design of Critical Bridges Subjected to Blast Loads." *Journal of Bridge Engineering,* ASCE, Vol. 131, No. 8, pp. 1243–1255.

Zehrt Jr., W. H., and P. M. LaHoud. (1998). "Development of Design Criteria for Reinforcing Steel Splices in Blast Resistant Concrete Structures." *Special Publication,* ACI, Vol. 175, pp. 131–140.

LIST OF VARIABLES

A_c = area of concrete core (in.^{2})
A_g = gross cross-sectional area (in.^{2})
A_s = area of longitudinal reinforcement (in.^{2})
A_{sh} = area of transverse reinforcement (in.^{2})
A_v = area of shear reinforcement within a distance s (in.^{2})
b = effective width of cross section (in.)
c = concrete clear cover (in.)
C_{age} = age of concrete (months)
d = effective depth of cross section (in.)
d_b = nominal diameter of reinforcing bar (in.)
d_v = effective moment arm (in.)
D = diameter or width (in.)
D_{core} = diameter or width of concrete core (in.)
D_r = diameter or width passing through longitudinal reinforcement (in.)
DIF = dynamic increase factor
E_s = steel modulus of elasticity (ksi)
f_{du} = dynamic ultimate strength of reinforcing bars (psi)
f_{dy} = dynamic yield strength of reinforcing bars (psi)
f_u = ultimate strength of reinforcing bars (psi)
f_y = yield strength of reinforcing bars (psi)
f'_c = specified compressive strength of concrete at 28 days (psi)
f'_{dc} = dynamic compressive strength of concrete (psi)
F_e = force applied to a single-degree-of-freedom system
h_c = core dimension of column in the direction under consideration (in.)
H = charge height above ground surface
H_T = height of triple point above ground surface
i_r = unit positive normal reflected impulse (psi-ms)
i_s = unit positive incident impulse (psi-ms)
I_{BEL} = BEL equivalent impulse (psi-ms)
I_x = moment of inertia (in.^{4})
k_e = stiffness of a single-degree-of-freedom system
K_A = age increase factor for concrete
K_E = strength increase factor for concrete and steel
L = height of column (in.)
L_o = column height between supports (in.)
L_w = wavelength of positive phase (ft)

m_o(x) = mass per unit length of a member
M_e = mass of a single-degree-of-freedom system
M_n = nominal moment capacity (kip-ft)
M_P = plastic moment capacity (kip-ft)
P = applied load (lb)
P_{BEL} = BEL equivalent uniform pressure (psi)
P_o = ambient atmospheric pressure (psi)
P_r = peak positive normal reflected pressure (psi)
P_s = peak incident overpressure at Mach front (psi)
P_{so} = peak positive incident pressure (psi)
R = standoff, distance between center of blast source and target (ft)
s = center-to-center spacing or pitch of transverse reinforcement (in.)
S = section modulus (in.^{3})
S_x = distance from nearest free edge to point of interest (ft)
t_A = time of arrival (s)
t_{BEL} = BEL duration (ms)
t_c = clearing time (s)
t_o = positive phase duration (s)
t_o^- = negative phase duration (s)
U_s = shock front velocity (ft/s)
V_{base} = maximum shear at base (lb)
V_c = nominal shear strength provided by concrete (lb)
V_N = nominal shear strength (lb)
V_s = nominal shear strength provided by steel (lb)
w = charge weight parameter
w_o = maximum magnitude of assumed blast load shape applied to a member
$w_o(x)$ = assumed blast load shape applied to a member
W = charge weight of explosive
W_{TNT} = charge weight of explosive (lb equivalent TNT)
z = standoff distance parameter
Z = scaled standoff (ft/lb$^{1/3}$)
Z_x = plastic section modulus (in.^{3})
α = angle of incidence (degrees)
γ_v = average shear strain across section
γ_c = concrete unit weight (lb/ft^3)
δ = displacement
$\Delta_{elastic}$ = displacement at the elastic limit (in.)
Δ_{max} = maximum displacement of a member (in.)
$\Delta(x)$ = displaced shape of a beam
θ = support rotation (degrees)
θ_{SBEDS} = SBEDS support rotation (psi)
μ = flexural ductility ratio
μ_{SBEDS} = SBEDS flexural ductility (psi-msec)
ρ_s = volumetric reinforcement ratio
ρ_L = longitudinal reinforcement ratio
$\phi(x)$ = normalized displaced shape of a beam

Abbreviations and acronyms used without definitions in TRB publications:

AAAE	American Association of Airport Executives
AASHO	American Association of State Highway Officials
AASHTO	American Association of State Highway and Transportation Officials
ACI–NA	Airports Council International–North America
ACRP	Airport Cooperative Research Program
ADA	Americans with Disabilities Act
APTA	American Public Transportation Association
ASCE	American Society of Civil Engineers
ASME	American Society of Mechanical Engineers
ASTM	American Society for Testing and Materials
ATA	Air Transport Association
ATA	American Trucking Associations
CTAA	Community Transportation Association of America
CTBSSP	Commercial Truck and Bus Safety Synthesis Program
DHS	Department of Homeland Security
DOE	Department of Energy
EPA	Environmental Protection Agency
FAA	Federal Aviation Administration
FHWA	Federal Highway Administration
FMCSA	Federal Motor Carrier Safety Administration
FRA	Federal Railroad Administration
FTA	Federal Transit Administration
HMCRP	Hazardous Materials Cooperative Research Program
IEEE	Institute of Electrical and Electronics Engineers
ISTEA	Intermodal Surface Transportation Efficiency Act of 1991
ITE	Institute of Transportation Engineers
NASA	National Aeronautics and Space Administration
NASAO	National Association of State Aviation Officials
NCFRP	National Cooperative Freight Research Program
NCHRP	National Cooperative Highway Research Program
NHTSA	National Highway Traffic Safety Administration
NTSB	National Transportation Safety Board
PHMSA	Pipeline and Hazardous Materials Safety Administration
RITA	Research and Innovative Technology Administration
SAE	Society of Automotive Engineers
SAFETEA-LU	Safe, Accountable, Flexible, Efficient Transportation Equity Act: A Legacy for Users (2005)
TCRP	Transit Cooperative Research Program
TEA-21	Transportation Equity Act for the 21st Century (1998)
TRB	Transportation Research Board
TSA	Transportation Security Administration
U.S.DOT	United States Department of Transportation